THE UNIVERSITY
of EDINBURGH

This thesis has been submitted in fulfilment of the requirements for a postgraduate degree (e.g. PhD, MPhil, DClinPsychol) at the University of Edinburgh. Please note the following terms and conditions of use:

This work is protected by copyright and other intellectual property rights, which are retained by the thesis author, unless otherwise stated.
A copy can be downloaded for personal non-commercial research or study, without prior permission or charge.
This thesis cannot be reproduced or quoted extensively from without first obtaining permission in writing from the author.
The content must not be changed in any way or sold commercially in any format or medium without the formal permission of the author.
When referring to this work, full bibliographic details including the author, title, awarding institution and date of the thesis must be given.

Genetic Dissection Reveals Distinct Roles for the Transcription Factor ZHOUPI in Controlling *Arabidopsis* Endosperm Cell Death and Embryonic Cuticle Development

Qian Xing

Supervisor Dr. Gwyneth Ingram

Thesis submitted for the Degree of Doctor of Philosophy

University of Edinburgh

2012

II. Declaration

I declare that the results and other statements included in this thesis are my own work and contributions made by others are clearly cited.

III. Abstract

Angiosperm seed development requires co-ordinated development of the embryo and a second zygotic tissue, the endosperm. In *Arabidopsis thaliana*, the endosperm is ephemeral and is largely consumed by the embryo during seed development. In addition to a role in embryo nutrition, it is also likely that the endosperm may play a more direct role in signalling to the embryo to regulate development. Despite their importance for embryo development, these processes are very poorly understood. The *ZHOUPI* (*ZOU*) gene provides an important tool to address these problems. Firstly, *ZOU* likely regulates endosperm breakdown. Whereas wild-type seed have a single layer of endosperm at maturity, *zou* seed has a large persistent endosperm and a correspondingly small embryo. The small *zou* embryo does not fill the seed so that the seed shrivels as it desiccates during maturation. Secondly, *zou* embryos have defects in their cuticle, so that the endosperm adheres to the embryo throughout seed development. After seed germination, *zou* cotyledons develop holes in their epidermis as they expand, probably due to the defects in the cuticle. *ZHOUPI* (*ZOU*) encodes a bHLH transcription factor and is expressed in the embryo surrounding region (ESR) of endosperm but not in the embryo itself. The role of *ZOU* in cuticle development is partly mediated by the *ABNORMAL LEAF SHAPE1* (*ALE1*) gene. Thus, *ale1* mutants also show defects in embryonic cuticle development and *ALE1* is specifically expressed in ESR in a *ZOU*-dependent fashion.

It was unclear whether the effects of *ZOU* upon embryo development are an indirect consequence of the persistent endosperm mechanically impeding embryo expansion, or rather reflect a more direct role of the ESR in signalling to the embryo.

The main aims of this thesis were 1) to provide evidence that *ZOU* regulates endosperm cell death and 2) to test whether *ZOU* function in controlling endosperm cell death could be separated from that in embryonic epidermal cuticle development. To achieve this goal, 1) TUNEL assays were performed in the seeds to confirm the *zou* endosperm cell death phenotype, 2) *ALE1* expression in the ESR in *zou* mutants was rescued using the *ZOU*-independent *AtSUC5* promoter to investigate whether one or both of *zou* phenotypes were complemented, 3) Candidate *ZOU* target genes were validated and characterized to determine their functions in endosperm cell death and/or embryonic epidermal cuticle development. The TUNEL assays revealed that *zou* mutants display less DNA fragmentation in the ESR than that of the wild-type, but that *zou* did not have defects in cell death outside the seeds suggesting *ZOU* specifically regulated endosperm cell death. The *AtSUC5*::*ALE1* transgene partially rescued *zou* defects in epidermal cuticle but not in endosperm cell death. This shows that the defects in the *zou* cuticle are not caused by the defective endosperm, rather *zou* has distinct, separable functions. Lastly, I characterised several novel *ZOU* targets and showed that *RGP3* may be a direct *ZOU* target as it is expressed in ESR in *ZOU* dependent fashion, whereas *RGP4* is likely indirect as it is expressed in the testa and up-regulated in *zou* mutants. In conclusion, *ZOU* has independent roles in endosperm cell death and embryonic epidermal cuticle development. Because *ALE1*, which largely mediates the role in cuticle development, is less widely conserved than is *ZOU*, the role in promoting endosperm cell death may be the ancestral function of *ZOU*.

IV. Acknowledgement

I would like to thank China Scholarship Council and the University of Edinburgh for the funding of my study and my supervisors Dr. Gwyneth Ingram and Dr. Justin Goodrich for giving me the opportunity to carry out my PhD in their groups.

I am mostly influenced by Gwyneth's enthusiasm for science and discovery, and not to mention her more than nine hours hard working in the lab every day. I was really lucky to be recruited as PhD student to her lab during my most difficult time. Gwyneth not only teaches me techniques hand by hand, but also leads me to think, to ask why and most importantly to find out the answers by myself. Without her encouragement I could not finish my work and I really appreciate her supervision.

Unfortunately Gwyneth left Edinburgh during the last one and half year of my PhD study and I luckily joined my second supervisor, Justin Goodrich's lab which provides me with research materials and mental guidance. From Justin I have learned how to make a balance between pursuing science in earnest during the work and relaxing and enjoying the life after the work. Justin has put a lot of efforts on guiding me to finish my thesis and I sincerely and deeply thank him.

I had great time of working with my colleagues from the former Gwyneth Ingram group, Zareen, Rita and Quique, and the 'big lab', which is consisted of Justin Goodrich group, Andrew Hudson group, Richard Milne group, Catherine Kidner group, Peter Doerner group, and Steven Spoel group. I would like to thank Andrew W, Shih, Erica, Pumi, Andrew H, Hayley, Abby, Joa, Poay, Tanyarat, Byung-Ho, Zafar, Peter, Anne, Eric, Julie and members from Steven Spoel group, and Sophie for being the versatile lab manager, and special thanks to Jessica Fitzgibbon for helping

with the double blind tests. I apologize for people whose names are not listed here and thank you.

Lastly, I would like to thank my big family in China, my much-loved Mum and Dad and thank you for your emotional and financial supports. I would like to thank my beloved husband Ralf for the inspirations from your analytical and scientific criticism and spontaneous creativities.

V. Abbreviations

2-ME	2-mercaptoethanol
ABA	Abscisic acid
APP	Amyloid beta precursor protein
bp	Base pair
BSA	Bovine serum albumin
cDNA	Complimentary DNA
CTAB	Cetyl trimethylammonium bromide
dATP	2'-deoxyadenosine 5'-triphosphate
dCTP	2'-deoxycyidine 5'-triphosphate
DDM	n-dodecyl beta-D- maltoside
DEPC	Diethylpyrocarbonate
dGTP	2'-deoxyguanosine 5'-triphosphate
DNA	Deoxyribonucleic acid
dNTPs	Deoxyribonucleotide triphosphate
dTTP	2'-deoxythymidine 5'-triphosphat
EDTA	Diaminoethanetetraacetic acid
SEM	Scanning electron microscopy
EtOH	Ethanol
GA	Gibberellic acid
GFP	Green fluorescent protein

HRP	Horse radish peroxidase
JA	Jasmonic acid
kb	Kilo base
L	Litre
LB	Lauria broth
M	Molar
mg	Milligram
min	Minute(s)
ml	Millilitre
mM	Millimolar
mRNA	Messenger RNA
MW	Molecular weight
MS	Murashige and Skoog
ng	Nanogram
O/N	Over night
PBS	Phosphate-buffered saline
PVP 40	Polyvinyl pyrrolidone (vinylpyrrolidine homopolymer), Mw 40,000
RNA	Ribonucleic acid
RNAase	Ribonuclease
SDS	Sodium dodecyl sulfate
SSC	Standard saline citrate
TE	Tris-EDTA buffer

Tween	Polyethylenesorbitan monolaurate
µl	Microlitre
V	Volt
X-gal	5-bromo-4-chloro-indolyl-galactopyranoside

VI. Contents

1 Introduction

1.1 Angiosperm seed development

In the past half-century, there has been remarkable growth in the world food production. Considering the major cereal grains (wheat, barley, maize, rice and oats) as an example, since 1961 their production has increased by 3 fold (Godfray et al., 2010). Nevertheless, the global population is continuously growing and today more than 14% of people are still not obtaining enough protein and energy from their food intake, with many suffering from malnutrition (Godfray et al., 2010). It is predicted that by the year 2050 there will be 9 billion people on the earth and by the same date the world will demand a 70% to 100% increase in food production with an average increase of 44 million metric tons/year, which is equal to maintaining a rate of increase 38% higher than that achieved over the past 40 years (Tester and Langridge, 2010). Seeds from cereals and the *Brassicaceae* family species contributed over 44% of calories consumed in the world in 2005, and seed storage proteins, carbons, lipids and other macro and micro-molecules which are vital to seed nutritional qualities have been shown to play an indispensable role in reducing malnutrition and maintaining a healthy condition (Kawakatsu and Takaiwa, 2010). Therefore, increasing both seed yield and seed nutritional quality are ways of maintaining global food security. In order to achieve this goal, it is essential to elucidate the biological and physiological nature of seed development.

1.1.1 Double fertilization

Angiosperms seed development is initiated by double fertilization of the female gametophyte. In summary, the pollen tube germinates from the male gametophyte

(the pollen grain), is guided to the ovule by signals from both the sporophytic and gametophytic maternal tissues, penetrates the female gametophyte and releases two haploid sperm cells. One sperm cell fuses with the haploid egg cell and the other fuses with the diploid central cell of the female gametophyte, ultimately giving rise to the diploid embryo and triploid endosperm respectively (Friedman, 1990). In reaction to double fertilization, the *Arabidopsis* seed coat or testa which originates from the sporophytic, maternally derived integuments of the ovule starts to develop. The two/three-layered inner integument and the two-layered outer integument synthesize various chemical compounds, such as flavonoids and mucilage, and undergo programmed cell death. This development is coordinated with the growth of the endosperm and embryo (Haughn and Chaudhury, 2005).

In *Arabidopsis* the female gametophyte is a structure containing seven cells and eight nuclei. It consists of three antipodal cells at the chalazal (proximal) pole of the sac, one egg cell and two synergid cells at the micropylar (distal) pole of the sac and a large central cell containing two central nuclei in the middle of the sac (Yadegari and Drews, 2004). The female gametophyte is developed from a diploid megaspore mother cell which undergoes one round of meiosis generating four haploid cells, only one of which becomes a megaspore while the others die. The megaspore undergoes three rounds of mitosis and cellularization to form the final female gametophyte (Yadegari and Drews, 2004). The male gametophyte is developed from a diploid pollen mother cell which undergoes one round of meiosis forming a tetrad of haploid microspores, all microspores survive and each of which then undergoes one round of mitosis to form a bicellular pollen grain consisting of a generative cell within a vegetative cell. The generative cell undergoes a second round of mitosis late in

development, to form the tricellular pollen consisting of two hapoid sperm cells within one vegetative cell (McCormick, 1993).

1.1.2 Embryogenesis in *Arabidopsis*

Arabidopsis seed development is staged with reference to the major stages of embryo morphogenesis (Figure 1.1) and the developmental processes involved in embryogenesis have been extensively reviewed (Baud et al., 2002; Capron et al., 2009; De Smet et al., 2010; Dumas and Rogowsky, 2008; Nawy et al., 2008). At the preglobular stage (Figure 1.1 A), the zygote elongates and divides asymmetrically giving rise a smaller apical cell and a bigger basal cell (Figure 1.2 A). These two cells have very different cell fates: The basal cell only undergoes horizontal division forming a filamentous structure, the suspensor (Figure 1.2 B). In contrast the apical cell contains dense cytoplasm, and is very active in cell division. After its formation it undergoes three rounds of division, two in the vertical plane and one in the horizontal plane to form the upper tier and the lower tier of cells at the octant stage. At the early globular stage (Figure 1.1 B), the eight cells of the octant embryo undergo a first round of tangential cell division defining the outer layer which forms protoderm and inner layer which forms the ground and vascular tissues (Figure 1.2 C). Meanwhile, the upper most suspensor cell which is called the hypophysis becomes incorporated into the embryonic root meristem (Figure 1.2 D). At the early heart stage (Figure 1.1 C), the embryo displays a triangular shape because of the different growth pattern of cells in the upper and the lower tier, and in particular because of the initiation of the primordia of the major organs of the seedling, the cotyledons. The precursors of the hypocotyl, primary root, provascular tissue and cortex have also formed at this stage (Figure 1.2 E). After the heart stage, the embryo

elongates (Figure 1.1 D) to give the torpedo stage. Subsequently the embryo bends over within the confines of the seed coat to give the bent cotyledon stage and mature stage (Figure 1.1 F). At the torpedo stage and the bent cotyledon stage the cotyledons continuously elongate and bend from the micropylar zone to the chalazal zone, and by the torpedo stage the patterning of shoot apical meristem (SAM), cotyledons, hypocotyl, primary root and root apical meristem (RAM) is complete and is basically equal to that of the seedling (Figure 1.2 G).

At the mature stage, the embryo enters a phase of growth arrest and becomes osmotolerant. The endosperm is maintained as a single layer of living cells which are surrounded by a layer of dead outer integument (testa) (Belin and Lopez-Molina, 2010). Once the seed is exposed to germination promoting factors, such as moisture, light, cold treatment or chemicals, seed dormancy can be overcome and the seed starts to germinate (Bentsink and Koornneef, 2008). Recent evidence has shown that dormancy is regulated by endosperm associated ABA production (Bethke et al., 2007; Lee et al., 2010; Lefebvre et al., 2006). ABA and GA have long been known to play opposing roles in the regulation of dormancy (Finkelstein et al., 2008). Lee and colleagues (2010) have shown that imbibed dormant seeds show a high expression of *RGA-like 2* (*RGL2*), which is negative regulator in GA response (Lee et al., 2002) and *ABA1* which is involved in generating epoxycarotenoid precursors for the ABA biosynthetic pathway (Barrero et al., 2005) in the seed coat and the one layer endosperm. This generates high levels of ABA to repress embryo germination. The RGL2 protein may have an additional role in promoting ABA biosynthesis in the endosperm.

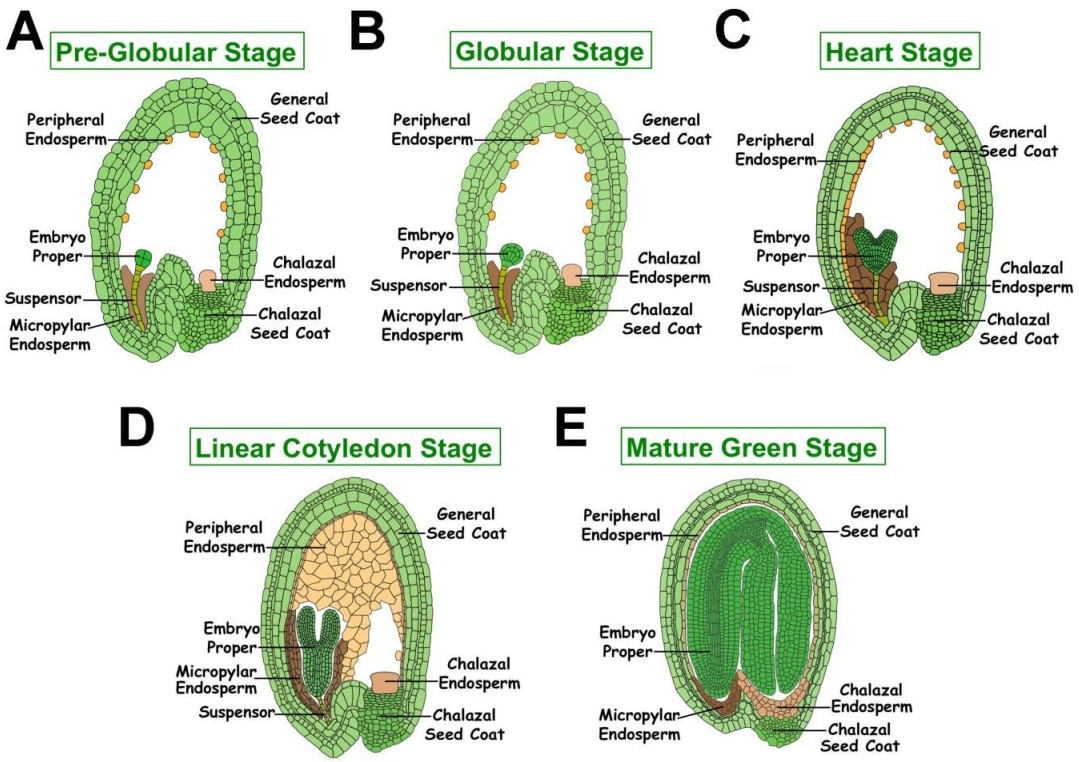

Figure 1.1 Schematic models of major stages of *Arabidopsis* seed development

The major stages of *Arabidopsis* seed development were specified according to the morphogenesis of the embryo. The names of each organ in the seed are marked and the original figures were downloaded from the website: http://seedgenenetwork.net/arabidopsis.

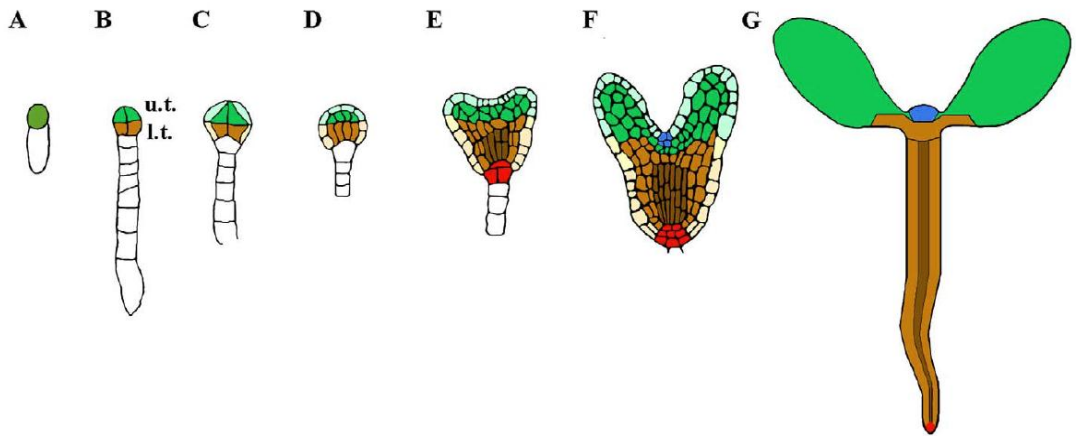

Figure 1.2 *Arabidopsis* embryo patterning

A, asymmetrical division of the zygote forming the apical cell (green domain) and the basal cell (white domain). B, octant stage (8-cell stage). Four cells form the upper tier (u.t., green domain) and four cells form the lower tier (l.t., light brown domain) of the apical domain. The basal domain (white) undergoes horizontal divisions forming the suspensor. C, dermatogen stage (16-cell stage). One tangential division of the cells in the apical domain leads to the generation of inner cells (green and light brown regions) and protoderm cells (epidermis, light blue and ivory regions). D, early globular stage. Further division of inner cells to give the precursors of ground and vascular tissues. E, heart stage. Cotyledons (green region), ground tissue (light brown region), vascular tissue (dark brown region) and the primary root meristem (red region) have formed. F, linear stage (torpedo stage). Cotyledons elongate and the primary shoot meristem is initiated (blue region). G, seedling after the germination. The colour scheme is maintained. Figures were taken from Capron et al., (2009).

1.1.3 Molecular mechanisms of embryo patterning

i) The role of auxin in embryo patterning

During early embryo development, auxin directional transport and auxin signalling play an important role (Weijers et al., 2006; Wisniewska et al., 2006). Auxin flux during embryogenesis is polarized and controlled by PIN-FORMED (PIN) proteins which are auxin efflux carriers and have a polar subcellular localization. PIN proteins play an essential role in forming the major axis of the globular stage embryo (Wisniewska et al., 2006). During the two cell stage of embryogenesis, PIN7 is localized to the apical membrane of the basal cell and drives the auxin flux from the basal domain to the apical domain triggering the specification of the apical pole (Friml et al., 2003). During the early globular stage of embryogenesis, free auxin is produced in the apical domain, transported from the apical domain towards the basal domain, and accumulates in the hypophysis in a PIN1 and PIN4 dependent manner, to trigger the specification of root pole (Friml et al., 2003). PIN1 polarization in cell membranes is dependent on an adenosyl ribosylation factor guanine nucleotide exchange factor GNOM/EMBRYO DEFECTIVE30 (GNOM). *gnom* mutants lose their apical-basal polarity both during embryo development and post-embryogenesis, suggesting a critical role for PIN1 and polarized auxin transport in establishing embryo polarity (Geldner et al., 2003). It has also been shown that PIN1 polarity is controlled by PINOID (PID) protein kinase. Overexpression of PID causes a basal-to-apical shift of PIN1 localization in embryo and seedling roots, and loss of PID function causes an apical-to-basal shift of PIN1 localization in inflorescence apices and consequently a defect in organogenesis. This further supports the role of auxin flux in patterning (Friml et al., 2004). Genetic and biochemical studies have shown

that the phosphorylation status of PIN proteins, which is controlled by PP2A phosphatase and PID kinase (acting antagonistically), mediates the apical-basal patterning (Michniewicz et al., 2007).

Auxin signalling involves SCF-E3-protease regulated transcriptional activation. When there is no auxin present in the cytosol, transcription factors called AUXIN RESPONSE FACTORS (ARFs), are bound to transcriptional repressors of the Aux/IAA family, and are thus rendered inactive (Dharmasiri and Estelle, 2004; Kepinski and Leyser, 2005). However, when auxin is transported and accumulated in the cytosol, auxin receptors in the auxin-signalling F-box (AFB) family of proteins, such as TRANSPORT INHIBITOR RESPONSE1 (TIR1), which form the SKP1-CULLIN-F-BOX (SCF) E3 ubiquitin ligase complex, are activated and target the degradation of the Aux/IAA transcriptional repressors. This degradation releases the ARFs which are then free to activate down-stream gene expression (Dharmasiri and Estelle, 2004) . The *Arabidopsis* genome encodes 23 ARFs (Okushima et al., 2005), many of which are expressed during early embryogenesis (Rademacher et al., 2011). Loss of function alleles of *MONOPTEROS* (*MP*)/*ARF5*, one of the ARF family members, shows severe defects in forming the embryo axis including fused cotyledons and replacement of the hypocotyl and root by an undifferentiated basal domain, suggesting that MP is required for forming basal body plan (Berleth and Jurgens, 1993). *BODENLOS (BDL)* encodes one of the Aux/IAA transcriptional repressors. Gain of function mutants in *BDL* display defects as early as two cell stage. *bdl* mutants display horizontal division of the apical cell instead of vertical divisions. Subsequently the upper most basal cell fails to produce the quiescent centre of the root meristem resulting in lack of the hypocotyl and the root (Hamann et al., 2002).

mp bdl double mutants resembles the two single mutants (Hamann et al., 2002), and consistent with this observation it has also been shown that MP protein and BDL protein interact with each other *in vivo* and that BDL inhibits MP transportation to the nuclei (Weijers et al., 2006). More recent studies have thrown light on roles of ARFs and IAA proteins in other aspects of embryo patterning, which were obscured by extensive functional redundancy (Rademacher et al., 2012). In summary, auxin plays a critical role in apical-basal patterning.

ii) The role of WOX family homeodomain transcription factors in embryo patterning

The expression of *WUSCHEL-RELATED HOMEOBOX (WOX)* genes, which encode homeodomain transcription factors, has also been shown to play an important role in defining apical and basal domain during early embryo developmental (Chandler et al., 2008). During the one cell zygote stage, *WOX2* and *WOX8* mRNAs accumulate in the zygote, but during the apical-basal two cell stage, their expression is separated into two distinct zones, with *WOX2* only expressed in the apical cell and *WOX8* together with *WOX9* specifically expressed in the basal cell. The expression of these genes therefore mirrors the establishment of the two different cellular identities during formation of the apical-basal axis of the embryo (Haecker et al., 2004). When *WOX2* function is lost, mutants display mild phenotypes, such as abnormal cell division at the apex of globular stage embryos and occasionally seedlings with only one cotyledon (Haecker et al., 2004). However, removing *WOX1*, *WOX3* and *WOX5*, all of which show expression patterns overlapping with that of *WOX2*, in a *wox2* background results in strong enhancement of the *wox2* phenotype resulting in shootless embryos. This suggests that *WOX2* has an important but redundant role in controlling apical patterning in embryos (Breuninger et al., 2008).

Although *WOX8* and *WOX9* are expressed in the basal domain and suspensor during early embryo development, they likely play a role in controlling the apical domain differentiation through a non-cell autonomous mechanism (Breuninger et al., 2008). *wox8 wox9* double mutants display abnormal proembryo and suspensor, and the expression of the early proembryo marker gene *ZLL* is abolished, suggesting that *WOX8* and *WOX9* play a role in maintaining apical cell lineage. *WOX5* expression which marks the development of the shoot meristem and the quiescent centre in the root meristem is also abolished, suggesting that *WOX8* and *WOX9* play a role in maintaining the basal cell lineage. However, some embryo pattering genes are expressed in *wox8 wox9* double mutants, including *AtML1* which controls the protoderm specification (see below), suggesting that not all embryo development related genes are affected (Breuninger et al., 2008).

To summarize *WOX* genes are indispensable for early embryonic gene programming and maintaining the normal apical-basal cell linages during early embryo development.

iii) Shoot *vs* root fate in embryo patterning

The specification of shoot and root fates requires an antagonistic interaction between the class III homeodomain-leucine zipper (HD-ZIPIII) transcription factors which are expressed in the upper tier and the PLETHORA (PLT) family of AP2-domain transcription factors which are expressed in the lower tier (Galinha et al., 2007; Smith and Long, 2010). There are five genes encoding HD-ZIP III transcription factors in the *Arabidopsis* genome: *PHABULOSA* (*PHB*), *PHAVOLUTA* (*PHV*), *REVOLUTA* (*REV*), *INCURVATA4* (*ICU4*, also known as *CORONA* and *CNA*), and

ARABIDOPSIS THALIANA HOMEOBOX-8 (*ATHB-8*). Expression of all these genes has been shown to be suppressed in basal regions of the embryo by microRNA *miR165/6* (Floyd and Bowman, 2004; Mallory et al., 2004). When *miR165/6* production is compromised, ectopic expression of HD-ZIPIII transcription factors in the basal zone leads to impaired root pole formation and embryo lethality (Grigg et al., 2009).

PLETHORA1 (PLT1) a member of the AINTEGUMENTA-like (AIL) subclass of the AP2/EREBP family of transcription factors, is expressed throughout the whole lower tier at the globular stage of embryogenesis and later its expression is confined in the vascular precursors in the centre of the proembryo and the quiescent centre (Galinha et al., 2007). In the upper tier, *PLT1* expression is suppressed by the transcriptional corepressor *TOPLESS* (*TLP)* and in *tpl-1*loss of function mutants *PLT1* is ectopically expressed in the shoot apex and produces root-like structures (Smith and Long, 2010). Genetic analysis of *TPL*, *PLT1* and dominant gain of function alleles of the *HD-ZIP III* class genes has shown that the functions of *PLT1* in specifying basal fate, and *HD-ZIP III* genes in specifying apical cell fate are antagonistic (Grigg et al., 2009; Smith and Long, 2010).

In addition to transcription factors, cell-cell signalling components have been shown to be important in specifying cell identities in the developing embryo. For example the MAP kinase *YODA* (*YDA*) and the putative inactive receptor-like kinase *SHORT SUSPENSOR* (*SSP*) have been shown to control apical cell fate and the normal division of the basal cell (Bayer et al., 2009). *SSP* mRNA is delivered to the zygote by the sperm cell containing *SSP* mRNA, *SSP* protein is produced after fertilization and the transient accumulation of SSP protein on the plasma membrane

activates *YDA* and the functionally redundant MAP kinases *MPK3* and *MPK6*, and downstream kinase cascade components including *MKK4*, *MKK5*, *MKK7* and *MKK9* (Lukowitz et al., 2004; Wang et al., 2007). *YDA* loss of function mutants display defects in zygote elongation. The cells from the basal lineage adopt an embryonic fate rather than forming the suspensor, whilst gain-of-function mutants display the opposite phenotype with enlarged suspensor and suppressed embryo development, suggesting that *YDA* plays a critical role in first cell fate decision during embryogenesis (Lukowitz et al., 2004).

iv) Setting up the embryonic shoot meristem

The founding member of the WOX transcription factor family, *WUSCHEL* (*WUS*), is expressed in the inner cells of the upper tier after the dermatogen stage, and from the heart stage *WUS* expression is only detected at the base of the shoot meristem (Mayer et al., 1998). The onset of *WUS* expression indicates the embryonic shoot meristem initiation, and the early expression of *WUS* has been suggested to play a role in maintaining stem cells in an undifferentiated state (Mayer et al., 1998). Ectopic expression of *WUS* in roots is able to direct root cells to leaf, floral organs or embryos (Gallois et al., 2004). Overexpression of *WUS* causes somatic embryogenesis irrespective of the tissue and organ type (Zuo et al., 2002), suggesting that *WUS* controls the formation of ectopic stem cell or even controls somatic embryogenesis, and that *WUS* expression is critical to locally restrict *WUS* function. Thus, regulation of *WUS* expression is important for regulating stem cell formation. This is achieved by a dynamic feedback loop involving *WUS*, *CLAVATA3* (*CLV3*) and *CLAVATA1* (*CLV1*). *WUS* expression activates the expression of peptide-encoding gene *CLV3* in the central zone of the shoot meristem distal to the *WUS*

expressing region during the late heart stage of embryo development. The spatial expression of *WUS* is in turn dependent upon the activity of *CLV3* which is the ligand for the *CLV1* receptor kinase, suggesting a feedback regulation in controlling the stem cell pool in the shoot meristem (Brand et al., 2000; Lenhard and Laux, 2003; Rojo et al., 2002; Schoof et al., 2000). It has also shown that during embryo development the ARGONAUTE (AGO) family member *ZWILLE* (*ZLL*; also known as *PINHEAD* and *AGO10*), which is specifically expressed in the vascular primordium, plays a role in controlling embryonic stem cell development non-cell autonomously (Tucker et al., 2008). AGO proteins are central components of RNA-induced silencing complexes (RISC) and play a role in translational inhibition by binding small RNAs to target mRNAs for degradation or to target genomic DNA for methylation (Franck, 2006). *ZLL/AGO10* functions in a similar manner but in a sequential order with *AGO1* which mediates RNA silencing, and loss of *ZLL* function results in loss of *CLV3* expression despite of the increased level of *WUS* expression, suggesting that the *WUS*-dependent stem cell maintenance in embryos is promoted by *AGO1* and provascular *ZLL*-dependent signalling pathway (Tucker et al., 2008).

A class I knotted-like homeobox (KNOX) gene, *SHOOTMERISTEMLESS* (*STM*), is expressed in the shoot meristem primordium from the globular stage of embryogenesis and is expressed postembryonically throughout the SAM (Jeff et al., 1996). *STM* also has a role in forming and maintaining the meristem, the stem cell specification regulated by *WUS* is not dependent on *STM*, and conversely *STM* suppression of stem cell differentiation does not require *WUS* activity (Lenhard et al., 2002). It has been suggested that although *WUS* and *STM* expression is co-localized

and both have a role in suppressing stem cell differentiation, *STM* likely has a role in promoting the amplification of stem cell daughters, and therefore maintaining the organ primordia which flank the meristem (Hay and Tsiantis, 2010; Lenhard et al., 2002).

The boundary between the centre of the meristem primordium and peripheral regions from which the cotyledon primorida grow out is controlled by *CUP-SHAPED COTYLEDON1* (*CUC1*), *CUC2* and *CUC3* which encode putative transcription factor homologue of the petunia NO APICAL MERISTEM (NAM) protein and which function redundantly (Aida et al., 1999; Hibara et al., 2006; Vroemen et al., 2003). *CUC* gene single mutants do not show visible defects, however *cuc1 cuc2* double mutants show cup-shaped cotyledons, *stm-1 cuc2* double mutants show fused cotyledon petioles, and *cuc1 cuc2 stm-1* triple mutants show an enhanced cup-shaped cotyledon phenotype suggesting a role for *CUC* genes in specifying the boundary between the hypocotyl and cotyledon petioles (Aida et al., 1999). *CUC* genes show a dynamic expression pattern during embryogenesis. *CUC1* and *CUC2* are expressed from the early globular stage of embryo development, then spread along the medial axis, and from the heart stage to torpedo stage of embryo development the expression is stripe like and between the cotyledon primordia (Aida et al., 1999). *CUC2* expression is only detected in the hypodermal cells but not in protoderm cells (Aida et al., 1999). *STM* expression requires *CUC1* and *CUC2*, and *STM* in turn promotes *CUC1* expression and together with *PIN1* and *STM* is necessary for correct spatial expression of *CUC2*, suggesting a regulatory network of transcription factors in the apical domain specifying the central zone and the

peripheral zone where the cotyledons develop during embryogenesis (Aida et al., 1999; Aida et al., 2002; Kwon et al., 2006; Spinelli et al., 2011; Takada et al., 2001).

1.1.4 Protoderm specification

As early as the dermatogen stage (16-cell stage; Figure 1.2 C), the protoderm (epidermis) is specified by the localized expression of HD-ZIP IV class of homeodomain transcription factor *MERISTEM LAYER1* (*ATML1),* and *PROTODERMAL FACTOR2 (PDF2*) in the outer cells of the apical domain (Abe et al., 2003; Lu et al., 1996). *ATML1* expression is first detected in the apical cell after the first asymmetric division of the zygote and its expression continues in all cells of the embryo proper until the 16-cell stage when its expression becomes restricted to the protodermal layer (L1 layer) (Lu et al., 1996). During embryo development, *PDF2* expression overlaps with that of *AtML1* (Abe et al., 2003). *atml1* or *pdf2* single mutants do not show distinguishable defects, whilst *atml1 pdf2* double mutants show severe defects in forming normal epidermis at the later stages of embryogenesis, suggesting that *PDF2* and *AtML1* play redundant roles in protoderm specification in the apical domain of the embryo (Abe et al., 2003).

Two receptor-like kinases *ARABIDOPSIS CRINKLY4* (*ACR4*) and *ABNORMAL LEAF SHAPE2* (*ALE2*) have also been shown to have a role in epidermal formation. *ACR4* is expressed in the protoderm of all aerial organ primordia and of developing embryos (Gifford et al., 2003; Tanaka et al., 2002). *acr4* loss of function mutants display defects in ovule and leaf epidermal differentiation and sepal margin outgrowth, although *acr4* seeds are viable. The *acr4* phenotype is consistent with a role for *ACR4* in maintaining epidermal cell fate (Gifford et al., 2003; Tanaka et al.,

2002). ACR4 protein has a lateral and basal plasma membrane subcellular localization in leaf epidermal cells, suggesting that ACR4 controls epidermal cell fate possibly by receiving and transmitting signals from neighbouring and underlying cells (Watanabe et al., 2004). *ale2* loss of function mutants display epidermal defects both in seedlings and adult tissues and are sterile due to ovule development defects (Tanaka et al., 2007). *ale2* loss of function mutants are epistatic to *acr4* mutants suggesting that *ACR4* and *ALE2* function in the same pathway in controlling epidermal differentiation. In contrast, mutations in the subtilisin serine protease-encoding encoding gene *ABNORMAL LEAF SHAPE1* (*ALE1*), enhance the phenotypes of both *ale2* and *acr4.* In *acr4 ale1* double mutants the expression of *ATML1* and *PDF2* is more severely compromised than in either single mutants suggesting that *ACR4* and *ALE1* function in parallel pathways controlling epidermal differentiation (Tanaka et al., 2007; Tanaka et al., 2002; Watanabe et al., 2004). *ALE1* is an important element in the work carried out in this thesis and will be discussed further in later sections.

The transmembrane protein DEFECTIVE KERNEL1 (AtDEK1) has also been shown to have a role in protoderm differentiation (Johnson et al., 2005). AtDEK1 loss of function mutants display abnormal embryo development showing abnormal cell divisions in suspensor, embryo proper and a disorganized L1 layer. Moreover, in *atdek1* mutants the expression of protoderm markers, such as *ATML1* and *ACR4* is down-regulated (Johnson et al., 2005). However, *AtDEK1* does not show a protoderm specific expression pattern. From the dermatogen (8-cell) stage to torpedo stage of embryo development *AtDEK1* is expressed all over the embryo proper but not in the suspensor. In vegetative organs *AtDEK1* is expressed throughout the shoot

apical meristem, young leaf primordia and axillary meristems. In inflorescence apices *AtDEK1* is expressed in the inflorescence and floral meristems.

AtDEK1 is also expressed in developing ovules, which suggests that the role of *AtDEK1* in maintaining epidermal cell fate may be through signalling pathways (Johnson et al., 2008). *AtDEK1* encodes an integral plasma membrane protein with a C-terminal cytoplasmic calpain cysteine proteinase domain which may catalyse the autolytic cleavage of the calpain domain after reception of either an extracelluar or plasma membrane-located signal, releasing the calpain domain to activate downstream targets controlling protodermal identify (Johnson et al., 2008). Although it is not clear how the *DEK1* pathway relates to all the other epidermis specifying pathways in the embryo, preliminary data from *Arabidopsis*, suggest that it may act in a parallel pathway to *ACR4* (Johnson et al., 2005).

To summarize, after double fertilization embryos undergo apical-basal patterning, protoderm specification, axial patterning, radial pattering, and shoot and root meristem establishment. Together these processes define the whole body plan of the seedling. By applying new techniques, such as cell sorting, laser dissection, microarray based expression profiling and deep sequencing, more genes which play a role in embryogenesis will be identified (De Smet et al., 2010).

1.1.5 Endosperm patterning in *Arabidopsis* and cereals

In angiosperms, endosperm is formed by the fusion of two haploid central-cell nuclei with one of the haploid male sperm-cell nuclei during double fertilization. In *Arabidopsis* the resulting triploid endosperm zygote nucleus undergoes several rounds of semi-synchronous mitosis without cytokinesis and the resulting nuclei

spread as a syncytium from the micropylar zone to the chalazal zone. This process begins while the embryo is still at the zygote stage of development (Boisnard-Lorig et al., 2001). In cereals, such as barley the triploid nucleus is localized in the basal cytoplasm of the central cell. After three rounds of nuclear division the resulting eight endosperm nuclei are localized in a plane in the basal domain of the endosperm. At two DAF (Days After Fertilization) the syncytial nuclei spread along the peripheral cytoplasm (Olsen, 2004). In *Arabidopsis*, from the late globular stage of embryo development, the syncytial endosperm nuclei start to cellularize from the micropylar zone along the peripheral endosperm towards the chalazal zone. By the linear cotyledon stage (torpedo stage) of embryo development, the embryo is surrounded by cellularized endosperm cells (Berger, 2003; Boisnard-Lorig et al., 2001) (Figure 1.1 C to D). In maize, cellularization starts at about three DAF and completes at about six DAF, and the cellularization proceeds from the peripheral region towards the central region of the embryo sac until the central cavity is filled with cells (Olsen, 2004).

In *Arabidopsis*, endosperm patterning is defined by specification of three regions, the micropylar endosperm which is near the embryo at the anterior pole (also known as the Embryo Surrounding Region or ESR), the peripheral endosperm which includes the central and peripheral region of the endosperm, and the chalazal endosperm which is situated towards the posterior pole (Berger, 2003). Genes have been identified which are specifically expressed in the *Arabidopsis* ESR. *AtSUC5* which encodes a sucrose transporter is specifically expressed in the ESR during early stage of embryo development and has a role in seed storage lipid accumulation (Baud et al., 2005). *ALE1*, which encodes a subtilisin-like serine protease, was shown to be

expressed in the ESR and has a role in embryonic epidermal cuticle formation (Tanaka et al., 2001). The central and peripheral endosperm has mainly been characterized in cereals (see below). At the early stage of embryo development, *Arabidopsis* central endosperm plays a similar role as that of the cereals, as a major nutrient reserves of the seeds in the forms of lipids and proteins, however, this reserve is transient and at the late stage of embryo development cotyledons become the nutrient reserve centre (Costa et al., 2004). The cellularization of endosperm was well studied in *Arabidopsis* peripheral endosperm cells. The endosperm cellularization initiates at the micropylar region at the late globular stage of embryo development, extends to the peripheral region, and spreads as a wave during early heart stage to finally reaches the chalazal endosperm at the late heart stage (Sørensen et al., 2002). The chalazal endosperm never cellularizes fully. The cellularization of the peripheral region initiates with the formation of a cell plate between sister nuclei and subsequent rapid cell wall assembling, which is very similar to somatic cytokinesis. This results in a layer of cells at the periphery of the central vacuole (Sørensen et al., 2002).

In *Arabidopsis* the extent of endosperm proliferation and cellularization, is regulated by *Fertilization Independent Seed* (*FIS*) class of genes. The *FIS* genes encode homologues of *Drosophila* Polycomb group (PcG) Repressive Complex 2 (also known as PRC2) members. The *Arabidopsis* PRC2 proteins regulating endosperm development consist of MEDEA (MEA)/FIS1which is closely related to the *Drosophila* SET-domain protein E(z) (Kinoshita et al., 1999), FIS2 which is a zinc finger protein related to *Drosophila* Su(z)12 (Chaudhury et al., 1997), FERTILIZATION INDEPENDENT ENDOSPERM (FIE)/FIS3 which is a WD-40

domain protein and related to *Drosophila* Esc (Ohad et al., 1996) and MULTICOPY SUPPRESSOR of IRA1 (MSI1) which is a homologue of p55 protein (Kohler et al., 2003). Mutation of any of these genes gives a so called *fertilization independent seed (fis)* phenotype, which consists of initiation of endosperm development without fertilization. In addition, if fertilization occurs, seeds carrying a mutated maternal allele of a *FIS* gene show continuous syncytial growth of endosperm towards the chalazal zone and embryo arrest (Guitton et al., 2004). Thus, for example *MEA/mea* heterozygotes display autonomous endosperm development in 50% of embryo sacs without fertilization. Likewise, after self-fertilization *mea* mutants display non-cellularized endosperm and arrested embryo development in 50% of seeds (Grossniklaus et al., 1998). When a *MEA*/*mea* mutant silique is pollinated with wild-type pollen, the silique produces 50% arrested embryos and seeds, whilst when a wild-type silique is pollinated with pollen from a *MEA/mea* heterozygote, it produces wild-type seeds, showing a maternal effect which is due to differential expression of maternal alleles caused by parental genomic imprinting (Grossniklaus et al., 1998). This genomic imprinting is controlled epigenetically by specifically silencing maternal or paternal target alleles through histone modifications and DNA methylation (Bauer and Fischer, 2011; Raissig et al., 2011; Rodrigues et al., 2010; Wollmann and Berger, 2012).

In cereals, for example in maize, the endosperm is considered to consist of four zones: the Basal Endosperm Transfer Layer (BETL), the ESR, the aleurone layer and the starchy endosperm (Becraft, 2001). The BETL is localized at the base of the endosperm adjacent to the maternal vasculature, and the transfer cells within the BETL display an extended cell wall and plasma-membrane area, and cytoplasm

which is rich with mitochondria (Davis et al., 1990). Genes specifically expressed in the BETL have been identified. Transient expression of the genes *BETL1-4* in cells in the BETL has been suggested to have a role in pathogen resistance (Cai et al., 2002; Serna et al., 2001). Maize *Miniature 1* (*Mn1*) which encodes a cell wall invertase has been shown to be exclusively expressed in BETL cells during seed development (Kang et al., 2009). Loss-of -function mutants of *Mn1* display compromised cell wall and plasma-membrane expansion, abnormal endoplasmic reticulum formation and reduced Golgi density compared to the wild-type BETL cells, suggesting that *Mn1* may be involved in BETL cell secretory pathways (Kang et al., 2009). *Myb-Related Protein-1* (*MRP-1*) is another BETL specific gene and plays an important role in controlling transfer cell differentiation (Gómez et al., 2009).

Maize ESR refers to cells that surround the cavity in which the embryo develops and cells that are predominantly localized underneath the developing embryo (Balandín et al., 2005; Opsahl-Ferstad et al., 1997). ESR is also defined by genes specifically expressed in that region, such as *Esr1-3* (Opsahl-Ferstad et al., 1997), *Ae1, Ae3* (Magnard et al., 2000) and *ZmESR-6* (Balandín et al., 2005). Although the function of these ESR genes yet to known, *ZmESR-6* encodes a protein homologue of plant defensins and the recombinant ZmESR-6 protein purified from *E. coli* displayed strong inhibitory activity against bacterial and fungal pathogens, suggesting a role of ESR in plant defence (Balandín et al., 2005). Esr3 shares a conserved motif with *Arabidopsis* CLAVATA3 which is the ligand of the receptor-like kinase CLAVATA1 (Brand et al., 2000; Ogawa et al., 2008), suggesting that

Esr3 could play an important role in endosperm signalling to the embryo (Bonello et al., 2002).

The aleurone layer in cereals is defined as one or more cell layers in the peripheral region of the central starchy endosperm. Marker genes for aleurone cells include *Ltp2*, *Ole-1*, *Ole-2* in barley and *C1* in maize (Olsen, 2004). In *Arabidopsis*, the endosperm is consumed during embryo growth, and by the mature stage only a peripheral aleurone-like layer remains. This cell layer has been shown to be critically important in controlling embryo dormancy (Lee et al., 2010). In contrast, in cereals, the aleurone layer produces hydrolases, glucanases and proteinases in response to GA, and mobilizes starch and storage protein from the starchy endosperm to the germinating embryo (Becraft, 2001). In maize the receptor like kinase Crinkly4 (Cr4) (Tian et al., 2007), the calpain family protease Defective kernel1 (Dek1) which shares 70% amino acid identity with *Arabidopsis* DEK1 (Lid et al., 2002) and *Supernumerary aleurone layers1* (*Sal1*) which encodes a protein likely involved in intra-cellular trafficking, have been shown to have a role in aleurone cell fate specification (Shen et al., 2003). Maize *DEK1* and *Cr4* are co-localized in the outer cell layer of the endosperm. Neither *dek1* mutants nor *cr4* mutants specify aleurone cell fate, suggesting a role for both proteins in initiating and maintaining aleurone identity (Becraft et al., 2001; Becraft et al., 2002).

Starchy endosperm in cereals mainly functions in the accumulation of starch and proclamin storage proteins. Thus starchy endosperm serves as a major source of carbohydrate and proteins for both human and animal nutrition. Maize proclamin storage protein aggregation in starchy endosperm cells involves the endoplasmic reticulum (ER) pathways and likely shares a common trafficking mechanism with

wheat and barley (Reyes et al., 2011). Because of the economic importance of the starchy endosperm, genetic manipulations of starchy endosperm cells have been studied. Using starchy endosperm specific gene promoter to drive *CELLULOSE SYNTHASE-LIKE F6* (*CSLF6*) gene expression, which encodes a putative β-glucan synthase, in RNAi constructs has decreased the level of β-glucan in wheat wholemeal flowers, which has been suggested to be useful for enhancing the health benefits of wheat products (Nemeth et al., 2010). Starchy endosperm cells transformed by *Agrobacterium tumefaciens* are able to express epitope-tagged storage proteins that can be used for biochemical and immuno assays, making cell biological and biochemical studies on endosperm cells possible (Reyes et al., 2010). Mutants with defects in producing starchy endosperm during seed development have also been identified, for example, maize *discolored1* (*dsc1*) (Scanlon and Myers, 1998) and *empty pericarp2* (*emp2*) (Fu et al., 2002).

The endosperm is a unique structure, found only in Angiosperms. Interestingly, however, it shares developmental and functional similarities with the nutritive tissue formed by proliferation of the female gametophyte in gymnosperms. Based on this observation, the leading hypothesis addressing the origin of the endosperm is that it evolved from the nutritive gametophyte of a gymnosperm-like ancestor, which became sexualized by linking its development to the fertilization of the central cell (Baroux et al., 2002). A second, and less widely accepted hypothesis is that the central cell derives from a second egg cell in ancient seeds or seed like structures. Double fertilization gave rise to two embryos, and during the course of evolution one of the embryos became sterile and evolved the function of nurturing the other embryo in modern flowering plants (Friedman, 1995). In angiosperms, regardless of

its origin, the endosperm tissue not only plays a role in nourishing the embryo during seed development, but also it integrates seed growth by mediating inter-compartment signalling, and it is the site of action of parental control of female gametophyte formation and sexual seed development mediated the Polycomb group (PcG) genes of the plant Fertilization Independent Seed (FIS)-class (Berger et al., 2006; Springer, 2009).

1.2 Epidermis and Epidermal Cuticle

1.2.1 The structure of epidermis

Epidermis is the outmost cell layer of almost all multicellular land plants, and consists of many specialized cell types or structures. The *Arabidopsis* leaf epidermis consists of trichomes, stomata and pavement cells. Trichomes are unicellular and are specified during leaf development within the epidermal layer. In mature leaves they protrude from the epidermal surface with varying shapes, the most common of which is one central stalk with three or four branches (Hülskamp et al., 1994). Although trichomes have very diverse functions, they are mainly involved in light reflectance to reduce leaf heat, absorbing water from moist air, and defence against biotic attack (Martin and Glover, 2007). Stomata are specialized epidermal structures composed of two guard cells which surround a central, regulatable pore. The differentiation of stomata is initiated by asymmetric cell divisions of meristemoid mother cells (MMC) which originate from the protodermal cells during primordium formation. These divisions result in one small triangular meristemoid and a large neighbouring cell. The meristmoid undergoes further rounds of asymmetric cell division before producing a guard mother cell (GMC) which eventually divides symmetrically to give two guard cells. Neighbouring cells can also undergo asymmetric cell division producing satellite stomata (Nadeau and Sack, 2002). The main function of stomata is to regulate water loss and assist gas exchange (O_2 and CO_2) (Martin and Glover, 2007).

Pavement cells are the most frequently occurring cell type in the epidermis. The pavement cells from different organs have different shapes reflecting the functions of

the organ. The dicot leaf pavement cells are usually shaped like the interlocked pieces of a jigsaw-puzzle (Glover, 2000). The morphogenesis of the jigsaw shaped (wavy) pavement cells is initiated by the positional arrangement of cortical microtubules in a young pavement cell (Panteris and Galatis, 2005). During the pavement morphogenesis, cortical microtubules form bundles and radial arrays, cell walls are formed following the pattern of cortical microtubules resulting in the wavy anticlinal cell wall reinforcement and the interlocked jigsaw-puzzle shape (Panteris and Galatis, 2005). The basic function of pavement cells is to maintain the integrity of epidermis during the development of the organ, whilst other functions of pavement cells are also suggested, such as affecting stomata and trichome arrangement (Martin and Glover, 2007).

1.2.2 The structure and biosynthesis of epidermal cuticle

Aerial plant epidermal surfaces are covered by a continuous hydrophobic layer called the cuticle which seals the outer cell walls of epidermal pavement cells, stomatal guard cells and trichomes. The ultrastructure and composition of cuticle vary, and depend on developmental stage, cell and organ type, and plant species. In addition, cuticular composition can be modified by plants in response to environmental conditions (Riederer and Schreiber, 2001; Suh et al., 2005). Biochemically plant cuticle consists of three types of cuticular lipids, cutin, cutan and wax (Pollard et al., 2008). Cutin is composed of unsubstituted fatty acids (1% to 25%), ω-hydroxy fatty acids (1% to 32%), α,ω-dicarboxylic acids (usually less than 5%, although in *Arabidopsis* these represent more than 50% of cutin monomers), epoxy-fatty acids (0 to 43%) and polyhydroxy-fatty acids (16% to 92%) (Molina et al., 2006). In addition to fatty acids, fatty alcohols, glycerol and phenolics contribute to cutin, but at much

lower abundance (Molina et al., 2006). Although the biochemical compositions of cutan is not clear, compared to cutin which can be depolymerized by cleavage of ester bonds, cutan is more rigid and cannot be depolymerized (Molina et al., 2006).

Genes that encode cutin biosynthetic enzymes have been identified. A cytochrome P450-dependent fatty acid oxidase (encoded by *CYP86A2* or *ABERRANT INDUCTION OF TYPE THREE 1* (*ATT1*)) (Duan and Schuler, 2005), an acyl-CoA synthetase (encoded by *LATERAL ROOT DEVELOPMENT 2* (*LACS2*)) (Schnurr et al., 2004) and two acyltransferases (encoded by *GLYCEROL-3-PHOSPHATE ACYLTRANSFERASE 4* and *8* (*GPAT4* and *8*)) (Chen et al., 2011; Li et al., 2007) have been shown to play critical roles in ω-hydroxy fatty acids biosynthesis, and in *att1* single mutants, *lacs2* single mutants and *gpat4 gpat8* double mutants cutin monomer loads are significantly compromised compared to the wild-type. There is evidence suggesting that cutin biosynthesis is co-ordinately regulated at the level of transcription. Constitutive over-expression of an Ethylene Response Factor (ERF)-type transcription factor *WIN*, caused a glossy leaf phenotype in *Arabidopsis* and up-regulated the expression of *GDSL-motif lipase* (*At2g04570*), *LACS2*, *GPAT4*, *CYP86A4* and *CYP86A7* which are involved in lipid metabolism and cutin biosynthesis (Broun et al., 2004).

Cuticular wax mainly consists of C_{20} to C_{60} aliphatic very long chain fatty acid (VLCFA) derivatives, and a certain amount of secondary metabolites including triterpenoids, flavonoids and phenylpropanoids (Samuels et al., 2008). Wax is synthesized by extending the C_{16} and C_{18} fatty acids to VLCFA chains by reaction with C_2 acetyl-coenzyme A (acetyl-CoA). When acids reach a length of C_{26}, the wax biosynthesis pathway splits into the primary alcohol pathway, which produces wax

esters, and the alkane pathway which produces ketones (Millar et al., 1999). The extension of VLCFA chain requires enzymes called fatty acid elongases, and at different stages of the VLCFA elongation, substrate specific elongases are recruited. For instance, β-keto acyl-CoA synthases (KCS), which are encoded by *ECERIFERUM 6* (*CER6*)/*CUTICULAR 1* (*CUT1*) and enoyl-CoA reductase (ECR), which is encoded by *CER10*, catalyse C_{24}/C_{26} formation. Loss of function mutants of these two enzymes have reduced wax load in stems (Millar et al., 1999; Zheng et al., 2005). Fatty acyl-CoA reductase (FAR), which is encoded by *CER4*, catalyses C_{26}/C_{28} formation in the primary alcohol pathway, and loss of function mutants have reduced primary alcohol and wax ester loads (Doan et al., 2009; Kamigaki et al., 2009). A mid-chain alkane hydroxylase, which is encoded by *CYP96A15*/ *MID-CHAIN ALKANE HYDROXYLASE 1* (*MAH1*) catalyzes the formation of secondary alcohols and ketones in the alkane pathways (Greer et al., 2007). Recent evidence suggests that a gene specifically expressed in aerial epidermis *ECERIFERUM 1* (*CER1*) is coexpressed with *CER3* and *MAH1* and is involved in alkane pathways during cuticular wax biogenesis (Bourdenx et al., 2011). *cer1* T-DNA insertion mutants display significant reductions in the amount of n-alkanes and total cuticular wax loads in rosette leaves, and *CER1* over-expression lines display significant increases in the amount of n-alkanes and total cuticular wax load in rosette leaves, suggesting a role of *CER1* in promoting wax VLC alkane biosynthesis (Bourdenx et al., 2011).

One of the interesting observations regarding cuticle formation is that cutin and waxes are synthesized in the cytoplasm, but their final destination is in the outer layers of the epidermal cell wall, suggesting that a transportation mechanism for high

molecular weight lipidic molecules is involved in epidermal cuticle formation (Pollard et al., 2008). The chemical reactions for cutin/wax biosynthesis are localized on the endoplasmic reticulum (ER) membranes and the products are transported by unknown cytoplasmic components to the plasma membrane possibly *via* the Golgi associated secretion pathways (Pollard et al., 2008). On the plasma membrane ATP-binding cassette (ABC) transporters have been shown to be associated with cutin/wax transportation, and loss of function mutants of an ABC transporter gene *WHITE-BROWN COMPLEX 11* (*WBC11* or *ABCG11*) displays reduced cutin and wax load (Pighin et al., 2004). On the extracellular side of plasma-membrane glysosylphosphatidylinositol (GPI)-anchored lipid transfer proteins (LTPGs), with the GPI-anchor attached to the plasma-membrane and the lipid binding domain attached to the cell wall, are involved in transporting cuticular monomers to the cuticle layers (DeBono et al., 2009). The *Arabidopsis BODYGUARD* (*BDG*) gene encodes a lipase domain containing protein which might be involved in cutin cross-linking or lipid signalling in the epidermal cell wall. *BDG* knock-out mutants show typical features of epidermal cuticle defects such as organ fusions, Toluidine Blue staining, and gaps between epidermal pavement cells (Kurdyukov et al., 2006). GDSL-lipase family proteins which have a GDSL domain at the N-terminal of protein sequence have also been suggested to be involved in cutin/wax metabolism, especially in the cutin/wax secretion pathways (Volokita et al., 2011).

Defects in cuticle biogenesis can lead to a series of developmental abnormalities, including abnormal seed development or seed abortion, destruction in pollen surface structure and pollen sterility, and organ deformation and fusions. *Arabidopsis RESURRECTION 1* (*RST1*) encodes a novel protein, *rst1* loss of function mutants

remove most wax precursors away from alkane synthesis and into the primary alcohol producing branch of the wax biosynthesis pathway resulting in altered wax composition, and *rst1* loss of function mutants produce approximately 70% shrunken and nonviable seeds compared to wild-type plants, suggesting a link between wax biosynthesis and embryo development (Chen et al., 2005). *Arabidopsis ACC1* and *ACC2* encode two acetyl-CoA carboxylases (ACCases) which catalyse the carboxylation of acetyl-CoA and formation of precursors for fatty acid elongation in plastid and cytosol (Baud et al., 2003). Both *acc1* and *acc2* mutants produce lethal embryos showing no cotyledons, shortened hypocotyls and roots, and a complete lack of very long chain fatty acids (VLCFA) in seeds, which again shows a relationship between fatty acid metabolism and embryo morphogenesis (Baud et al., 2003).

Transmission electron micrographs showed that during *Arabidopsis* seed development, before the fertilization an electron-dense layer with lipid nature which was considered to be the cuticle layer was observed on the surface of inner integument layer 1 (ii1) which is in direct contact with the embryo sac but not on the surface of other integument layers, and this cuticle layer was observed until the mature stage of embryo development (Beeckman et al., 2000). During embryogenesis, protoderm (epidermis) specification starts at the dermatogen stage and cuticle is a trait of epidermis, suggesting that the cuticle deposition of the embryo could start at the dermatogen stage. Tanaka et al. (2001) reported that at the globular stage of embryo development an electron-dense layer was observed in the outmost region of the epidermal cell walls of the embryo which separated the embryo from the syncytial endosperm, at the late globular stage the electron-dense layer

became thicker, and by the early heart stage the endosperm became detached from the embryo and the thick cuticle layer had covered the whole embryo. In *ale1* mutants, at the globular stage of embryo development the boundary between the endosperm and the embryo was not clear, at the heart stage the mutant embryo displayed discontinuous cuticle and cellularized endosperm adhered to the embryo, and at the torpedo stage beside the boundary blur between the endosperm and the embryo some regions between two cotyledons were fused (Tanaka et al., 2001). These results suggest that cuticle plays a critical role in defining boundaries between organs and preventing organ fusions. Another embryo cuticle defect which resulted in organ fusions was studied in *gassho1* and *2* (*gso1 and 2*) mutants (Tsuwamoto et al., 2008). *GSO1* and *GSO2* encode leucine-rich repeat containing receptor-like kinases which are specifically expressed in embryos, germinated cotyledons and pollen (Tsuwamoto et al., 2008). *gso1 gso2* double mutants display abnormal embryo development showing fused cotyledons, and adherence of cotyledons to the peripheral endosperm and inner integument which results in inverted bending of cotyledons (bend to micropylar zone instead of chalazal zone), ectopic organ fusions, and severe epidermal cuticle defects after germination (Tsuwamoto et al., 2008). These results indicate that embryonic epidermal cuticle formation may involve receptor kinase related signalling to the prodermal cells during protoderm specification.

1.2.3 Biological function of the cuticle

Biosynthesis pathways of cuticular polyesters are not only essential for cuticle formation but also control other cellular process such as organ separation. *FIDDLEHEAD* (*FDH)*/*3-ketoacyl-CoA synthase 10* (*KCS10*) shows similarity to a

large class of genes encoding beta-ketoacyl-CoA synthases and chalcone synthases and has a role in the biosynthesis of long-chain lipids in the cuticle (Pruitt et al., 2000; Yephremov et al., 1999). *fdh* mutants display abnormal compositions of cuticular wax, Toluidine Blue permeability of epidermis and fusion of rosette leaves (Voisin et al., 2009). Another gene *LACERATA* (*LCR*) which encodes a cytochrome P450 monooxygenase, CYP86A8, has a role in catalysing ω-hydroxylation of fatty acids ranging from C12 to C18:1 in the biosynthesis of cutin in the epidermis (Wellesen et al., 2001). *lcr* loss-of-function mutants display similar abnormal cuticle composition and organ fusions to those seen in *fhd* mutants and *bdg* mutants, suggesting that cuticle biosynthesis pathways controlling epidermal cell differentiation and preventing organ fusions may share some elements (Voisin et al., 2009).

Very long chain fatty acids not only contribute to epidermal cuticle composition, but also are very important components of the extracellular pollen coat (Wolters-Arts et al., 1998). CER6/CUT1 functions as a fatty acid-condensing enzyme and catalyses very long fatty acid elongation (>28 carbon long) in epidermal cuticle formation and pollen coat lipids synthesis (Millar et al., 1999). *cer6* mutants display defects in stem wax formation and loss of pollen coat lipids which results in disrupted pollen interaction with the stigma, inhibiting pollen hydration and causing pollen sterility, and it has been shown that CER6 regulates long-chain lipid content in pollen coat and stem wax formation likely through different pathways (Fiebig et al., 2000). Recent evidence has shown that two long-chain acyl-CoA synthases (LACS1 and 4), which provide CoA-activated very long chain fatty acids to the wax biosynthesis pathways, have also a role in controlling pollen coat lipid contents and consequently controlling pollen germination and preventing male sterility (Jessen et al., 2011).

Cuticle covers almost the entire plant aerial surface, and being at the interface with the environment, has a major function in protection, especially in preventing the uncontrolled loss of water (Buschhaus and Jetter, 2011). Therefore cuticle integrity is key in ensuring that water loss is controlled and mediated exclusively via stomatal pores (Bird and Gray, 2003). The permeability of cuticle also has big impact on agriculture, since in some situations nutrients and many synthetic compounds (such as pesticides, herbicides and other xenobiotics) are applied onto leaf surfaces. The penetrance of ions depends on the molecular size of ions, temperature, wax constitution and humidity, whilst the permeability of non-ionic molecules (pesticides, herbicides and xenobiotics) which are usually lipophilic, mainly depends on their molecular weight and their mobilities across lipophilic wax and cutin domains of the cuticle (Schreiber, 2005). Cuticle also plays a key role in plant-pathogen interactions. *Arabidopsis att1* mutants display less condensed cuticle, an enhanced expression of bacterial type III virulence genes *avrPto* and *hrpL* in the intercellular spaces of leaves or at the leaf surface when *att1* mutants are inoculated with *Pseudomonas syringae*, and an increased susceptibility towards virulent bacterial infections, suggesting that *ATT1* not only encodes an important fatty acid synthase in cuticle biosynthesis but that is able to repress bacterial virulence gene expression (Xiao et al., 2004). Interestingly, although cuticle defects appear to make plants more susceptible to virulent bacterial pathogens, loss of cuticle synthase function, for example in *bdg* and *lacs2* mutants leads to increased resistance to the necrotrophic fungal pathogen *Botrytis cinerea* and enhanced susceptibility to avirulent *Pseudomonas syringae* (Tang et al., 2007). Over-expressing the VLC alkane synthesis gene *CER1* increases susceptibility to the virulent pathogen *Pst* and the necrotrophic fungal pathogen

Sclerotinia (Bourdenx et al., 2011). It has therefore been suggested that compromising cuticle integrity could induce the production of anti-fungal effectors repressing the growth of necrotrophic fungi and could promote the growth of biotrophic fungi and virulent bacterial pathogens (Xiao et al., 2004). A recent study has shown that reactive oxygen species may be amongst the anti-fungal components released in plants with defective cuticles (L'Haridon et al., 2011).

Besides playing a role in plant-environment interactions, the cuticle also plays a role in stomatal development. Two wax biosynthesis mutants, *cer1* and *cer6* have higher stomatal indices than wild-type plants, which means that *cer1* and *cer2* have a higher ratio of guard cells to pavement epidermal cells than wild-type plants. One explanation that has been proposed to explain this phenomenon is based on the observation that guard cells produce different waxes to the surrounding pavement cells. It could be that wax composition affects the developmental interactions between stomatal precursors and surrounding pavement cells, which are necessary for determining when and where stomatal pores develop. For example changes in the cuticle could alter the rate of diffusion of a signalling molecule (Bessire et al., 2007).

To summarize, epidermal cuticle plays an important role in protecting plants from biotic/abiotic stress, and also cuticle mediates the interaction between plants and the environment and modulates a series of developmental processes. However, through what mechanism cuticle biogenesis accounts for the developmental processes and plants' interaction with the environment is waiting to be elucidated in the future.

1.3 *ZHOUPI* (*ZOU*)

Previous members of our lab have identified a novel transcription factor ZHOUPI (ZOU) which is required for normal embryo development, embryonic cuticle formation, desiccation tolerance and epidermal integrity in the cotyledons of young *Arabidopsis* seedlings (Yang *et al.*, 2008). The seeds of homozygous *zhoupi* (*zou*) mutants are mis-shapen and appear shrivelled. Visible differences between *zou* and wild-type seeds first appear from the mid-late heart stage of embryogenesis. Before the early heart stage, *zou* embryos appear normal and the surrounding endosperm cellularizes around the early heart stage, as in wild-type. Subsequently, *zou* embryos stop elongating at later stages and appeared shorter and wider than wild-type at the torpedo stage. In wild-type the cotyledons continue to elongate and bend over, resulting in a large embryo filling the seed (Figure 1.3). In wild-type seeds, the endosperm in the ESR separates from the embryo from the heart stage onwards and at the torpedo stage, little or no endosperm remains between the cotyledons. In contrast, *zou* embryos adhere to endosperm throughout embryogenesis and considerable amounts of endosperm persist between the cotyledons. Another typical defect in *zou* mutants is the presence of a discontinuous cuticle layer on the outside of embryo epidermal cells and epidermal defects in germinated cotyledons. When examined by transmission electron microscopy (TEM), compared with wild-type plants, *zou* mutant embryos at torpedo stage were not covered by a continuous cuticle layer. After germination, cotyledons of *zou* seedling, but not true leaves, are strongly stained by Toluidine Blue (Figure 1.4), which is used to detect epidermal cuticle defects in plants (Tanaka et al., 2004).

The *ZOU* gene was cloned, and found to encode a novel basic helix-loop-helix (bHLH) transcription factor which contains all the sequences normally associated with DNA binding. *ZOU* was only expressed in developing seeds, with expression initiating immediately after fertilization in the central cell nucleus and then becoming restricted to the ESR by the globular stage. No *ZOU* RNA or ZOU protein was ever detected in developing embryos.

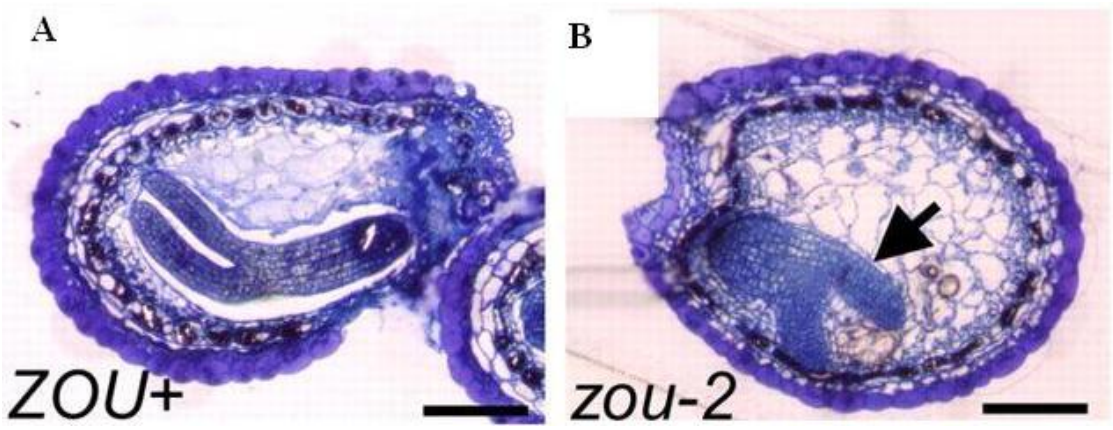

Figure 1.3 Wild-type and *zou* seed morphology

A, wild-type seed; B, *zou* mutant seed. Seed were embedded in resin, sectioned, stained in toluidine blue and examined using light microscopy. Arrow indicates the *zou* embryo (adapted from Yang et al., 2008).

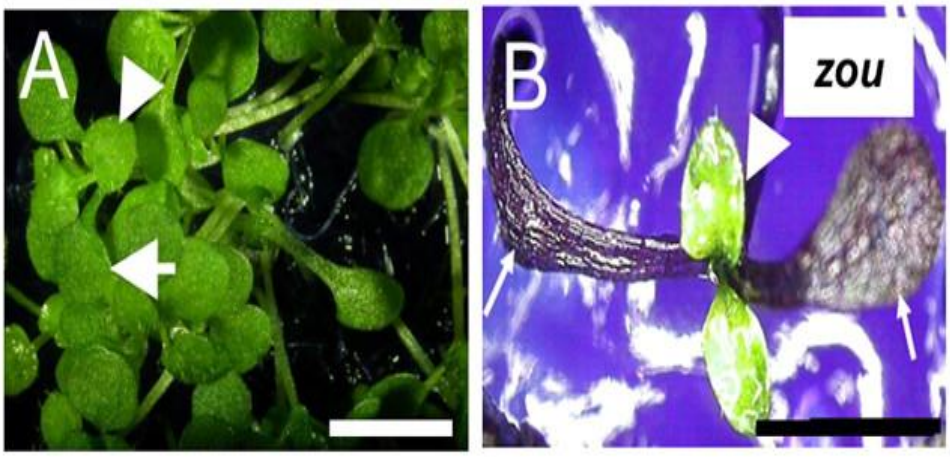

Figure 1.4 Toluidine Blue staining of wild-type plants and *zou* mutant plants

A, wild-type plants; B, *zou* mutant plants. Arrow indicates cotyledons and arrow head indicates young leaves (adapted from Yang et al., 2008).

1.4 Transcriptome profiling of *ZOU* regulated genes

To identify the *ZOU* associated targets and pathways, RNA from siliques containing seeds at the heart stage of embryogenesis from *zou* mutants and wild-type plants were isolated and used to make cDNAs. A next-generation (Illumina Solexa platform) sequencing of the resulting cDNA populations was performed by the GenePool facility at Edinburgh University (J Goodrich and G Ingram, unpublished results). The expression of approximately 13,000 genes was detected through the sequencing. Genes with greater than five folds change in expression levels are of great interest, and among these genes 233 genes show down-regulation in *zou* mutants and 64 genes show up-regulation in *zou* mutants compared to the wild-type plants. These *ZOU* responsive genes are mainly involved in plant immune response and cell wall/cuticle related pathways. A summary of *ZOU* responsive genes and pathways identified by SOLEXA cDNA sequencing is shown in Table 1.1 and Figure 1.5.

Putative Identity	Reading in the WT	Reading in *zou*	Ratio of WT/*zou*	Up/Down-regulation in *zou*
Nucleotide binding-leucine rich repeat (NB-LRR) family protein				
Disease resistance TIR-NBS-LRR class				
AT5G41750	11	1	0.1	Down
AT1G72900	28	6	0.2	Down
AT5G11250	21	5	0.2	Down
AT3G04210	10	1	0.1	Down
LRR family				
AT5G45770	0	24	0	Up
AT1G24650	13	2	0.2	Down
Calcium dependent protein kinase/Protein kinases				
CPK24 (AT2G31500)	3	19	6.3	Up
SnRK1.3 (AT5G39440)	27	3	0.1	Down
AtMKK9 (AT1G73500)	55	14	0.3	Down
AtMPK5 (AT4G11330)	39	10	0.3	Down
MAPKKK9 (AT4G08480)	21	6	0.3	Down
MAPKKK14 (AT2G30040)	37	11	0.3	Down

MKS1 (AT3G18690)	17	0	0	Down
AT1G76360	26	4	0.2	Down
AT1G67470	27	5	0.2	Down
JA response				
MYC2 (AT1G32640)	264	52	0.2	Down
JAZ7 (AT2G34600)	20	1	0.1	Down
JAZ6 (AT1G72450)	284	53	0.2	Down
JAZ1 (AT1G19180)	22	5	0.2	Down
JAZ5 (AT1G17380)	48	12	0.3	Down
Ethylene response				
ACO4 (AT1G05010)	14	3	0.2	Down
AtERF13 (AT2G44840)	11	1	0.1	Down
AtERF4 (AT3G15210)	314	74	0.2	Down
AtERF11 (AT1G28370)	94	21	0.2	Down
AtERF1 (AT4G17500)	20	5	0.3	Down
Disease response TFs and genes				
AtWRKY54 (AT2G40750)	17	3	0.2	Down
AtWRKY40 (AT1G80840)	59	12	0.2	Down
AtWRKY22 (AT4G01250)	17	2	0.1	Down
PR5 (AT1G75040)	32	9	0.3	Down
Cell death regulators				
LOL2 (AT4G21610)	2	12	6.0	Up
DOX1 (AT3G01420)	8	42	5.3	Up
Cell wall biosynthesis/remodelling				
CSLA11 (AT5G16190)	10	2	0.2	Down
ATXTH19 (AT4G30290)	11	1	0.1	Down
RGP3 (AT3G08900)	43	0	0	Down
RGP4 (AT5G50750)	29	147	5.1	Up
FLA5 (AT4G31370)	2	41	21	Up
Galactosyltransferase family (AT3G06440)	2	10	5.0	Up
Cuticle biogenesis				
GDSL-motif lipase (AT1G71250)	57	0	0	Down
GDSL-motif lipase (AT5G03820)	55	1	0.0	Down
Lipid transfer protein (AT2G44300)	18	5	0.3	Down

Table 1.1. Selected examples of genes that are mis-expressed in *zou* mutants compared to that of the wild-type identified by SOLEXA cDNA sequencing.

1.4.1 Genes involved in plant immunity showed significant changes in expressions in *zou* mutants

Plants respond to a range of biotic signals in order to protect themselves from infection. These signals include universal responses to microbe-associated and pathogen-associated molecular patterns (MAMPs or PAMPs), such as the 22 amino acids (flg22) in the N-terminus of bacterial flagellin and specific recognition events between pathogen specific effector proteins (also known as avirulence (AVR) proteins) and plant resistance (R) proteins. Responses to a range of different stimuli share common machinery including receptor proteins, calcium signalling, kinase cascades, the production of reactive oxygen species, plant hormone responses and the expression of WRKY transcription factors involved in transcriptional regulation (Tsuda and Katagiri, 2010).

In the *ZOU* regulated gene profile, a group of nucleotide binding-leucine rich repeat (NB-LRR) family proteins were down-regulated in *zou* mutants. This type of nucleotide binding-leucine rich repeat (NB-LRR) family protein mediates the recognition of effectors by R proteins in R-protein mediated responses to specific pathogens. These interactions are commonly associated with rapid programmed cell death in the infected regions, which is thought to halt the spread of infection (Elmore et al.,). *CPK24*, which encodes a calcium or calmodulin dependent protein kinase and responds to biotic stresses was up-regulated in *zou* mutants. A group of protein kinases including *SnRK1.3* and *MKS1* were down-regulated in *zou* mutants. The sucrose non-fermenting-1 (SNF1)-related protein kinases (SnRKs) are involved in sucrose metabolism, abscisic acid-induced signalling pathways, salinity tolerance, nutritional stress and disease responses (Coello et al., 2011; Zheng et al., 2010).

MKS1 is involved in signalling via mitogen-activated protein kinase (MAPK) cascades. MKS1 interacts with MAP kinase 4 (MPK4) and the WRKY33 transcription factor, which acts downstream of innate immune receptors, indicating that MKS1 has a role in defence responses (Petersen et al., 2010). The PP2C-Type Phosphatase AP2C1 negatively regulates MPK4 and MPK6 and thus regulates stress hormone levels and defence responses (Schweighofer et al., 2007). *AP2C1* was down-regulated in *zou* mutants. These results suggest that *ZOU* function may regulate a set of signalling pathways which have previously been shown to play important role in disease recognition.

Plant hormones jasmonic acid (JA), ethylene (ET) and salicylic acid (SA) are major endogenous signalling molecules that regulate defence responses. In *Arabidopsis*, JA and ET signalling pathways are critical to necrotrophic pathogen resistance, such as *Botrytis cinerea* and *Erwinia carotovora*, whilst SA signalling is necessary for biotrophic pathogen resistance, such as *Erysiphe orontii* and *Pseudomonas syringae* (Thomma et al., 2001). Cross-talk among the plant hormones, JA, ET and SA plays a very important role in plant immune responses. JA responses are at the core of plant hormone cross-talk and mediate a broad range of pathogen defense responses including, wound responses, production of secondary metabolites as well as developmental processes including senescence (Kazan and Manners, 2008). Genes implicated in JA biosynthesis (such as lipoxygenase genes) and JA signalling pathways (including *JASMONATE INSENSITIVE 1* (*JIN1*/*MYC2*) and *JAZ1, 5, 6, 7*) were down-regulated in *zou* mutants. JAZ proteins are repressors of JA signalling, binding to MYC2 and preventing its action. *MYC2* encodes a bHLH type transcription factor which possibly binds to the conserved G-box elements in the

promoter region of JA-responsive genes and therefore modulates the transcriptional cascades of JA-dependent functions (Lorenzo et al., 2004). MYC2 is also involved in regulating the expression of ABA response genes (Staswick, 2008), and this might be the cause of the up-regulation of the ABA-response related gene (*AT5G08350*) in *zou* mutants.

Genes encoding components of ethylene signalling pathways, including *1-AMINOCYCLOPROPANE-1-CARBOXYLATE OXIDASE*/*ETHYLENE FORMING ENZYME* (*ACO4*/*EFE*) and *ethylene-responsive element binding factors 1, 4, 11 and 13* (*ERF 1, 4, 11*, and *13*) were also down-regulated in *zou* mutants. Ethylene regulates many important aspects of plant life cycle, which includes flowering, seed development, fruit ripening, senescence, abscission, and also responses to biotic (such as pathogen attack) and abiotic (such as wounding, cold and hypoxia) stresses (Lin et al., 2009). 1-aminocyclopropane-1-carboxylate oxidase (ACO) catalyses the final step in ethylene biosynthesis, which converts 1-aminocyclopropane-1-carboxylic acid (ACC) to ethylene, CO_2, and HCN. *Arabidopsis* genome encodes 5 *ACO* genes and it has been suggested that *ACO* genes are regulated at the transcriptional level in response to different developmental and environmental signals, such as floral organ development, ripening, senescence, wounding, pathogens, ozone and UV-B in all plant species that have been studied (Lin et al., 2009). Ethylene-responsive element binding factors (ERFs) are a family of transcription factors that specifically bind to GCC-box and plays an important role in downstream ethylene signalling which is involved in perceiving ethylene by the receptors on the membrane, activating kinase pathways, transmitting the signal to the nucleus, and activating the expression of ERFs which bind to GCC-box and activate

the expression of ethylene response genes (Solano et al., 1998). As stress signal responsive factors, *Arabidopsis* ERFs are able to interact with GCC-box containing stress response genes *via* an ethylene-dependent pathway or an ethylene-independent pathway. When there are stress signals (cold, salt, drought, wounding and pathogen attacks) *AtERF3/4/11/12* transcription is activated without ethylene signalling, producing AtERF3/4/11/12 proteins which act as the repressors for the expression of GCC-box containing stress response genes. In contrast, but also independent of ethylene signalling, AtERF1/2/5 act as the activators of the same genes (Fujimoto et al., 2000; Yang et al., 2005). *AtERF1* expression can also be activated by ethylene signalling and the resulting protein acts as activator for GCC-box containing stress response genes (Solano et al., 1998). It has been shown that *AtERF4* expression can be induced by JA and ABA, and acts as a negative regulator in ABA responses (Yang et al., 2005). Together with AtMYC2 which is a positive regulator of ABA response (Kazan and Manners, 2008) and down-regulated in *zou* mutants, AtERFs may play an critical role in hormone cross talk. Taken together, *ZOU* may have the potential to coordinate JA, ET and ABA responses during seed development.

Many AtWRKY transcription factors act down-stream of the MAPK cascades regulating the expression of the disease response genes such as *PR1, PR5* and *CYP81F2* (Ronald and Beutler, 2010). In our SOLEXA sequencing dataset, we identified that *WRKY 22*, *40* and *54* were down-regulated in *zou* mutants, which suggests again a compromised expression of down-stream disease response-associated genes.

1.4.2 Genes involved plant cell wall and cuticle biogenesis showed significant change in expression in *zou* mutants

The plant cell wall is highly heterogeneous and dynamic matrix. It not only provides stability and mechanical support for the cells, but also likely provides source of metabolizable energy for some plants such that wall polysaccharides in the seeds serve as seed storage macromolecules (Burton et al., 2010). Cell wall polysaccharides are composed of cellulose, hemicelluloses and pectins. Glycosyltransferases are involved in hemicellulose biosynthesis. *Cellulose synthase-like A11* (*CSLA11*) which belongs to the Cellulose synthase-like superfamily of glycosyltransferases was down-regulated in *zou* mutants. The *cellulose-synthase-like* (*CSL*) family of genes catalyze the biosynthesis of the mannan, galactomannan and glucomannan back-bones of xyloglucan which is the major component of hemicellulose (York and O'Neill, 2008). The other groups of glycosltransferases are believed to modify the side chains which are appended to the back-bone, for example the galactosyltransferases add (1,6)-α-galactopyranosyl residues to the back-bone of (1,4)-β-mannans or (1,4)-β-glucomannans (Burton et al., 2010). In *zou* mutants, a galactosyltransferase family protein (*AT3G06440*) was found to be up-regulated. A group of hydrolases including *XYLOGLUCAN ENDOTRANSGLUCOSYLASE/HYDROLASE 19* (*XTH19*) were also down-regulated in *zou* mutants. These hydrolases are usually co-expressed with polysaccharide biosynthetic enzymes and are predicted to regulate the dynamics of hemicelluloses during their transportation and incorporation into the wall (Scheller and Ulvskov, 2010). These results suggest that *ZOU* may regulate the expression of cell wall biosynthesis and modifying enzymes.

Recently, reversibly glycosylated proteins (RGPs) from *Arabidopsis* were identified as being involved in the constitution of the plant cell wall (Rautengarten et al., 2011). There are five RGPs (RGP1, 2, 3, 4, 5) in *Arabidopsis*, and they have been shown to be located in the Golgi, and somewhat perplexingly, on the cytoplasmic side of the membrane. RGP1, RGP2 and RGP3 have been shown to have mutase activity, which can interconvert UDP-arabinopyranose to UDP-arabinofuranose, but RGP4 and RPG5 do not have this mutase activity. In *zou* mutants, *RGP3* was down-regulated and *RGP4* was up-regulated. However, *RGP1*, *RGP2* and *RGP5* did not show differences in expression between wild-type plants and *zou* mutants. Both *RGP4* and *RGP3* show seed specific expression, with *RGP4* apparently restricted to the testa, and *RGP3* to the endosperm (Winter et al., 2007). This suggests that *ZOU* might affect the interconvertion of UDP-arabinopyranose to UDP-arabinofuranose in the endosperm. However, the function of RGP4, since it appears to be catalytically inactive, is still not clear.

Beside polysaccharides, glycoproteins, which have a protein back-bone decorated by diverse sugar residues, form another important component of the plant cell wall (Ellis et al., 2010). Some cell wall associated glycoproteins have extensin motifs and a glycosylphosphatidylinositol (GPI) membrane anchor and which could trigger a cascade of signal transduction events (Seifert and Blaukopf, 2010). In *zou* mutants, a seed (micropylar endosperm) specific extensin protein and a GPI-membrane anchored protein, *FLA5*, were up-regulated, suggesting a potential role of *ZOU* in regulating cell wall signalling.

The plant cuticle, as discussed previously, consists of wax and cutin, which are made from fatty acids and their derivatives (Nawrath, 2006). Cuticular wax

biosynthesis is initiated in ER and the wax molecules are transported to the plasma-membrane and then transported through the plant cell wall to the outer layers of the plant cell wall. The expression of known wax biosynthesis genes, such as *fatty acid elongases* (*FAEs*), *β-keto acyl-CoA synthases* (*KCSs*) and *wax synthases* (*WAXs*) were not affected in *zou* mutants. However, two *GDSL-motif lipases* have been found down-regulated in *zou* mutants. The GDSL-motif lipases family is predicted to be involved in plant defense responses and secretion of cuticle wax (Volokita et al., 2011). One of the *GDSL-motif lipases* (*AT1G71250*) has been shown to be involved in metabolism of cuticular waxes and is down-regulated in cuticle associated mutants (*win1/shn*) (Kannangara et al., 2007). Several *lipid transfer proteins* (*LTPs*) which are involved in lipid transfer were also down-regulated in *zou* mutants. LTPs are associated with the cell wall, once the hydrophobic wax is exported from the cell it has to cross the hydrophilic cell wall and reach the cuticle. LTPs in the cell wall are very likely involved in facilitating this process (DeBono et al., 2009). These results suggest that *ZOU* may not be involved in cuticle biosynthesis, but possibly might play a role in the secretion of wax from the ER through the cell wall. Taken together, *ZOU* might be involved in cell wall biosynthesis pathways, cell wall signalling pathways as well as lipid transport pathways.

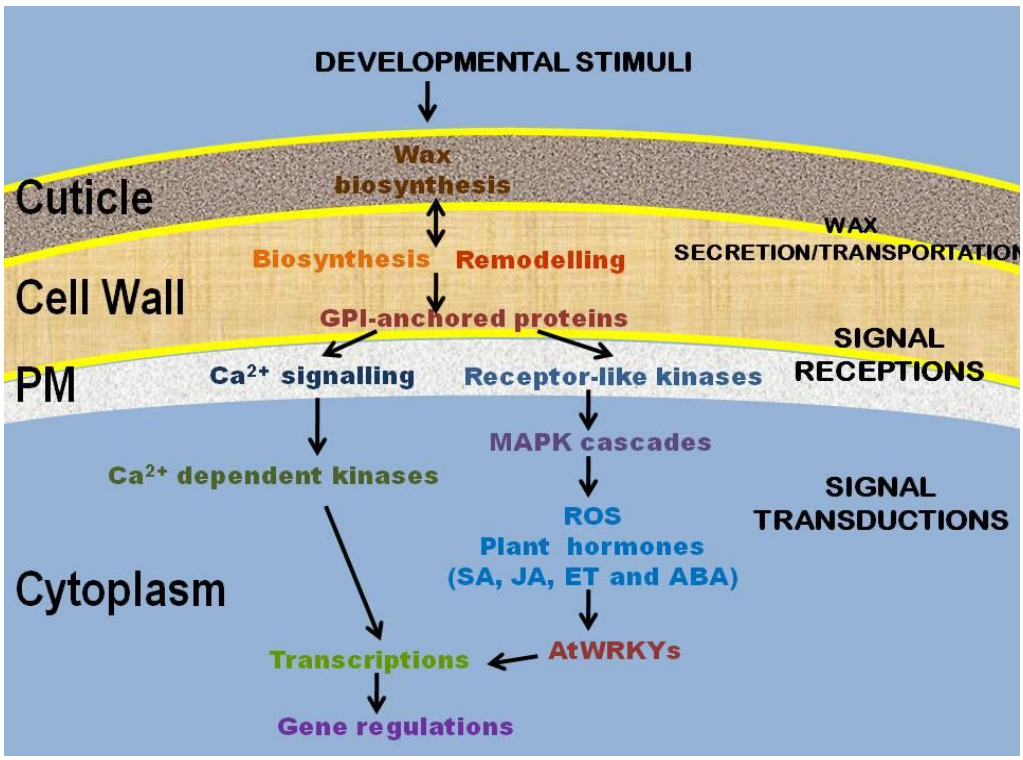

Figure 1.5 Summary of *ZOU* responsive genes and pathways identified by SOLEXA cDNA sequencing

Genes that either up-regulated or down-regulated in zou mutants are represented in metabolic processes (wax biosynthesis, cell wall biosynthesis and remodelling, Ca^{2+} signalling, ROS, plant hormone signalling, etc), or grouped into clusters of genes that may have similar functions (GPI-anchored proteins, Ca^{2+} dependent kinases, receptor-like kinases, MAP kinases, AtWRKY transcription factors). Black coded components on the right hand side represent the subcellular localizations of the cellular processes that might be regulated by *ZOU*: the wax secretion/transportation happens between the cytoplasm and the cuticle, signal reception happens on the outside face of plasma-membrane and the signal transduction happen in the cytoplasm.

In summary, *ZOU* appears to function by regulating the expression of a large number of genes which have previously been described as playing roles in responses to pathogen attack. Since many plant responses to pathogen challenge ultimately lead to forms of programmed cell death, with the aim of preventing disease spread to healthy neighbouring tissues, it is possible that many of these genes are actually cell death regulators and/or respond to cell death-induced signals such as the release of active oxygen species into the apoplast. Consistent with a potential role for *ZOU* in regulating programmed cell death, *LOL2*, which was predicted to be a negative regulator of plant cell death is up-regulated in *zou* mutants (Petra Epple et al., 2001). ZOU, as a transcription factor might regulate the early signalling in plant immune response at transcriptional level, which triggers programmed cell death.

1.5 Aims of this thesis

The main aims of this thesis were 1) to provide evidence that *ZOU* regulates endosperm cell death, 2) to test whether the function of *ZOU* in controlling endosperm cell death could be separated from its function in controlling embryonic epidermal cuticle development, and 3) to identify novel *ZOU* targets that may have a role in endosperm cell death and/or embryonic epidermal cuticle development.

2 Materials and Methods

2.1 Plant materials and growth conditions

2.1.1 Plant materials

The wild-type background used in this study was the Columbia-0 (Col-0) ecotype. If not specified, 'wild-type' refers to Col-0. The mutant alleles that were used in this thesis are listed in Table 2.1.

Mutant line	Seed stock	Mutation type	Reference
zou-4	GABI_584D09	T-DNA	(Yang et al., 2008)
ale1-1		dAc-I-RS-tagged line	(Tanaka et al., 2001)
lol2-3	SALK_144734	T-DNA	(Petra Epple et al., 2001)
dp1	SAIL_60_D04	T-DNA	(Matsuda et al., 2010)
dox1-1	SALK_113614C	T-DNA	(De León et al., 2002)
rgp3-1	SALK_113532	T-DNA	(Rautengarten et al., 2011)
rgp3-2	SALK_116503	T-DNA	(Rautengarten et al., 2011)
rgp4-1	SALK_150951	T-DNA	(Rautengarten et al., 2011)
rpg4-2	SALK_094267	T-DNA	(Rautengarten et al., 2011)
glip3-1 (at1g71250)	SALK_094513	T-DNA	(Kwon et al., 2009; Lee et al., 2009; Volokita et al., 2011)
glip4-1 (at5g03820)	GK-359A07	T-DNA	(Kwon et al., 2009; Lee et al., 2009; Volokita et al., 2011)
atenodl10-1	SALK_107590	T-DNA	(MASHIGUCHI et al., 2009)
csy1-1	SALK_007026	T-DNA	(Pracharoenwattana et al., 2005)
jar1-1	CS8072	substitution	(Staswick and Tiryaki, 2004)

Table 2.1 Mutant alleles used in this thesis

All mutant lines were obtained from the National Arabidopsis Stock Center (NASC), except for *ale1-1* which was kindly provided by Dr Tanaka.

2.1.2 Growth conditions

Arabidopsis seeds were sterilized and spread on tissue culture medium containing 0.5× MS salts (Duchefa), 0.3% (w/v) sucrose, and 1% (w/v) agar. After three days cold treatment (4°C), seeds were germinated in continuous light for about ten days. When the first pair of true leaves was easily visible, seedlings were transferred to soil. The growth room conditions were 24°C, 60% relative humidity and 16 h/8 h (light/dark) cycles. For desiccation tests, the wild-type, *zou-4*, *ale1-1* and *pSUC5::ALE1 zou-4* lines were germinated on the media plates, one week later the seedlings transferred to the soil carefully without causing mechanical harm, and covered with a loosely fitting lid, which was removed after one week. After three weeks the number of survivors was scored.

2.2 Plant cell death analysis

2.2.1 Terminal deoxynucleotidyl transferase-mediated dUTP Nick End Labelling (TUNEL) assays

Individual siliques were collected, both ends were cut off, and the rest of the siliques were plunged into cold fixative immediately. Fixative was 4% (w/v) paraformaldehyde in PBS buffer (pH 7.4). Siliques were fixed over night at 6°C with moderate agitation and washed three times with fresh PBS buffer (pH 7.4) after the fixation. Siliques were dehydrated through an ethanol series (30% 2 h, 50% 1 h, 70% 1 h, 80% 1 h, 95% 1 h and 100% 1 h) and the dehydrated siliques were put into tissue processing/embedding cassettes (Histo-prep, Fisher Scientific). The siliques were infiltrated with xylene (three times for one hour each) then infiltrated with liquid paraffin wax (four changes for one hour each at 60^{o}C) using a Leica ASP300 S automated tissue processor. After the wax infiltration the siliques were taken out of the cassettes and transferred into a mould filled with hot wax that best corresponded to the size of the tissue. The mould was then left to solidify on a cold plate for at least 30 min. When the wax was completely cooled and hardened the paraffin block was removed from the mould. The wax block was fixed to the microtome and tissue samples were sectioned in 10 μm slices. The wax ribbons were cut in to small pieces and stretched by floating the sections on distilled water on the surface of poly-lysine-coated glass slides (ProbeOn Plus, Fisher Biotech) at 44°C until no wrinkles were observed in the sections. The water was removed from the slides and the slides were left at 42°C overnight to allow the tissues to bond to the glass. The TUNEL reactions were performed with the DeadEnd^{TM} Colorimetric TUNEL Kit (Promega Corp., Madison, WI, USA) according to the manufacturer's instructions. As positive

controls, samples were treated with 10 U/ml DNAse-I for one hour. Negative controls were treated without adding Terminal Deoxynucleotidyl Transferase during the labelling reaction. Experiments were repeated three times. The samples were examined using bright field illumination on a Nikon Eclipse E600 microscope and photographed using a Leica DFC425 C digital microscope camera.

2.2.2 Dark-induced leaf senescence and wounding of leaves

Leaf number six (counted from the bottom of the rosette of three-week-old plants) was excised and placed on water-wetted filter paper in Petri dishes, abaxial-side facing down. The Petri dishes were kept in darkness at 24°C for four days and photographed. For the leaf wounding experiments, leaf number six was cut longitudinally. Both cut leaves and uncut leaves from above the cut leaves on the same rosette were taken as samples at time point 0 h, 2 h, 6 h, 12 h and 24 h.

2.2.3 Bacteria culture and plant inoculation

Bacteria strains *Pseudomonas syringae pv tomato* DC3000 expressing *avrRps4* or *avrB* were cultured in King's B medium (prepared by mixing 10 g proteose peptone, 1.5 g anhydrous K_2HPO_4, 15 g glycerol and 1 L H_2O, and then adjusting the pH to 7.0 with HCl, autoclaving and then adding 5 mL of sterile 1 M $MgSO_4$) with 50 mg/L rifampicin and 50 mg/L kanamycin overnight at 30°C. Bacterial cultures were centrifuged at 4,000 rpm for 5 min (Qiagen microcentrifuge), the supernant was discarded and the cells were resuspended in 10 mM $MgCl_2$ to give of OD_{600} 0.2 or 0.02. Three-week-old plants were used to observe the pathogen-induced hypersensitive response. Bacterial suspensions were infiltrated into one side of the

leaf using a 1.5 ml needleless syringe. Photographs were taken three days after the treatment.

2.3 Toluidine Blue tests

2.3.1 Toluidine Blue staining of seedlings

Sterilized seeds were plated on 0.5× MS salts (Duchefa) + 0.4% (w/v) phytogel (gum allum). After three days cold treatment (4°C), seeds were germinated in continuous light for about seven days in the growth room. 0.05% (w/v) Toluidine Blue with 0.4% (v/v) Tween 20 was dissolved in water. For the staining, Toluidine Blue solution was poured onto the plates and left for 2 min. The Toluidine Blue solution was poured off, and the plates were rinsed with distilled water three to five times. Photos of the seedlings were taken immediately after the staining, using the dissecting microscope.

2.3.2 Double blind tests

Double blind tests were performed to distinguish the quality of the Toluidine Blue staining in cotyledons among Col-0, *zou-4* and *pSUC5::ALE1 zou-4* lines. The level of staining was classified into three categories: 1) almost no staining, 2) medium staining, and 3) heavy staining, and given a score 1, 2 and 3 to each category respectively. Approximately 100 stained seedlings from each line were randomly placed on white filter paper and the genetic background of each seedling was labelled at the back of the paper without being revealed during the tests. People who were chosen to score the quality of Toluidine Blue staining of each seedling had never known the genetic backgrounds and phenotypes of the lines. For each genetic background, the number of plants that were either categorized as category 1),

category 2) or category 3) was summed. The blind scoring was performed three times by the same person.

2.3.3 Quantification of Toluidine Blue

Seedlings were stained by Toluidine Blue, rinsed with distilled water as previously described and dried on filter paper for half an hour. Hypocotyls and roots of the stained plants were cut off, and the remaining parts of the seedlings were put into the destaining solution (80% ethanol) with continuous moderate shaking for the extraction of Toluidine Blue. For each genotype, 20 treated seedlings were put into an eppendorf tube and extracted into 2 ml of extraction solution with three biological replicates. The concentration of Toluidine Blue was measured at 30 min, 1 h and 12 h of extraction. 400 µl extraction solution was taken each time and optical absorbance was measured at 626 nm using a BECKMAN DU® 520 spectrophotometer. Non-stained seedlings were used as a control and 80% ethanol was used as a blank.

2.4 DNA manipulation and transgene techniques

2.4.1 Plant genomic DNA extraction for genotyping and PCR amplifications

2-ME was added to the required amount of CTAB extraction solution (100 ml was prepared by mixing 2.0 g CTAB, 10.0 ml 1 M Tris pH 8.0, 4.0 ml 0.5 M EDTA pH 8.0, 28.0 ml 5 M NaCl, 40.0 ml H_2O, and 1 g PVP 40, and adjusting to pH 8.0 with HCl and making up to 100 ml with H_2O). The extraction solution was heated to 65°C. Two-three leaves were collected and placed in a 1.5 ml Eppendorf tube. Three steel beads and 500 µl warm CTAB-extraction solution with 2-ME were added. The tubes were placed in a TissueLyser (Qiagen) and shaken twice at 30 rps for 3 min, until the tissues were pulverized. The tubes were incubated at 65°C for 40 min with occasional slow vortexing. After the incubation 500 µl chloroform/isoamyl alcohol (24:1) was added to each tube and mixed well by inversion. The tubes were centrifuged in a microcentrifuge at 14,000 rpm for 10 min. The top phase (the aqueous supernatant) was recovered to a new tube. The chloroform/isoamyl alcohol extraction was repeated once and an equal volume of iso-propanol was added to the final supernantant, mixed well, and placed on ice for 30 min. The tubes were centrifuged at 14,000 rpm at 4°C for 15 min (Qiagen microcentrifuge). The supernatant was removed completely and the pellets were washed twice with 70% ethanol. The pellets were air dried. 100-200 µl TE was add to each tube to dissolve the pellets.

2.4.2 Plasmid mini preparations from *E. coli* for enzyme digestion and sequencing

A small amount (a little on the end of a spatula) of lysozyme was dissolved in 5 ml freshly made boiling buffer (8% w/v Sucrose, 0.5% v/v Triton×100, 50 mM EDTA,

10 mM Tris-HCl pH 8.0). 1.5 ml of fresh bacterial culture was centrifuged at 7,000 rpm for 3 min (Qiagen microcentrifuge). The supernatant was discarded and the pellet was re-suspended in 350 µl boiling buffer plus lysozyme. The tubes were boiled in a water bath for 1 min and placed immediately on ice for 2 min. The tubes were then centrifuged at 14,000 rpm at 4°C for 20 min (Qiagen microcentrifuge). The slimy pellet was quickly removed with a tooth-pick. 40 µl of NaOAc 3 M (pH 5.2) and 400 µl of isopropanol were added to the tubes and mixed by inverting several times. The tubes were centrifuged at 14,000 rpm for 5 min (Qiagen microcentrifuge) and the supernatant was quickly discarded. The pellet was rinsed in 1 ml 70% EtOH, air-dried, and re-suspended in 50 µl R40 (TE with 40 µg/ml RNAase A). If the plasmid was Bluescript, pGEM or pGEMT, 1 µl was used for restriction digest. If the plasmid was a binary vector, 5 µl was used for restriction digestions. 20 µl was purified for sequencing reactions (5 µl reactions consisting of 5 µM primer and 300 ng purified DNA) which were performed at the GenePool, School of Biological Sciences, the University of Edinburgh and analysed using an ABI3730 (Applied Biosytems) capillary electrophoresis system.

2.4.3 Alkaline Lysis Plasmid Isolation from *E. coli*

A miniprep method was used for large plasmids (>10 kb binary vectors) (Sambrook and Russell, 2001). 1.5 ml of fresh bacterial culture was harvested, centrifuged at 5,000 rpm for 3 min (Qiagen microcentrifuge), and the supernatant was removed. Cells were resuspended in 100 µl solution 1 (50 mM Tris-HCl pH 8.0, 10 mM EDTA) and left to sit on ice for10 min. 200 µl solution 2 (0.2 M NaOH, 1% SDS) was added and mixed, and left on ice for 5 min. 150 µl solution 3 (3 M potassium acetate, pH 4.3 with acetic acid) was added and mixed, and left on ice for 10 min. The tubes

were centrifuged at 12,000 rpm at 4°C for 5min (Qiagen microcentrifuge), and 400 µl supernatant was transferred to a new tube. 1ml isopropanol was added to the tubes and left at -60°C for 20 min. The tubes were centrifuged at 12,000 rpm for 10 min (Qiagen microcentrifuge). The supernatant was discarded and the pellets were washed with 70% ethanol. The pellets were dried and dissolved in 50 µl TE.

2.4.4 Plasmid enzyme digestion and ligations

Restriction digests were performed according to the manufacturers' instructions (New England Biolabs, Ipswich, MA, USA). 1 µl of boiling mini-prep prepared DNA was digested in a 15 µl final volume for 1 h at the recommended temperature with the recommended buffer and BSA. 5 µl boiling mini prepared DNA or alkaline lysis prepared DNA was digested for binary vectors. Digested products were mixed with 10× loading dye (40% w/v sucrose, 0.25% w/v bromophenol blue) and separated on agarose gels at 70 V for 1 to 2 h.

Ligations into commercially available vectors were performed according to the manufacturers' instructions. Ligations with the binary vectors were carried out with T4 DNA ligase according to the manufactures' guidelines ((NEB). Typically 50-60 ng insert DNA and 10-20 ng linearised plasmid DNA were included in a 10 µl reaction (5µl 2×buffer and 0.5 µl T4 DNA ligase) and incubated at 16°C overnight. 5 µl of the resulting ligation was used for transformation of competent *E. coli* cells (Inoue et al., 1990).

2.4.5 *E. coli* transformation by heat shock

E. coli DH5α competent cells which were prepared according to Inoue el al. (1990) by lab members were thawed on ice for 10 min. 100 µl aliquots of thawed cells were

mixed with the DNA to be transformed and incubated on ice for at least 20 min. Cells were heat shocked for 1 min at 42°C, and immediately chilled on ice for 5 min. 1 ml LB (1% tryptone, 0.5% yeast extract, 0.5% NaCl; pH 7.0) liquid medium was added to the tubes and cells were allowed to recover at 37°C for 30 min. Cells were centrifuged at 7,000 rpm for 3 min (Qiagen microcentrifuge), pellets were resuspended in 100 µl LB and plated on LB agar (LB with 1% bactoagar [Difco, Haarlem, The Netherlands]) containing the necessary antibiotics for selection of transformed cells. For vectors carrying the *LacZ* reporter gene (e.g. pGEM-T easy, pBluescript), blue/white selection could be used to identify cells with recombinant plasmid and plates were spread with 100 µl X-gal solution (20 mg/ml dissolved in dimethylformamide). Plates were incubated overnight at 37°C. Individual white colonies (i.e. likely recombinants lacking *LacZ* activity) were picked using a sterile tooth stick and cultured in 3 ml LB media with antibiotics at 37°C with shaking for 16 h. Plasmid DNA was prepared from fresh *E. coli* culture by either the boiling or the alkaline lysis method.

2.4.6 Transgene construction

To generate *pSUC5::ALE1* transgene construct, the *ALE1* cDNA was amplified from a silique cDNA population using primers ALE1-F and ALE1-R, the *pSUC5* promoter was amplified from genomic DNA using primers pSUC5-F and pSUC5-R (primer sequences see Table 2.2), and both sequences were cloned into pGEM-T easy vector (Promega, Madsion, USA) and sequenced to verify that no mutations had been introduced during PCR amplification. The *ALE1* cDNA was excised from the pGEM-T easy vector with *Xba*I and *Sph*I, and subcloned into the pGEM-T easy vector derivative containing the *pSUC5* promoter to generate the *pSUC5::ALE1*

fusion. The *pSUC5::ALE1* fragment was then excised from the pGEM-T easy vector using *Hind*III and *Sph*I, and subsequently cloned into the pBIB-hyg binary vector and introduced into plants using the *Agrobacterium tumefaciens* mediated floral dip method.

2.4.7 *Agrobacterium tumefaciens* cold shock transformation

Competent *Agrobacterium tumefaciens* GV3101 cells were available in the laboratory, prepared according to the freeze thaw method of Hofgen and Willmitzer (1988). Before the transformation, competent *Agrobacterium* cells were thawed on ice for 1.5 h. 10 µl (1 µg) DNA was added to 100µl cells, mixed gently and left on ice for 30 min. Tubes were snap froze in liquid nitrogen for 1 min and then thawed in a 37°C water bath for 1-2 min. 1ml YEP medium (1% yeast extract, 1% tryptone peptone, 0.5% NaCl, pH 7.0) was added to the tubes and they were incubated at 28°C in an agitating incubator for 2-3 h. Tubes were centrifuged at 7,000 rpm in a microcentrifuge for 1min and the bacteria was resuspended in 100µl of supernatant and plated out on YEP plates (YEP media with 15 g/L agar) with 50 mg/L Kanamycin and 80 mg/L Gentomycin. The plates were incubated at 28°C for 2-3 days.

2.4.8 *Agrobacterium* mini plasmid preparations.

Bacterial colonies were picked in 3 ml YEP and cultured overnight at 28^{o}C. The bacteria were harvested by centrifuging at 14,000 rpm for 3 min (Qiagen microcentrifuge). The pellet was resuspended in 100 µl ice-cold lysis buffer P1 (50 mM TrisHCl, 10 mM EDTA 100 mg/ml lysosyme), and left at room temperature for 30 min. 200 µl Buffer P2 (0.2 M NaOH, 1% SDS) was added and tubes were mixed

by inverting 2-3 times, and left on ice for 5 min. 150 µl ice-cold Buffer P3 (3 M KAc, pH 4.8) was added, tubes were gently vortexed, and left on ice for 5 min. Tubes were centrifuged at 4°C, 14,000 rpm for 5 min (Qiagen microcentrifuge) and the supernatant was transferred a new tube. 0.7 volume of isopropanol was added to the supernantant, mixed, and centrifuged at 4°C 14,000 rpm for 10 min (Qiagen microcentrifuge). The pellet was washed with 70% ethanol, air dried and dissolved in 10 µl R40 (TE with 40mg/L Rnase). 2 µl of DNA was used to retransform *E. coli* and the resultant transformants were analysed to check that the plasmid was intact. Glycerol stocks were made with equal volumes of bacterial culture and 80% glycerol and stored at -80°C.

2.4.9 *Agrobacterium*-mediated floral dip transformation

Arabidopsis plants for flower dip transformation (Clough and Bent, 1998) were grown under short day conditions (8 h light/16 h dark, 22°C) for 6 weeks, before being transferred to long days (16 h light/8 h dark, 22°C) and allowed to bolt. Inflorescences were cut off to stimulate auxiliary inflorescence formation, and plants were allowed to grow for a further two weeks. *Agrobacterium* strains harbouring the appropriate plasmids were propagated from glycerol stocks in 5 ml YEP (kanamycin/gentamycin) media overnight at 28°C with shaking, and then used to inoculate 500 ml cultures. Cells were pelleted and resuspended in 5% (w/v) sucrose with 400 µl/L 'Silwet' detergent (Lehle Seeds, Round Rock, USA). *Arabidopsis* flowers were dipped in bacterial solution for 5 min and plants were covered with a plastic bag for 24 h. The plants were then kept in normal growth condition until the seeds were dry. Transformants were selected on 0.5× MS media containing 200 mg/L Timentin (Galaxo Smith-Kline, Brentford, UK) and 15 mg/L Hygromycin B

(Calbiochem, Darmstadt, Germany) or 50 μg/ml kanamycin, depending on the binary vector. Transformed T1 lines were selected to identify lines carrying one insertion (segregating 3 resistant: 1 susceptible plant). Homozygous T2 lines were then identified as those segregating 100% resistance to antibiotics.

2.5 Gene expression analysis and in situ hybridization

2.5.1 Reverse transcription polymerase chain reaction (RT-PCR)

Total RNA was extracted using the RNeasy Mini Kit (Qiagen) following the manufacturer's instructions. For extracting RNA from siliques, the Lysis Buffer RLC was used. The quality of RNA was checked on a 2% agarose gel and the quantity of RNA was measured using a nanodrop spectrophotometer (Thermo Scientific). cDNA was synthesized using RevertAid^{TM} First Strand cDNA Synthesis Kit (Fermentas) and for each reaction 1 μg total RNA was used as template. PCR was carried out using the GoTaq® Flexi DNA Polymerase (Promega) or PfuTurbo DNA polymerase (Stratagene) according to manufacturers' instructions, and primers that were used are shown in in Table 2.2. PCR products were analysed by electrophoresis using 2% agarose gels.

Primer Name	Sequence (5' to 3')	Purpose
ZOU RT-F	GCAAAAAGGGTAAAATGAGCA	RT-PCR, *ZOU* expression
ZOU RT-R	TGGTGTGAGGAGAGCTGTTG	RT-PCR, *ZOU* expression
TUB-F	GTTCTTGATAACGAGGCCTT	RT-PCR, *TUBULIN* expression
TUB-R	ACCTTCTTCCTCATCCTCG	RT-PCR, *TUBULIN* expression
pSUC5-F	TAAGCTTTGAGTAAGAACAGGTAGTCC	Amplification of *AtSUC5* promoter
pSUC5-R	CTCTAGATATGAAAAGAAAAACGAGCAG	Amplification of *AtSUC5* promoter

ALE1-F	CTCTAGAATGGAAACC AATCCAAGAAAAC	Amplification of *ALE1* coding region
ALE1-R	GGTACCTCAAATGGTTT TAACTGACAACGG	Amplification of *ALE1* coding region
ALE1qRT-F	CTTCTCAGGCCAAGAA ACTC	Q-PCR analysis of *ALE1* expression
ALE1qRT-R	TTTGCCAGACTTGTTGA GGA	Q-PCR analysis of *ALE1* expression
ALE1-1F	CGTGCTAGAATAGACG AAGG	Genotyping *ale1-1* allele
ALE1-1R	CGTGGTGGAGATGGCA G	Genotyping *ale1-1* allele
ALE1-DS	CCGTTTTGTATATCCCG TTTCCGT	Genotyping *ale1-1* allele
LOL2-F	GTCAGGTGAATTGCAA CAATTGC	RT-PCR, *LOL2* expression and genotyping
LOL2-R	ACTGCTTAAACTTTTGA GTGGTC	RT-PCR, *LOL2* expression and genotyping
DP1-F	TGAGTTTGGTCTTGAAT GTAGCG	RT-PCR, *DP1* expression and genotyping
DP1-R	TGAAACCTTTGGGACT AGGG	RT-PCR, *DP1* expression and genotyping
DOX1-F	ATGAACTGAATCCAAG AAGCTGC	RT-PCR,*DOX1* expression and genotyping
DOX1-R	TGCATGGAGTGGATAA GATGG	RT-PCR, *DOX1* expression and genotyping
R4-01F	ACCATTACCACCTGATC ATTGTC	RT-PCR, *RGP4* expression and genotyping
R4-02F	TGTATCTCCTACAAAGA TGGTGG	RT-PCR, *RGP4* expression
R4-qPCR-F	ACGTAACACGAGGTAT GTGG	RT-PCR, *RGP4* expression
R4-probe02F	TCTCTCGAAAGAATCTG ACAC	*RGP4* RNA *in situ* hybridization probes
R4-03R	CCAAGGATCCTGTTGAT ATCATTACGGTT	RT-PCR, *RGP4* expression
R4-01R	ACCACACATTGGCTAC AATACTC	RT-PCR, *RGP4* expression
R4-02R	CATATAACATTTAGCTG CAGTGTC	RT-PCR, *RGP4* expression and genotyping
R4-probe02R	TCAACGAAGTCATCCA TGTAC	*RGP4* RNA *in situ* hybridization probes
R3-02F	GATGATTGCTTTGTTGC AAAGG	RT-PCR, *RGP3* expression
R3-01F	TATGAACCTTGCTTTTG ACCG	RT-PCR, *RGP3* expression and genotyping
R3-probeF	ACTCTTCCTAAAGAGTG	*RGP3* RNA *in situ*

	CACT	hybridization probes
R3-02R	ACCAGGTGCCTTATTCAGTGACC	RT-PCR, *RGP3* expression and genotyping
R3-01R	TCAACATACCTGGAATT	RT-PCR, *RGP3* expression
R3-probeR	ATGCATAGAGCACATTACACC	*RGP3* RNA *in situ* hybridization probes
GDSL1g71250-F	GTATTGACTGAGAAGTAGATTGGC	RT-PCR, *GDSL1g71250* expression and genotyping
GDSL1g71250-R	TGACTTTCATTGATCTGCTAG	RT-PCR, *GDSL1g71250* expression and genotyping
GDSL5g03820-F	TGATGACCTTTTCGGTTATCGC	RT-PCR, *GDSL5g03820* expression and genotyping
GDSL5g03820-R	TGGTACTCTTTGTAGTTTTTCAGC	RT-PCR, *GDSL5g03820* expression and genotyping
PLASTO-F	CTTCCCTTGTTCATGATATGAGC	RT-PCR, plastocyanin-like protein *5g57920* expression and genotyping
PLASTO-R	AGAATCTAGAGATGAAACACTAAACC	RT-PCR, plastocyanin-like protein *5g57920* expression and genotyping
CSY1-F	AATTTGAAGATCGTCGATGAGCG	RT-PCR, *CSY1* expression and genotyping
CSY1-R	TTCTCTGAATAAGAAAGGTTGCTC	RT-PCR, *CSY1* expression and genotyping

Table 2.2 Primers that were used in this thesis

2.5.2 Quantitative real time polymerase chain reaction (Q-PCR/qPCR/qRT-PCR)

Q-PCR analysis was carried out using SYBR Green JumpStart Taq ReadyMix (SIGMA). cDNA templates were diluted in distilled water from stocks using the protocol detailed above, and the following components were mixed: 1 µl template cDNA, 5 µl SYBR Green JumpStart Taq ReadyMix, 1 µl forward and reverse primer mix (3 µM), and 3 µl distilled water. The PCR amplifications were performed on the LightCycler® 480 machine (Roche) in triplicates. The programme used for PCR amplification was denaturation at 95°C for 1 s in the first cycle, denaturation at 95°C for 0 s in further cycles, annealing at 55°C for 10 s, elongation at 72°C for 10 s, and with a transition rate of 20 °C/s between temperature plateaus for a total of 45 cycles.

The melting curve analysis, which was used to check that a single product was amplified, and the Cp (crossing point) value which referred to the cycle at which the change in the fluorescence of a sample increased at maximum rate were obtained using the second derivative max method in the Roche LightCycler® software 2.0. The primers used are listed in Table 2.2. The mean normalized gene expression was calculated by normalising the amount of cDNA of the target gene relative to the amount of cDNA of the reference gene (e.g. *Actin* gene). The mean normalized expression (MNE) was calculated by averaging the threshold cycles (the Cp values) of the target genes and the reference genes, respectively and using the equation

$$MNE = (E_{reference})^{Cp\ ref\ gene,\ mean}/(E_{target})^{Cp\ target\ gene,\ mean}$$

, where E is the efficiency of a primer calculated by calibration using a dilution series of template cDNA. The standard error of the mean normalized expression (ΔMNE) was calculated by using the differential equation of Gauss for calculating the error propagation and was performed by Microsoft Excel software using the equation

$$\Delta MNE = MNE \cdot [(\ln(E_{target}) \cdot SE_{Cp\ target\ gene,\ mean})^2 + (\ln(E_{reference}) \cdot SE_{Cp\ ref\ gene,mean})^2\ ]^{½}$$

, where $SE_{Cp\ target\ gene,\ mean}$ referred to standard error of mean threshold cycle of the PCR amplification of the target gene and $SE_{Cp\ ref\ gene,mean}$ referred to standard error of mean threshold cycle of the PCR amplification of the reference gene (Pfaffl et al., 2002; Simon, 2003).

2.5.3 RNA *in situ* hybridizations

i) Fixation

A 4% paraformaldehyde solution was prepared by dissolving 8 g of paraformaldehyde in 200 ml 1×PBS, the pH of which had been pre-adjusted to 10.5

with NaOH and which had been pre-heated heated to 50-60°C. Once the dissolved solution was cooled on ice the pH was adjusted to 7.0 with H_2SO_4 and Triton 100 and Tween 20 were added, each to a final concentration of 0.1%. Tissue samples were put in the cold fixation buffer and vacuum infiltrated on ice twice for 30 min. Samples were transferred to fresh fixation buffer and left over night at 4°C with constant gentle agitation. The next day, samples were processed through the following solutions: 1×PBS wash 30 min, 1×PBS wash 15 min, 30% EtOH 1 hour, 50% EtOH 1-2 hour and 70% EtOH overnight in cold room. The tissues were embedded in paraffin wax blocks and sectioned, and the sections were attached to the surface of polylysine-coated glass slides using the same protocols as that of the TUNEL assays (see 2.2.1).

ii) Preparations for the probes

Plasmids containing cDNA sequences were linearized with enzymes that create 5' overhangs (10 μg plasmids, digested for 4-5 h in a volume of 50-100 μl). DNA digestions were diluted to 200 μl and mixed thoroughly with 200 μl phenol/chloroform. Tubes were centrifuged at 13,000 rpm for 5 min (Qiagen microcentrifuge). The upper phase (~185 μl) was transferred to a new tube and mixed with an equal volume of chloroform. Tubes were centrifuged at 13,000 rpm for 5 min (Qiagen microcentrifuge). The upper phase (~170 μl) was transferred to a new tube, mixed with 17 μl NaAc (3M, pH 5.2) and 400 μl of EtOH, and left at -20°C for 2 h. Tubes were centrifuged at 13,000 rpm and 4°C for 10 min. The supernatant was discarded and the pellet was washed with 70% EtOH. The pellet was air dried and dissolved in 10 μl DEPC-water. The DNA was quantified by the nanodrop spectrophotometer (Thermo Scientific).

iii) In vitro transcription

~300 ng of template DNA was used for each reaction. 15.5 µl DNA in water (DEPC-treated), 2.5 µl 10× buffer (from enzyme supplier), 1.0 µl RNAase inhibitor (RNAaseOUT, Promega), 2.5 µl NTP mix (ATP, CTP, GTP; 5 mM each), 2.5 µl DIG-UTP (1 mM) and 1.0 µl RNA polymerase (5 U, NEB) were mixed together to a total volume of 25.0 µl. Tubes were incubated at 37°C for 60 min in a PCR cycler and then 75 µl H_2O, 1 µl tRNA (100 mg/ml) and 1 µl DNAase (RNAase-free, Strategene RQ) were added to the tube. Tubes were incubated at 37°C for 10 min and 100 µl NH_4OAc (4M) and 400 µl EtOH were added to the tube. The tubes were incubated at -80°C, overnight. The DNA pellet was precipitated by centrifugation at maximal speed for 30 min at 4°C in a microcentrifuge. The pellet was air dried, dissolved in 100 µl 50% de-ionised formamide in DEPC-treated H_2O and stored at -80ºC.

iv) Hybridizations

1.5 L of 1× PBS, 300 ml of 2×SSC (3M NaCl, 0.3M sodium citrate for 20× concentration), 300 ml of 2% glycine (dissolved in 1×PBS), 600 ml of triethanolamine buffer (8 ml of triethanolamine dissolved in 600 ml H_2O and the pH adjusted to 8.0 with HCl) and 300 ml of 4% Paraformaldehyde (prepared as for fixative, but without the addition of detergents) were prepared. 300 ml of 100 mM Tris 8.0, 50 mM EDTA (Proteinase K buffer) was warmed to 37ºC. The slides were placed in racks and incubated twice for 10 min in Histo-Clear clearing solution (National Diagnostics) to remove wax, then rehydrated using an ethanol series consisting of two washes for 1-2 min in 100% EtOH, then 1-2 min each in 95%

EtOH, 90% EtOH, 80% EtOH, 60% EtOH, 30% EtOH and finally H_2O. The slides were then incubated for 5 min in 2× SSC, permeabilised by light digestion for 30 min in 1 µg/ml proteinase K at 37°C (add 15 µl of 20 mg/ml proteinase K stock to the warmed buffer just before use), and the digestion stopped by incubating for 2 min in 2% glycine (room temperature). Slides were then treated two times for 2 min in PBS (room temperature), re-fixed for 10 min in 4% formaldehyde (room temperature), and washed for two times 2 min in PBS (room temperature). To block the positively charged slides and reduce background during hybridization, slides were incubated for 10 min in triethanolamine buffer in the fume hood with 3 ml acetic anhydride added drop by drop into the solution while stirring, then washed two times 5 min PBS (room temperature), and dehydrated by passage for 30 s in each of the ethanol series from 30% EtOH to 100% EtOH. The slides were then stored in a closed box containing a small amount of 100% ethanol.

v) Making probe mixes for hybridization (for one two-slide 'sandwich' reaction)

For each 'sandwich' comprising two slides, 250 µl of hybridisation buffer was prepared using 25 µl of 10× *in situ* salts (3 M NaCl, 100 mM Tris-HCl pH 8.0, 100 mM sodium phosphate buffer pH 6.8, 50 mM EDTA), 42.5 µl of DEPC treated H_2O, 2.5 µl of 100× Denhardt's solution (Amresco, USA), 2.5 µl of tRNA (100 mg/ml), 100 µl of de-ionised formamide (Amresco, USA), 50 µl of 50% dextran sulfate (warmed at 65°C before use) and 2.5 µl 10% Triton ×100 were mixed in the above order. Four layers of dampened paper towels were put at the bottom of a long box, and covered completely with Parafilm, so that the slides would not touch the towels. 1 µl probe was added to 250 µl hybridisation probe mix. The hybridisation probe mix was denatured by heating at 80°C for 3 min and briefly cooled on ice. 250 µl probe

mix was added to one slide and covered with a second slide with the sections inwards to make a ‘sandwich’. The slide ‘sandwiches’ were put in the prepared parafilm-lined box which was then sealed and incubated at 55ºC overnight.

vi) Post-hybridisation

The slides were washed in three changes of 0.2×SSC for 3 h at 52°C. They were then incubated in 1% Boehringer block (Roche, dissolved in 1×TBS buffer) at room temperature for 45 min. Prior to anti-DIG antibody incubation, slides were blocked in BSA solution (1% BSA, 0.3% Triton X-100, 100 mM Tris-HCl pH 7.5, 150 mM NaCl) for 45 min, and 4.8 µl antibody was diluted in 6 ml BSA solution which could be used for 48 slides (24 ‘sandwiches’). 500 µl of antibody solution was puddled on Parafilm. The slides were paired with the samples facing each other, and allowed to take up the antibody solution by capillarity. The paired slides were incubated in large Petri dishes for 2 h. Unbound antibody was removed with four 20 min washes in BSA solution. The slides were briefly washed in revelation buffer (100 mM Tris-HCl pH 9.5, 100 mM NaCl, 50 mM $MgCl_2$) and incubated with NBT/BCIP (4.5 µl NBT (30 mg/ml in 70% DMF), 3.5 µl BCIP (15 mg/ml in DMF) in 1 ml revelation buffer) at room temperature in the dark for 1-3 days. The reaction was stopped by rinsing the slides in TE, H_2O, 70% EtOH and 100% EtOH. Dry slides were mounted with Entellan (Sigma). The results were examined using a Nikon Eclipse E600 microscope.

2.6 Microscopy

For dry seed size analysis and young seedling analysis, images were taken under the Nikon SMZ1500 binocular microscope. For embryo development analysis, green seeds were cleared in Hoyer's solution (chloral hydrate:water:glycerol in proportions 8 g: 2 ml: 1 ml) overnight and examined using a Nikon Eclipse E600 microscope under differential interference contrast (DIC) conditions.

Cryo-scanning electron microscopy (SEM) studies were carried out using a Hitachi S-4700 scanning electron microscope (Hitachi High Technologies, Wokingham, UK). Specimens were placed on a flat metal stub which was provided with the microscope and the surface of the stub was coated with one layer of carbon. Fresh samples were transferred directly from the growth media or soil to the carbon coated metal stub. The stub with the specimens was frozen in liquid nitrogen and inserted immediately to the cooled preparation chamber (-140°C). If some ice crystals were observed on the surface of the specimen, the temperature of the preparation chamber were increased to about -95°C to allow the ice crystals to be sublimed. The samples were transferred to the SEM chamber and coated with gold and palladium to avoid charging of the samples and improve image quality, and then the samples were visualized and imaged at low accelerating voltage (1-2 kV) at -120°C.

2.7 Genetic crossings

Arabidopsis genetic crossings were performed on plants at six to seven weeks old. Flowers on the lateral shoots were emasculated before they had opened, using tweezers that were rinsed in 70% EtOH to avoid contaminations. Carpels were hand pollinated the next day with pollen from the donor plants. Mature siliques were harvested and seeds were stored in dry condition.

3 Programmed cell death in *Arabidopsis* seed development

3.1 Introduction

3.1.1 What is programmed cell death?

Programmed cell death is a controlled cell death process which selectively removes unwanted cells (Pennell and Lamb, 1997). Classification of programmed cell death is periodically reviewed by the Nomenclature Committee. In animals, programmed cell death can be mainly classified into three categories according to morphological appearance: apoptosis, autophagic cell death and necrosis (Kroemer et al., 2008). According to Kroemer et al. (2008), the morphological features of apoptosis include rounding-up of the cell, retraction of pseudopodes, chromatin condensation, nuclear segmentation and very little ultrastructural modification of cytoplasmic organelles. The hallmarks of apoptosis are regarded as blebbing of plasma membrane, fragmentation of the cell, formation of apoptotic bodies, and finally the engulfing of cells by phagocytes. Biochemical features of apoptosis include DNA fragmentation and/or activation of caspases. These phenomena can, however, be linked to the other types of cell death or non-lethal biological processes (Kroemer et al., 2008). Autophagic cell death is defined by an increased number of autophagosomes or autolysosomes (small lytic vacuoles) and the absence of chromatin condensation (Kroemer et al., 2008). Necrosis, compared to the above mentioned cell death types is defined in a negative fashion, which means cell death lacking the features of apoptosis or autophagic cell death (Kroemer et al., 2008). However, morphologically necrosis is characterized by gaining of cell volume, swelling of organelles (typically mitochondria), rupturing of the plasma membrane, depletion of ATP, degradation of

lipid which follows the activation of phospholipases, lipoxygenases and sphingomyelinases, and subsequently the loss of cellular contents (Kroemer et al., 2008). An increase in calcium (Ca^{2+}) concentration and membrane permeability, and production of reactive oxygen species (ROS) are also typical features of necrotic cell death in animals (Kroemer et al., 2008).

Divergent opinions exist in defining plant programmed cell death. Love et al. (2008) proposed two major forms of programmed cell death depending on the speed of the cell death process: autophagic cell death which is a slow form of cell death, and apoptosis-like programmed cell death which is rapid cell death. Plant autophagic cell death involves the formation of autophagosomes which fuse with lysosomes in which the cytoplasm is sequestered leading to rapid disappearance of the cellular contents. Plant autophagic cell death has been associated with vacuolar recycling of nutrients, accumulation of reactive oxygen species (ROS) and jasmonic acid (JA) and/or ethylene signalling. It can be considered to have a pro-survival function (Love et al., 2008). Plant apoptosis-like cell death is defined by rapid nuclear fragmentation, caspase-like activity, chromatin condensation, nuclear blebbing and DNA degradation, and involves ROS and SA signalling (Love et al., 2008). According to Love et al. (2008), developmentally regulated cell death during root formation and the differentiation of xylem and phloem show features of both autophagic cell death and apoptosis-like cell death; senescence and cell death triggered by mild environmental factors (such as drought and temperature) resemble autophagic cell death; and the hypersensitive response (Hatsugai et al., 2004) which is triggered by interaction between plants and avirulent pathogens and is associated with rapid and localized cell death at the infected sites of host plants, should be classified as

apoptosis-like cell death. Love et al. (2008) also proposed that there is an antagonistic effect between the autophagic and the apoptosis-like cell death pathways due to the cross-talk between the JA/ethylene signalling and the SA signalling pathways, and that the autophagic pathway might suppress the apoptosis-like pathway.

By comparing the morphological features of animal programmed cell death with the features of plant programmed cell death, van Doorn et al. (2011a) argued that it is incorrect to use the terms apoptosis or apoptosis-like in defining plant programmed cell death. Firstly, although apoptosis is often associated with activation of caspases and DNA fragmentation, these processes can also happen during non-apoptotic cell death, and are thus insufficient criteria. Secondly, apoptosis in animals is often accompanied by the rounding up of cells and the formation of apoptotic bodies. In plants, however, shrinking of protoplasts usually leads to damaged plasma membranes and, cells cannot further fragment into discrete bodies. The rigid plant cell wall thus prevents plant cells from forming apoptotic bodies.

Van Doorn et al. (2011a) recently proposed a new classification of plant programmed cell death into three categories based on both morphological and biochemical features: 1) vacuolar cell death, 2) necrotic cell death and 3) cell death that cannot be ascribed to either of categories 1) or 2). The morphological features of vacuolar cell death are manifested by the accumulation of autophagosomes and lytic vacuoles, rupture of the vacuolar membrane (tonoplast) and fusion of vesicles with the vacuole, followed by engulfment of the cytoplasm into the vacuole lumen (van Doorn et al., 2011a). This vacuolar cell death is often accompanied by rapid destruction of the entire protoplast and the plant cell wall. Biochemically, vacuolar

cell death often features acidification of vacuoles, reorganisation of the cytoskeleton, activation of vacuolar processing enzymes (VPEs) and, in some cases, the expression of *AUTOPHAGY* (*ATG)* genes (van Doorn et al., 2011a). Examples of vacuolar cell death can be found during aerenchyma formation, leaf perforation in the lace plant, petal senescence, xylem differentiation, embryo development, organ and tissue morphogenesis and senescence (van Doorn et al., 2011a). Van Doorn et al.'s (2011a) definition of necrotic plant cell death is consistent with the necrosis in animals. Because during necrotic plant cell death lytic vacuoles do not participate in clearing the cytoplasm, the cell corpse remains largely unprocessed. The third category suggested by van Doorn et al. (2011a) includes hypersensitive cell death, starchy endosperm cell death in cereals and cell death during the self-incompatibility (SI) response.

Van Doorn (2011b) subsequently updated the previous classification and proposed a new criterion to define programmed cell death in plants, which is whether rupture of the tonoplast followed by rapid clearance of the cytoplasm and the plant cell wall occurs. The cell death showing this feature is called 'autolytic' programmed cell death, and cell death that does not show this feature is called 'non-autolytic' programmed cell death (van Doorn, 2011b). 'Autolytic' programmed cell death occurs mainly during plant development such as shoot and root development, mild abiotic stress such as formation of aerenchyma in roots under the low oxygen condition, and senescence. 'Non-autolytic' cell death happens mainly during the hypersensitive response (van Doorn, 2011b).

Van Doorn (2011b)'s classification was mainly based on the morphological changes that was happening during the programmed cell death, and defining cell

death by Van Doorn (2011b)'s criteria requires morphological data during the whole course of cell death, which in some cases is hard to achieve. Love at al. (2008)'s classification were more general and were based on characterization of biological pathways that were involved in the cell death.

3.1.2 Programmed cell death during plant senescence

Senescence is an age dependent deterioration process which occurs at the cell, tissue or organ level or in the whole organism leading eventually to death or the end of the life cycle (Lim et al., 2007). Leaf senescence has been extensively studied. Ultrastructual characterization of chloroplast morphology during leaf senescence was performed in wheat, rice and barley (Gregersen et al., 2008). In general, the changes in chloroplasts during senescence include a reduction in the thylakoid membrane system, a loss of grana stacks, swelling of the intrathylakoid space and an increase in the number and the size of plastoglobuli (Gregersen et al., 2008). In wheat flag leaves, there is a progressive destruction of the thylakoid membrane system and the loss of the integrity in the plastid envelope. By the later stage of the leaf senescence, the outer membrane of the chloroplasts which is adjacent to the tonoplast, appears to break down whilst the inner membrane remains integral (Gregersen et al., 2008).

Biochemical studies show that during leaf and petal senescence, there is a massive change in protein composition and extensive degradation of DNA, RNA, lipids and carbohydrate complexes. These cellular components degrade to sucrose, amino acids and amides which are transported through the phloem out of the dying organ and into the other organs (van Doorn, 2004). The biochemical changes during leaf and petal programmed cell death might be caused by the loss of selective permeability of both

the tonoplast and the plasma membrane and the leakage of the chloroplast components, which allows the contact between the degradative vacuolar lytic enzymes and the membrane systems, causing the degradation of cytoplasm and organelles (Gregersen et al., 2008; van Doorn, 2004).

Genetic and molecular approaches are also used to study leaf senescence. Forward genetic screening methods have been used to identify mutants with an early or delayed leaf senescence phenotype, which allows researchers to identify various positive or negative regulators in the leaf senescence process. Many such mutants result from altered hormone pathways, such as delayed senescence mutants with reduced ethylene signalling and increased cytokinin signalling (Lim et al., 2007). Forward genetic methods have also been used to identify genes that show different expression patterns during senescence. *AtNAP* encodes a NAC family transcription factor which has been shown to be nuclear localized and up-regulated in expression during natural senescence and dark-induced leaf senescence. T-DNA knockout mutants of *AtNAP* showed a significant delay in leaf senescence suggesting that *AtNAP* may be a positive regulator in leaf senescence (Guo and Gan, 2006). Identification of other transcription factors, for example the WRKY family transcription factor WRKY53, that are involved in early events of leaf senescence, suggests that leaf senescence is highly complex and is regulated by many endogenous and exogenous signals (Miao and Zentgraf, 2007). In order to reveal the global picture of senescence regulatory networks, an RNA microarray based high resolution time-course profile of gene expression during development of a single leaf over a three-week period of senescence was performed (Breeze et al., 2011). Using the 7th leaf from individual *Arabidopsis* plants, samples from a time course of 19

days after sowing to 39 days after sowing were analysed. Over 6000 genes showed change of expressions during this period (Breeze et al., 2011). Among those differently expressed genes, down-regulated genes are significantly enriched for genes linked to plastid and thylakoid proteins required for photosynthesis and carbohydrate and amino acid metabolism (Breeze et al., 2011). This is consistent with the destruction of chloroplasts and other cellular structures during senescence. Among the up-regulated genes, genes that are linked to peroxisome and vacuole function, transport, protein binding, and transcription are overrepresented There is also a significant enrichment in genes involved in stress response such as osmotic, salt and water stress, and catabolic processes (Breeze et al., 2011).

Hormone responses during the senescence process are complex. The timing of expression of specific hormone biosynthesis genes shows that rapid up-regulation of JA biosynthesis genes occurs at the early stage of senescence, whereas ABA and SA biosynthesis genes show a later increase in expression with a peak at the final stage of senescence (Breeze et al., 2011). Ethylene biosynthesis genes show an increase in expression in the middle of senescence with a steady increase as senescence proceeds (Breeze et al., 2011). It seems that ABA, ethylene, and possibly SA synthesis and signalling are co-ordinately regulated during senescence, whereas JA shows a different pattern of regulation.

The expression of many autophagy-related (*ATG*) genes is enhanced at the starting point of senescence, nine out of 15 up-regulated *ATGs* show an increased expression from the onset of senescence, with the other five *ATGs* showing a slightly delayed activation. *ATG7* has been shown to be up-regulated at the 29th day after sowing (Breeze et al., 2011). The timing expression of *ATG7* may provide an important

control for cell death activation during leaf senescence. LSD1, a zinc finger protein which monitors a superoxide-dependent signal and negatively regulates a plant cell death pathway, is induced at the 21st day after sowing as is the mitogen-activated protein kinase MPK7 which is induced by hydrogen peroxide and enhances plant defense responses (Breeze et al., 2011), further suggesting a chronologically controlled cell death during leaf senescence.

To summarize, plant senescence is a finely regulated and complex process that incorporates both developmental and environmental signals. Morphological and biochemical analysis has revealed some common cell death features during senescence. Genetic and molecular analysis has identified important regulators and revealed a global picture of senescence regulatory networks. Further experiments are needed to validate the function of the key regulatory genes and pathways during senescence.

3.1.3 Programmed cell death during seed development

Features of programmed cell death in the seeds of both cereals and non-cereal plants have been characterized. Although PCD has been proposed to play an important role in coordinating the development of different parts of the seed, our understanding of the true function of this process in many tissues remains fragmentary. In maize, programmed cell death has been reported in the central starchy endosperm cells and apical cells near the silk scar at about 16 days after pollination (DAP), and then spreads towards the base of the kernel between 24 DAP and 40 DAP (Young and Gallie, 2000). The decline in DNA concentration in the central endosperm happens simultaneously with the initiation of programmed cell death in these cells, and the

subsequent spread of cell death throughout the other parts of the endosperm follows the pattern of starch deposition. Mutant analyses in maize and barley further indicated a mutual coordination between endosperm cells and maternal tissue. In maize *minature1* (*mn1*) mutants, loss of invertase in basal endosperm cells and adjacent maternal tissues results in a premature cell death in maternal cells, indicating a nutrient transportation between basal endosperm cells and maternal tissue which could be mediated by cell death (Miller and Chourey, 1992). In maize, DNA laddering was detected in the scutellum, coleoptile, root cap and suspensor, suggesting a programmed cell death during embryogenesis (Giuliani et al., 2002). In barley, cell death in the aleurone which is the outermost cell layer of the starchy endosperm, was well characterized by Fath et al (1999). Three nucleases, which are regulated by GA and ABA in barley aleurone cells, are responsible for initiating a non-apoptotic cell death programme, which does not display DNA fragmentation, plasma membrane blebbing or the formation of apoptotic bodies. A barley cysteine protease, cathepsin B, although universally expressed was only positively regulated by GA and negatively regulated by ABA in isolated aleurones (Martínez et al., 2003), suggesting that there might be a cysteine protease mediated programmed cell death pathway in barley aleurones. Programmed cell death in wheat was first observed in the nucellus (Young and Gallie, 2000). In the wheat nucellus, programmed cell death initiates at about 4 to 6 DAP, and is thought to make space for rapid expansion of the developing endosperm. In contrast to maize, the onset of programmed cell death in wheat endosperm is not confined to a specific region, but instead it initiates randomly across the whole area of endosperm at about 30 DAP. The pharmacological analysis of programmed cell death inducers and inhibitors in wheat

aleurone cells suggests that decrease of the haem oxygenase (HO) activity by zinc protoporphyrin IX before the exposure to GA accelerates the aleurone programmed cell death. Moreover, inducing haem oxygenase (HO) activity by using the HO inducer haematin, inhibits programmed cell death in the aleurone (Wu et al., 2011). As haem oxygenase is triggered by various exogenous and endogenous stimuli, such as heavy metals, hypoxia, UV, ROS (such as H_2O_2) and NO, haem oxygenase might be a key modulator of the signals controlling the programmed cell death in aleurone cells.

In castor bean seeds (*Ricinus communis*), cell death takes place in a different pattern. After fertilization, the endosperm expands rapidly and nutrients are transferred from nucellar cells, which function as the major seed storage organ, into endosperm cells. This process coincides with rapid nucellar degeneration through programmed cell death. DNA fragmentation was observed in nucellar cells adjacent to the expanding endosperm. This was accompanied by expression of a pro-cysteine endopeptidase (CysEP) in ricinosomes which are a subset of precursor protease vesicles involved in certain types of plant programmed cell death in nucellar cells, indicating that CysEP may digest the nucellar cells (Greenwood et al., 2005). By maturity, the living endosperm forms the major storage body, stocking both proteins and oil. During seed germination, programmed cell death takes place in endosperm cells and DNA fragmentation is observed in endosperm cells surrounding the cotyledons. This cell death is characterised by the presence of a large central vacuole in endosperm cells, cellular collapse, and gradual disappearance of the endosperm, leaving a thin layer of collapsed endosperm cells surrounding the cotyledons (Schmid et al., 1999).

Programmed cell death regulators were studied using Norway spruce somatic embryogenesis as the model system and it has been shown that animal caspase-like VEIDase is involved in programmed cell death pathway during embryogenesis (Bozhkov et al., 2003). Biochemical analysis has shown that cell extracts from Norway spruce embryos contain a specific protease with the substrate preference for VEID-containing peptides similar to those of mammalian caspase-6 which are critical for controlling programmed cell death during both embryonic and postembryonic development (Bozhkov et al., 2003). The programmed cell death in embryo cells especially in embryo suspensor cells detected by TUNEL assays is correlated with the VEIDase activity, and inhibition of the VEIDase activity affects the normal embryo patterning showing defects in suspensor development and reduced DNA fragmentation in the suspensor illustrated by less TUNEL positively stained nuclei in the suspensor (Bozhkov et al., 2003). These results suggest that the mammalian caspase-like protease VEIDase plays a major role in promoting Norway spruce programmed cell death in the beginning of the execution phase (suspensor degradation) and is critical for embryo patterning.

In *Arabidopsis*, a 25-amino-acid peptide Kiss of Death (KOD) has been suggested to have a role above the caspase-like protease activity in promoting programmed cell death (Blanvillain et al., 2011). *kod* mutants display reduced PCD in suspensor cells during embryo development and reduced PCD in root hairs, and KOD expression is induced during biotic and abiotic stress, particularly in HR associated plant defence response, suggesting a general role of KOD in regulating PCD during embryogenesis and outside the seeds (Blanvillain et al., 2011). In the dexamethasone-induced *KOD* expression lines, the plant PCD hallmarks, caspase 3-like protease and ion leakage

which have been implicated in a wide range of PCD pathways including HR and self-incompatibility (Bonneau et al., 2008) were well correlated with *KOD* expression level, suggesting that *KOD* has a role in the early stage of cell death initiation (Blanvillain et al., 2011). However, which signal triggers the processing of KOD and how the death signal is mediated by KOD are yet to know.

Cell death is not only observed in endosperm, nucellus, aleurones and embryo, but is also observed during seed coat development. The seed coat (testa) is the maternal part of the seed which derives from the outer and inner integuments of the ovule. The outer integument of *Brassica napus* seed coat consists of four cell layers and the inner integument consists of six to eight cell layers at the time of flowering (Wan et al., 2002). The cell layers of the outer integument of *Brassica napus* seed remain unchanged during early embryo development, whereas the inner integument cell layers go through a remarkable reduction. At four days after flowering (DAF), the inner integument cells undergo cell expansion and vacuolation, and show a reduction in starch granules. At 10 DAF, the inner integument loses half of its cell layers and starch is actively turned over so that by 10 to 14 DAF, the inner integument has only two to three cell layers left. By 20 DAF, as the embryo is reaching its full size, the inner integument cells are completely crushed, whereas the outer integument retains four cell layers at this stage (Wan et al., 2002). A nuclear DNA fragmentation was observed in the cells of the inner integument at 10 DAF, but not at 6 DAF by fluorometric terminal deoxynucleotidyl transferase-mediated dUTP nick end labelling (TUNEL) assays, indicating a DNA fragmentation associated programmed cell death in the inner integument during embryogenesis in *Brassica napus* (Wan et al., 2002).

Arabidopsis seed coat development has been studied in even more detail. In *Arabidopsis,* after the fertilization, cells from the outer and the inner integument undergo cell division, cell expansion, a set of morphological and physiological changes, and die sequentially during different stages of seed development. The two cell layers of outer integument and the three cell layers of the inner integument (named ii1, ii2 and ii3 from the inside to the outside) have distinct fates: Cells of the innermost layer (the endothelium, ii1) synthesize proanthocyanidin (PA) flavonoid compounds giving a brown colour to the seed coat. Cells of the other two inner integument layers (ii2 and ii3) do not differentiate and are crushed together. Cells of both outer integument layers accumulate starch-containing granules. While the sub-epidermal layer differentiates into palisade with thickened cell walls, the cells of the epidermal layer synthesize and secrete a large amount of mucilage. Modification of a secondary cell wall, and cytoplasmic constriction cause these cells to form a volcano-shape in the mature seed (Haughn and Chaudhury, 2005).

Programmed cell death during *Arabidopsis* seed coat development is characterized by cell shrinkage and partial destruction and fusion of the plasma membrane and tonoplast, followed by disruption of cellular organelles. This process is first initiated in the ii2 cell layer at the torpedo stage of embryogenesis, when cells in the ii1 and ii3 layers are still intact. Later in development cells in the ii2 layer also die and are crushed into the ii1 layer (Nakaune et al., 2005). An *Arabidopsis* vacuolar processing enzyme, δVPE, which is a cysteine proteinase, was identified to be specifically and transiently expressed in the ii2 and ii3 layers of the integument at early stages of seed development. The δVPE loss of function mutants showed delayed cell death in the ii2 and ii3 layers compared to the wild-type seeds. *in vitro*, the δVPE protein exhibits

caspase 1-like activity which has been shown to have a function in various types of plant cell death, suggesting that δVPE is involved in programmed cell death in the inner integument during seed coat formation (Nakaune et al., 2005). Cysteine proteases involved in the programmed cell death of the cells of the ii1 layer (the endothelial cells) were also reported in the developing seeds of *Arabidopsis*. Protein disulfide isomerase 5 (PDI5) which interacts with the cysteine proteases CP43 and RD21 in vitro, is associated with the endoplasmic reticulum trafficking through Golgi to vacuoles in the endothelial cells (Andème Ondzighi et al., 2008). PDI5 is preferentially expressed in floral tissues and developing seed, and exclusively localized in the ER and protein storage vacuoles and lytic vacuoles of endothelial cells before the onset of programmed cell death. Expression of PDI5 promotes the programmed cell death in the endothelium cells, which is manifested by disruption of vacuoles, shrinkage of cytoplasm, nuclear condensation and fragmentation, and breakdown of the cell wall. Loss of PDI5 function leads to premature initiation of programmed cell death in the endothelium cells and seed abortions, suggesting that PDI5 is required for seed development and temporally controls endothelium programmed cell death by chaperoning and inhibiting cysteine proteases function (Andème Ondzighi et al., 2008).

3.1.4 Cell death in the Embryo Surround Region (ESR)

The Embryo surrounding region (ESR) is characterized as a zone within the endosperm which is directly adjacent to the embryo. Both in cereals and *Arabidopsis* the development of the ESR is very similar: As the embryo grows, the ESR progressively shrinks, providing the space for the embryo to expand (Olsen, 2004). The ESR exists both in cereals and castor beans, where a large proportion of the

endosperm is persistent and used as an energy source post-germination, and in species with largely transient endosperms such as *Phaseolus coccineus* L. (the runner bean) and *Arabidopsis*. In the latter, endosperm is largely absorbed by the growing embryo before maturation. Despite its importance very little, if any work on cell death processes involved in ESR degeneration has been published. Programmed cell death was reported by Lombardi et al (2007) in suspensor cells of the runner bean embryo, which start to degenerate from the neck region to the knob region after the degeneration of the endosperm. Although degeneration of endosperm in the runner bean was not specifically characterised by Lombardi et al (2007), interestingly, a DNA fragmentation is seen in the embryo surrounding region (ESR) in the runner bean in Lombardi et al's work. Although this was not discussed, it could indicate a very active programmed cell death taking place in the ESR. However, what is going on in the other parts of endosperm is not known. Programmed cell death in the *Arabidopsis* ESR during seed development has yet to be analysed, and forms the main subject of this chapter.

3.1.5 Technical approaches for the analysis of PCD

As was mentioned previously, the classical features of programmed cell death in plants include shrinking of the cytoplasm, changing permeability of the plasma membrane, condensation of chromosomes, alteration in nuclear morphology and DNA fragmentation (Reape et al., 2008). Several techniques can be used to characterize these features. Terminal deoxynucleotidyl transferase-mediated dUTP Nick End Labelling (TUNEL) assays are one of the most widely used methods in detection of programmed cell death as they can label the free 3'-OH end of the

nicked DNA in cells undergoing DNA fragmentation *in situ,* which can subsequently be observed by microscopy. The TUNEL system used in this study is called the DeadEnd™ Colorimetric TUNEL System and it is a commercially available kit. It can detect programmed cell death *in situ* at a single cell level. It is used to detect nuclear DNA fragmentation in both tissue sections and cultured cells. The 3'-OH ends of the fragmented DNA are labelled with biotinylated dUTPs by the enzyme Terminal Deoxynucleotidyl Transferase (TdT). Horseradish-peroxidase-labeled streptavidin (Streptavidin HRP) is then bound to these biotinylated dUTPs, and can be detected using the peroxidase substrate, hydrogen peroxide, and the stable chromogen, diaminobenzidine (DAB). Nuclei of cells undergoing DNA fragmentation are stained dark brown. This DeadEnd™ Colorimetric TUNEL System is widely used for detecting apoptosis in human and animal cells and tissues. Examples where this kit has been successfully used include human breast cancer and mouse cancer cell lines (Muraoka-Cook et al., 2007), *Fgf21*-knock down zebrafish embryos sections (Yamauchi et al., 2006), sections of mouse lung tissue (Teder et al., 2002), and rat embryo sections (Arthur et al., 2000).

TUNEL assays in plants are not as widely used as in human and animals, although in recent years, several published studies have used TUNEL assays to characterize programmed cell death in plant cells. The DeadEnd™ Fluorometric TUNEL System is the most commonly used. This system uses fluorescein-12-dUTP to label 3'-OH DNA ends instead of biotin. The fluorescein-12-dUTP-labeled DNA can then be visualized by fluorescence microscopy directly. In wild-type *Arabidopsis* plants, during pollen mitosis, a TUNEL fluorescence positive signal was observed in the tapetal nuclei, which indicates that the degeneration of tapetum is a type of

programmed cell death (Vizcay-Barrena and Wilson 2006). In maize embryo development, a DNA fragmentation was detected by the Fluorometric TUNEL assay in the scutellum layers surrounding the coleoptile at 14 DAP (Giuliani et al., 2002). In tomato protoplasts and leaflets, programmed cell death was characterized by both Fluorometric TUNEL assay and Colorimetric TUNEL assays (Wang et al., 1996). Programmed cell death of inner integument cells during *Brassica napus* seed development was characterized by Fluorometric TUNEL assay (Wan et al., 2002).

Several other methods have been used to look at programmed cell death in plant cells. Staining with Fluorescein diacetate (FDA) in combination with propidium iodide (PI) has been used to distinguish dead and living cells, living cells will actively convert the non-fluorescent FDA into a yellowgreen fluorescent compound; a sign of viability, while the nuclei of membrane-compromised cells stain with PI; a sign of cell death (Harvey et al., 2008b). This FDA/PI staining requires the natural exposure of the cells and is not suitable for cells within the tissues, such as endosperm cells. Using transmission electron microscopy to look at morphological change of sub-cellular organelles in resin embedded cells is another alternative (Greenwood et al., 2005), but this requires specialized equipment, and a level of fixation which is difficult to achieve in the delicate endosperm cells. DNA laddering on agarose/EtBr gel is a classical method to look at DNA fragmentation during programmed cell death, however, this method cannot look at cells *in situ*. Ion leakage is detected by measuring the conductivity of freshly harvested leaves or leaf discs in cell death assays (Coll et al., 2010). Again this method is not suitable for endosperm cells which are enclosed within the developing seed and are impossible to separate

without damage from the surrounding tissues. Analysing cell death marker genes is another alternative way to study programmed cell death.

In animals, caspases which are proteases acting as key components in apoptosis have been studied as the markers for programmed cell death (Tsiatsiani et al., 2011). Plants do not have orthologous caspase genes in their genome, however, plants and fungi metacaspases have been discovered as proteases that are the most related homologues to animal caspases (Bonneau et al., 2008). *Arabidopsis* has 9 metacaspases, and He and colleagues have shown that metacaspase-8 (AtMC8) positively modulates programmed cell death induced by oxidative stresses such UV light and hydrogen peroxide, by analyzing the expression of *AtMC8* and recombinant AtMC8 protein activities during the stresses (He et al., 2008). *Arabidopsis* metacaspase 2d (also known as AtMC4) has recently been shown as a positive mediator of programmed cell death induced by biotic and abiotic stresses, such as bacterial pathogens and oxidative stresses (Watanabe and Lam, 2011). Other plant proteases which have a caspase-like active have been shown to be involved in embryo development (Bozhkov et al., 2003) and seed coat development (Nakaune et al., 2005). Although the expression patterns and the enzyme activities of plant cell death marker proteins have been extensively studied in *Arabidopsis*, there are disadvantages of using these marker proteins to study endosperm cell death. Firstly, different cell death regulators are expressed at different levels in different parts of the plant (He et al., 2008). Secondly, due to the large gene families of plant proteases, some members of the family are involved in programmed cell death, and some members are involved in other cellular processes (Bonneau et al., 2008). Thirdly, and

again due to the technical difficulties, it is not easy to isolate RNA and proteins specifically from endosperm cells.

3.1.6 Background: *ZOU* is a potential cell death regulator

As previously described, in *zou* mutants, after the heart stage, embryos cannot elongate properly and fail to invade into the endosperm (Yang et al., 2008). The *zou* endosperm cells around the embryo do not appear to break down as they do in wild-type. In addition they adhere to the embryo epidermis and there is no empty space between the developing embryo and the endosperm. Both hypocotyls and cotyledons are squashed and forced to expand along the radial axis but not along the longitudinal axis, resulting in a smaller embryo. At maturity the persistent endosperm present in *zou* mutants collapses making a smaller and shrivelled seed (Yang et al., 2008). Based on this phenotype it was proposed that *ZOU* might regulate cell death in the ESR. Moreover, by analyzing the SOLEXA cDNA profiling of *zou* mutants, we identified several genes which were known cell death regulators as being either up or down-regulated in *zou* mutants seeds compared to wild-type. For example, two known negative regulators of cell death, *DOX1* and *LOL2* which are negative regulators of plant cell death (De León et al., 2002; Petra Epple et al., 2001) were found to be up-regulated in *zou* mutants.

3.1.7 Aims of this chapter

The aims of this chapter are to visualise cell death in the *Arabidopsis* ESR and to ascertain whether there is an altered cell death programme in *zou* mutant ESR. In additional I have examined whether *ZOU* might be involved in other cell death pathways in *Arabidopsis*.

3.2 Results

3.2.1 Visualisation of Programmed cell death in the endosperm of wild-type plants and *zou* mutants by colorimetric TUNEL assays

As previously described, in *zou* mutants, after the heart stage, embryos cannot elongate properly and fail to invade into endosperm (Yang et al., 2008). The *zou* endosperm cells around the embryo do not appear to break down as they do in wild-type. In addition they adhere to the embryo epidermis and there is no empty space between the developing embryo and the endosperm. Both hypocotyls and cotyledons are squashed and forced to expand along the radial axis but not along the longitudinal axis (Yang et al., 2008). In order to find out whether the squashed *zou* embryos are caused by the persistence of endosperm cells around the developing embryo which lacks programmed cell death and physically inhibits the elongation of the embryos, it is first necessary to ascertain whether programmed cell death can be detected in the ESR of wild-type seeds. Colorimetric Terminal deoxynucleotidyl transferase-mediated dUTP Nick End Labelling (TUNEL) assays were performed on Col-0 wild-type plants and *zou-4* mutant seeds. Colorimetric TUNEL is used to detect nuclear DNA fragmentation which is the typical feature of programmed cell death in both tissue sections and cultured cells (Concetta Giuliani, 2002; Harvey et al., 2008a; Lombardi et al., 2003; Vizcay-Barrena and Wilson, 2006). The free 3'-OH ends of the nicked DNA can be labelled with biotinylated dUTPs by the enzyme Terminal Deoxynucleotidyl Transferase (TdT). Horseradish-peroxidase-labelled streptavidin (Streptavidin HRP) is then bound to these biotinylated DNA, which can be detected by using the peroxidase substrate, hydrogen peroxide, and the stable chromogen, diaminobenzidine (DAB) giving rise to a dark brown colour. Nuclei of cells which

contain fragmented DNA with free 3'-OH ends are stained dark brown and can be visualized by light microscopy.

In wild-type plants, at the globular stage, the endosperm is not yet cellularized and the free nuclei are distributed along the peripheral endosperm from the micropylar zone to the chalazal zone. In Figure 3.1 A and C (arrows), chromagen stained nuclei in the endosperm of wild-type plants at the globular stage are shown. This might suggest nuclear DNA in the endosperm is undergoing fragmentation as early as the globular stage of embryogenesis. In *zou* mutants at the globular stage (Figure 3.1B and D), a lighter staining of nuclei compared to the wild-type in endosperm was observed suggesting that in *zou* mutants less DNA fragmentation is occurring. After the heart stage, the hypocotyls and the cotyledons of wild-type plants start to elongate and accumulate storage nutrients. The endosperm of the wild-type plants start to break down providing nutrients and space for the growing embryo, so there is an empty space between the embryo and the endosperm. Dark staining of the nuclei of the endosperm cells around the embryo are observed in wild-type plants (Figure 3.1 E, G and I, arrows), which suggests that the endosperm cells around the developing embryo are undergoing active programmed cell death.

In *zou* mutants, at the early torpedo stage very few nuclei in the endosperm surrounding region were stained, with the exception of occasional staining of endosperm just near the tip of the cotyledons and some staining in the peripheral endosperm (Figure 3.1 F). This weak staining suggests the considerably less DNA fragmentation occurs in the ESR of *zou* mutants than in wild-type plants. After the late torpedo stage, the defects in *zou* endosperm break-down and embryo elongation have become more severe. Wild-type embryos at this stage have fully elongated and

properly bent; the endosperm of wild-type plants has almost totally degraded and chromogen stained endosperm nuclei in the remaining cells are rarely observed (Figure 3.1 K). However, at the maturing stage *zou* mutants embryos cannot elongate and bend to the chalazal zone. *zou* endosperm cells around the embryo are persistent and adhesive, leaving no space between the embryo and the endosperm (Figure 3.1 J and L). Chromagen stained nuclei can be observed in the peripheral endosperm of *zou* mutants but not in the cells around the embryos, suggesting *zou* has a defect in degrading endosperm cells, and especially the cells surrounding the embryo (Figure 3.1 J, arrows). As a positive control (Figure 3.1 M), samples were treated with DNase I to create artificial DNA fragmentation. Chromagen stained dark brown nuclei were universally observed in suspensors (Figure 3.1 M, red arrow head), embryos (Figure 3.1 M, red arrow), endosperm cells (Figure 3.1 M, green arrow heads) and the seed coat (Figure 3.1 M, black arrow).

To summarize, TUNEL assays on wild-type and *zou* seeds show that DNA fragmentation occurs in the endosperm during wild-type seed development and less DNA fragmentation occurs in *zou* mutant endosperm.

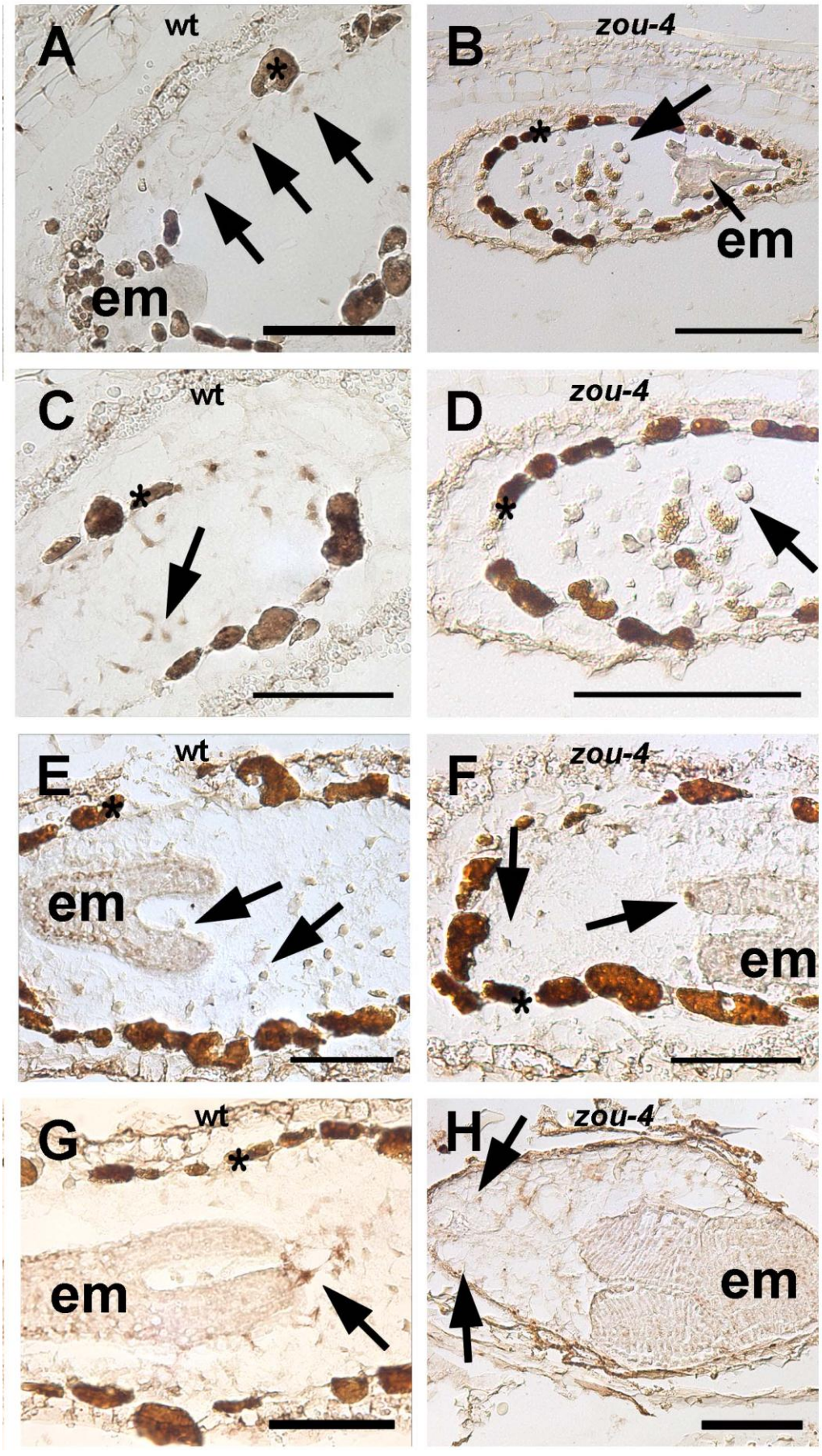
A
wt
em
B
zou-4
em
C
wt
D
zou-4
E
wt
em
F
zou-4
em
G
wt
em
H
zou-4
em

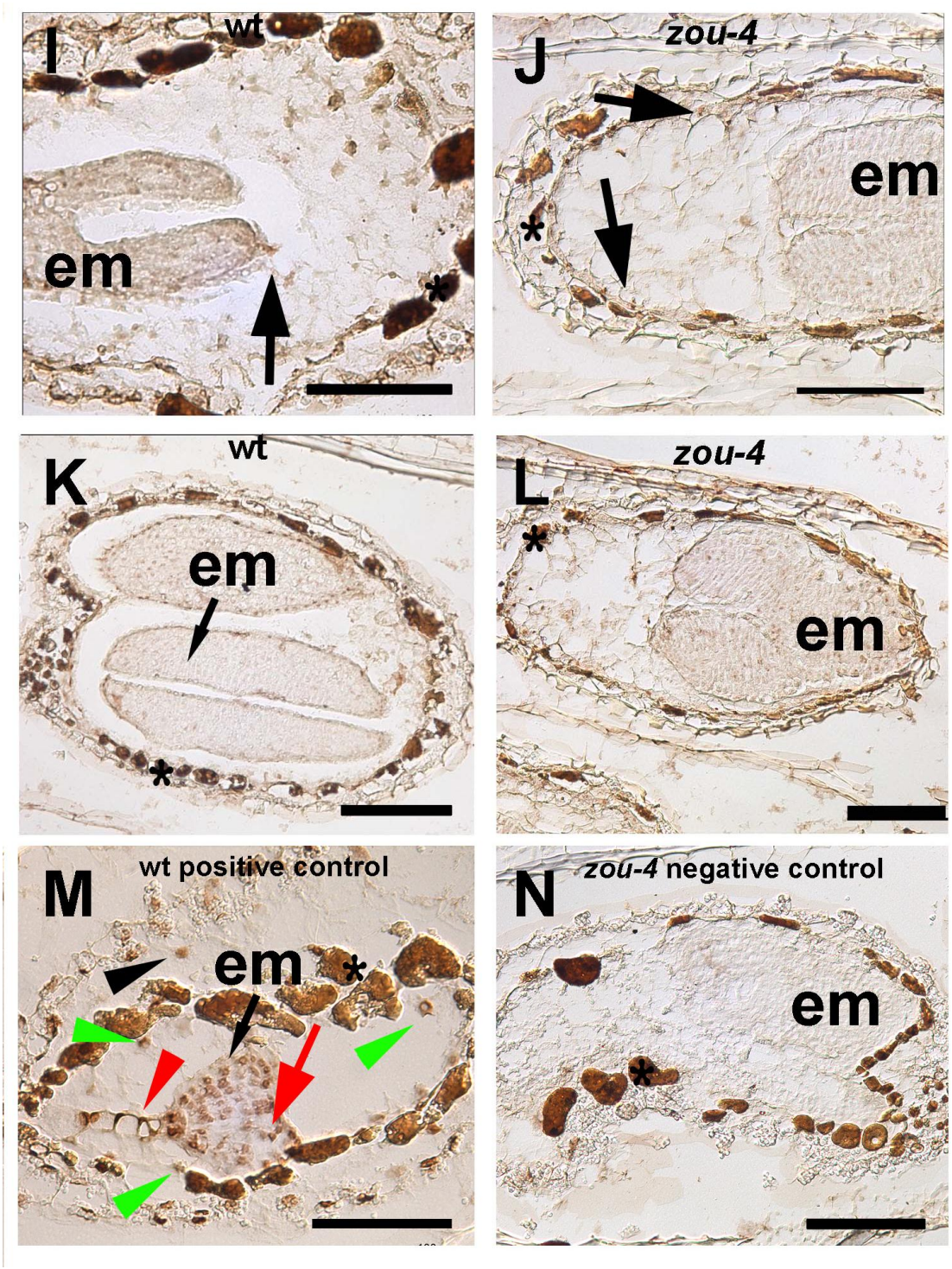
I
wt
em
*
J
zou-4
em
*
K
wt
em
*
L
zou-4
*
em
M
wt positive control
em
*
N
zou-4 negative control
em
*

Figure 3.1 DNA fragmentation in endosperm in wild-type plants and *zou* mutants by colorimetric TUNEL assays

A, C, E, G, I, K and M are wild-type seeds. B, D, F, H, J, Land N are *zou-4* mutants. A to D, globular stage embryo; E and F, early torpedo stage embryo; G to I, and N, torpedo stage embryo; J and K, maturing stage embryo; M, heart stage embryo. M, positive control, samples were treated with DNase I to create artificial DNA fragmentation in the nuclei; the red arrow head indicates the nuclei in the suspensor cells, the red arrow indicates the nuclei in the embryo cells, the green arrow heads indicate the nuclei in the endosperm cells, and the black arrow indicates the nuclei in the seed coat cells. N, negative controls were treated without adding Terminal Deoxynucleotidyl Transferase during the labeling reaction. Photos were taken under differential interference contrast (DIC) microscopy. In A to J, black arrows without labelling indicate the chromagen stained nuclei in endosperm. Asterisks indicate endothelium which was stained as background peroxidase activity. em, embryo; scale bar represents 100 μm.

3.2.2 Programmed cell death during seed coat development and embryo development in wild-type plants by colorimetric TUNEL assays

In this study, colormetric TUNEL assays were used to explore the cell death of testa cells. During the ovule development, the outer and inner integuments expand to cover the embryo sac forming five cell layers. This cell-layer arrangement is

maintained post fertilization and the layers are indicated by the numbers 1 to 5 in Figure 3.2 B and C. Cell layers 1 and 2 (oi1 and oi2) are from the outer integument of the ovule. Layer 1 (oi1) is the epidermis of the seed. Cells of this layer synthesize and secrete the mucilage which will later contribute to forming the volcano-shaped epidermal cells (Figure 3.2 E and F). Layer 2 (oi2), which is called palisade, produces a thickened wall on the inner tangential side of the cell (Figure 3.2 F). Both outer integument layers accumulate starch-containing amyloplasts during the growth phase which can be seen in Figure 3.2 B as transparent crystals. All these features make the outer integument easily distinguishable from the inner integument layers. Layers 3 to 5 are from the inner integument (ii3 to ii5), chromagen stained dark brown nuclei are observed in layer 3 and 4 (ii3 and ii4, Figure 3.2 B and C, indicated by arrow heads). This TUNEL staining might come from the fragmented nuclear DNA formed during the programmed cell death which has previously been shown to occur in the cells of the ii2 and ii3 layers in *Arabidopsis* by TEM (Nakaune et al., 2005). Most cells of ii5 layer (the endothelium) are occupied by dark brown mass composed of flavonoids and other metabolites (Figure 3.2 B and C). During the heart- stage (Figure 3.2 D), as mucilage deposition continues, the vacuole of the epidermal cells contracts making the volcano-shaped epidermal cells more distinguishable. The ii3 and ii4 layers have collapsed. During the mature stage (Figure 3.2 E and F), the oi2 cell layer crushes to the epidermis. By the end of embryo development, all cell layers die and crush together leaving only the endothelium and the epidermis. In *zou* mutants, TUNEL labelled nuclei were also observed in the ii3 and ii4 cell layers (data not shown), showing that *zou* mutants do not have defect in testa programmed cell death. To summarize, my results support

previously published data showing that programmed cell death demonstrated by DNA fragmentation during testa development first occurs in the inner integuments.

The suspensor is part of the embryo which derives from the basal cell of the two-cell embryo proper. It connects the embryo proper to the maternal organism and absorbs nutrients and growth regulators from the endosperm cavity which are required by the developing embryo (Kawashima and Goldberg, 2010). By embryo maturity, the suspensor degenerates and disappears and, with the exception of the uppermost cell (the hypophysis, which is incorporated into the root meristem), it does not contribute to the postembryonic morphogenesis. Here I observed chromagen stained dark brown nuclei which indicated fragmented DNA in the suspensor cells of both wild-type seeds (Figure 3.2 G and H, arrows) and *zou* mutant seeds (data not shown) during late heart stage and early torpedo stage. These results suggest that programmed cell death in suspensor cells is very active during late heart stage and early torpedo stage, and also support the hypothesis that *ZOU* is only involved in controlling the programmed cell death specifically in the endosperm.

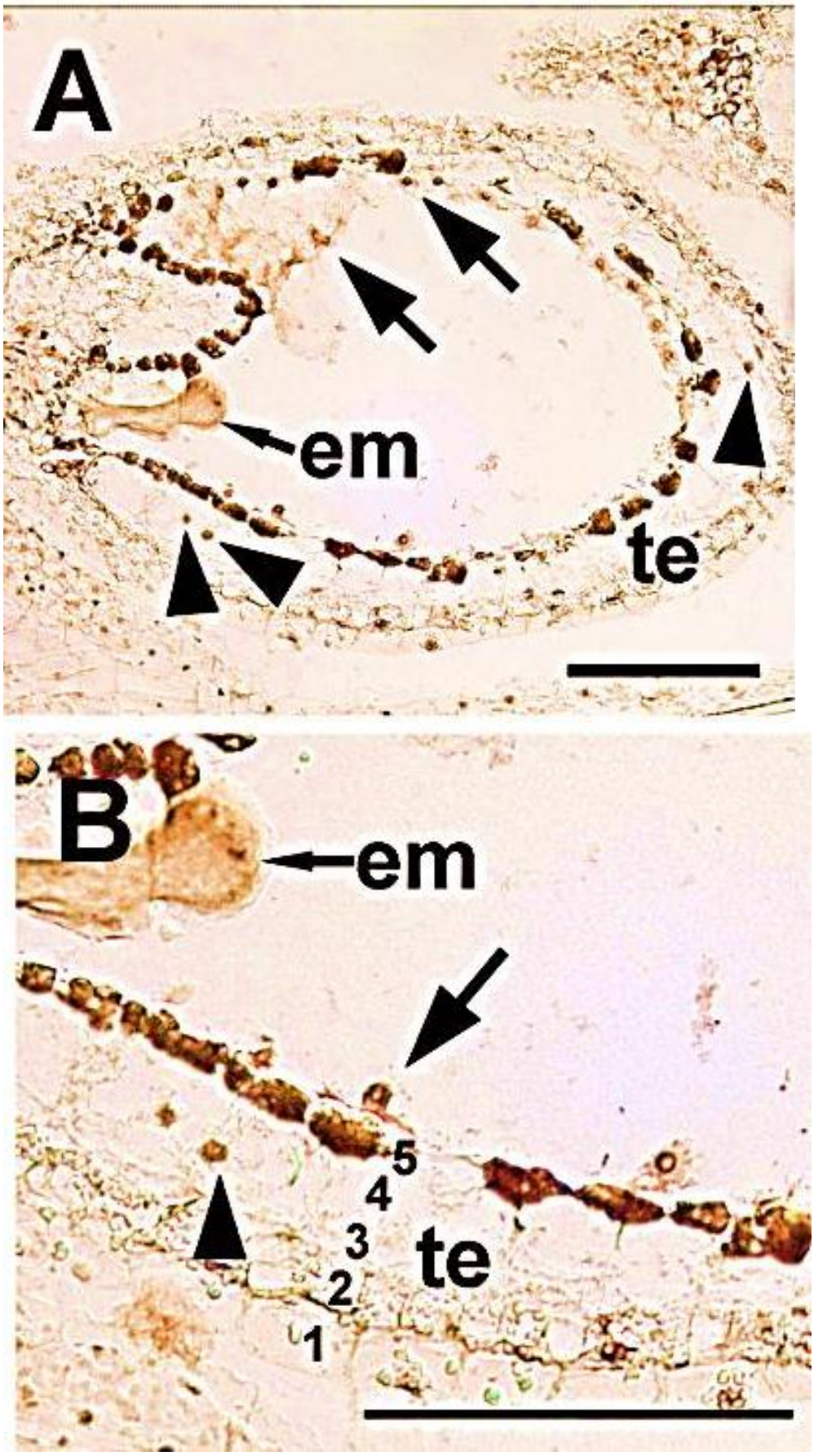
A
em
te
B
em
5
4
3
2
1
te

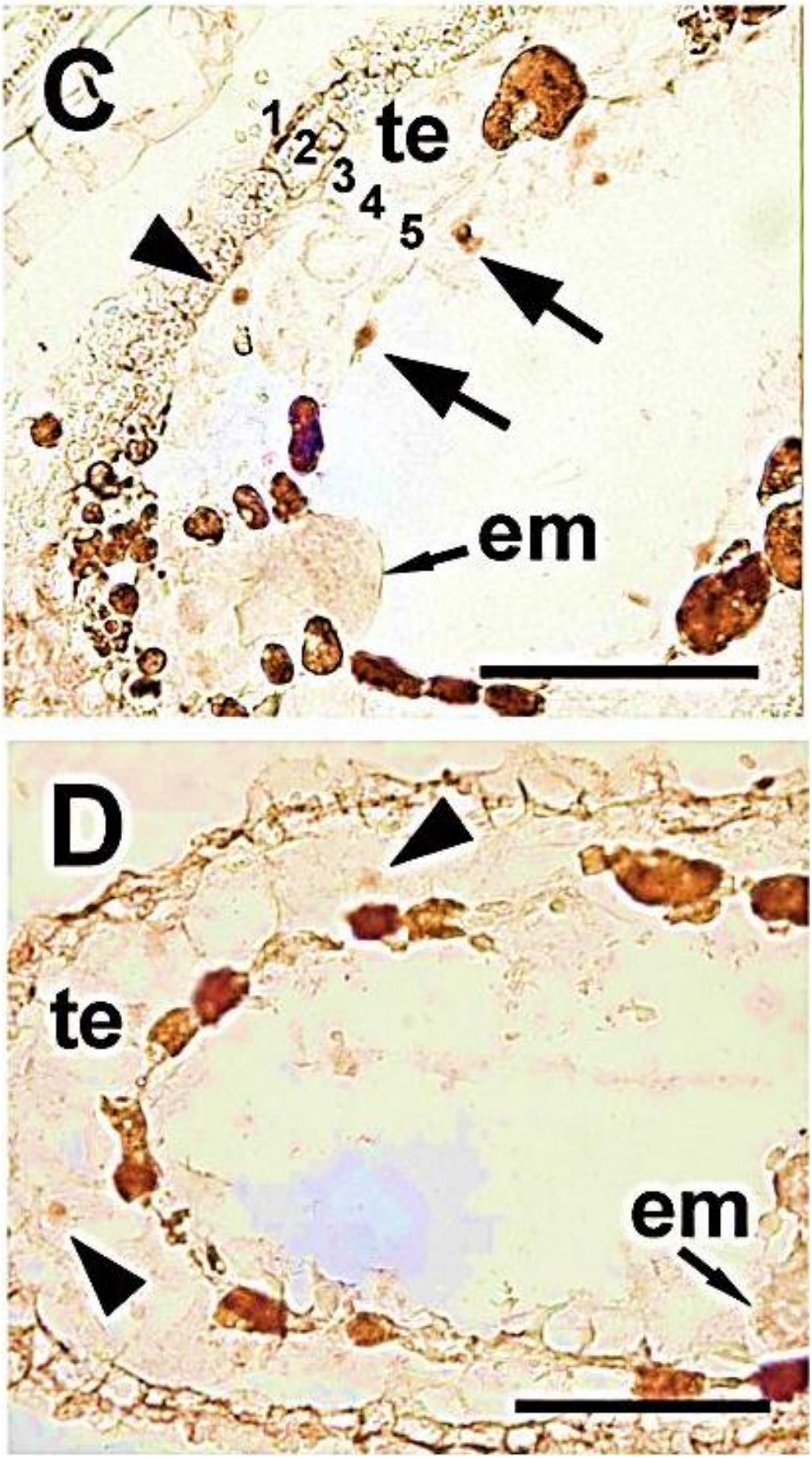
C
1
2
3
4
5
te
em
D
te
em

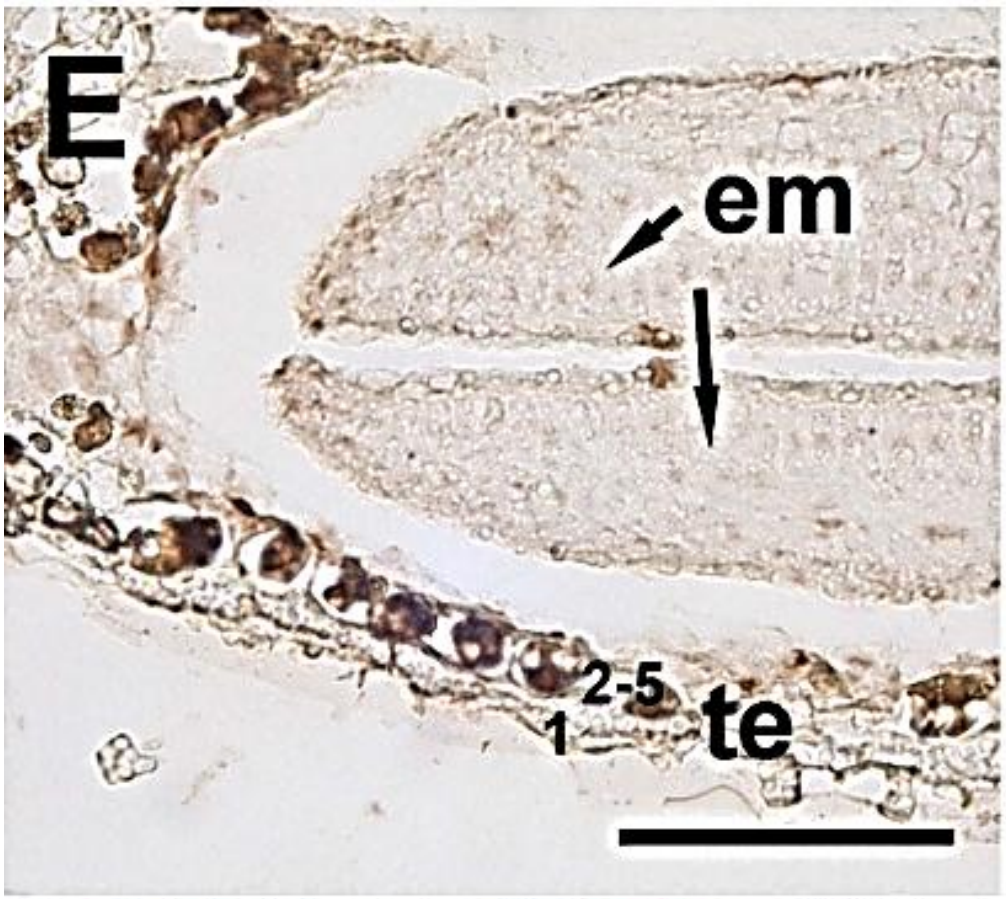
E
em
2-5
1
te

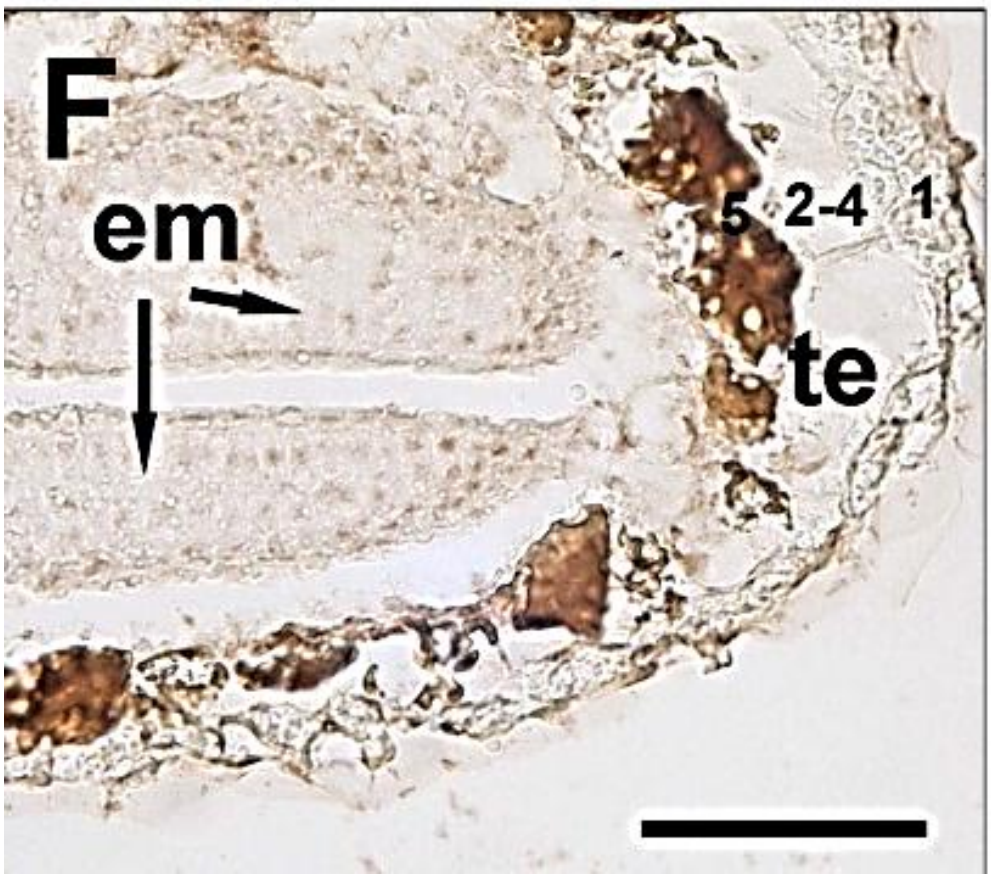
F
em
5
2-4
1
te

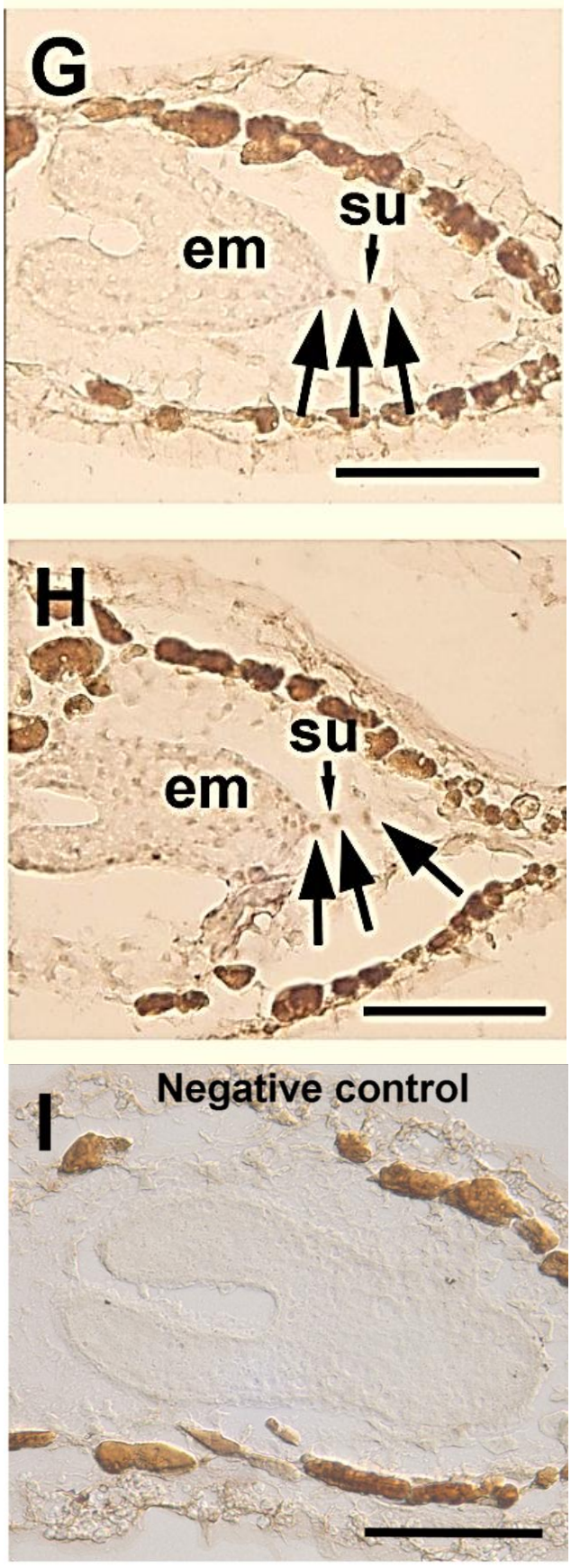
G
su
em
H
su
em
I
Negative control

Figure 3.2 Programmed cell death during seed coat development and embryo development in wild-type plants by colorimetric TUNEL essays.

A to C, globular stage; D, heart stage; E and F, late torpedo stage; G and H early torpedo stage. I, negative control in torpedo stage. A, wax embedded globular stage ovule, arrow heads point to the nuclei of the testa cells, which were stained dark brown by insoluble chromagen produced by DeadEndTM Colorimetric TUNEL kit, indicating that testa cells were undergoing programmed cell death. Arrows point to the chromagen stained nuclei in endosperm which were also going through programmed cell death. B, zoom in of A, number 1-5 marked the cell layers of the testa, outer integument (labelled by number 1 and 2), inter integument (labelled by number 3-5). Arrow head is pointing to a dark brown nuclear in an inner integument cell indicating that during globular stage programmed cell death initiates from the inner integument. C, another globular stage ovule, programmed cell death was observed in the outer-most layer of inner integument (number 3) as indicated by arrow head. Stained endosperm cells were labelled by arrows. D, programmed cell death was observed in the inner integument during heart stage. E, F, during late torpedo stage, inner integument cells have already died and collapse in to one layer (number 2-5), leaving only the epidermal cells of the outer integument (1). G, H, chromagen stained nuclei were observed in suspensor cells shown by arrows, indicating programmed cell death in suspensors. I, Negative controls were treated without adding Terminal Deoxynucleotidyl Transferase during the labeling reaction. Photos were taken under differential interference contrast (DIC) microscopy. em, embryo; te, testa; su, suspensor; scale bar represents 100 μm.

3.2.3 *zou* mutants do not show differences in plant senescence or bacterial pathogen induced hypersensitive response compared to wild-type plants

The expression of *ZOU* suggests that it has a seed specific role. However it was important to test whether *ZOU* might play roles either in other developmental programmes involving cell death, or in cell death programmes induced in response to wounding or pathogen attack. In order to test whether *zou* mutants have delayed whole plant senescence, *zou-4* mutants and Col-0 wild-type plants were grown side by side in the growth room. At early developmental stages, *zou* mutants are smaller than wild-type plants (Figure 3.3 A). Three weeks later, the differences in size between *zou* and wild-type are not obvious (Figure 3.3 B), and in fact *zou* plants tend to produce more rosette leaves than wild-type plants, possibly due to the delay in their early development. At later stages, *zou* mutants senesce similarly to wild-type (Figure 3.3 C). There was no difference observed in rosette leaf senescence between *zou-4* mutants and the wild-type plants (Figure 3.3 D).

Developmental senescence is a progressive process; even in a senescing leaf the progress of each cell is not synchronous. Dark induced leaf senescence is one method used to induce synchronous leaf senescence which can be characterized by losing chlorophyll (Guo and Gan, 2006). In my study, rosette leaves that were at the same developmental stage from *zou-4* mutants and wild-type plants were excised and placed in the dark for 4 days. There were no visible differences in chlorophyll loss observed between *zou-4* and wild-type (Figure 3.3 E). Taken together these results suggest that consistent with the lack of *ZOU* expression outside the seeds, *zou* mutants do not show defects in either natural senescence or dark induced senescence.

During plant-pathogen interaction, plants have developed a set of mechanisms to recognize the invasion and protect themselves from pathogen attack (Hann et al., 2010). When *Arabidopsis* (Col-0) are challenged by the bacteria *Pseudomonas syringae* expressing the avirulence proteins/effectors *avrB* or *avrRps4*, the plants can recognize the effector via the activity of a specific R-protein and activate the innate immune system which causes the hypersensitive response. This pathogen triggered hypersensitive response is a type of localized programmed cell death which can restrain the spreading of the disease (Nishimura and Dangl, 2010). In order to test whether *zou* has a defect in pathogen activated programmed cell death, both *zou-4* mutants and wild-type plants rosette leaves were challenged with avirulent bacteria *Pseudomonas syringae pv tomato* DC3000 *avrRps4* and *avrB* at low and high concentrations (OD_{600} 0.02 and 0.2). Programmed cell death was monitored 72 h after challenging (Figure 3.3 F and G). Both *zou* mutant leaves and wild-type leaves developed hypersensitive response against *Pseudomonas syringae pv tomato* DC3000 *avrRps4* and *avrB* as indicated by the formation of lesions on leaves. In $MgCl_2$ treated (control) leaves, neither *zou* nor wild-type developed lesions. Taken together, these results suggest that *zou* mutants do not have defect in pathogen induced hypersensitive response.

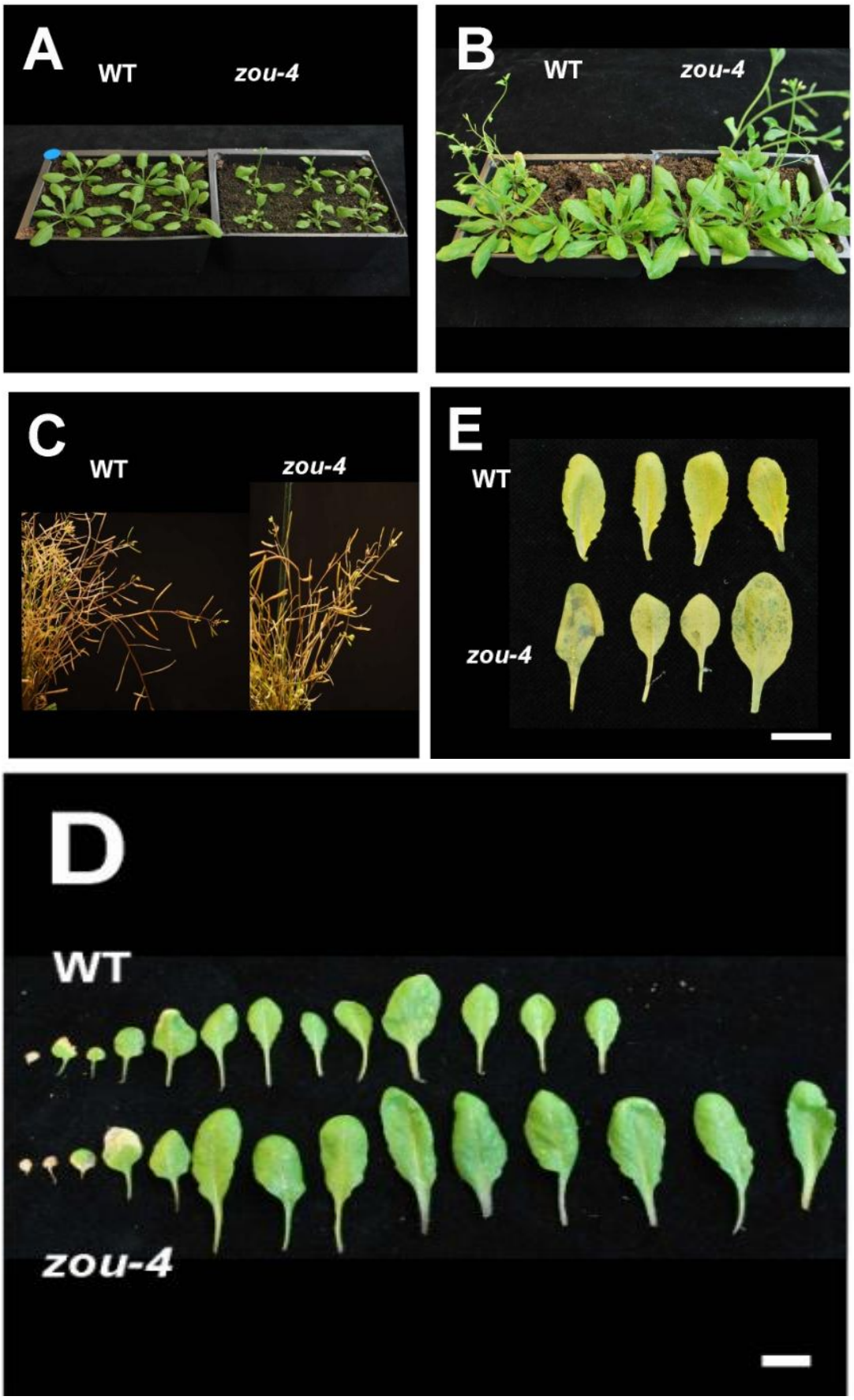
A
WT
zou-4
B
WT
zou-4
C
WT
zou-4
E
WT
zou-4
D
WT
zou-4

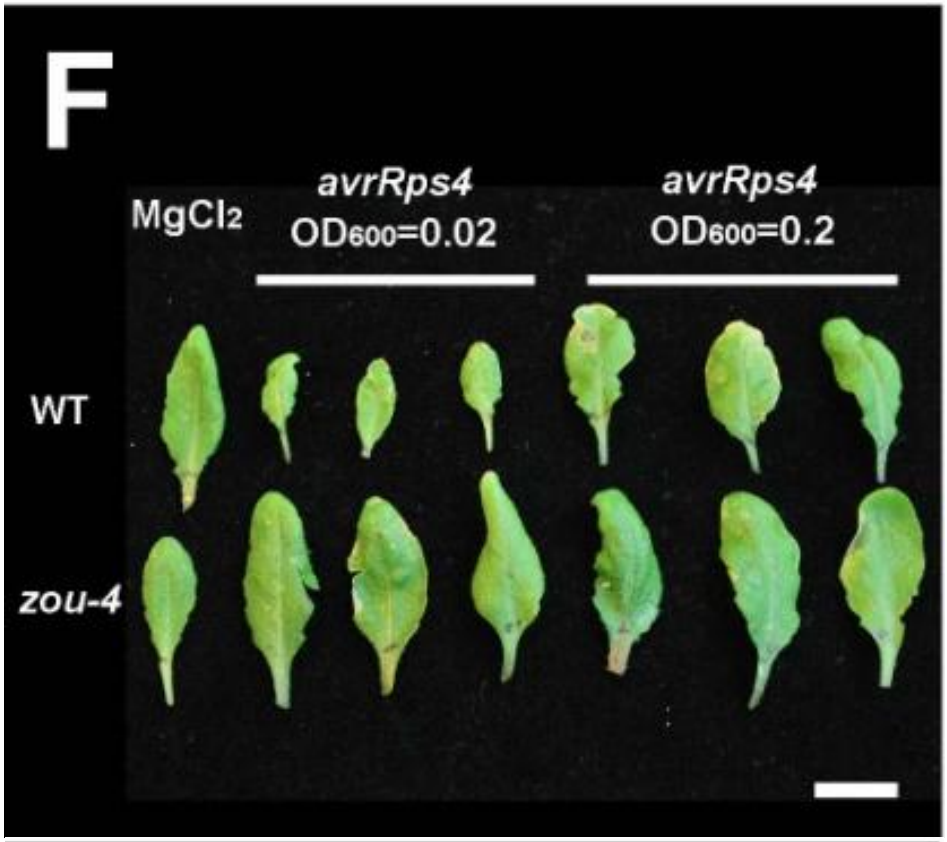
F
MgCl2
avrRps4
OD600=0.02
avrRps4
OD600=0.2
WT
zou-4

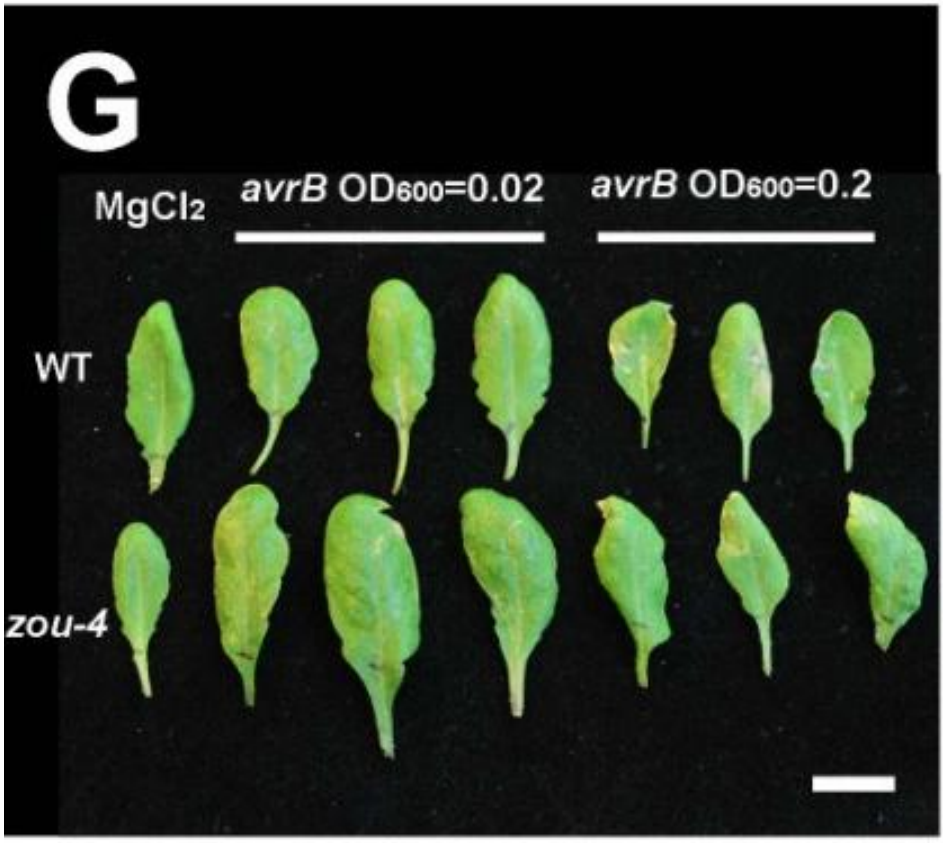
G
MgCl2
avrB OD600=0.02
avrB OD600=0.2
WT
zou-4

Figure 3.3 Plant senescence and avirulent pathogen induced hypersensitive response in wild-type plants and *zou-4* mutants

A, early stages of plant development in wild-type plants (left) and *zou-4* mutants (right); B and C, whole plant senescence in wild-type plants (left) and *zou-4* mutants (right) at four-week-old (B) and eight-week-old (C); D, rosette leaf senescence in wild-type plants (upper) and *zou-4* mutants (lower); E, dark induced rosette leaf senescence in wild-type plants (upper) and *zou-4* mutants (lower), the sixth rosette leaf of each plant counted from the bottom to the top were excised; F and G, rosette leaves challenged by bacteria pathogen *Pseudomonas syringae avrRps4* (F) and *avrB* (G) after 72 h in wild-type plants (upper) and *zou-4* mutants (lower). Scale bars represent 2 cm.

3.2.4 *ZOU* expression cannot be ectopically activated outside the seeds by pathogen treatment and wounding

Although pathogen challenge results suggested that *zou* mutants had a normal HR response, we wished to confirm that *ZOU* expression was not ectopically activated by pathogens outside the seeds. Both *zou-4* mutant and wild-type rosette leaves were challenged with the avirulent bacteria *Pseudomonas syringae pv tomato* DC3000 *avrRps4* and *avrB*. RNA samples were extracted from the infected rosette leaves and leaves above the infected leaves at 12 h and 24 h. *ZOU* expression cannot be detected by RT-PCR analysis in the infected leaves at 12h (Figure 3.4 A) or 24 h, or in the leaves above the infected leaf at 24 h (Figure 3.4 B). As a positive control, RNA was extracted from the siliques that grew under the same conditions but without pathogen challenging. *ZOU* expression was detected in siliques containing globular stage and heart stage embryos. As a negative control, *ZOU* expression was checked in rosette

leaves of non-challenged plants and in $MgCl_2$ treated rosette leaves. In neither case was *ZOU* expression detected. In order to test whether *ZOU* expression can be ectopically activated outside the seeds by wounding, rosette leaves were cut several times but without cutting the leaves off. RNA was made from the wounded leaves at 24 h. *ZOU* expression could not be detected in the wounded leaves (Figure 3.4 B). In addition, *ZOU* expression was also tested in senescing rosette leaves, however, again, *ZOU* expression could not be detected (Figure 3.4 A). To summarize, *ZOU* expression cannot be ectopically activated during basal defense and systemic acquired defense against *Pseudomonas syringae*. Neither can *ZOU* expression be ectopically activated by wounding. *ZOU* is therefore unlikely to be involved in the effector triggered immune system or wounding responses.

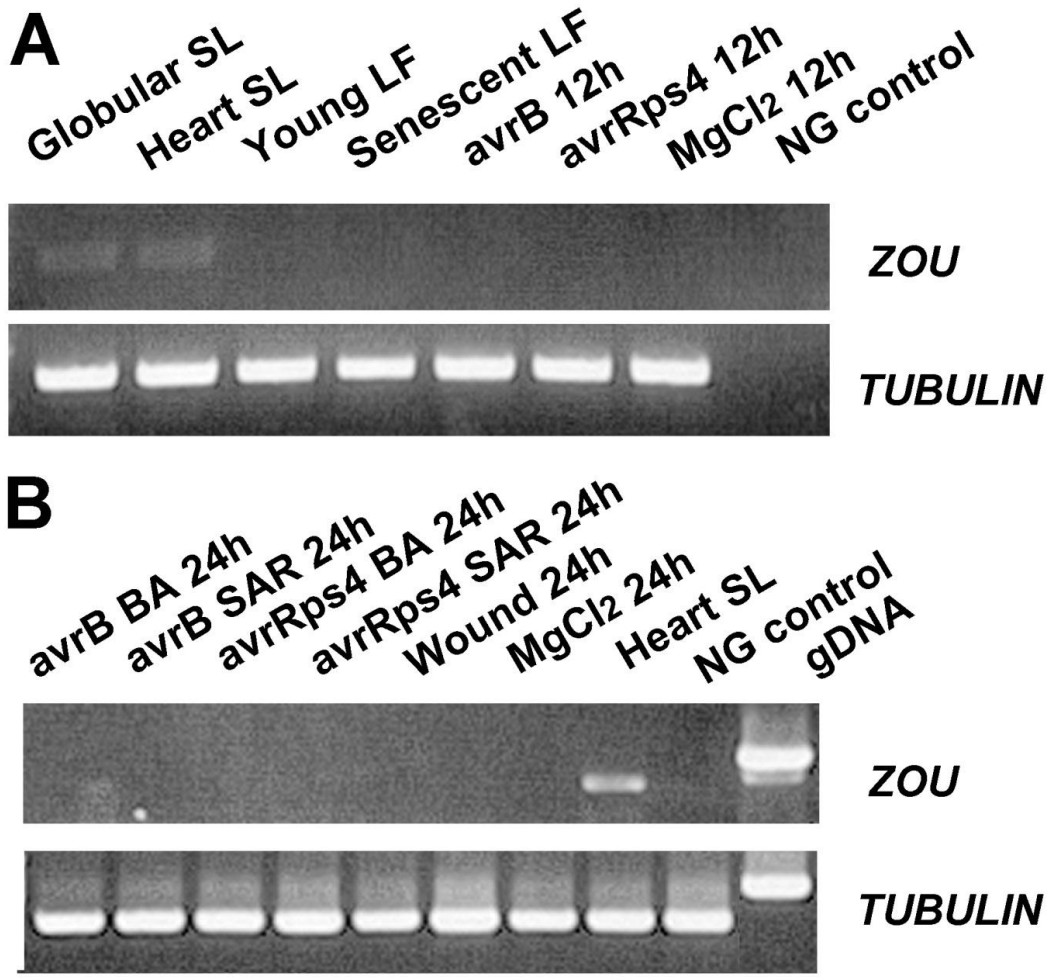
A
Globular SL
Heart SL
Young LF
Senescent LF
avrB 12h
avrRps4 12h
MgCl2 12h
NG control
ZOU
TUBULIN
B
avrB BA 24h
avrB SAR 24h
avrRps4 BA 24h
avrRps4 SAR 24h
Wound 24h
MgCl2 24h
Heart SL
NG control
gDNA
ZOU
TUBULIN

Figure 3.4 RT-PCR analysis of expression of *ZOU* in wild-type plants under biotic or abiotic stress

A, upper lane, RT-PCR analysis of *ZOU* expression in (from left to right) globular stage siliques, heart stage siliques, young rosette leaves, senescent rosette leaves, rosette leaves infiltrated by bacterial pathogen *Pseudomonas syringae avrB* at 12 h, rosette leaves infiltrated by bacterial pathogen *Pseudomonas syringae avrRps4* at 12 h, rosette leaves infiltrated with 10mM $MgCl_2$ at 12 h and negative control for PCR with H_2O as the template; lower lane, RT-PCR analysis of *TUBULIN* expression under the same conditions. B, upper lane, RT-PCR analysis of *ZOU* expression in (from left to right) rosette leaves infiltrated by *Pseudomonas syringae avrB* at 24 h (to test for BA, basal defence), rosette leaves above the *avrB* infiltrated leaves at 24 h (to test for SAR, systemic acquired resistance), rosette leaves infiltrated by *Pseudomonas syringae avrRps4* at 24 h, rosette leaves above the *avrRps4* infiltrated leaves at 24 h, scissors wounded rosette leaves at 24 h, rosette leaves infiltrated by 10 mM $MgCl_2$ at 24 h, heart stage siliques, negative control for PCR with H_2O as the template, positive control for PCR with gnomic DNA as the templates; lower lane, RT-PCR analysis of *TUBULIN* expression under the same conditions.

3.3 Discussion

In order to investigate whether the persistent endosperm in *zou* mutant was caused by defects in programmed cell death, I first looked at the programmed cell death in the ESR of wild-type seeds. TUNEL assays suggest that in the wild-type in the endosperm DNA fragmentation initiates as early as the globular stage of embryogenesis, and that after the heart stage of the embryogenesis active DNA fragmentation occurs in the ESR accompanied by the disappearance of the ESR cells. By the mature stage, ESR cells have disappeared and no DNA fragmentation can be observed. By contrast, *zou* mutants have less DNA fragmentation occurring in the ESR from the globular stage of embryogenesis to the torpedo stage of embryogenesis. By the mature stage, no DNA fragmentation is observed in the persistent ESR cells in *zou* mutants, except for a weak DNA fragmentation in the peripheral endosperm. Taken together, *zou* mutants have defects in programmed cell death in the ESR during the embryogenesis, indicated by a lack of nuclear DNA fragmentation.

Programmed cell death during seed development has been studied in different species and with different methods (Andème Ondzighi et al., 2008; Bozhkov et al., 2003; Concetta Giuliani, 2002; Greenwood et al., 2005; Lombardi et al., 2003; Sreenivasulu et al., 2006; Suarez et al., 2004; Wan et al., 2002; Young and Gallie, 2000a; Young and Gallie, 2000b). For example, in maize, programmed cell death was observed in the nuclei of the scutellum layers surrounding the coleoptile, in the coleoptiles and in the root cap by TUNEL essays from 14 to 27 DAP (Concetta Giuliani, 2002). During these developmental stages in maize, there was no programmed cell death observed by TUNEL assays in the ESR and the starchy endosperm (Concetta Giuliani, 2002). So far there has also been no evidence of DNA

fragmentation in the endosperm cells in *Arabidopsis*. In my study, in wild-type *Arabidopsis* DNA fragmentation was observed in the endosperm as early as globular stage of the embryogenesis (about 2 DAP), and there was a very active DNA fragmentation in the ESR during early torpedo stage of the embryogenesis (about 6 DAP), and the DNA fragmentation disappeared as the ESR was consumed (so did the nuclei). The difference in endosperm DNA fragmentation between maize and *Arabidopsis* may be because of the general difference between cereal seed development and that of dicots. In cereals the ESR starts to differentiate by the completion of endosperm cellularization (i.e. at about 4 DAP), and as the embryo develops the ESR cells shrink, so that by 12 DAP the ESR has almost disappeared, leaving only vestigial remnants at the bottom of the endosperm (Sabelli and Larkins, 2009). In *Arabidopsis*, DNA fragmentation in the ESR lasts until the mature embryo stage. This difference between cereals and *Arabidopsis* may also suggest a difference in the function of the ESR.

A second point of note is that cereals have a starchy endosperm which accumulates starch granules and storage proteins. This takes up the majority of the seed volume at maturity, and during germination the starchy endosperm cells break down providing nutrients for the germinating embryo (Olsen, 2004). In *Arabidopsis*, nutrients are stored in the expanding embryo and the endosperm degrades through programmed cell death. Therefore, it has been suggested that the cell death in cereal starchy endosperm, which has a nutrient storage function, and that in the *Arabidopsis* ESR, which mainly has a role in nutrient recycling and space creation, are regulated through different mechanisms.

TUNEL assays also showed DNA fragmentation occurring during testa development and in the suspensor cells in both wild-type seeds and *zou* mutant seeds. Suspensors have been used as a model to study programmed cell death. DNA fragmentation in the maize suspensor was detected by TUNEL assays at 14 DAP (Concetta Giuliani, 2002), and DNA fragmentation has also been observed in suspensors in runner bean (*Phaseolus* coccineus) and Norway spruce somatic embryos by TUNEL assays (Bozhkov et al., 2003; Lombardi et al., 2003). Blanvillain et al. (2011) report that in *Arabidopsis*, the occurrence of suspensor programmed cell death varies among different genetic backgrounds, and that in Col-0 plants the last stage at which the suspensor is visible is at the bent-cotyledon stage, which is consistent with my observation that DNA fragmentation in the suspensor occurred from the late heart stage of embryogenesis until the early torpedo stage of embryogenesis. Taken together, my results suggest that DNA fragmentation occurs during *Arabidopsis* seed development in the embryo suspensor, the seed coat and the endosperm at different developmental stages. However, only one of these processes is affected in *zou* mutants suggesting that *ZOU* is likely involved in the endosperm programmed cell death specifically.

ZOU is specifically expressed in the ESR (Yang et al., 2008) and *ZOU* expression cannot be ectopically activated by pathogen challenges and wounding outside the seeds. These results suggest that *ZOU* functions only in the seeds. I have shown that *zou* mutants do not show defects of programmed cell death in non-embryonic organs. Neither do *zou* mutants show differences in hypersensitive response upon pathogen attack, or in senescence, compared to the wild-type plants. Again these results indicate *ZOU* controls endosperm cell death exclusively.

Cysteine proteases are believed to play a role in plant cell death in response to environmental and developmental cues (van der Hoorn, 2008). During the castor bean (*Ricinus communis* L.) seed development, ricinosomes which are the precursors of protease vesicles containing a cysteine protease CysEP were observed during the programmed cell death of the nucellar cells that are adjacent to the expanding endosperm (Greenwood et al., 2005). It is suggested that the CysEP might have a function in digesting the nucellar cells and the digesting products might be taken up by the growing endosperm. Other type of proteases that have been extensively studied in programmed cell death are caspases, and in animals the caspases are hallmarks for apoptotic cell death (van Doorn, 2011a). However, in plants no caspase homolog have been identified (Bonneau et al., 2008). Norway spruce VEIDase was discovered to process a caspase-like activity, and this caspase-like activity has been suggested to play an important role in programmed cell death during embryo pattern formation (Bozhkov et al., 2003). Vacuolar processing enzymes (VPEs) have been designated as a novel family of cysteine protease (Hatsugai et al., 2004; Nakaune et al., 2005). Tobacco VPEs are expressed in the vegetative organs and play a key role in virus-induced hypersensitive response (Hatsugai et al., 2004), whilst *Arabidopsis* δVPE is specifically and transiently expressed in the inner integument (ii2 and ii3 layer) during early seed development and has an role in seed coat programmed cell death (Nakaune et al., 2005). *ZOU* encodes a basic helix-loop-helix (bHLH) class transcription factor, which preferably binds to E-box (5'-CANNTG-3') and G-box (5'-CACGTG-3') promoter elements (Toledo-Ortiz et al., 2003). By analysing the whole transcriptome profiling of *zou* mutants and the wild-type, we did not see any caspase-like proteases regulated by *ZOU* at the transcription level except for the

substilisin-like serine protease ALE1 which does not appear to have functions in cell death (Tanaka et al., 2001). However, we cannot rule out the possibility that *ZOU* regulated transcripts which are below the limits of detection of our experiment could encode peptides or proteases involved in cell death regulation.

Two known negative regulators of plant programmed cell death, *DOX1* and *LSD1* were up-regulated in *zou* mutants, which fits the facts that *zou* mutants have less cell death than the wild-type. Moreover, in *zou* mutants the JA signalling pathways and the ethylene signalling pathways were significantly down-regulated, as were genes annotated as being involved in disease resistance including those encoding 6 TIR/NBS/LRR proteins and WRKY 22, 40 and 54. Furthermore a cluster of genes implicated in REDOX homeostasis were also down-regulated. Our experimental data fit with the key features of Love et al.'s (2008) criteria for the definition of autophagic cell death. Firstly, the cell death in the endosperm is a progressive and slow form of cell death. Secondly, according to our SOLEXA sequencing results *zou* mutants have down-regulated JA, ethylene and REDOX signalling pathways whereas genes that were involved in SA signalling did not show significant changes in expression compared between the wild-type and *zou* mutants. Although the TUNEL assays have provided some evidence on programmed cell death in endosperm during embryogenesis, transmission electron micrographs of programmed cell death in *zou* and wild-type endosperm are still missing, as the morphological features are often used in literature to classify the programmed cell death (van Doorn et al., 2011b). This would be a valuable complement to the work described in this chapter.

To conclude, *zou* mutants have a dramatic defect in programmed cell death during seed development. The relationship between this defect and the defect in embryonic

epidermal cuticle development also seen in *zou* mutants will be dissected in more detail in the following chapter.

4 Genetic dissection of *ZOU* function by endosperm specifically expressing *ALE1*

4.1 Introduction

4.1.1 SOLEXA whole transcriptome sequencing reveals that *ZOU* regulates genes involved in cuticle biogenesis

Angiosperm seed development requires the coordinated growth of the testa, endosperm and embryo. In the model species *Arabidopsis thaliana*, during seed development, the testa undergoes proliferation, expansion and programmed cell death, the endosperm is transient and undergoes proliferation, cellularization and breakdown by programmed cell death, and the embryo undergoes proliferation and differentiation to set up the body plan of the seedling. By the mature stage of seed development the dormant embryo takes almost all the space inside the testa leaving only one cell layer of endosperm tissue surrounding the embryo. Previous members of our lab identified a mutant, *zhoupi* (*zou*) which has persistent endosperm and a smaller embryo at the mature stage, and epidermal cuticle defects in cotyledons (Yang et al., 2008). *ZOU* was cloned and shown to encode a predicted bHLH transcription factor with an ESR specific expression pattern.

In order to identify the developmental pathways that are regulated by *ZOU*, SOLEXA whole transcriptome sequencing of wild-type and *zou* siliques were performed. In the SOLEXA datasets we identified several genes which have previously been shown known to be involved in cuticle biosynthesis or cuticular wax transportation. Two *GDSL-LIPASE*s (*AT1G71250* and *AT5G03820*) were found to be down-regulated in *zou* mutants. These two *GDSL-LIPASE*s are predicted to be

expressed in the endosperm and might have a function in hydrolysing very long-chain fatty acids and their derivatives during cuticular wax biosynthesis (Takahashi et al., 2010; Zimmermann et al., 2004). One plasma membrane associated ABC transporter gene (*AT3G47780*) was also down-regulated in *zou* mutants, and the plasma membrane associated ABC transporters have been shown to be involved in cutin/wax transportation from the cytosol to the apoplastic space (Pighin et al., 2004) . In addition, a gene encoding a GPI-membrane anchored protein *FLA5* which was predicted to be expressed in the testa was up-regulated in *zou* mutants, and the GPI-membrane anchored proteins were implied to be involved in wax secretion to the cell wall and cell wall signalling (Caffall and Mohnen, 2009). Taken together with the *zou* phenotype these data support the possibility that *ZOU* may be required for cuticle biogenesis.

4.1.2 *ABNORMAL LEAF SHAPE1* (*ALE1*) is regulated by *ZOU*

Among the *ZOU* regulated genes identified by SOLEXA sequencing, *ABNORMAL LEAF SHAPE1* (*ALE1*) had previously been identified as a potential *ZOU* target. In the SOLEXA dataset, *ALE1* expression was 5-fold down-regulated in *zou* siliques compared to the wild-type, which was consistent with a 5-fold decrease in expression previously shown by Q-PCR analysis (Yang et al., 2008). *ALE1* encodes a subtilisin-like protease (subtilase, SBT), which contains a N-terminal signal peptide, S8 protease domain with catalytic residues in the order Asp, His and Ser, and a C-terminal domain likely be processed during protein maturation (van der Hoorn, 2008). In *Arabidopsis*, 56 subtilase genes have been identified. According to the protein structure these 56 genes are divided into six subfamilies, expressed in different organs, subcellularly localized in different organelles, and have diverse but likely

overlapping functions (Rautengarten et al., 2005). Forward genetic screen has identified a developmental role for *STOMATAL DENSITY AND DISTRIBUTION 1* (*SDD1*) which encodes a subtilisin-like Ser protease. *SDD1* is highly expressed in stomatal mother cells, and the protein is likely to be secreted to the apoplastic space and associated with the plasma membrane (von Groll et al., 2002). When *SDD1* function is lost, plants display disrupted stomatal patterning including clustered stomata and increased stomatal density (von Groll et al., 2002). It is suggested that SDD1 cleaves an inactive precursor peptide activating the peptide which functions as a ligand for the receptors, one of which could be the transmembrane leucine-rich repeat (LRR) receptor-like protein TOO MANY MOUTHS (TMM), and subsequently activates the downstream MAPK cascades via the mitogen-activated protein kinase kinase (MAPKK) kinase YODA (YDA) to supress stomata proliferation (Shpak et al., 2005).

Also identified by forward genetic screen, *ALE1* was also first identified in a forward genetic screen, and shown to control embryonic cuticle development (Tanaka et al., 2001). By RNA in situ hybridizations, *ALE1* expression was only detected in the ESR and the signal was detectable from the early globular stage of embryo development onwards (Tanaka et al., 2001). Publically available microarray data from the *Arabidopsis* eFP browser shows that *ALE1* expression is very low at the globular embryo stage, at the heart stage *ALE1* expression increases sharply by 200 times, and after the heart stage it gradually decreases to the same level as that in the globular stage of embryo development (Winter et al., 2007). *ale1* mutants display embryo cuticle defects. During early embryo development the embryo surface cannot separate from the surrounding endosperm and during late embryo development some

regions of cotyledons are fused. TEM analysis showed that *ale1* mutants had discontinuities in the cuticle layer on the surface of developing embryos (Tanaka et al., 2001). After the germination, *ale1* mutants displayed fused cotyledons and leaves and the young seedlings were very sensitive to desiccation. It was suggested that ALE1 protein could be secreted to the apoplast and might be required for processing some signal peptides in the endosperm which act as ligands for receptors and act in a non-cell autonomous manner to control embryo epidermal cuticle development (Rautengarten et al., 2005; van der Hoorn, 2008). However, by what mechanism *ZOU* regulates *ALE1* in controlling embryonic epidermal cuticle formation is still not known.

4.1.3 Visualization of epidermal cuticle defects by using Toluidine Blue

Epidermal cuticle can be visualized by TEM, which requires fixation, staining with osmiun tetroxide, embedding, ultrathin sectioning, and finally transmission electron microscopy (Yang et al., 2008). This process is laborious and slow and is not suitable for examining large numbers of samples. Alternatively, cuticle permeability can be visualized by staining with toluidine blue (Tanaka et al., 2004). Toluidine blue is a hydrophilic dye which is commonly used for histological staining. The plant cuticle consists of a hydrophobic cutin and wax matrix which is not permeable to water-soluble molecules, such as Toluidine Blue. Thus if plants have a discontinuous cuticle the internal cell walls of the organ affected are exposed and can be stained by Toluidine Blue giving patchy blue staining. If plants have a complete loss of the cuticle layer, the underlying organ can be completely stained by Toluidine Blue showing all-over dark blue colouration (Tanaka et al., 2004). Toluidine Blue tests have been applied to *ale1* mutants, which have defects in embryonic epidermal

cuticle development, giving patchy staining patterns in cotyledons. *fiddlehead* (*fdh*) mutants which have a defect in cuticle biosynthesis, show complete dark blue staining in young leaves when treated with toluidine blue. Other cuticle biosynthesis mutants such as *cer5, cer14* and *cer19* showed patchy or complete dark blue staining in leaves (Tanaka et al., 2004).

Toluidine Blue has also been used as precipitate to extract radiolabeled anionic glycoconjugates such as proteoglycans and glycosaminoglycans which originate from cellulose or other extracellular matrices, based on the fact that Toluidine Blue can form dissociable complexes with anionic glycoconjugates and can be precipitated by ethanol (Terry et al., 2000). The absorption spectrum of Toluidine Blue dissolved in water shows a single strong peak at 626 nm (Merrill and Spencer, 1948), suggesting that the concentration of Toluidine Blue can be quantified by using a spectrophotometer.

4.1.4 *AtSUC5*: an ESR expressed gene which is not regulated by *ZOU*

During the initial analysis of *ZOU* function, a study of several different ESR-specific genes was carried out in order to understand whether *ZOU* regulates ESR identity *per se,* or only a subset of genes expressed in the ESR. A gene encoding a sucrose transporter, *AtSUC5* had previously been investigated with the aim of identifying genes involved in endosperm nutrient transportation to the developing embryo (Baud et al., 2005). *AtSUC5* expression was detected in roots, leaves, flowers and siliques. During seed development the expression started to increase at 4 DAF (early globular stage of embryo development), reached its maximum at 6 DAF (late heart stage of embryo development) and decreased gradually there after (Baud et al., 2005). RNA

microarray analysis from the *Arabidopsis* eFP browser showed that *AtSUC5* was expressed in imbibed seeds, flowers and pollen and highly expressed in seeds. The expression was already detectable at the globular stage, reached its maximum at the heart stage of embryo development, and gradually decreased afterwards. However, *AtSUC5* expression was only detectable at very low levels in roots and leaves (Winter et al., 2007) (Figure 4.1). By RNA in situ hybridizations of seed, *AtSUC5* transcripts were detected exclusively in the ESR from globular stage to heart stage of embryo development. From the torpedo stage to U-shape stage of embryo development *AtSUC5* transcripts were not limited to the ESR but the whole endosperm (Baud et al., 2005).

Baud et al. analysed the activity of a 1.5 kb fragment of the *AtSUC5* promoter activity by fusing it with the *mGFP5-ER* gene. *pAtSUC5::mGFP5-ER* was expressed in the endosperm from the globular stage to the torpedo stage, and the expression decayed at the U-shape stage of embryo development, which was consistent with the expression pattern in RNA in situ hybridizations (Baud et al., 2005). *atsuc5* mutants displayed a transient reduction in fatty acid concentration in the seeds at 8 DAF (U-shape stage of embryo development) and a minor delay in embryo development, suggesting that *AtSUC5* may have a role in seed nutrient transportation from the endosperm to the embryo which is necessary for normal embryo development (Baud et al., 2005).When tested by real time qRT-PCR, *AtSUC5* expression was not affected in *zou* seed (Yang et al., 2008).

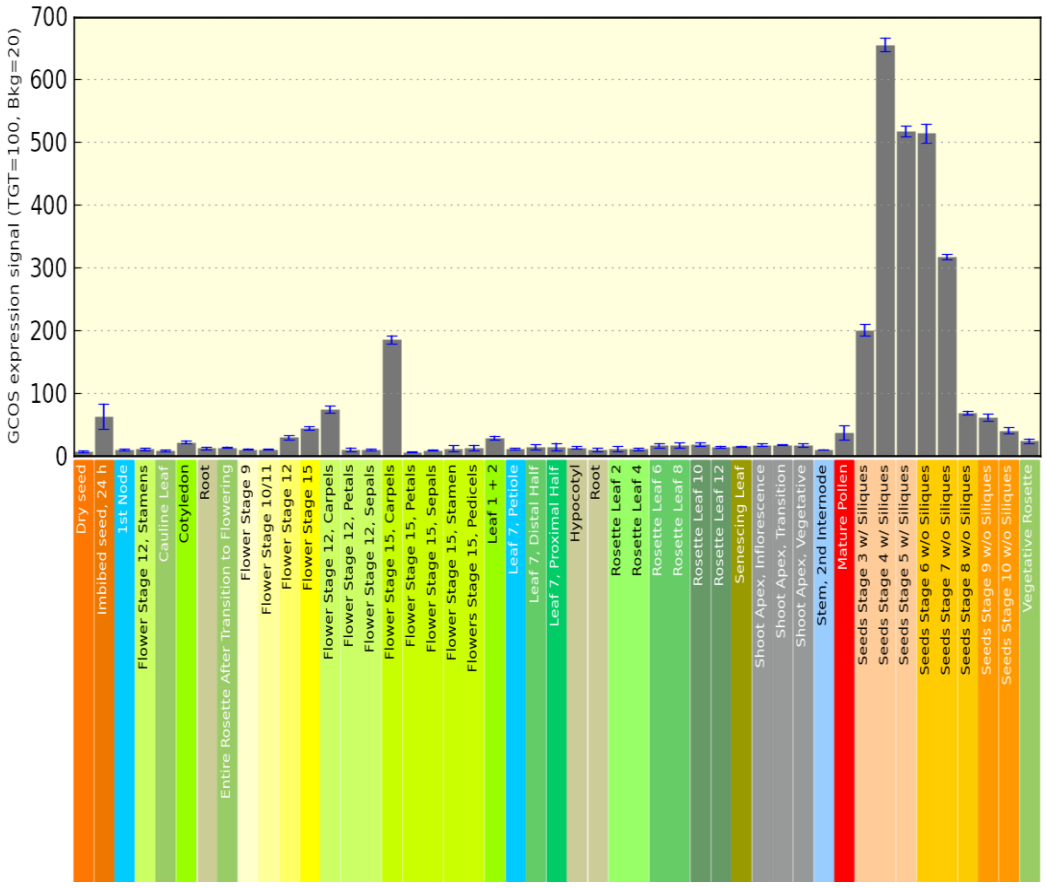

Figure 4.1 *AtSUC5* expressions by ATH1 GeneChip analysis (Schmid et al., 2005)

The X axis represents the gene ontology categories and the Y axis represents the *AtSUC5* expression signals calculated by GCOS 1.0 software (Affymetrix). Seed age is indicated by embryo development; seed stage3, globular stage; seed stage 4, early heart stage; seed stage 5, late heart stage; seed stage 6, torpedo stage; seed stage 7, walking-stick stage; seed stage 8 and 9; curled cotyledons (U-shape); seed stage 10, green cotyledons (Winter et al., 2007).

4.1.5 Two hypotheses for *ZOU* function

There are two possibilities that could explain *ZOU* function (Figure 4.2). Firstly, *ZOU* might regulate endosperm breakdown in a cell autonomous manner. Subsequently the breaking down endosperm might send signals to the developing embryo which are required for normal cell wall/cuticle formation, or physically provide space for cuticle specification (Figure 4.2 A). Alternatively, *ZOU* might regulate endosperm breakdown in a cell autonomous manner, whilst in a parallel pathway regulating cell wall/cuticle development in a non-cell autonomous manner, with both pathways being indispensable for normal embryo development (Figure 4.2 B).

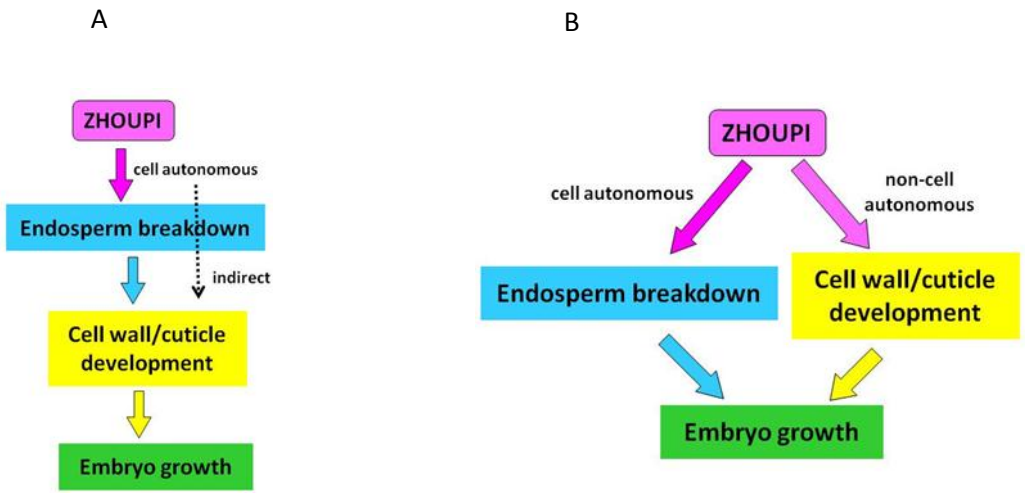

Figure 4.2 Two possible models for *ZOU* function

A, *ZOU* regulates endosperm cell breakdown in a cell autonomous manner. Endosperm breakdown subsequently affects embryo cell wall/cuticle formation and embryo growth. B, *ZOU* regulates endosperm cell breakdown and cuticle formation in two independent pathways.

4.1.6 Aims of this chapter

The aims of this chapter were to test the hypothesis that *ZOU* might regulate endosperm breakdown and epidermal cuticle development via one pathway, or whether alternatively *ZOU* might regulate endosperm breakdown and embryonic epidermal cuticle development via two independent pathways. To achieve this goal, the *ZOU* target *ALE1* was specifically expressed in the endosperm of *zou* mutants by using the *ZOU*-independent and largely endosperm specific *AtSUC5* promoter. If both the *zou* endosperm cell death phenotype and embryonic cuticle phenotype were rescued, it would suggest that *ZOU* regulates *ALE1*, endosperm breakdown and embryonic cuticle formation in one pathway. If only the *zou* embryonic cuticle phenotype was rescued, it would suggest that embryonic cuticle formation is not dependent upon endosperm breakdown and that *ZOU* regulates two independent developmental processes: endosperm breakdown (independently of *ALE1*), and cuticle formation (*via* an *ALE1*-dependent pathway).

4.2 Results

4.2.1 *ale1* mutants have defects in seed development

In order to better understand the role that loss of *ALE1* plays in the *zou-4* phenotype, detailed phenotypic analysis of *ale1* mutants was performed. 48% of *ale1-1* mutant seeds (186 out of 391) are abnormally shaped (Figure 4.3 C, arrows), and 52% of the *ale1-1* mutants have normal seed shape (Figure 4.3 C, arrow head). The abnormal seeds of *ale1-1* (Figure 4.3 D) are bigger than *zou-4* mutant seeds and in contrast, not shrivelled (Figure 4.3 B), but are rounder than wild-type seeds (Figure 4.3 A). To determine the origins of this seed shape defect, DIC images of the cleared wild- type and *ale1-1* seeds were examined. At the early torpedo stage, there is no difference in embryo development between *ale1-1* and wild-type. After the torpedo stage *ale1-1* starts to display abnormality. In wild-type after the torpedo stage the hypocotyl of the embryo elongates from the micropylar zone and pushes the growing cotyledons to bend to the chalazal zone (Figure 4.3 E), during germination the testa ruptures from the micropylar zone and the radicle protrudes from the rupture site. In the abnormal seeds of *ale1-1* mutant plants, after the torpedo stage the hypocotyl elongates, but the growing cotyledons cannot bend from the micropylar zone to the chalazal zone since they appear to adhere to the endosperm. Instead, the cotyledons bend to the micropylar zone (Figure 4.3 H). In contrast, in *zou-4* mutants after the torpedo stage the hypocotyl and the cotyledons cannot elongate and bend. The embryo appears to be squashed into the micropylar zone and the chalazal zone is occupied by the persistent endosperm (Figure 4.3 F).To summarize, *ale1* mutants do not display the same seed phenotype as that of *zou-4* mutants.

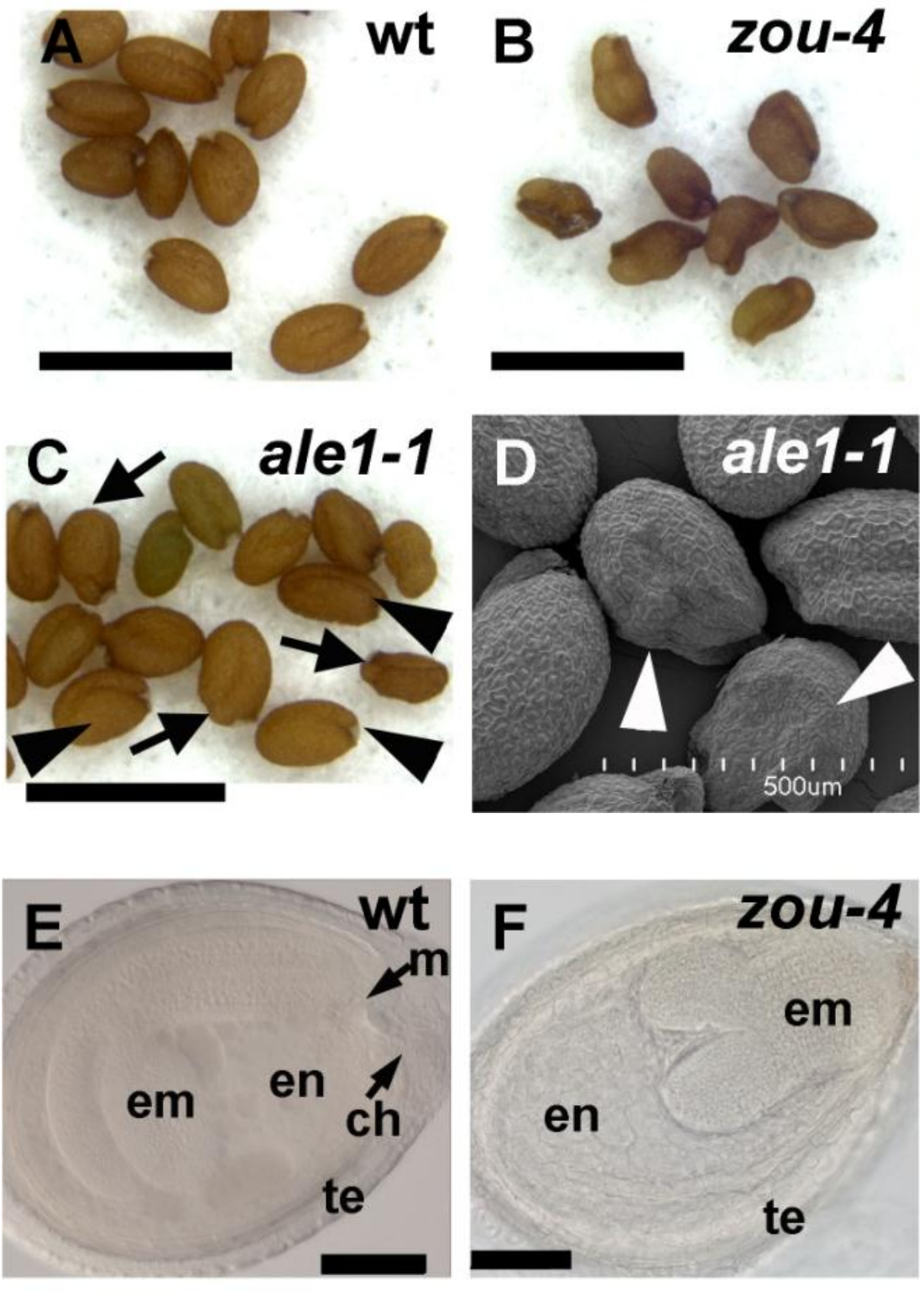
A
wt
B
zou-4
C
ale1-1
D
ale1-1
500um
E
wt
m
em
en
ch
te
F
zou-4
em
en
te

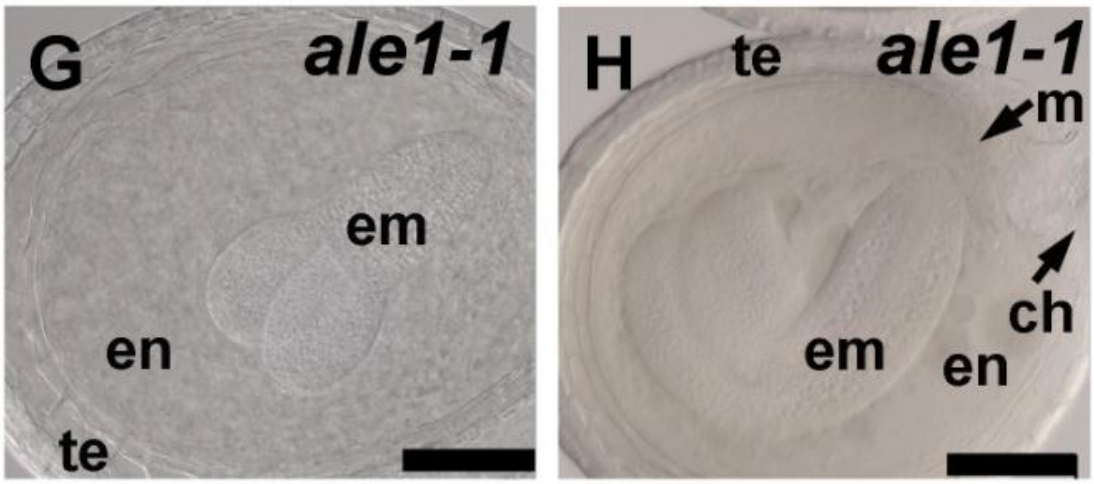

Figure 4.3 *ale1* mutants have defects in embryo development

A and E: wild-type seeds. B and F: *zou-4* mutant seeds. C-H: *ale1-1* mutant seeds. C, arrows indicate the abnormal seed shape phenotype of *ale1-1*, arrow heads indicate the wild-type seed shape phenotype of *ale1-1*. D, scanning electron microscopy (SEM) image of *ale1-1* dry seeds, arrow heads indicate the abnormal seed shape of *ale1-1*. E-H, cleared seeds viewed using DIC microscopy, E, F and H, late torpedo stage embryo, G, early torpedo stage embryo. m, micropylar zone, ch, chalazal zone, em, embryo, en, endosperm, te, testa. A-C scale bars represent 1 mm, D scale bar represents 500 µm, E-H scale bars represent 100 µm.

4.2.2 *ale1* mutants have no obvious defects in endosperm breakdown

As has been shown in the previous chapter, *zou* mutants have defects in endosperm breakdown. TUNEL assays showed that *zou* mutants have less nuclear DNA fragmentation in the ESR, which was shown by fewer chromagen stained nuclei in *zou* endosperm cells, especially in the ESR (Figure 4.4 B) in contrast to the wild-type

in which the nuclei in the ESR were strongly stained suggesting an active DNA fragmentation in those cells (Figure 4.4 A, arrows). In order to test whether the abnormal embryo development in *ale1-1* was caused by defects in endosperm breakdown in the ESR, TUNEL analysis was carried out in *ale1-1* seeds. During the early (Figure 4.4 C) and the late torpedo stage (Figure 4.4 D), chromagen stained nuclei were observed in the ESR in *ale1-1* in the same way as in wild-type seeds (Figure 4.4 C and D, arrows). These results suggest that it is unlikely that *ale1-1* has defects in endosperm breakdown in the ESR. This result is in agreement with microscopic analysis of *ale1-1* mutant seeds, in which no persistent endosperm was ever observed during late seed development or at seed maturity, suggesting that *ALE1* does not have a role in endosperm cell death.

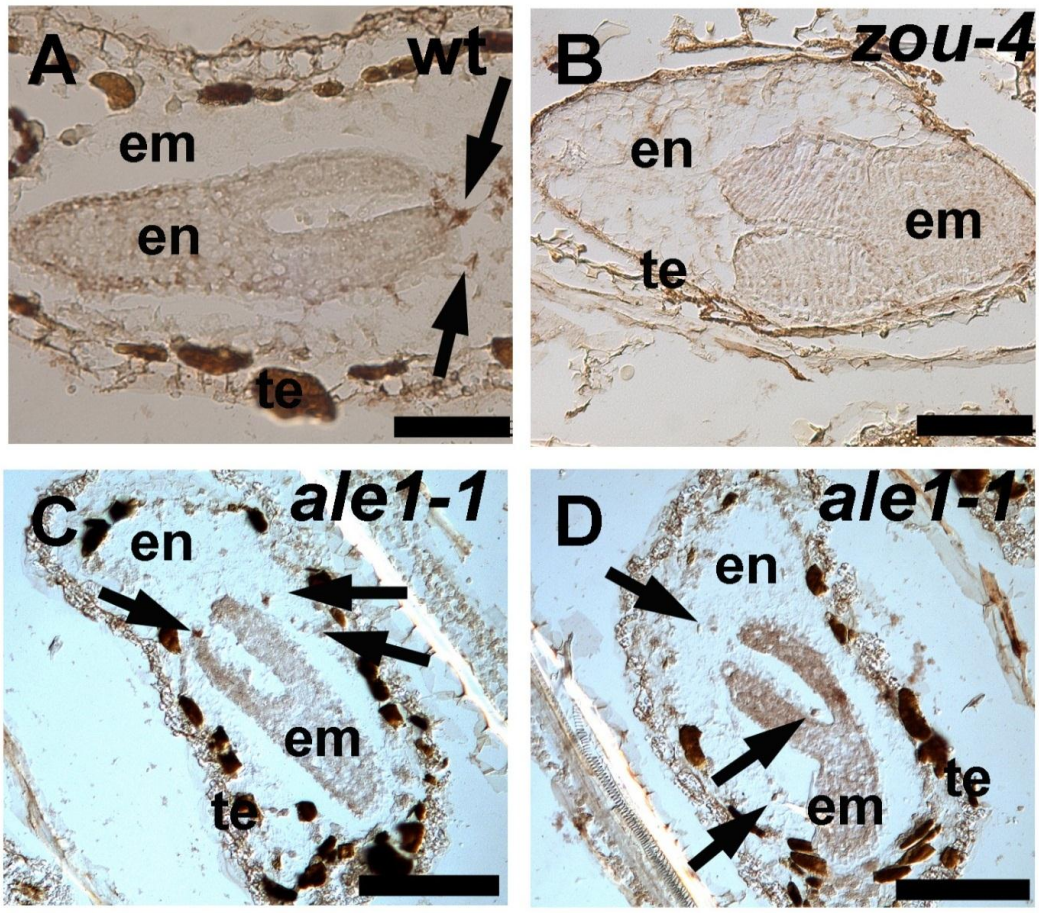

Figure 4.4 *ale1-1* mutants do not have defects in endosperm cell death

A-D, wax embedded torpedo stage embryo in Colorimetric TUNEL analysis. A, wild-type seed, arrows indicate the fragmented DNA in the nuclei which was stained dark brown by chromogen. B, *zou-4* mutants have defects in endosperm cell death, showing persistent endosperm cells and no chomagen stained nuclei in the ESR. C and D, *ale1-1* mutants do not show persistent endosperm cells and chromogen stained nuclei (arrows) were observed in the ESR. m, micropylar zone, ch, chalazal zone, em, embryo, en, endosperm, te, testa. E-L scale bars represent 100 µm.

4.2.3 *ale1* mutants have defects in embryonic epidermal development

ale1-1 in a Landsberg *erecta* (L*er*) background has been shown to produce embryos with fused cotyledons and which adhere to the endosperm during development (Tanaka et al., 2001). Moreover, young seedlings are extremely sensitive to desiccation because of the defective cuticle production on their cotyledons. However, if the young seedlings germinate in highly humid conditions, and are later transferred to soil, they survive and their true leaves have a normal cuticular structure, suggesting that the cuticle defects are derived from abnormalities during embryogenesis. The *ale1-1* allele was backcrossed 5x out of the *Ler* background into Col-0 by Hirokazu Tanaka. He then kindly provided us with the resulting seeds. I analysed the *ale1-1* cuticle phenotype in the Col-0 ecotype. In our growth conditions, the young *ale1-1* seedlings are healthier than previously described in the L*er* background (Tanaka et al., 2001), and tolerant to desiccation tests (data shown later).

In wild-type plants, germination can be divided into two physically distinct stages. First the testa at the micropylar side ruptures, and then the micropylar endosperm (the aleurone cell layer) is ruptured by the emerging radicle. Germination is then completed leaving the testa adhering to the radicle (Figure 4.5 M, arrows) (Bentsink and Koornneef, 2008). In the *zou-4* mutant, during germination, even though the testa ruptures apparently normally, cotyledons adhere to the endosperm making the testa adhere to the tip of the cotyledon after germination (Figure 4.5 B, arrow). *ale1-1* mutants show a similar testa adhesion to the tip of the cotyledon phenotype. However, unlike *zou* endosperm, *ale1-1* endosperm cells degrade normally during embryogenesis, suggesting that even in the Col-0 background the epidermis of *ale1-1* cotyledons may have an epidermal defect that causes them to physically adhere to the aleurone cell layer (Figure 4.5 C and D, arrows).

The epidermal phenotype of *ale1-1* in Col-0 was further examined. The epidermis of wild-type cotyledons shows jigsaw-shaped pavement cells and stomata are distributed following the "one-cell spacing rule" (Rowe and Bergmann, 2010) (Figure 4.5 E, arrows indicate the stomata). The epidermis of *zou-4* cotyledons does not show jigsaw-shaped pavement cells, instead the pavements cells show irregular shapes, and there are gaps between pavement cells (Figure 4.5 F, white arrows). Occasionally, the rupture of epidermis and clustering of stomata were observed in *zou* mutants as previously described (Yang et al., 2008) (Figure 4.5 F, red arrow). This defect is likely caused by the abnormality of the epidermal cuticle in the cotyledons rather than the defects of epidermal patterning.

The epidermis of *ale1-1* cotyledons that germinated from normal shaped seeds does not show any major difference from that of wild-type cotyledons (Figure 4.5 G).

However, the epidermis of *ale1-1* cotyledons that germinate from abnormal-shaped seeds have severe defects. The pavement cells are not always jigsaw shaped, and there can be gaps in the epidermis (Figure 4.5 H, white arrow). Occasionally, protrusions of epidermal cells with clumped stomata were observed (Figure 4.5 H, red arrow). These results are consistent with Tanaka et al.'s (2001) observation in the *ale1-1* allele in the L*er* ecotype. Although both *zou* and *ale1-1* have defects in embryonic epidermis, *ale1-1* has abnormalities in cotyledon shape which are different from those observed in *zou-4* cotyledons. Wild-type cotyledons at about 10 d after germination display an oval shape with a slightly pointed end (Figure 4.5 I). *zou-4* mutant cotyledons at the same age display an elongated petiole, smaller blade area and a blunt end (Figure 4.5 J, arrow). Compared to the wild-type, *ale1-1* cotyledons have similar size, however cotyledons that germinate from normal shaped seeds display a weak shape phenotype with rounder blades with indented edges (Figure 4.5 K, arrows). Cotyledons germinating from the abnormal shaped *ale1-1* seeds display a stronger phenotype with heavily indented edges (Figure 4.5 L, arrows).

To further investigate the epidermal cuticle defects in *ale1-1* cotyledons which may cause the gaps and other defects observed during the germination, Toluidine Blue staining which has been shown to provide a quick test for the epidermal cuticle defects was used (Tanaka et al., 2004). Neither cotyledons nor leaves of the wild-type could be stained by Toluidine blue (Figure 4.5 M). Consistent with previous experiments (Yang et al., 2008), *zou-4* cotyledons were heavily stained (Figure 4.5 N, arrows), but not the leaves, suggesting a strong epidermal cuticle defect only in cotyledons. The cotyledons of *ale1-1* which germinated from the normal shaped

seeds could be lightly stained by Toluidine Blue, as some dark blue dots were observed at the edge of the cotyledons (Figure 4.5 O, arrow). The cotyledons of *ale1-1* which germinated from the abnormal shaped seeds displayed darker blue staining compared to wild-type seedlings, and showed dark blue dots on the surface of the cotyledons (Figure 4.5 P, arrow). However the staining is weaker than in *zou* mutants, suggesting a weak epidermal cuticle defects in *ale1* mutants. These results are consistent with those of Tanaka et al (Tanaka et al., 2004). To summarize, *ale1-1* mutants have defects in embryo development after the early torpedo stage, which are likely due to abnormal embryonic epidermal cuticle development.

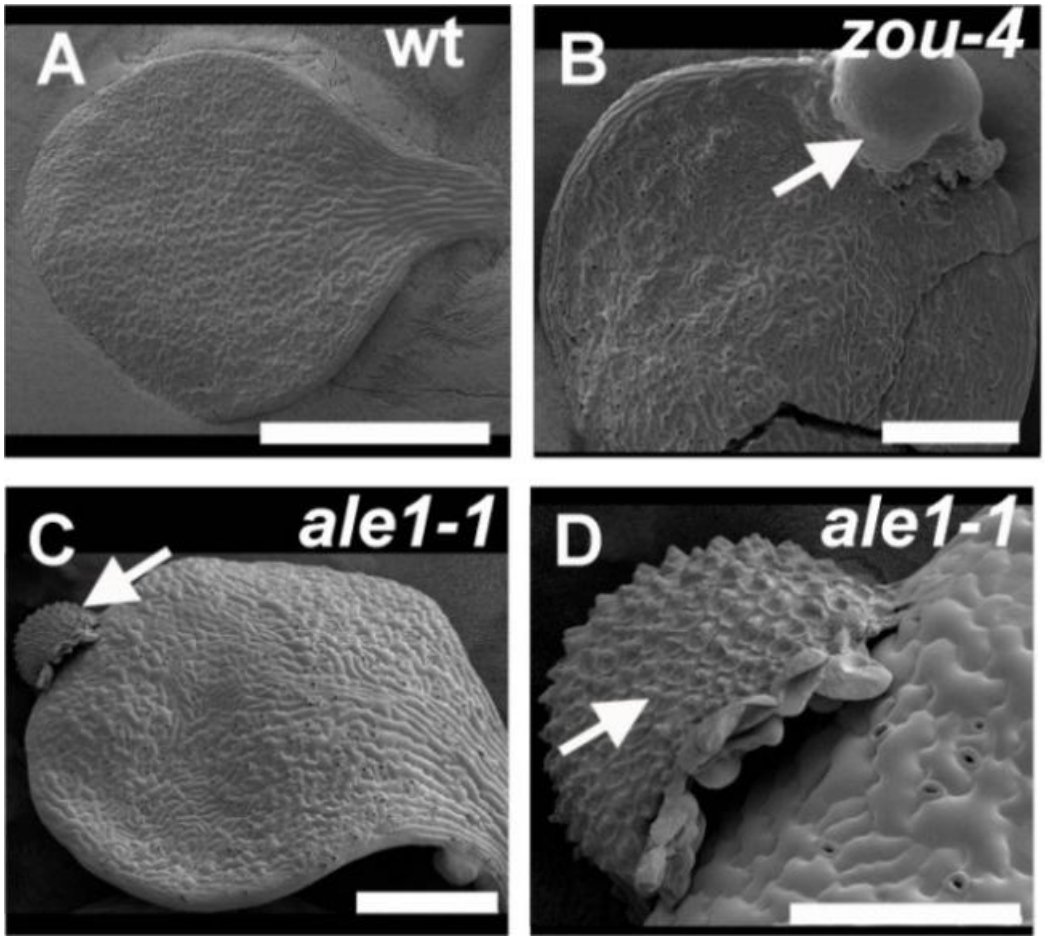

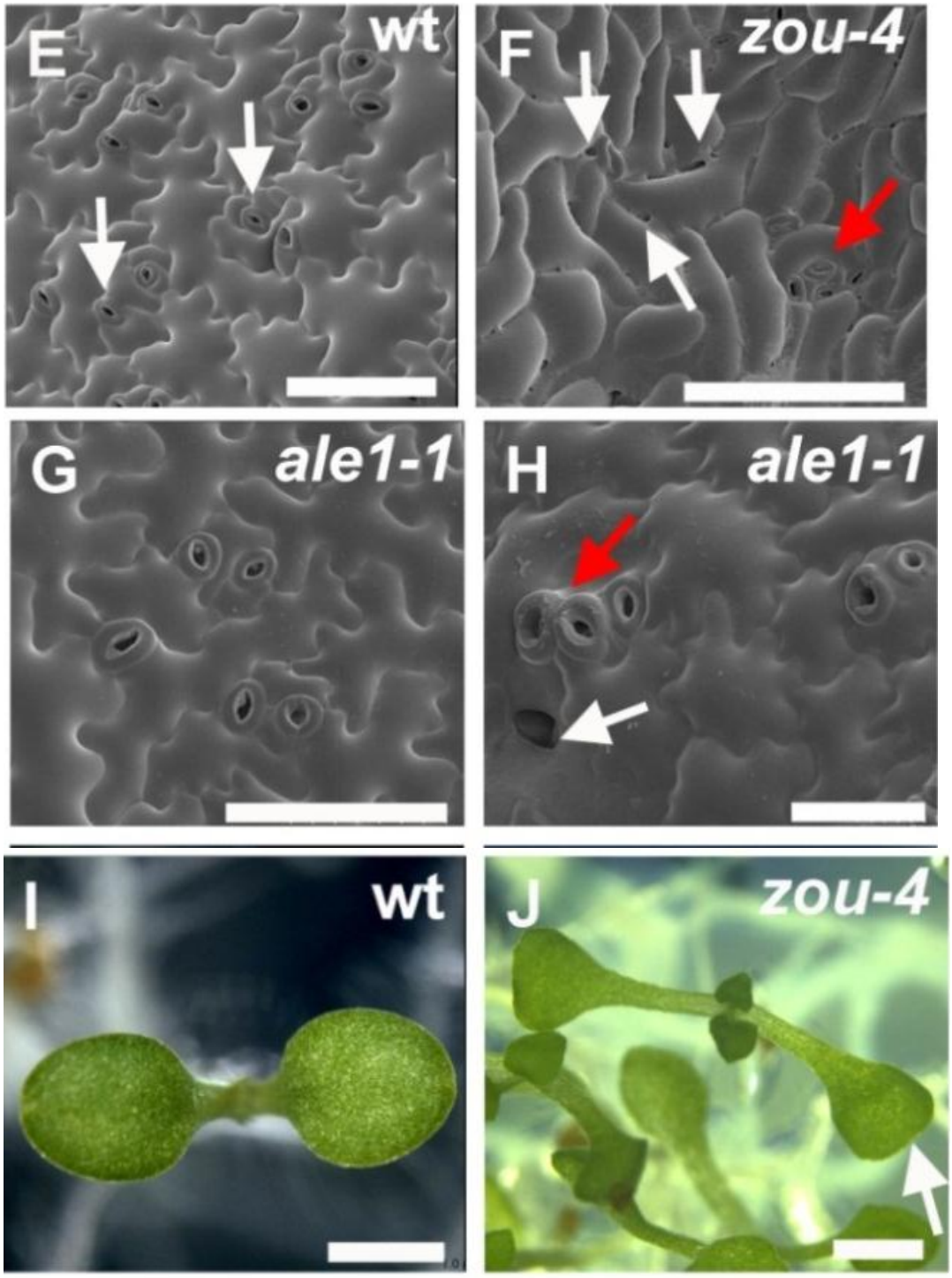
E
wt
F
zou-4
G
ale1-1
H
ale1-1
I
wt
J
zou-4

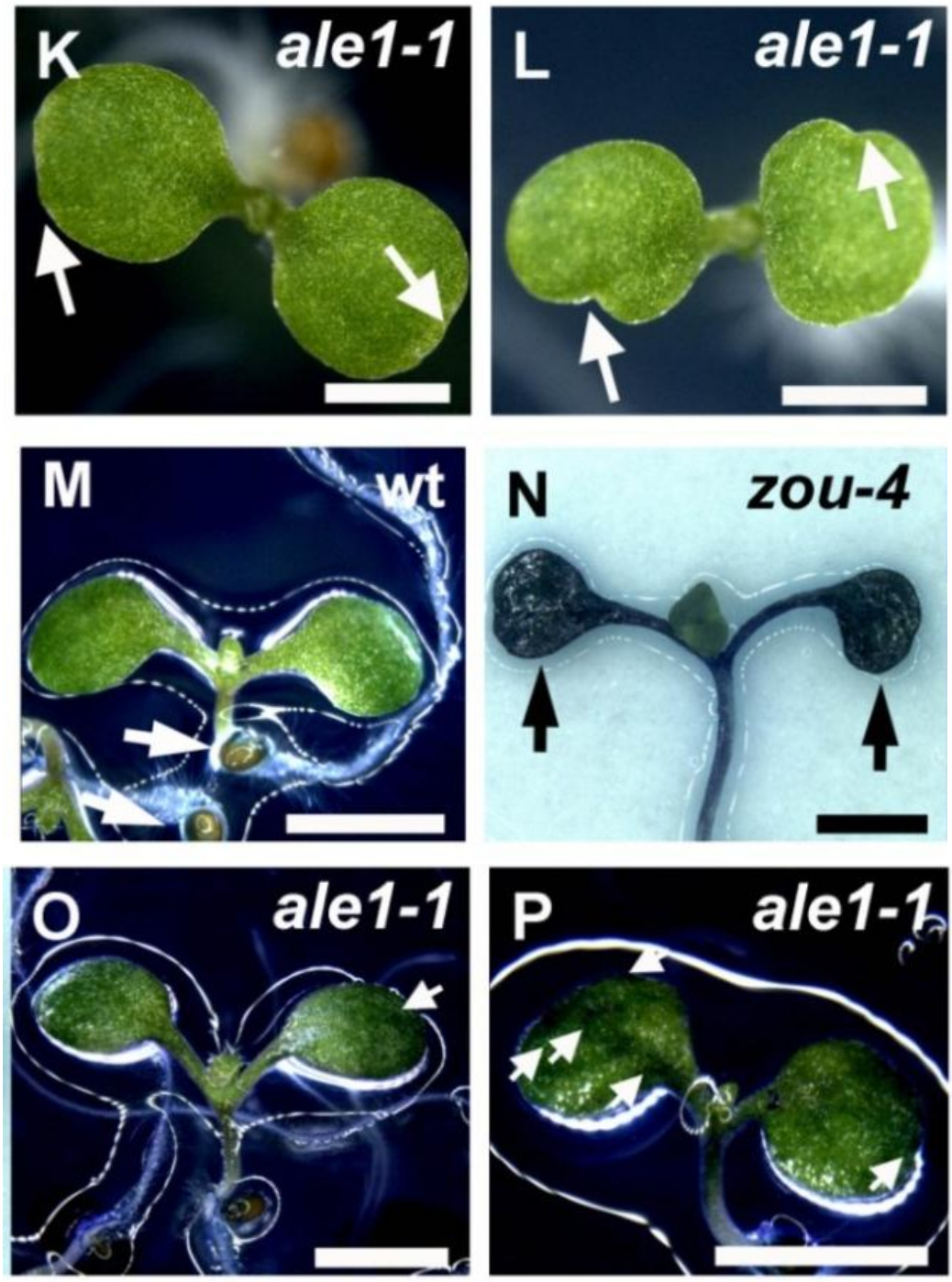
K
ale1-1
L
ale1-1
M
wt
N
zou-4
O
ale1-1
P
ale1-1

Figure 4.5 *ale1* mutants have defects in embryonic epidermal development

A, E, I and M are wild-type plants. B, F, J and N are *zou-4* mutants. C, D, G, H, K, L, O and P are *ale1-1* mutants. A-D, SEM images of the adaxial side of cotyledons at 10 d. B, arrow indicates the adhering seed coat to one of the cotyledons in *zou-4* mutants. C and D, arrows indicate the adhering seed coat to one of the cotyledons in *ale1-1* mutants. E-H, SEM images of adaxial epidermis of cotyledons at 10 d. E, arrows indicate the normal stomatal distribution in wild-type epidermis. F, red arrows indicate the abnormal distribution of stomata and white arrows indicate the gaps between pavement cells in *zou-4* mutant epidermis. G, epidermis of cotyledon germinated from wild-type shaped *ale1-1* seed. H, epidermis of cotyledon germinated from abnormal-shaped *ale1-1* seed, the red arrow indicates the abnormal distribution of the stomata and the white arrow indicates a hole in the *ale1-1* mutant epidermis. I-L, shapes of cotyledons at 10 d. I, wild-type cotyledons have an oval shape with a point at the end of the cotyledons. J, *zou-4* cotyledons have a narrower shape with a blunt end of the cotyledons indicated by the arrow. K, *ale1-1* cotyledons which germinated from the wild-type shaped seeds have a rounder shape with slightly dented edges indicated by the arrows. L, *ale1-1* cotyledons which germinated from the abnormal-shaped seeds have much more severe defects showing heavily dented edges indicated by the arrows. M-P, toluidine blue staining of the cotyledons at 10 d. M, the toluidine blue can hardly stain the wild-type cotyledons; arrows indicate that the seed coat is normally attached to the radicle in wild-type seedlings after germination. N, the cotyledons of *zou-4* mutants are stained dark blue by the toluidine blue.

Figure 4.5 continued.

O, the cotyledons of *ale1-1* mutants which germinated from wild-type shaped seeds can be partially stained by the toluidine blue showing blue dots indicated by the arrow. P, the cotyledons of *ale1-1* mutants which germinated from abnormal-shaped seeds can be stained by the toluidine blue with the dark staining on the edge of the leaves indicated by the arrows. H scale bar represents 0.05 mm; E and G scale bars represent 0.1 mm; D and F scale bars represent 0.2 mm; B, C and J scale bars represent 0.5 mm; A, K and L scale bars represent 1.0 mm; I and M-P scale bars represent 2.0 mm.

4.2.4 Expression of *ALE1* under the *pSUC5* promoter rescues the *ale1-1* seed phenotype, but does not complement the *zou-4* shrivelled seed phenotype

It has been shown that *ALE1* is a key component acting downstream of *ZOU* with the function of controlling embryonic cuticle formation. However, *ale1* mutant seeds are not shrivelled, and the TUNEL assays show no defect in nuclear DNA fragmentation in the ESR, suggesting normal endosperm breakdown in *ale1*. Thus *ALE1* may only be implicated in one of the proposed functions of *ZOU,* making *ALE1* an important tool for dissecting the *zou* phenotype. Another important tool, presented in detail in the introduction to this chapter, is the promoter of the *AtSUC5* gene. Based on *AtSUC5*'s ESR specific expression pattern, and the fact that *AtSUC5* is expressed normally in a *zou* mutant background, it is possible to use *AtSUC5* 1.5 kb promoter (*pSUC5*) to drive *ALE1* expression in the ESR of *zou* mutant seeds.

To achieve this goal, I fused the *AtSUC5* 1503 to -1 bp promoter region to the *ALE1* cDNA at the transcription start site, and then I cloned this *pSUC5::ALE1* fragment to the *pBIB* binary plant expression vector with a kanamycin resistance in the bacteria and a hygromycin resistance in plants. The schematic map of the construct is shown in Figure 4.6 B. Figure 4.6A shows the scheme of the strategy.

To test the functionality of the *pSUC5::ALE1* construct, I transformed it into Col-0 wild-type plants, and then crossed the *pSUC5::ALE1* Col-0 line 10 which had the highest *ALE1* expression in the siliques at the heart embryo stage tested by qPCR (Figure 4.6 C) into *ale1-1* mutants. This indirect strategy was necessary because the transposon insertion responsible for the lesion in the *ale1-1* mutant had the same hygromycin resistance as the construct. Homozygous *ale1-1* mutants harbouring the *pSUC5::ALE1* transgenes were confirmed by PCR. 99% of the *ale1-1* seeds carrying the *pSUC5::ALE1* transgene showed wild-type seed size and shape (Figure 4.7 F) suggesting that the *pSUC5::ALE1* construct was able to produce functional ALE1 protein.

I then introduced the *pSUC5::ALE1* transgene into *zou-4* mutants by *Agrobacterium*-mediated flower dip transformation. Quantitative real-time RT-PCR (qPCR) was used to test *ALE1* expression in the siliques of homozygous transformants at the heart embryo stage (Figure 4.6 C). *pSUC5::ALE1 zou-4* line 8-1, *pSUC5::ALE1 zou-4* line 26-3 and *pSUC5::ALE1* Col-0 line 10-1 were the lines used in subsequent analysis since they showed the highest *ALE1* expression levels. All *pSUC5::ALE1* Col-0 lines generated showed a wild-type seed phenotype (Figure 4.7 D). All *pSUC5::ALE1 zou-4* lines generated, including line 8-1 and line 26-3, showed a phenotype that was indistinguishable from that of *zou-4* seeds i.e. small,

dark and shrivelled (Figure 4.7 E). These results show that the *pSUC5::ALE1* transgene is not able to rescue the seed shrivelling phenotype of *zou4* mutants.

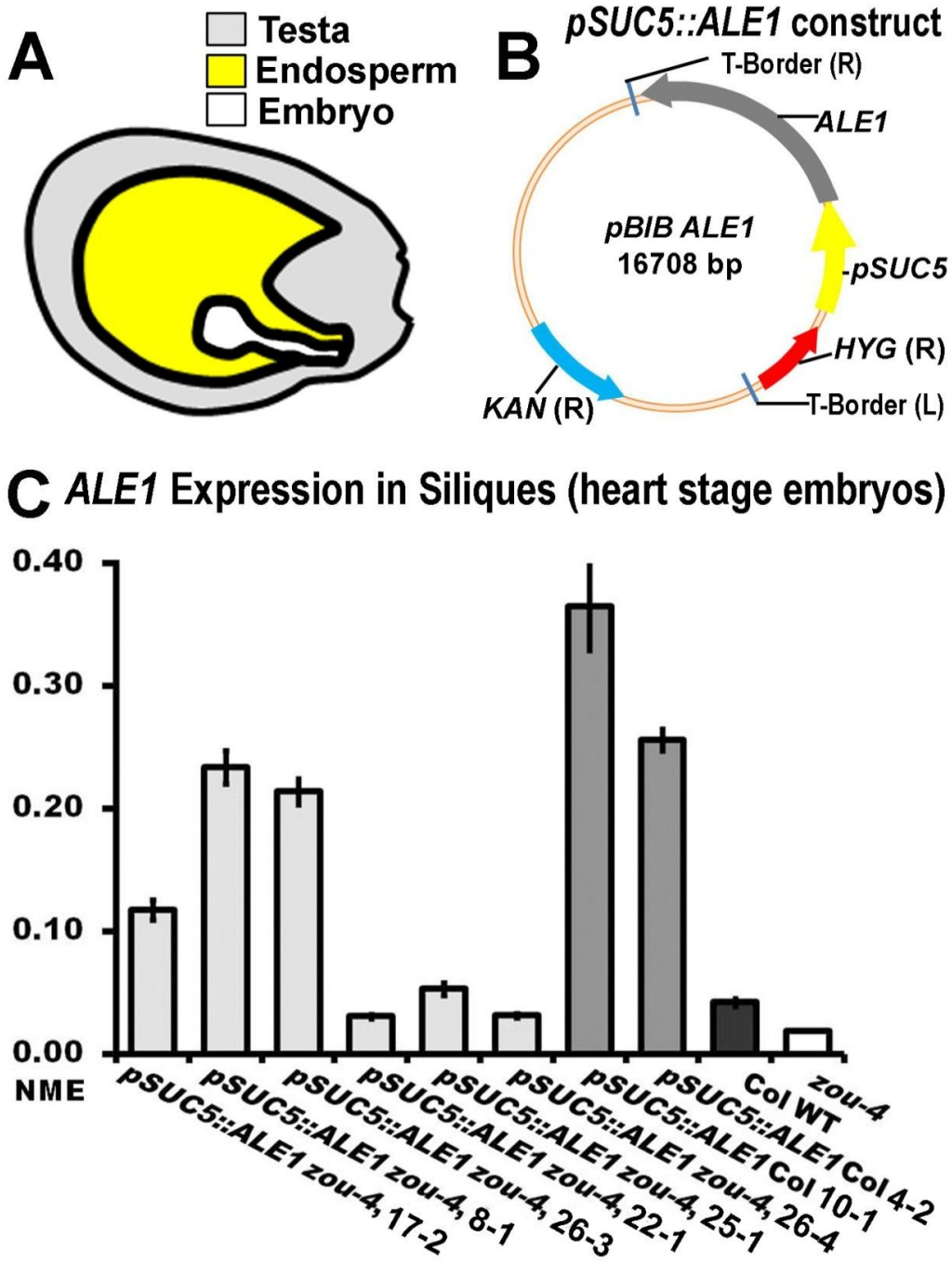

Figure 4.6 Expression of *ALE1* under the *pSUC5* promoter in Col-0 and *zou-4* mutants

A, schematic presentation of specifically expressing *ALE1* in the endosperm (the yellow region) under the *pSUC5* promoter in an *Arabidopsis* seed, the white region represents the embryo and the grey region represents the seed coat. B, construct design of *pSUC5::ALE1*, *ALE1* cDNA was fused in frame with the *SUC5* 1500 bp promoter region and cloned into the binary vector *pBIB*, conferring hygromycin resistance. The clone was transformed into *A. tumefaciens* and was introduced into *A. thaliana* Col-0 wild-type plants and *zou-4* mutants by floral dip transformation. C, *ALE1* expression in the siliques with heart stage embryos of *pSUC5::ALE1 zou-4* transgenic line 17-2, line 8-1, line 26-3, line 22-1, line 25-2 and line 26-4, *pSUC5::ALE1* Col-0 transgenic line 10-1 and line 4-2, Col-0 and *zou-4* mutants by the qPCR analysis.

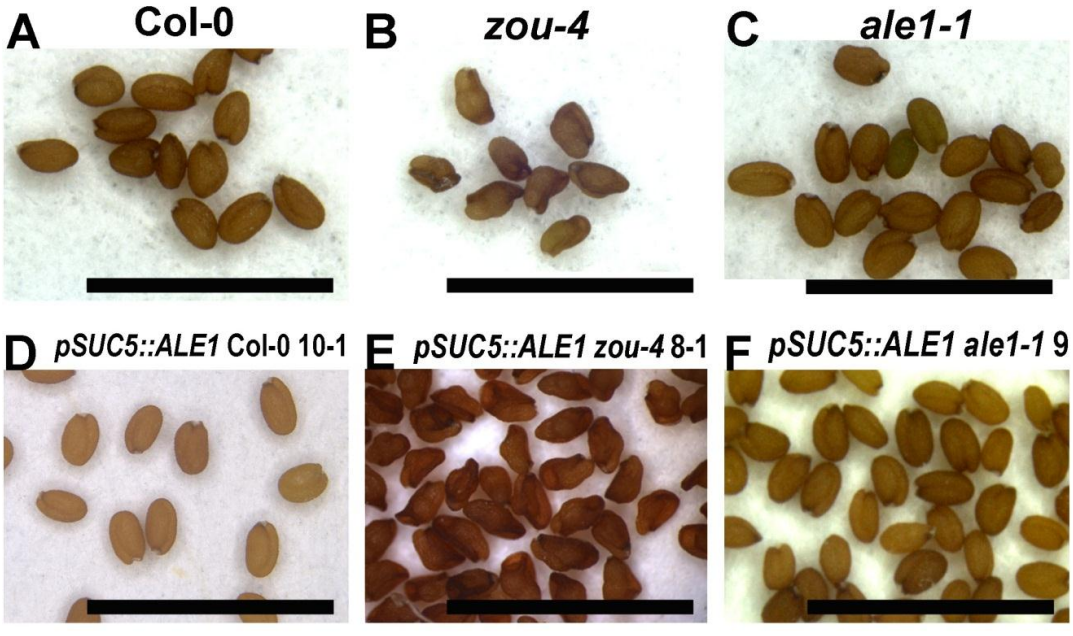

Figure 4.7 Expression of *ALE1* under the *pSUC5* promoter rescues *ale1-1* seed phenotype, but does not complement the *zou-4* shrivelled seed phenotype

A, Col-0 wild-type seeds. B, *zou-4* mutant seeds. C, *ale1-1* seeds. D, *pSUC5::ALE1* Col-0 line 10-1 seeds. E, *pSUC5::ALE1 zou-4* line 8-1 seeds. F, *pSUC5::ALE1 ale1-1* line 9 seeds and *pSUC5::ALE1* construct was introduced to *ale1-1* mutants by crossings. A-F scale bars represent 1.0 mm.

4.2.5 Expression of *ALE1* under the *pSUC5* promoter partially complements *zou-4* epidermal cuticle defects.

Expression of *ALE1* under the *pSUC5* promoter cannot complement *zou-4* shrivelled seed phenotype. However, the *pSUC5::ALE1* construct was able to rescue the *ale1-1* seed phenotype suggesting a functional ALE1 protein was produced under *pSUC5* promoter. Since the *ale1-1* phenotype is caused by epidermal cuticle defects, and there is no defect in cell death in the endosperm of *ale1-1* mutants, it was important to investigate the cuticular phenotype of *zou-4* mutants containing *pSUC5::ALE1*. When grown and stained by Toluidine Blue in the same conditions, *pSUC5::ALE1 zou-4* lines showed lighter blue staining than *zou-4* mutants, though still darker than the wild-type seedlings (Figure 4.8), suggesting a partial complementation of epidermal cuticle defect of *zou-4* mutants.

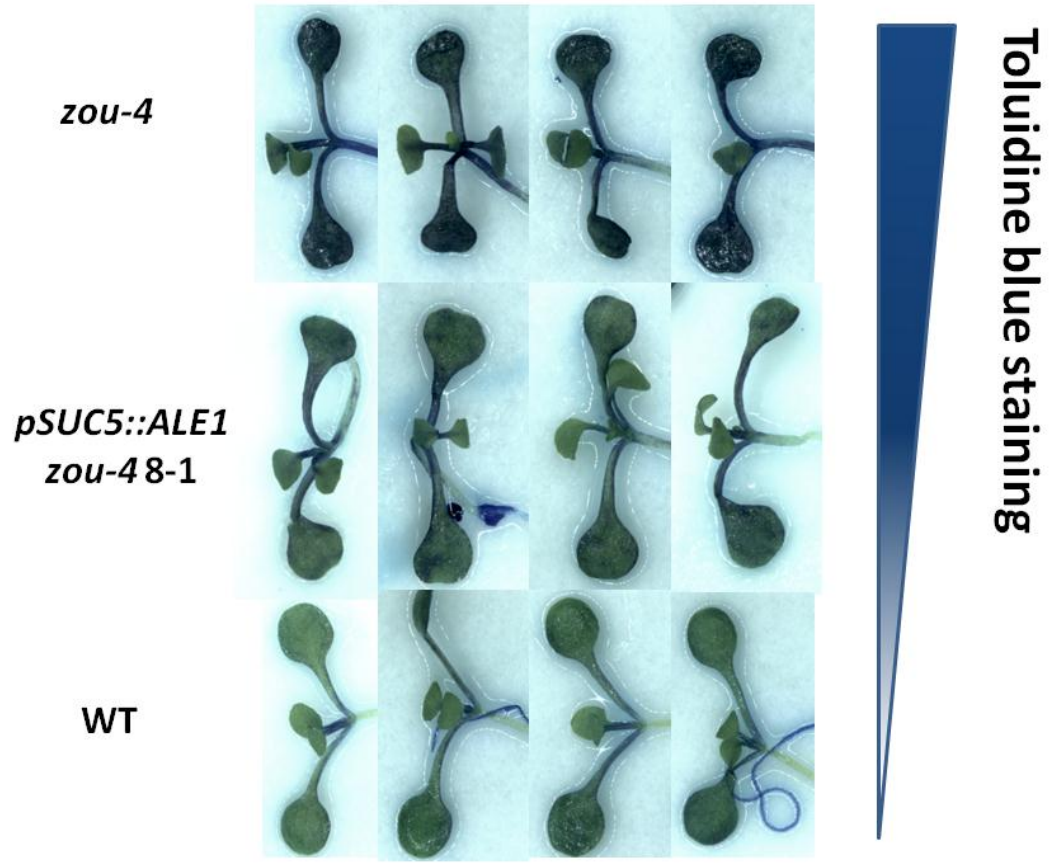

Figure 4.8 Expression of *ALE1* under the *pSUC5* promoter complements *zou* cuticle defects by toluidine blue tests

Toluidine blue staining on *zou-4*, *pSUC5::ALE1 zou-4* line 8-1 and wild-type cotyledons at 10 d. The cotyledons of *zou-4* mutants were strongly stained (the first row). The cotyledons of *pSUC5::ALE1 zou-4* line 8-1 were less stained compared to *zou-4* mutants (the second row). The cotyledons of wild-type plants were the weakest stained (the third row).

To further confirm the partial complementation of *zou* epidermal cuticle defect, double blind tests were performed to distinguish the quality of the Toluidine Blue staining in cotyledons among Col-0, *zou-4* and *pSUC5::ALE1 zou-4* lines (Figure

4.9). I first classified the level of staining into 3 categories: 1) almost no staining, 2) medium staining, and 3) heavy staining, and gave a score 1, 2 and 3 to each category respectively. Approximately 100 stained seedlings from each line were placed on white filter paper and the genetic background of each seedling was labelled at the back of the paper without being revealed during the tests. 82% of wild-type seedlings were grouped to category 1 (almost no staining), 18% of wild-type seedlings were grouped to category 2 (medium staining), and none were grouped to category 3 (heavy staining). 90% of *zou-4* seedlings were grouped to category 3 (heavy staining), 10% of *zou-4* seedlings were grouped to category 2 (medium staining), and none were grouped to category 1 (almost no staining). 58% of *pSUC5::ALE1 zou-4* line 8-1 was grouped to category 2 (medium staining), 20% of *pSUC5::ALE1 zou-4* line 8-1 was grouped to category 1 (almost no staining), and 22% of *pSUC5::ALE1 zou-4* line 8-1 was grouped to category 3 (heavy staining). 29% of *pSUC5::ALE1 zou-4* line 26-3 was grouped to category 2 (medium staining), 71% of *pSUC5::ALE1 zou-4* line 26-3 was grouped to category 3 (heavy staining), and none was grouped to category 1 (almost no staining). These results are summarised in Figure 5, and suggest that both *pSUC5::ALE1 zou-4* line 8-and *pSUC5::ALE1 zou-4* line 26-3 had less staining than *zou-4*, and that the *zou-4* epidermal cuticle defects were partially complemented by expressing *ALE1* under the *pSUC5* promoter.

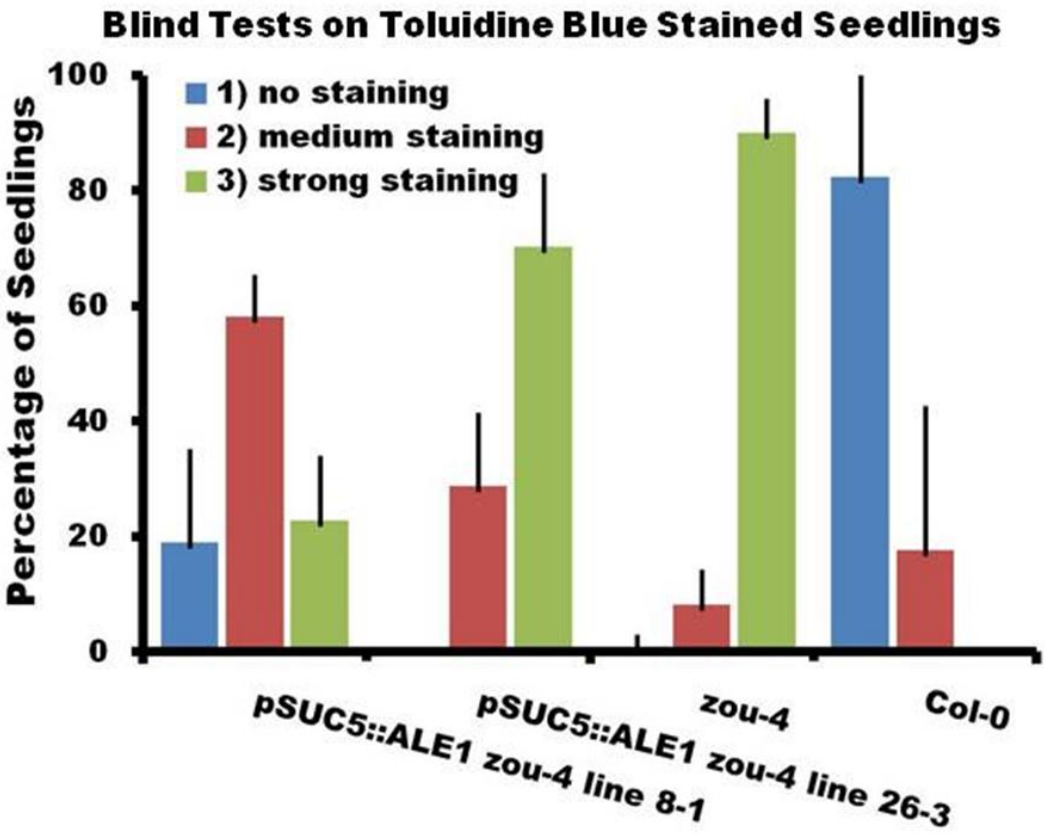

Figure 4.9 Blind tests on the Toluidine Blue stained *pSUC5::ALE1 zou-4* lines, *zou-4* mutants, and Col-0 wild-type seedlings

The X axis represents the genetic backgrounds of the seedlings that were used for the blind tests. The Y axis represents the average percentage of seedlings from the different genetic background that were scored as either category 1) almost no staining of cotyledons, or category 2) medium staining of cotyledons, or category 3) strong staining of cotyledons. Error bars represent the standard deviation.

Quantification of Toluidine blue that permeated through holes in the epidermal cuticle under controlled conditions is an alternative way to examine the level of the

cuticle integrity. The more Toluidine Blue is extracted from the stained cotyledons, the more severe the cuticle defects are. In order to test this hypothesis I designed a novel Toluidine Blue extraction and quantification protocol based on the observation that Toluidine blue is soluble in 80% ethanol (Terry et al., 2000). Twenty seedlings from each of wild-type, *zou* mutants and *pSUC5::ALE1* lines were grown and stained by Toluidine Blue under the same conditions with 3 replicates. The Toluidine Blue remaining in cotyledons after washing was extracted using 80% ethanol and quantified by spectrophotometry at the observed Toluidine Blue maximal absorbance peak of 626 nm (Merrill and Spencer, 1948). Measurements were made after 30 min, 1 h and 12 h of extraction. Observed by the naked eye, after a 12 h extraction, the *zou-4* cuvette showed the darkest blue colour in the 80% ethanol extraction solution, followed by *pSUC5::ALE1 zou-4* line 26-3, *pSUC5::ALE1 zou-4* line 8-1, wild-type, unstained *pSUC5::ALE1 zou-4* line 8-1 and the 80% ethanol (Figure 4.10 A). The colour from the unstained cotyledons is likely to come from chlorophylls. The amount of Toluidine Blue was quantified by spectrophotometer at 626 nm (Figure 4.10 B). After 30 min to 1 h of extraction, there was significantly higher amount of Toluidine blue from *zou-4* than from wild-type and the unstained seedlings, however no significant difference was observed between *zou-4* and *pSUC5::ALE1 zou-4* lines. After 12 h, there was significantly higher amount of Toluidine Blue extracted from *zou-4* than that was extracted from the *pSUC5::ALE1 zou-4* line 8-1, but no significant difference was observed between *zou-4* and *pSUC5::ALE1 zou-4* line 26-3. Interestingly, after a 12 h extraction period, wild-type and *pSUC5::ALE1 zou-4* line 8-1 did not shown an significant increase in the amount Toluidine Blue extracted, whilst *zou-4* and *pSUC5::ALE1 zou-4* line 26-3 showed

significant increase in the amount Toluidine Blue extracted. Taken together, *zou-4* was significantly more heavily stained by Toluidine Blue than *pSUC5::ALE1 zou-4* line 8-1, confirming that *zou* epidermal cuticle defects were complemented by expressing *ALE1* under the *pSUC5* promoter. The same Toluidine Blue quantification was performed on *pSUC5::ALE1 ale1-1* lines to further confirm that *pSUC5::ALE1* transgene was able to rescue *ale1-1* abnormal seed shape phenotype (Figure 4.7 F) and epidermal cuticle defects. As it was shown in Figure 4.11, the Toluidine Blue absorbance of *pSUC5::ALE1 ale1-1* lines was significantly reduced compared to those of *ale1-1* mutants and *zou-4* mutants showing similar level to that of the wild-type. These results suggest that *pSUC5::ALE1* transgene is able to completely complement both seed abnormality and cotyledon cuticle defects of *ale1-1* and the protein product of *pSUC5::ALE1* transgene is fully functional.

A

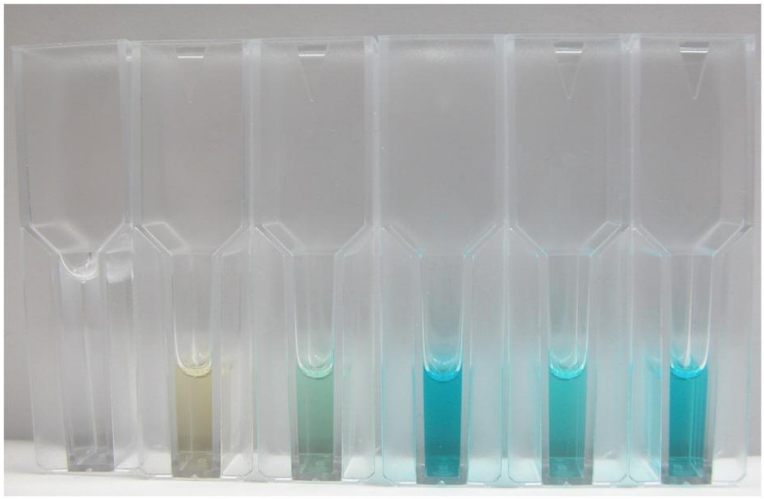
80% Ethanol
Unstained zou-4 8-1
TB stained Col-0
TB stained zou-4
TB stained zou-4 8-1
TB stained zou-4 26-3

B

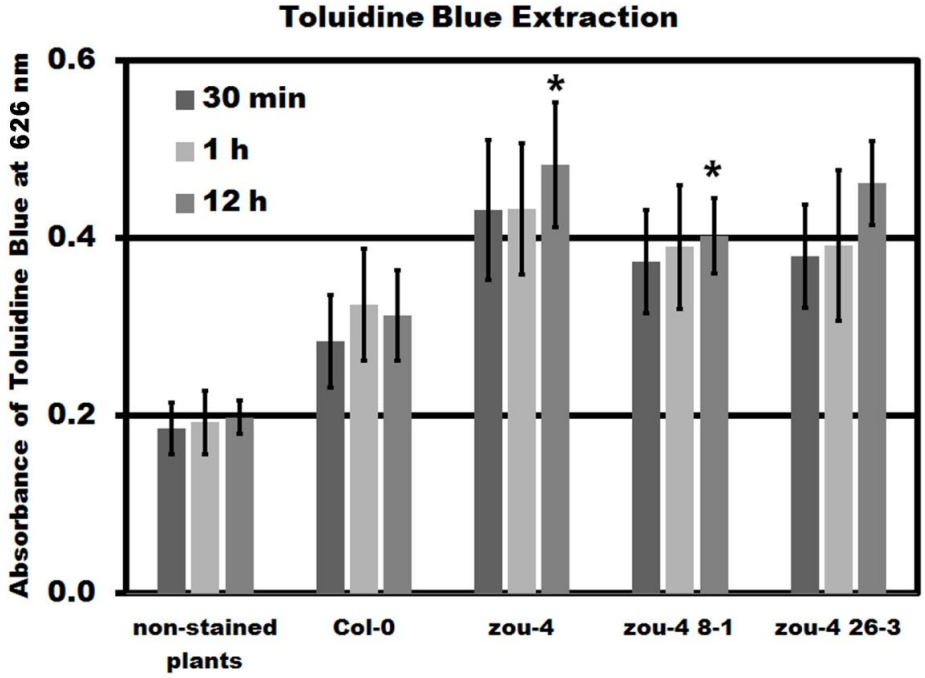
Toluidine Blue Extraction
Absorbance of Toluidine Blue at 626 nm
0.6
0.4
0.2
0.0
30 min
1 h
12 h
*
*
non-stained plants
Col-0
zou-4
zou-4 8-1
zou-4 26-3

Figure 4.10 Quantification of toluidine blue staining of cotyledons of wild-type plants, *zou-4* mutants and *pSUC5::ALE1 zou-4* lines by spectrophotometry

A, toluidine blue extracted in 80% ethanol from the cotyledons of different lines after 12 h. Cuvettes from the left to the right are 80% ethanol (blank), unstained *pSUC5::ALE1 zou-4* line 8-1, toluidine blue stained Col-0 wild-type plants, toluidine blue stained *zou-4* mutants, toluidine blue stained *pSUC5::ALE1 zou-4* line 8-1, toluidine blue stained *pSUC5::ALE1 zou-4* line 26-3. Toluidine blue stained *zou-4* mutants displayed the darkest blue colour, followed by the toluidine blue stained *pSUC5::ALE1 zou-4* line 26-3, toluidine blue stained *pSUC5::ALE1 zou-4* line 8-1, toluidine blue stained Col-0 wild-type plants, unstained *pSUC5::ALE1 zou-4* line 8-1 and the lightest, 80% ethanol. B, toluidine blue was extracted from the stained cotyledons of wild-type plants (Col-0), *zou-4* mutants, *pSUC5::ALE1 zou-4* line 8-1 (zou-4 8-1) and *pSUC5::ALE1 zou-4* line 26-3 (zou-4 26-3) and quantified by spectrophotometry at 626 nm after 30 min, 1 h and 12 h of the extraction. *zou-4* mutants showed the highest amount of the toluidine blue that was extracted from the cotyledons at all 3 time points. There was no significant difference between *zou-4* mutants and the *pSUC5::ALE1 zou-4* line 26-3 at all 3 time points ($P>0.05$). The amount of Toluidine Blue was significantly higher in *zou-4* mutants than in the *pSUC5::ALE1 zou-4* line 8-1 after 12 h of extraction ($P<0.05$). As a control, Col-0 wild-type showed the least amount of the toluidine blue extraction at all 3 time points compared to the other lines. Error bar=standard error of the mean.

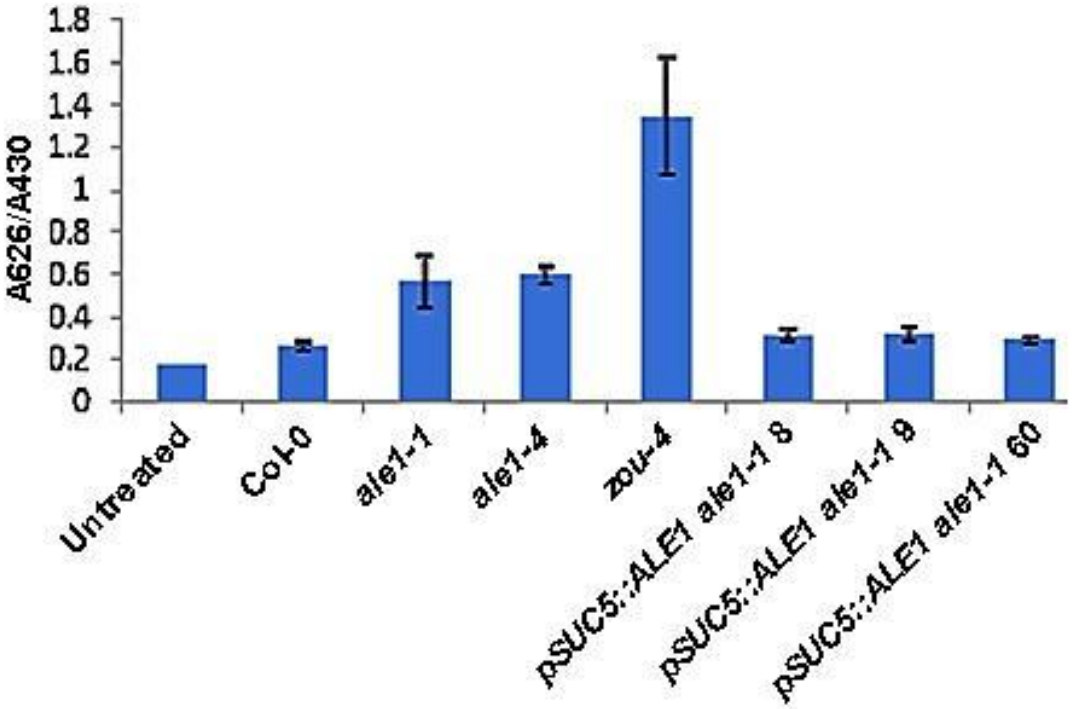

Figure 4.11 The presence of the *pSUC5-ALE1* transgene rescues the cuticle phenotype of *ale1-1*.

Seedlings from Col-0 wild-type, *ale1-1* mutants, *ale1-4* mutants, *zou-4* mutants and three independent lines of *pSUC5::ALE1 ale1-1* (line 8, 9 and 60) were subjected to Toluidine Blue staining which was quantified spectrophotometrically using the same methods described in Fig 4.10. Relative absorbance of Toluidine Blue at 626 nm divided by the background absorbance (the absorbance of chlorophylls at 430 nm) was calculated. Error bars represent standard deviation between three biological replicates each containing 20 seedlings. (The experiments were performed by Gwyneth Ingram.)

One of the critical roles of plant cuticle is controlling non-stomatal water loss (Samuels et al., 2008). In other words, if plants lose the integrity of their epidermal cuticle, their survival under low humidity conditions will be compromised. If the *pSUC5::ALE1*constuct can complement *zou* cuticle defects, the survival rate of *pSUC5::ALE1 zou-4* lines should be significantly higher than *zou*. To test this hypothesis, I germinated the wild-type, *zou-4*, *ale1-1*, *ale1-4* mutants and *pSUC5::ALE1 zou-4* lines on the media plates, one week later I transferred the seedlings to the soil carefully without causing mechanical harm. Three week later the number of survivors was scored. The experiments were repeated three times. Shown in figure 4.11, the Col-0 wild-type and *ale1* mutants under our condition had the highest survival rate, 100% and 99% respectively, and there was no significant difference among the wild-type seedlings *ale1-1* mutants, and *ale1-4* mutants ($P>0.05$). *zou-4* mutants had the lowest survival rate, 46.1%. Both *pSUC5::ALE1 zou-4* line 8-1and line 26-3 had significant higher survival rates than *zou-4* mutants ($P<0.05$). Again these results suggest *pSUC5::ALE1 zou-4* lines had significantly complemented *zou-4* cuticle defects.

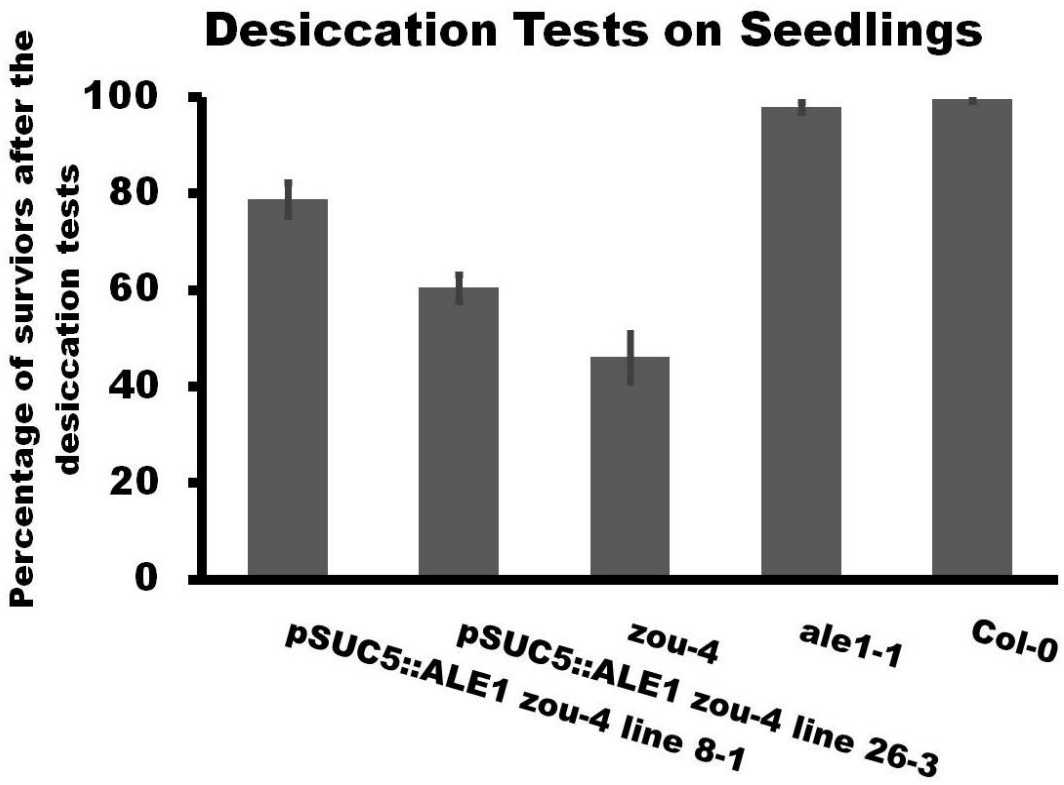

Figure 4.12 Desiccation tests on *pSUC5::ALE1 zou-4* line 8-1, *pSUC5::ALE1 zou-4* line 26-3, *zou-4*, *ale1-1* and Col-0 wild-type seedlings

The *pSUC5::ALE1 zou-4* lines, *zou-4* mutants, *ale1-1* mutants and Col-0 wild-type seeds were germinated on media. After one week, the seedlings were carefully transferred to soil. Three weeks later the number of survivors was scored. The experiments were repeated three times. Error bars represent the standard deviation. There was no significant difference between *ale1-1* and Col-0 wild-type ($P > 0.05$). zou-4 mutants had the lowest survival rate, 46.1%. Both *pSUC5::ALE1 zou-4* line 8-1and line 26-3 had significant higher survival rates than *zou-4* mutants ($P<0.05$).

4.3 Discussion

Angiosperm seed development requires co-ordinated growth of different compartments in the seeds, the embryo, endosperm and testa. In *Arabidopsis*, the endosperm is consumed during embryo growth and by the mature stage of seed development there is only a peripheral aleurone-like layer left (Olsen, 2004). Despite the importance of endosperm for embryo development, how the transient endosperm regulates embryo development is still poorly understood. The *ZOU* gene provides an important tool to address the question (Yang et al., 2008). *zou* mutants display two distinct phenotypes, lack of programmed cell death in the endosperm and loss of integrity in the embryonic epidermal cuticle layer, suggesting that *ZOU* has a role in endosperm cell death and embryonic cuticle formation (Yang et al., 2008). However, it was not clear whether the effects of *ZOU* upon embryo development are a direct role of the endosperm in signalling to the embryo, or rather reflect an indirect consequence of lack of cell death in the endosperm mechanically impeding embryo expansion. To test whether the two pathways could be separated, a previously identified *ZOU* target *ALE1* which controls epidermal cuticle development was specifically expressed in the ESR of *zou* mutants by using the *ZOU*-independent *AtSUC5* promoter to investigate whether one or both of the *zou* phenotypes were complemented. The *AtSUC5::ALE1* transgene partially complemented *zou* defects in epidermal cuticle but not in endosperm cell death. This shows that the defects in the *zou* cuticle are not caused only indirectly by the defective endosperm, but rather that *ZOU* has distinct, separable functions during seed development.

ALE1 has previously been shown to have a role in epidermal cuticle development (Tanaka et al., 2001). Besides the embryonic epidermal cuticle defect, *ale1-1* mutants

have bigger seeds than those of *zou-4* mutants, the hypocotyl and cotyledons from *ale1-1* mutants are more elongated than those of *zou-4* mutants, and TUNEL analysis showed that *ale1-1* ESR cells undergo normal programmed cell death during embryo development. These results suggest that *ALE1* does not have a role in endosperm cell death. However, some *ale1-1* mutant seeds have fatter cotyledons and an abnormal embryo shape. During the U-shape stage of embryo development, the cotyledons bend to the micropylar zone instead of chalazal zone as seen in wild-type seeds. The possible explanations for the abnormal embryo shape and inverted bending direction in *ale1-1* mutants could be that *ale1-1* embryonic cuticle defects result in adhesion between the embryo and the endosperm during early embryo elongation. Similar defects have been observed in other cuticle mutants such as the *gso1/gso2* double mutant (Tsuwamoto et al., 2008). In addition, the embryonic cuticle defect in *ale1-1* could cause cotyledons to fuse, which affects the normal elongation of cotyledons. The other evidence which supports the hypothesis that *ale1-1* embryo phenotype is not caused by endosperm cell death is that in *ale1-1* during the germination, the cotyledons epidermis often adheres to the aleurone layer and no remaining endosperm is observed. Finally, cell death related genes that are regulated by *ZOU* (shown by SOLEXA sequencing) are not regulated by *ALE1* (Gwyneth Ingram personal communication), suggesting that *ALE1* may not be involved in endosperm cell death pathways.

The *AtSUC5::ALE1* transgene only partially rescued *zou-4* epidermal cuticle defects. To confirm that *AtSUC5::ALE1* transgene was fully functional, the transgene was expressed in *ale1-1* mutants and *ale1-1* epidermal and cuticle defects were fully rescued, suggesting that the *AtSUC5::ALE1* transgene is able to produce functional

ALE1 protein. The *AtSUC5* expression pattern is to some extent different from that of *ALE1*. *AtSUC5* starts to be expressed at the globular stage of embryo development which is earlier than *ALE1*, *ALE1* transcript can hardly be detected during the globular stage of embryo development. However, after the globular stage, both *AtSUC5* and *ALE1* have very similar expression patterns which is showing a peak at the heart stage and a gradually decrease until the mature stage (Baud et al., 2005; Winter et al., 2007). It should nonetheless be born in mind that the protein expression patterns of *AtSUC5* and *ALE1* are still not known. It could be that *AtSUC5* and *ALE1* translation do not overlap and that *ALE1* has delayed protein accumulation which may be critical for *ALE1* function. *zou-4* mutants have more severe epidermal cuticle defects than those of *ale1-1*. *ale1-1* is not a null allele as in *ale1-1* mutants *ALE1* transcript fragments can be detected. Whether these transcripts can be translated into functional protein is not known (Gwyneth Ingram personal communication). Therefore, obtaining a null allele of *ale1* and analysing its effects on epidermal cuticle development needs to be done in the future. According to the SOLEXA dataset, besides *ALE1*, other genes that are involved in cuticle biosynthesis or cuticular wax transportation are regulated by *ZOU*. Two GDSL-lipases (*AT1G71250* and *AT5G03820*) that might have a function in cuticular wax biosynthesis (Takahashi et al., 2010; Zimmermann et al., 2004) and a plasma membrane associated ABC transporter gene (*AT3G47780*) which is involved in cutin/wax transportation (Pighin et al., 2004) are up-regulated by *ZOU*. However, these cuticle/wax related genes are not regulated by *ALE1* (Gwyneth Ingram personal communication), suggesting that *ZOU* may regulate other cuticle/wax pathways in parallel to *ALE1*. The expression pattern and functional analysis of these *ZOU* targets remain to be done.

Partial complementation of *zou* embryonic epidermal cuticle defects by expressing the *AtSUC5::ALE1* transgene, without alleviating the endosperm cell death in *zou*, suggests that endosperm cell death and embryonic epidermal cuticle development are likely controlled by different pathways. Nevertheless, we cannot rule out the possibility that the persistent endosperm might block the sending of signals from the endosperm to the embryo for the cuticle formation or that the cuticle biosynthesis might send signals to stimulate the endosperm breakdown. Furthermore, it is still formally possible that the expression of *ALE1* could be stimulated by the process of endosperm breakdown during normal seed development.

In conclusion, my results show that *ZOU* regulates endosperm breakdown independently of *ALE1* function. In addition *ZOU* up-regulates *ALE1* to promote embryonic epidermal cuticle development in a non-cell autonomous manner.

5 Genetic and functional analysis of *ZHOUPI* (*ZOU*) target genes

5.1 Introduction

5.1.1 Background

zhoupi (*zou*) mutants display persistent endosperm and a correspondingly small embryo, and *zou* mutants also display embryonic epidermal cuticle abnormalities and are extremely sensitive to dessication during seed germination. The intriguing phenotype of *zou* mutants raised the hypothesis that *ZHOUPI* (*ZOU*) might regulate programmed cell death in the endosperm, and that lack of cell death in the endosperm might indirectly cause epidermal cuticle abnormality. An alternative hypothesis was that *ZOU* might regulate the endosperm programmed cell death pathways and an embryonic epidermal cuticle pathway independently. Previously, a *ZOU* target *ALE1* was identified (Yang et al., 2008). *ALE1* expression is strongly down-regulated in *zou* mutants and *ALE1* has a strikingly similar ESR specific expression pattern to *ZOU*. *ale1* mutants display similar but milder epidermal cuticle defect to *zou*. When expressing *ALE1* specifically in the endosperm by using *pSUC5::ALE1* construct, the embryonic epidermal cuticle defect of *zou* mutants was complemented, whilst the cell death defects in *zou* endosperm was not complemented. This supports the hypothesis that *ZOU* regulates two independent pathways during seed development: the endosperm cell death pathway which does not require *ALE1*, and the embryo cuticle development pathway which involves *ALE1*.

SOLEXA whole transcriptome sequencing of wild-type and *zou* mutant siliques was performed to elucidate the pathways involved in cell death and cuticle

development, and to identify *ZOU* target genes that could be involved in these pathways. The SOLEXA sequencing results showed that 233 genes were significantly down-regulated in *zou* mutants and 64 genes were significantly up-regulated in *zou* mutants. The 233 genes whose expression is down-regulated in *zou* mutants are implicated in JA pathways, ethylene pathways, REDOX homeostasis, disease resistance, programmed cell death pathways and other pathways with diverse functions. The 64 genes whose expression is up-regulated in *zou* mutants are implicated in diverse functions and include genes encoding secreted peptides, receptor-like proteins and cell death regulators. To identify the genes involved in endosperm-embryo interactions, the expression patterns of these mis-regulated genes were analysed against the Genevestigator *Arabidopsis* microarray database (Zimmermann et al., 2004). About 20% of the mis-regulated genes were not included on the Affymetrix 22K microarray chip, including the *ZOU* gene itself. Among the up-regulated genes, a higher proportion showed silique/seed specific expression patterns than among the down-regulated genes. These seed specific genes could either be involved in *ZOU* mediated cell death pathways or *ZOU* mediated embryonic epidermal cuticle development. The summary of *ZOU* targets that were analysed is shown in Table 5.1.

5.1.2 *LSD1-like 2* (*LOL2*, *At4g21610*)

LOL2 was first identified by comparing the conserved zinc finger motif of *LSD1* (*Lesions Simulating Disease 1*) against the *Arabidopsis* genome. Two proteins were identified containing multiple conserved LSD1-like zinc fingers, and which were named *LSD1-Like 1* (*LOL1*) and *LSD1-like 2* (*LOL2*) (Epple et al., 2003). Structurally, LOL2 and LOL1 share a remarkable similarity within the internal zinc

finger domains of LSD1, which suggests that LOL2, LOL1 and LSD1 belong to a small protein family and that they might have similar functions. *lsd1* mutants are hypersensitive to various pathogen challenges and exogenous stimuli, and display spontaneous uncontrolled cell death which initiates throughout organs and will eventually kill the plants in 2 to 4 days. This phenomenon is known as runaway cell death (Dietrich et al., 1997). The proposed function of *LSD1* is that of negatively regulating the initiation of pathogen resistance responses and localized cell death (Dietrich et al., 1997). *lol1* mutants display reduced cell death upon pathogen challenge and a reduced expression level of *LOL1* compromises the runaway cell death phenotype of *lsd1*, suggesting *LOL1* functions as a positive cell death regulator and antagonizes *LSD1* function (Epple et al., 2003). *LOL2* has 2 splicing modes, which produce 2 proteins LOL2a and LOL2b. *LOL2a* is up-regulated by *Pseudomonas syringae* whilst *LOL1* is down-regulated, and *LOL1* is negatively regulated by *LOL2*, raising the hypothesis that *LOL2* is a negative regulator of cell death (Petra Epple et al., 2001). In *zou* mutants *LOL2* was 6 times up-regulated, which is consistent with the reduced cell death phenotype in the *zou* endosperm.

Table 5.1 List of genes that were selected for expression and functional analysis

Gene name	Locus	Reads in Col-0	Reads in *zou-4*	Proposed Function	Expression pattern	References
LOL2	AT4G21610	2	12	Negative regulator of cell death	Universally expressed, induced by *P. syringae*.	Dietrich et al., 1997; Epple et al., 2003
DP1	AT4G11180	3	16	Lignin biosynthesis in cell walls	Testa Specific, co-expressed with *ALE1* and *RGP3*.	Matsuda et al., 2010
DOX1	AT3G01420	8	42	Protection against oxidative stress and cell death.	High in roots and seeds, induced by SA and oxidative stress.	De León et al., 2002 Hamberg et al., 2003

RGP4	AT5G50750	29	147	Forming protein complex with RGP1 and RGP2	Seed coat specific	Rautengarten et al., 2011
RGP3	AT3G08900	43	0	UDP-Ara mutase	Endosperm specific	Rautengarten et al., 2011
GDSL-LIPASE 3	AT1G71250	57	0	Lipids degradation, cuticle development	Endosperm specific	Kwon et al., 2009; Lee et al., 2009; Volokita et al., 2011
GDSL-LIPASE 4	AT5G03820	55	1	Lipids degradation, cuticle development	Endosperm specific	Kwon et al., 2009; Lee et al., 2009; Volokita et al., 2011
AtENODL10	AT5G57920	80	5	Secretions, plama-membrane and cell wall signalling	Seed specific and high in endosperm, co-expressed with *ALE1, RPG3, RGP4* and *DP1*.	Borner et al., 2002; Ma et al., 2011
CSY1	AT3G58740	15	1	β-oxidation of fatty acids breakdown in the seeds	Seed specific and high in endosperm	Pracharoenwattana et al., 2005

The expression pattern of the candidate genes were analysed against the Genevestigator *Arabidopsis* Affymetrix 22K microarray database (Zimmermann et al., 2004) and coexpressed gene networks were inferred from ATTED-II Version 2.0.

5.1.*3 Dirigent protein 1* (*DP1, AT4G11180*)

Dirigent proteins were first discovered to have a role in oligomeric lignan biosynthesis which contributes to the heterogeneity of lignins during the formation of xylem cell walls and phloem fibres (Burlat et al., 2001). The evidence that dirigent proteins might participate in lignin assembly was the identification of metabolites that contain dirigent binding sites during lignin chain formation (Davin and Lewis, 2005). By examining the co-accumulation network of lignin and lignan metabolites, 10 putative dirigent proteins were identified, eight of which were root specific, one of which was universally expressed and one of which (*DP1)* was specifically expressed in the seeds. Genevestigator shows that *DP1* has a testa specific expression pattern (Zimmermann et al., 2004). This suggests that *DP1* might be involved in

lignin metabolism during seed development. Moreover, LC-MS analysis of seed extract showed that *dp1* T-DNA insertion mutants (*SAIL_60_D04*) had defects in producing SC(4-O-β)G 4'-O-hexoside which is a kind of neolignan, suggesting an important role of *DP1* in the biosynthesis of seed specific lignin (Matsuda et al., 2010). In *zou* mutants, *DP1* was up-regulated suggesting *ZOU* might regulate cell wall biosynthesis in seeds.

5.1.4 *α-dioxygenase 1* (*α-DOX1, AT3G01420*)

α-dioxygenases (α-DOXs) catalyse the initiation of the oxylipin biosynthesis pathways (De León et al., 2002). Oxylipins comprise a large group of fatty acid derivatives which play critical roles in defense response and programmed cell death. Importantly, jasmonate precursors are produced by oxylipin pathways (Vellosillo et al., 2007). The biochemical functions of the α-dioxygenases were characterized in tobacco leaves. The α-dioxygenase generated compounds, oxylipins, were strongly induced upon *Pseudomonas syringae* infection and overexpression of α-dioxygenases in bacteria infected leaves changed the composition of oxylipin derivatives suggesting that α-dioxygenases played an important role in defense response by affecting the oxylipin products (Hamberg et al., 2003). In *Arabidopsis*, two α-dioxygenases have been characterized, *α-DOX1* which is up-regulated in *zou* mutants and *α-DOX2* which did not appear in our SOLEXA datasets. *α-DOX1:GUS* has been detected in roots and senescing leaves (De León et al., 2002), and according to the e-FP Browser *α-DOX1* is highly expressed in the seeds (Winter et al., 2007). The expression of *α-DOX1* is induced by bacterial infections, SA and nitric oxide (NO), whilst reduced *α-DOX1* expression in plants compromises disease resistance, suggesting that *α-DOX1* has a role in protecting plants from biotic stresses (De León

et al., 2002). *α-DOX2* is not induced by pathogens and loss of function mutants do not show any visible phenotype, suggesting that *α-DOX2* may not be involved disease resistance (Bannenberg et al., 2009).

5.1.5 *Reversibly glycosylated polypeptides* (*RGP*s)

Reversibly glycosylated polypeptides (RGPs) are a group of enzymes involved in polysaccharide metabolism. In plants, *RGPs* have been suggested to have two different functions, modification of polysaccharide side chains during cell wall biosynthesis and initiation of starch biosynthesis during energy reserve accumulation (Langeveld et al., 2002). Genes encoding *RGPs* have been identified from different species including *Arabidopsis*, rice, wheat, potato, maize and cowpeas (*Vigna unguiculata*) (Langeveld et al., 2002). The characterization of rice *RGP* homologues have shown that they participate in transformation of uridine diphosphate (UDP)-arabinopyranose (UDP-Ara*p*) to UDP-arabinofuranose (UDP-Ara*f*) which is a key constituent of plant cell walls, suggesting that rice RGPs act as UDP-Ara*p* mutases (UAMs) in the biosynthesis of plant primary and secondary cell wall polysaccharides (Konishi et al., 2007). Down-regulation of an endogenous rice *RGP*-encoding gene, OsUAM1, by RNAi in vascular tissues, caused compromised UAM activity and decreased *Araf* content in the cell walls, resulting in their deformation (Konishi et al., 2011). In *Arabidopsis*, five *RGP* genes, *AtRGP1* to *5* have been identified, amongst which *AtRGP1* and *AtRGP2* share more identity than the other *RGP* genes (Drakakaki et al., 2006). *AtRGP1* was shown to have a glycosylase activity when it was expressed in *E. coli* and could be reversibly glycosylated when using UDP-glucose and UDP-galactose as substrates (Delgado et al., 1998). *AtRGP1* and *AtRGP2* are strongly expressed in apical meristem, root tips and flowers, and RGP1

and RGP2 proteins are localized in both the Golgi and the cytoplasm (Drakakaki et al., 2006). *rgp1*and *rgp2* single mutants did not show visible defects in development compared to the wild-type, however, *rgp1 rgp2* double mutants displayed defects in pollen morphology, suggesting that *RPG1* and *RGP2* are critical for pollen development. Interestingly, *RGP2* was also shown to be localized in the plasma-membrane and plasmodesmata in leaf epidermal cells, with a role in restricting virus spread and starch accumulation (Sagi et al., 2005; Zavaliev et al., 2010). How RGPs are transported from the Golgi to the plasma-membranes and plasmodesmata is still unclear. In a recent study *AtRGP1*, *AtRGP2* and *AtRGP5* transcripts were detected universally with high accumulation in flowers, seedlings, and siliques, whilst *AtRPG3* and *AtRGP4* transcripts were only detected in siliques with highest levels seen at the torpedo stage of embryo development (Rautengarten et al., 2011). *Promoter-YFP* reporter lines showed that *AtRGP1*, *AtRGP2* and *AtRGP5* were expressed in all major organs, whilst *AtRPG3* was expressed in the endosperm from the heart to walking stick stage of embryo development and *AtRGP4* was detected in the epidermal cells of seed coat from the heart to mature stage of embryo development (Rautengarten et al., 2011). *RGPpro:RGP-YFP* reporter lines confirmed that AtRGP1, AtRGP2 and AtRGP5 were localized in the Golgi and the cytosol, however, no conclusive data on the subcellular localizations of AtRPG3 and AtRGP4 was presented (Rautengarten et al., 2011).

Biochemical analysis showed that only AtRGP1, AtRGP2 and AtRGP3have UDP-*Ara* mutase activity which can interconvert UDP-*Arap* and UDP-*Araf*. This activity is absent from AtRGP4 and AtRGP5 (Rautengarten et al., 2011). In *zou* mutants, *AtRGP3* is down-regulated, in contrast to *AtRGP4* which is up-regulated in *zou*

mutants. Considering the different expression pattern and biochemical activities of AtRGP3 and AtRGP4, it is likely that RGP3 and AtRGP4 have different roles in seed development.

5.1.6 *GDSL-Lipases* (*GLIP*s)

GDSL-Lipases are named after the consensus amino acid sequence, Gly, Asp, Ser and Leu around their active site (Akoh et al., 2004). *GDSL-Lipases* belong to a large gene family across the land plants, which comprises three major subfamilies according to the consensus motifs in the amino-terminal GDSL and/or carboxy-terminal W/FDXXH regions. 604 *GDSL-Lipases* from seven species have been identified by searching the published genomic databases (Volokita et al., 2011). In *Arabidopsis*, over 30 *GDSL-Lipase*s have been annotated with diverse functions, including regulation of hormone responses, stress tolerance, disease resistance, cuticular wax biosynthesis, root nodulation, pollen coat protein functions, esterase activity in germinating seeds, etc (Volokita et al., 2011). *Arabidopsis Cuticle Destructing Factor 1* (*CDEF1*) encodes a member of GDSL-Lipase family protein and has a cutinase activity which degrades plant cuticle (Takahashi et al., 2010). Overexpression of *CDEF1* increases surface permeability and disrupts the epidermal cuticle layer suggesting a role of GDSL-Lipase in hydrolysing very long-chain fatty acids and their derivatives of cuticular wax (Takahashi et al., 2010). *GDSL-Lipase 3* (*GLIP3*, *AT1G71250*) and *GDSL-Lipase 4* (*GLIP4*, *AT5G03820*) are predicted to be only expressed in the endosperm by the Genevestigator microarray database (Zimmermann et al., 2004), and they are down-regulated in *zou* mutants suggesting that they might be involved in endosperm breakdown and/or embryonic epidermal cuticle development.

5.1.7 *Plastocyanin-like protein*/*nodulin-like protein 10* (*AtENODL10*, *AT5G57920*)

Plastocyanin-like proteins belong to phytocyanin protein family (PCs) which are ancient mono copper binding proteins, thus are predicted to have functions in electron transportation (Borner et al., 2002). Based on their domain structure and phylogenetic relationships, *Arabidopsis* phytocyanin proteins are composed of six groups of proteins, namely uclacyanins (UCs), stellacyanins (SCs), plantacyanins, early nodulin-like (ENODL) proteins, Plastocyanin-like domain (PCLD)-containing proteins and chimeric arabinogalactan proteins (AGPs) (Ma et al., 2011; MASHIGUCHI et al., 2009). *AT5G57920* is classified in the group of early nodulin-like proteins, and is also known as *AtENODL10*. Domain analysis has shown that AtENODL10 has a signal peptide at the amino end, a PCLD and an AGP-like domain in the middle, and a glycosylphosphatigylinositol (GPI)-anchor signal at the carboxyl end (Ma et al., 2011). The N-terminal signal peptide of AtENODL10 suggests that it might be secreted, whilst the AGP-like domains suggest that it could act as a cell surface glycoprotein. AGP proteins typically have a protein backbone glycosylated by AG polysaccharides involved in interactions with cell wall compositions, and a GPI-anchor which attaches the protein to the plasma-membrane (Borner et al., 2002). However, AtENODL10 does not appear to contain a GPI-anchor domain. *AtENODL10* (*AT5G57920*) is down-regulated in *zou* mutants. It is predicted to be specifically expressed in the endosperm and co-expressed with several other *ZOU* regulated seed specifically expressed genes, such as *ALE1*, *RGP3*, *RGP4* and *DP1* which are likely involved in cell wall and cuticle development (Zimmermann et al., 2004). Taken together, it is likely that *AtENODL10* might be involved in cell surface signalling or/and cell wall and cuticle pathways.

5.1.8 *Citrate synthase 1* (*CSY1*)

Citrate synthases (CSYs) are a group of enzymes essential for β-oxidation which involves metabolism of fatty acid *via* the glyoxylate cycle in the peroxisome (Graham, 2008). TEM data and biochemical analysis have suggested that storage oil metabolism in *Arabidopsis* seeds is linked to β-oxidation and the glyoxylate cycle. During oil body breakdown triacylglycerol (TAG) is hydrolysed to fatty acids in the cytosol and transported into peroxisomes by ATP-binding cassette (ABC) transporters. Fatty acids are subsequently converted into acetyl-CoA *via* β-oxidation and the glyoxylate cycle, and the products of β-oxidation are then transported to the mitochondria to be used either for gluconeogenesis or for respiration (Graham, 2008). In *Arabidopsis*, five citrate synthases have been identified and phylogenetically divided into two groups, CSY1 to 3 in one group and CSY4 to 5 in the other (Pracharoenwattana et al., 2005). RT-PCR analysis has shown that *CSY1* is specifically expressed in the siliques, whilst *CSY2* and *CSY3* are not only expressed in the siliques but also expressed in flowers and leaves (Pracharoenwattana et al., 2005). Moreover, Genevestigator microarray data show that *CSY1* expression is localized in the endosperm (Zimmermann et al., 2004), suggesting *CSY1* might have a role in endosperm catabolism. *cys1*, *cys2* and *cys3* single mutants did not show significant differences in CSY activities in seedlings. *csy2 cys3* double mutants cannot break dormancy; however this phenotype can be overcome by removing the seed coat. In addition *csy2 csy3* seedlings cannot be maintained until adulthood (Pracharoenwattana et al., 2005). TEM showed that five days after germination *csy2 cys3* double mutants displayed enlarged and persistent oil bodies in the seedlings compared to the wild-type, suggesting that *CSY*s have a role in lipid breakdown

(Pracharoenwattana et al., 2005). Consistent with a role in endosperm catabolism, *CSY1* is down-regulated in *zou* mutants.

5.1.9 Aims of this chapter

The aims of this chapter are to identify novel regulators of cell death and cuticle development that may be represented in the SOLEXA cDNA sequencing datasets of wild-type *vs zou* mutant siliques. Criteria for selecting the genes to be analysed were based on the type of protein and their expression patterns. I sought to validate the regulation of candidate genes by *ZOU* and ascertain the expression patterns of some of the candidate genes. In addition I sought to pinpoint potential functions for these genes in seed development, and test their genetic interactions with *ZOU*.

5.2 Results

5.2.1 Validation of *ZOU* regulated genes by RT-PCR

SOLEXA whole transcriptome sequencing of the wild-type and *zou* mutant heart stage siliques have shown that 64 genes are significantly up-regulated in *zou* mutants and over 233 genes are significantly down-regulated in *zou* mutants. Among these genes we picked out *LOL2* (*AT4G21610*), *DP1* (*AT4G11180*), *DOX1* (*AT3G01420*) and *RGP4* (*AT5G50750*) which are up-regulated in *zou* mutants, and *RGP3* (*AT3G08900*), *GLIP3* and *4* encoding genes (*AT1G71250* and *AT5G57920*, repectively), and *CSY1* (*AT3G58740*) which are down-regulated in *zou* mutants, to examine their genetic and molecular relationship to *ZOU*. In order to validate the SOLEXA sequencing results, gene specific primers were designed and RT-PCR analysis was performed. Siliques from Col-0 wild-type plants and *zou-4* mutants containing late heart stage embryos were harvested and RNA was made from the siliques. An *Arabidopsis TUBULIN* gene transcript was used as a control for loading and RNA integrity. Gel image showed that there was less expression of *LOL2*, *DP1*, *DOX1* and *RGP4* in the wild-type than in *zou* mutants, suggesting an up-regulation of these genes in *zou* mutants, and there was more expression of *RGP3*, *GLIP3* and *GLIP4*, and *CSY1* in the wild-type than in *zou* mutants, suggesting a down-regulation of these genes in *zou* mutants (Figure 5.2). These results were consistent with the SOLEXA results.

Figure 5.2 RT-PCR analysis on gene expressions in the sililques of Col-0 wild-type plants and *zou-4* mutants.

Primer sets that were specific for the genes listed on the left side of the gel image were used. An *Arabidopsis* TUBULIN-encoding gene was used as a control for loading and RNA integrity. The siliques that were used for RNA extraction contained heart stage embryos.

5.2.2 Phenotypic analysis of T-DNA insertion mutants of genes regulated by *ZOU*

T-DNA insertion mutants of genes regulated by *ZOU* were ordered from NASC, and lines containing homozygous, heterozygous and no T-DNA insertions for each gene were identified by PCR based genotyping. The structure of genomic regions and the position of T-DNA insertions are shown in Figure 5.3. The T-DNA lines used were all in the Col-0 ecotype. *lol2-3* contains a T-DNA insertion localized in the last exon (*SALK_144734*). *dp1-1* contains a T-DNA localized in the middle of the exon (*SAIL_60_D04*). *dox1-1* contains a T-DNA localized in the second exon (*SALK_113614C*). Two *rgp4* alleles were identified (*rgp4-2* and *rgp4-1*), one contains a T-DNA localized in the promoter region (*SALK_094267*) and the other contains a T-DNA localized in the second exon (*SALK_150951*). Two *rgp3* alleles were identified (*rgp3-1* and *rgp3-2*), both of which contain a T-DNA localized in the last exon (*SALK_116503* and *SALK_113532*). *gdsl-lipase3-1* (*glip3-1*) contains a T-DNA insertion localized in the first exon (*SALK_094513*). *gdsl-lipase4-1* (*glip4-1*) contains a T-DNA insertion localized in the second exon (*GK-359A07*). *atenodl10-1* contains a T-DNA insertion localized in the second exon (*SALK_107590*). *csy1-1* contains a T-DNA insertion localized in the fifth exon (*SALK_007026*).

JAR1 showed no significant difference in expression between the wild-type and *zou* mutants in the SOLEXA whole transcriptome sequencing. This gene plays very important roles in JA biosynthesis (Katsir et al., 2008). However, as the JA signalling pathway is massively down-regulated in *zou* mutants according to the SOLEXA sequencing results, it was important to verify the seed phenotype of *jar1* mutants and *jar1-1,* a functionally null allele (*CS8072*) (Staswick and Tiryaki, 2004), was therefore included in the analysis.

The seed phenotype and epidermal cuticle phenotype of the cotyledons were examined for each mutant line described (Figure 5.4 to Figure 5.6). Mature seeds from the homozygous plants of the each mutant allele were harvested and dried. No seed abnormality was observed in seeds of any of the mutants that were examined under the dissecting microscope (Figure 5.4).

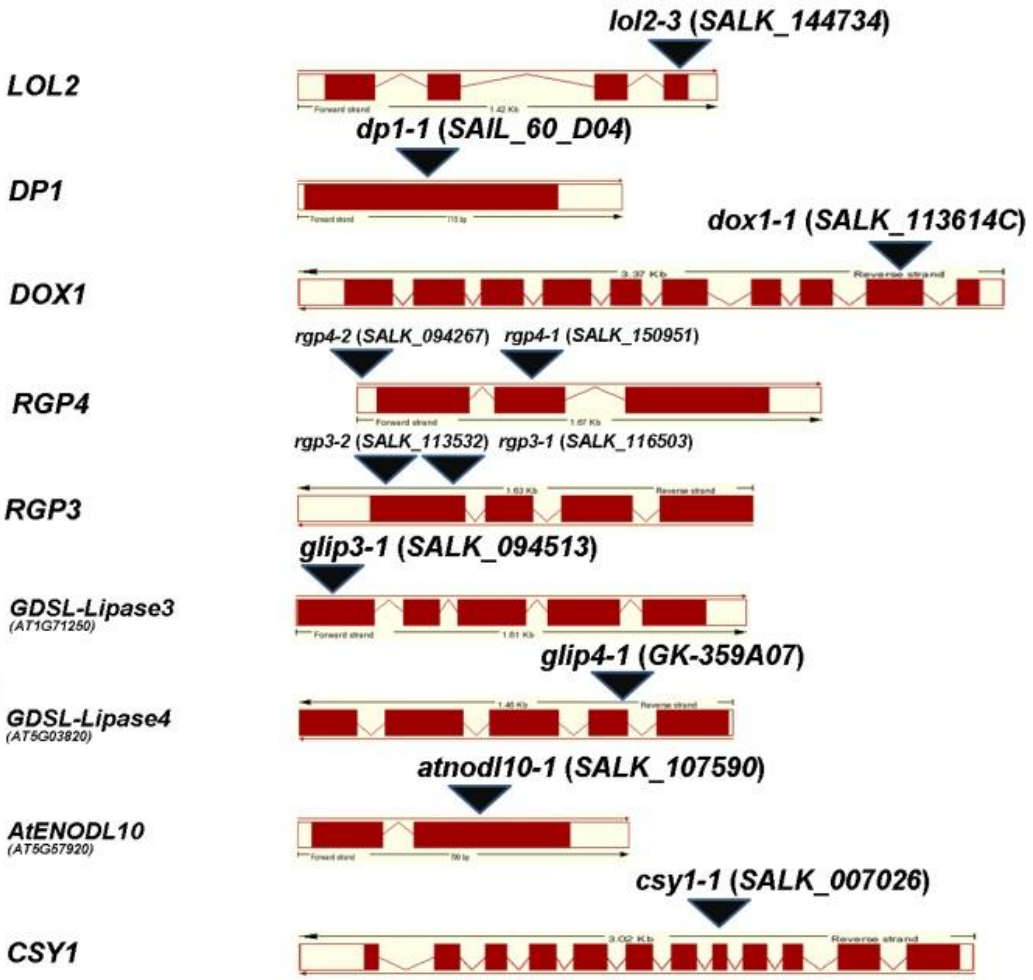

Figure 5.3 Structures of *ZOU* regulated gene mutant alleles.

ZOU regulated gene names are listed on the left side. The structures of genomic regions are shown in red colour and the exons are indicated by red rectangles. The 5' and the 3' UTRs are indicated by white rectangles. The long red arrow lines indicate the directions of the gene transcription and the black arrow lines indicate the length of the genomic region. The positions of T-DNA insertions are shown as black triangles on which the names of T-DNA alleles are marked. The genomic structure of each gene was downloaded and modified from the NASC Ensembl website.

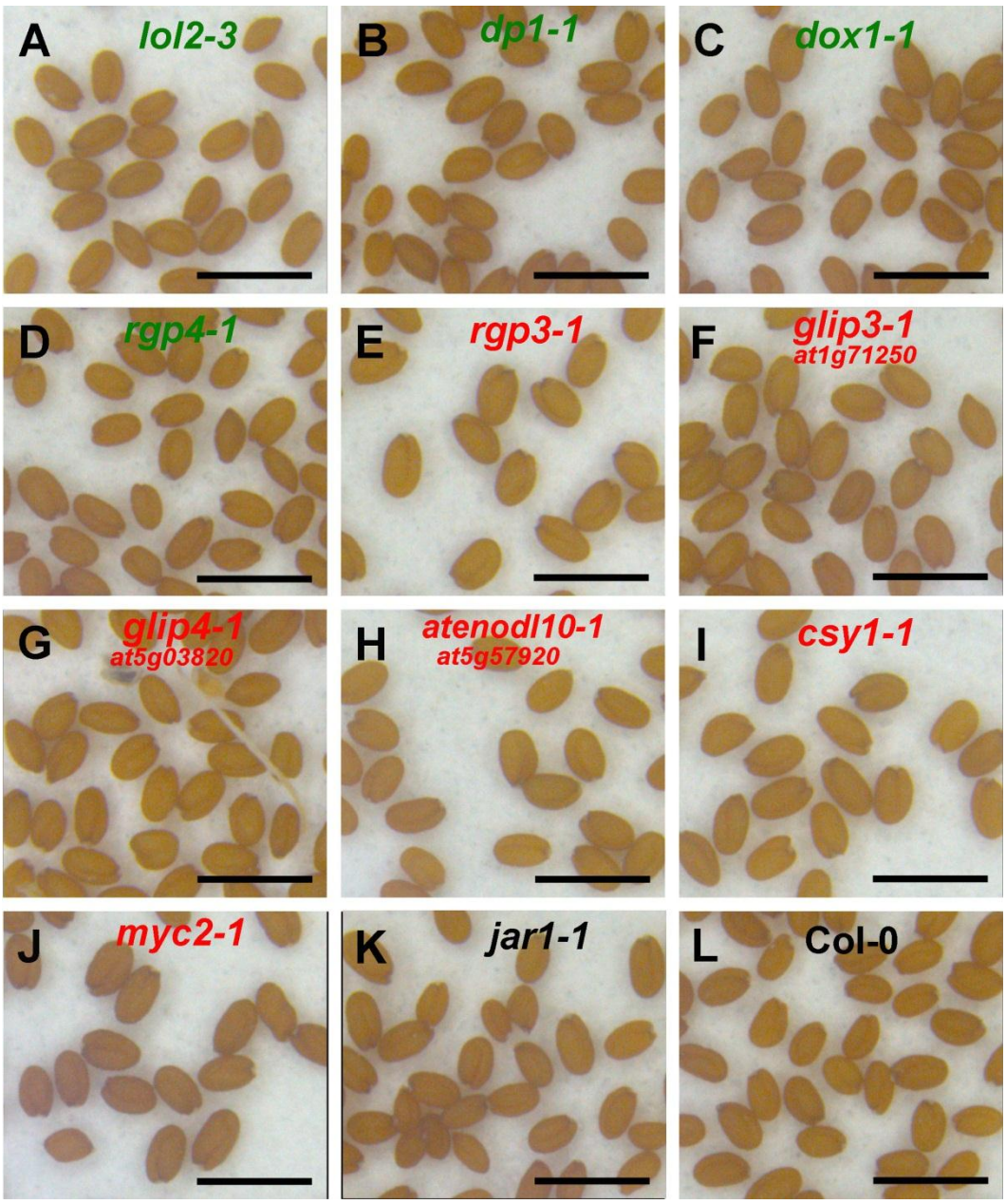

Figure 5.4 Seed phenotype of the T-DNA insertion lines

The names of the T-DNA insertion mutants are marked in either red (indicating the genes that are down-regulated in *zou* or green (indicating the genes that are up-regulated in *zou*). *JAR1* is not regulated by *ZOU*. Scale bars represent 2 mm.

In order to further analyse the seed size and seed shape of the mutants, the seed images of homozygous, heterozygous and wild-type *lol2-3*, *dp1-1*, *dox1-1*, *rgp4-1*, *rgp3-1*, *glip3-1*, *glip4-1*, *atenodl10-1* and *csy1-1* mutants were taken and converted into grey scale. ImageTool 2.0 was used to measure the area, the length of the major axis and the length of the minor axis of the seed images. At least 50 seeds from each allele were analysed. ANOVA was performed to analyse the variance among the homozygotes, heterozygotes and the wild-type. Among all the T-DNA lines that were analysed, there was no significant difference observed among homozygotes, heterozygotes and the wild-type in dry seed area, length of the major axis and length of the minor axis ($P>>0.01$). Some of the results are shown in Figure 3. For instance, in *lol2-3* mutants, seeds from 2 homozygous lines, 2 heterozygous lines and 2 wild-type lines which were identified by genotyping were used for the analysis. However, no significant difference were identified in seed area, length of the major axis and length of the minor axis among the 2 homozygous lines, 2 heterozygous lines and 2 wild-type lines (Figure 5.5, the first panel). To summarize, there was no abnormality observed in seed colour or seed size among the T-DNA insertion mutants of the genes regulated by *ZOU*.

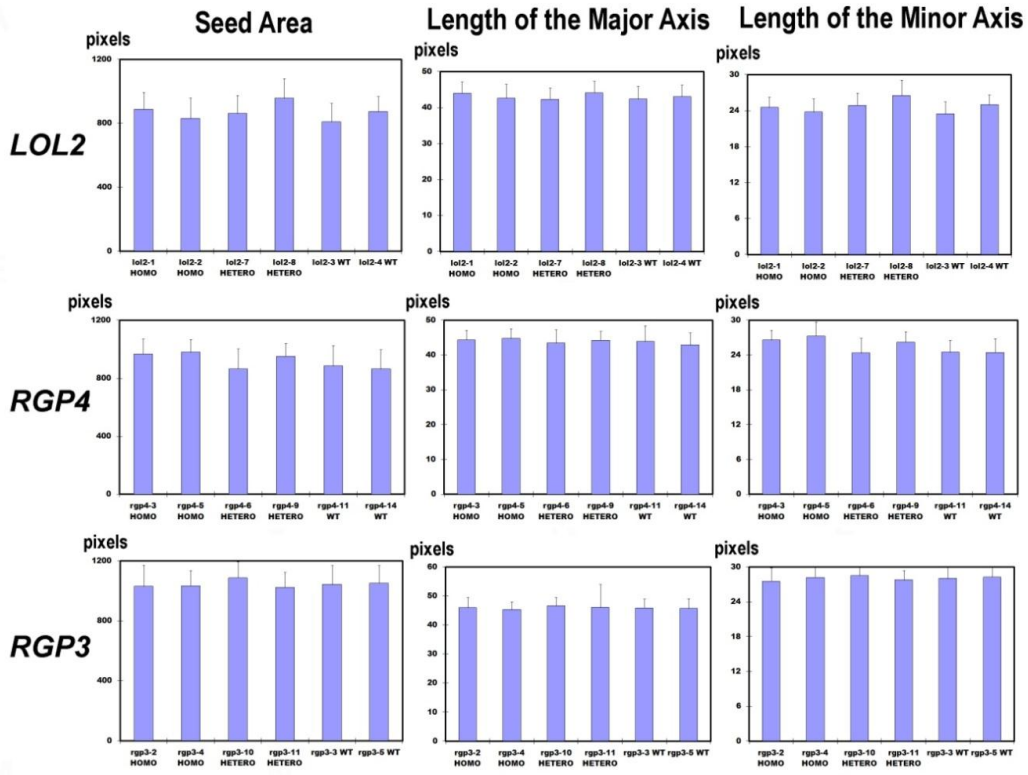

Figure 5.5 Measurement of seed size of *lol2-3*, *rgp4-1* and *rgp3-1* mutants.

For each T-DNA insertion line, at least 50 seeds were measured. The images of the seeds were taken and converted into grey scale. UTHSCSA ImageTool 2.0 was used to measure the area, the length of the major axis and the length of the minor axis of the seeds. The unit used for the measurement was pixels. The error bar=S.D. of biological replicates.

ZOU regulates embryonic epidermal cuticle development. *ZOU* targets might therefore also regulate embryonic epidermal cuticle development. In order to test this hypothesis, the cuticle development in cotyledons of the T-DNA insertion mutants of *ZOU* regulated genes was examined. Toluidine Blue tests were used to examine cuticle development (Tanaka et al., 2004). Two-week-old seedlings of homozygous

lol2-3, *dp1-1*, *dox1-1*, *rgp4-1*, *rgp3-1*, *glip3-1*, *glip4-1*, *atenodl10-1*, *csy1-1*, *zou-4* mutants and the wild-type were stained with Toluidine Blue and washed several times with distilled water. The results are shown in Figure 5.6. The cotyledons of the T-DNA insertion mutants did not stain any more than wild-type. In contrast, the cotyledons of *zou-4* mutants were stained a dark blue colour (Figure 5.6 K, arrow). Moreover, there were no visible morphological defects observed in the cotyledons of T-DNA insertion mutants. To summarize *lol2-3*, *dp1-1*, *dox1-1*, *rgp4-1*, *rgp3-1*, *glip3-1*, *glip4-1*, *atenodl10-1*, and *csy1-1* mutants do not show embryonic epidermal cuticle defects.

Figure 5.6 Toluidine Blue tests on epidermal cuticle integrity of cotyledons of the T-DNA insertion mutants.

The names of the T-DNA insertion mutants are marked in yellow (indicating that the genes are down-regulated by *ZOU*) or in red (indicating that the genes are up-regulated by *ZOU*). Cotyledons of two-week-old seedlings were stained by Toluidine Blue and washed several times with distilled water. K, arrow indicates the dark blue cotyledons of *zou* mutants that were stained by the Toluidine Blue.

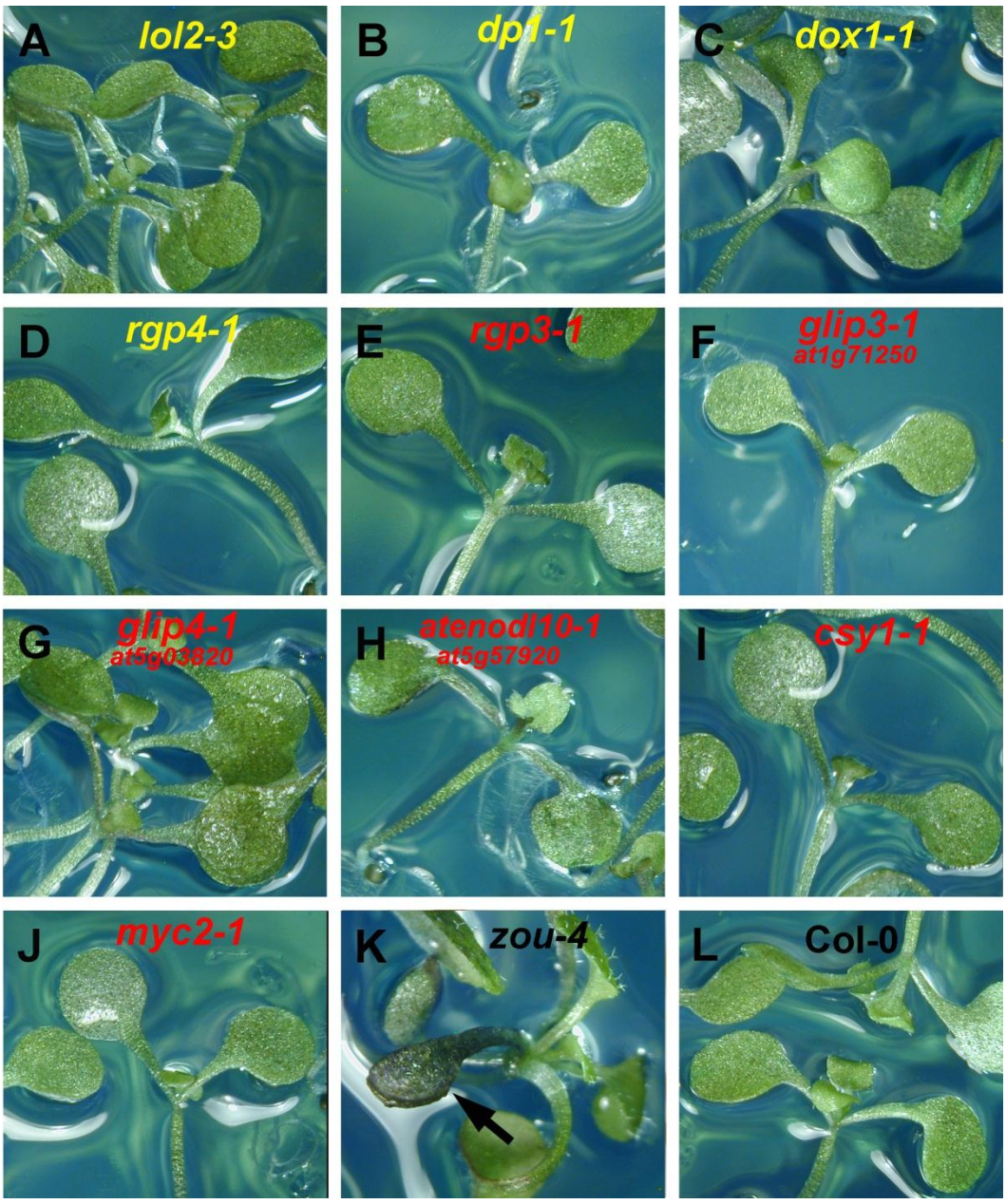

5.2.3 Gene expression analysis on siliques of *rgp4-1* and *rgp3-1* T-DNA insertion mutants

We were intrigued by the fact that two closely related members of the *RGP* gene family were oppositely regulated in *zou* mutants. We therefore decided to study these genes in more detail. The expression of *RGP4* and *RGP3* was analysed in the siliques

of *rgp4-1* (*SALK_150951*) and *rgp3-1* (*SALK_116503*) mutants containing heart stage and torpedo stage embryos by RT-PCR. Gene specific primer sets were designed upstream of the T-DNA insertion, spanning the T-DNA insertion and downstream of the T-DNA insertion. *RGP4* expression was detected in *rgp4-1* mutant siliques containing heart and torpedo stage embryos respectively when using the primer sets upstream of the T-DNA insertion (Figure 5.7 A, primer set 1), first panel of the gel image). However, no *RGP4* transcript was detected when using the primer sets spanning the T-DNA insertion and downstream of the T-DNA insertion in *rgp4-1* siliques (Figure 5.7 A, second to forth panel of the gel image). As a positive control, *RGP4* expression was detected by all the primer sets in Col-0 wild-type siliques containing heart and torpedo stage embryos. It seems likely that this allele of *RGP4* is functionally null based on the position of the T-DNA insertion in the gene.

RGP3 expression was detected in both *rgp3-1* mutants, in siliques containing heart and torpedo stage embryos when using the primer sets upstream of the T-DNA insertion (Figure 5.7 B, primer set 1), first panel of the gel image) and using the primer set downstream of the T-DNA insertion (Figure 5.7 B, primer set 3), third panel of the gel image). However, *RGP3* expression was not detected when using the primer sets spanning the T-DNA insertion (Figure 5.7 B, primer set 2), second panel of the gel image). As a positive control, *RGP3* expression was detected by using all the primer sets in Col-0 wild-type siliques containing heart and torpedo stage embryos.

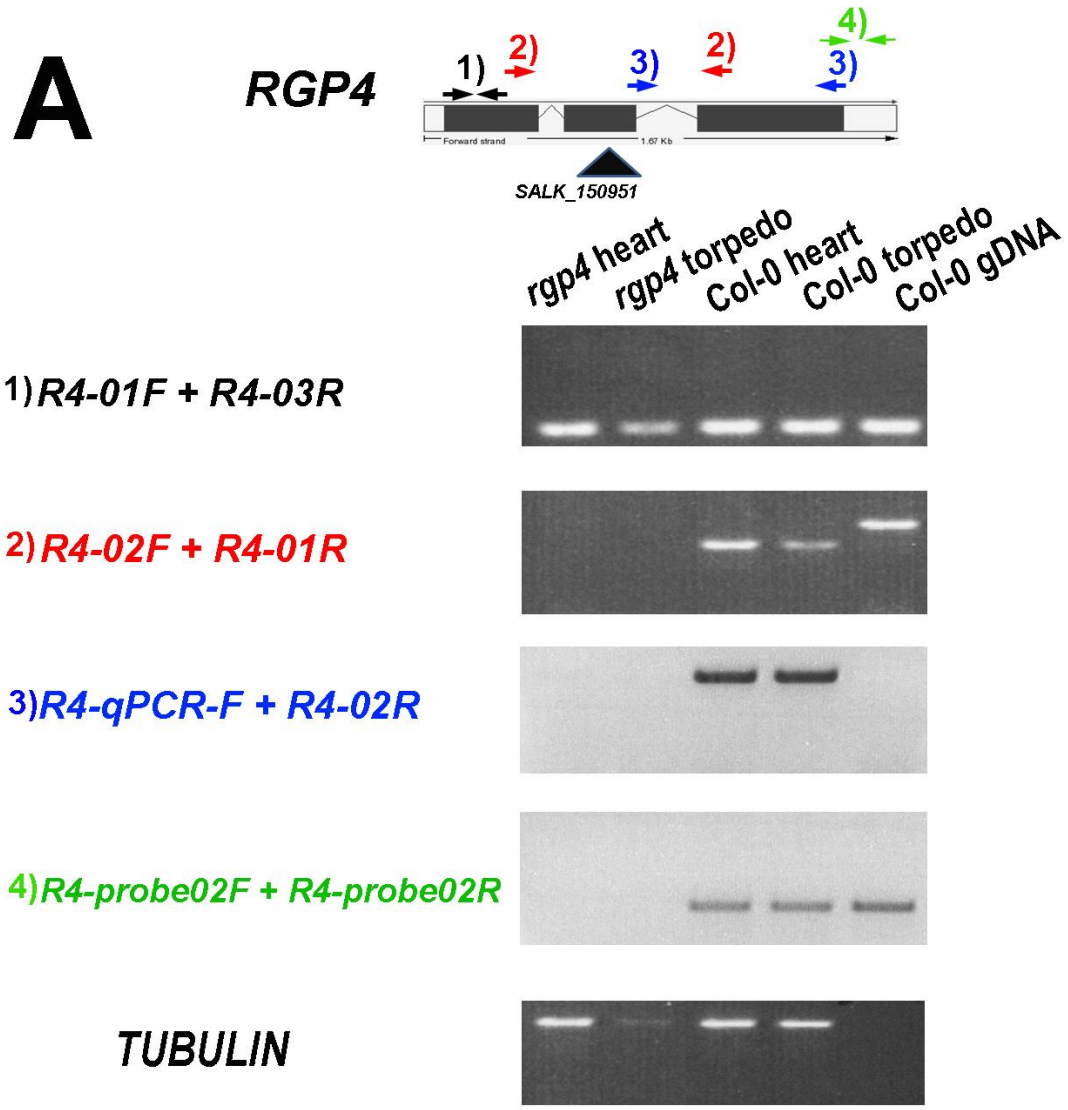

Figure 5.7 RT-PCR analysis on *RGP4* and *RGP3* transcription in *rgp4-1* and *rgp3-1* mutants.

A and B, the structures of *RGP4* and *RGP3* genomic regions are shown. The exons are indicated by black rectangles and the 5' and the 3' UTRs are indicated by white rectangles. The long arrow lines indicate the directions of the gene transcription and the length of the genomic region. The positions of T-DNA insertions are shown as black triangles below which the names of T-DNA alleles are marked. The gene specific primer sets that were used for RT-PCR are labelled on the left side of the gel images.

Figure 5.7 Continued.

Arrows marked on the genomic structure indicate the position of the primers. The number with a half bracket on top of the arrows matches the number of the primer sets. The genomic structure of each gene was downloaded and modified from the NASC Ensembl website. An *Arabidopsis* TUBULIN-encoding gene was used as a control for loading and RNA integrity. A, RNA was prepared from *rgp4-1* mutant siliques containing heart stage embryos (labelled as *rgp4-1* heart) and torpedo stage embryos (labelled as *rgp4-1* torpedo), and from Col-0 siliques containing heart stage embryos (labelled as Col-0 heart) and torpedo stage embryos (labelled as Col-0 torpedo). Genomic DNA made from Col-0 (labelled as Col-0 gDNA) was used as control.

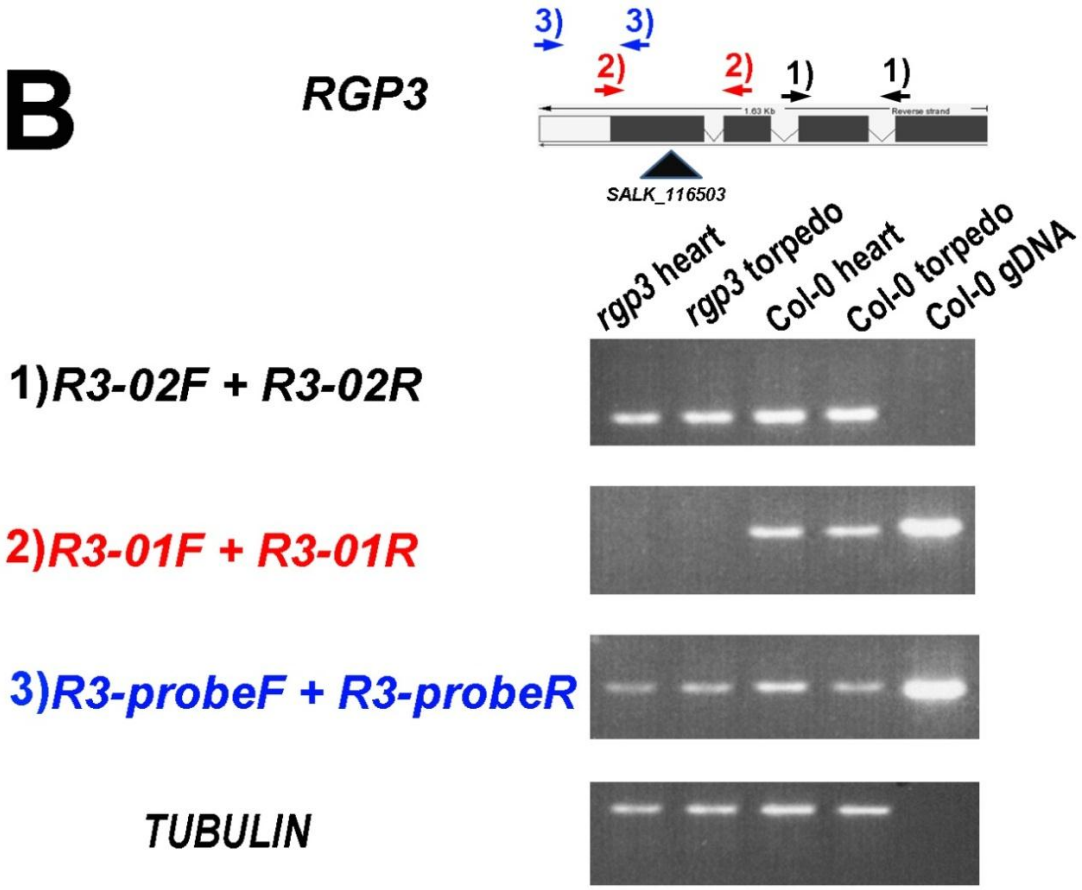

Figure 5.7 Continued.

B, RNA was prepared from *rgp3-1* mutant siliques containing heart stage embryos (labelled as *rgp3-1* heart) and torpedo stage embryos (labelled as *rgp3-1* torpedo), and from Col-0 siliques containing heart stage embryos (labelled as Col-0 heart) and torpedo stage embryos (labelled as Col-0 torpedo). Genomic DNA made from Col-0 (labelled as Col-0 gDNA) was used as control.

5.2.4 *RGP4* expression pattern during seed development

RPG4 is predicted to be expressed exclusively in the seed by the Arabidopsis eFP browser (Winter et al., 2007). In order to localize the *RGP4* expression in the seed, RNA *in situ* hybridization using *RGP4*-specific antisense probes was performed on wax embedded seed sections. In Col-0 wild-type seeds, from the globular embryo stage to the heart embryo stage *RGP4* is weakly expressed in the inner integument cells (the ii2 layer) (Figure 5.8 A and 5.8 B, red arrows). After the heart embryo stage, the inner integument (ii2 and ii3 layer) collapses and *RGP4* expression is detected in the inner cell layer of the outer integument with increasing intensity (Figure 5.8 C, red arrow). Sense *RGP4* probes were used as the negative control and no signal was detected in the seeds (Figure 5.8 D). *RGP4* expression is up-regulated in *zou* mutant siliques containing heart stage embryos by both SOLEXA whole transcriptome sequencing and RT-PCR analysis (Figure 5.2).

In *zou* mutants, by early heart stage of embryo development there was not an increase in *RGP4* expression detected by *in situ* hybridization in the inner integument (Figure 5.8 E, red arrows) compared to the wild-type seeds at the same stage (Figure

5.8 B, red arrows). However, in *zou* mutants at the late heart stage of embryo development there was a sharp increase in *RGP4* expression in the outer integument. After the heart stage, the difference in *RGP4* expression level in the testa between *zou* mutants and the wild-type was less clear (Figure 5.8 G). *ZOU* up-regulates *ALE1* and down-regulates *RGP4* (Figure 5.2), and so it is possible that *ALE1* down-regulates *RGP4*. In *ale1* mutants, from the heart stage (Figure 5.8 I and 5.8 J) to the torpedo stage (Figure 5.8 K) of embryo development there was no visible increase in *RGP4* expression detected in the testa of *ale1-1* mutants compared to the wild-type (Figure 5.8 C), and the expression of *RGP4* is weaker in *ale1* (Figure 5.8 J) than in *zou* (Figure 5.8 F) at the heart stage of embryo development. These results suggest that *ALE1* does not down-regulate *RGP4*, in other words *ZOU* regulates *RGP4* in an *ALE1* independent fashion.

To confirm this hypothesis, *RGP4* expression was examined in *pSUC5::ALE1 zou-4* line 8-1 and *pSUC5::ALE1* Col-0 line10-1 by *in situ* hybridization. *RGP4* expression was up-regulated in the testa in *pSUC5::ALE1 zou-4* line 8-1at the heart stage of embryo development (Figure 5.8 M) compared to the expression in *pSUC5::ALE1* Col-0 line10-1 at the same stage of embryo development (Figure 5.8 O, red arrows). *RGP4* expression was also up-regulated in *pSUC5::ALE1 zou-4* line 8-1at the torpedo stage of embryo development (Figure 5.8 N) compared to the expression in the wild-type at the same stage of embryo development (Figure 5.8 C, red arrow). These results confirm that *ZOU* regulates *ALE1* and *RGP4* independently. To summarize, *RGP4* has a testa specific expression pattern, and its expression level increases after the heart stage of embryo development. *ZOU* down-regulates *RGP4* expression independently from regulating the expression of *ALE1*.

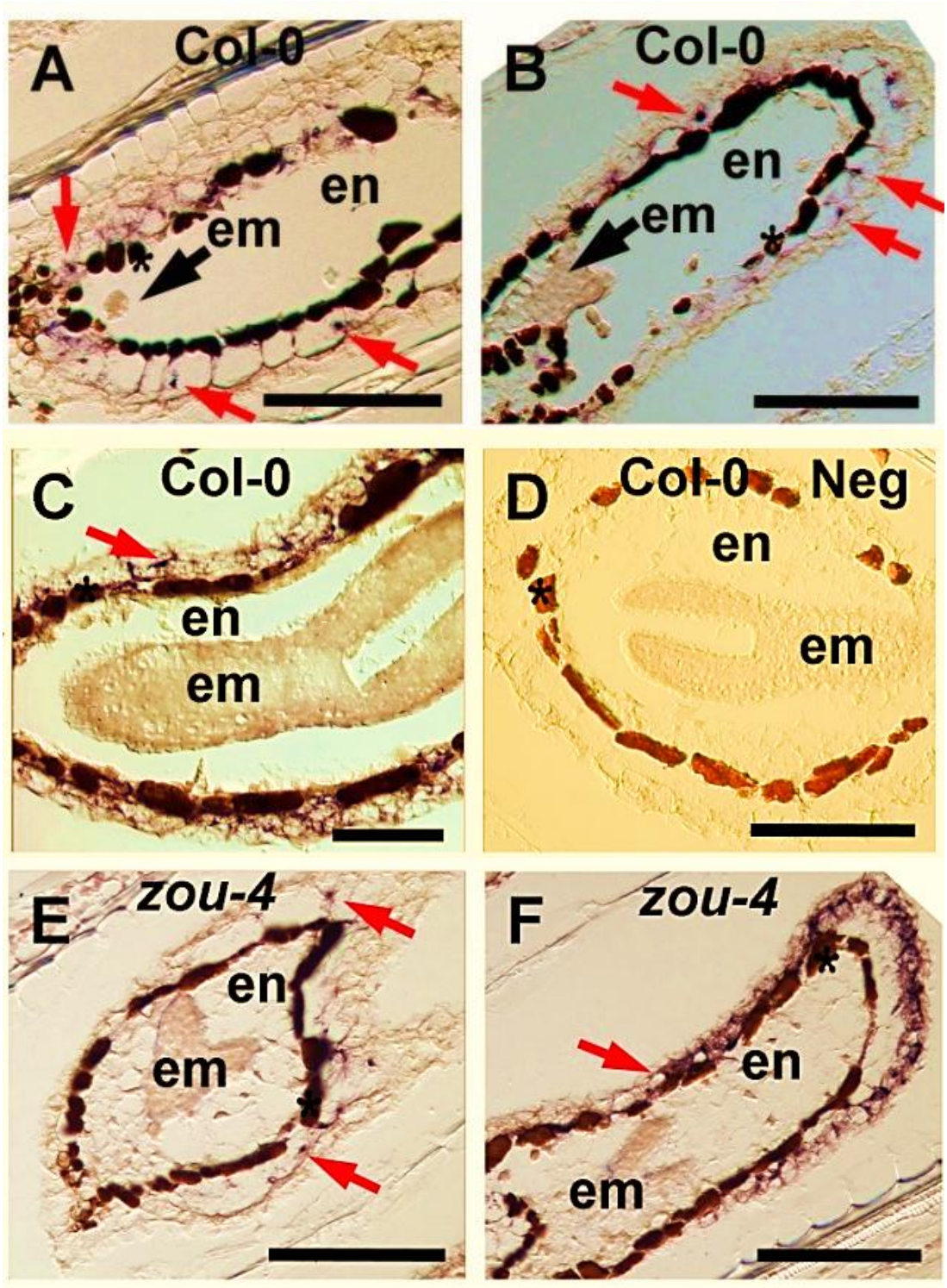
A
Col-0
en
em
B
Col-0
en
em
C
Col-0
en
em
D
Col-0
Neg
en
em
E
zou-4
en
em
F
zou-4
en
em

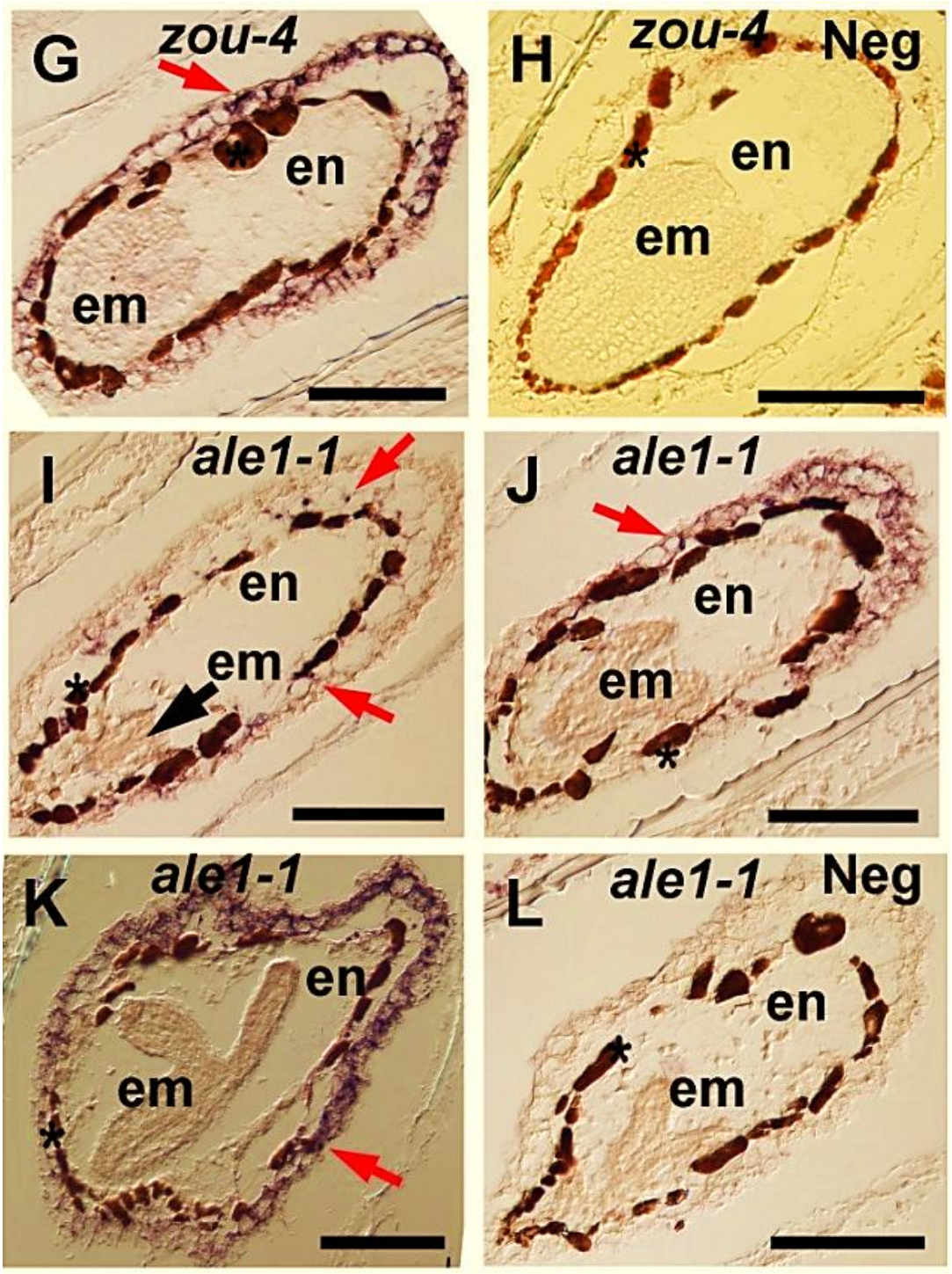
G
zou-4
en
em
H
zou-4
Neg
en
em
I
ale1-1
en
em
J
ale1-1
en
em
K
ale1-1
en
em
L
ale1-1
Neg
en
em

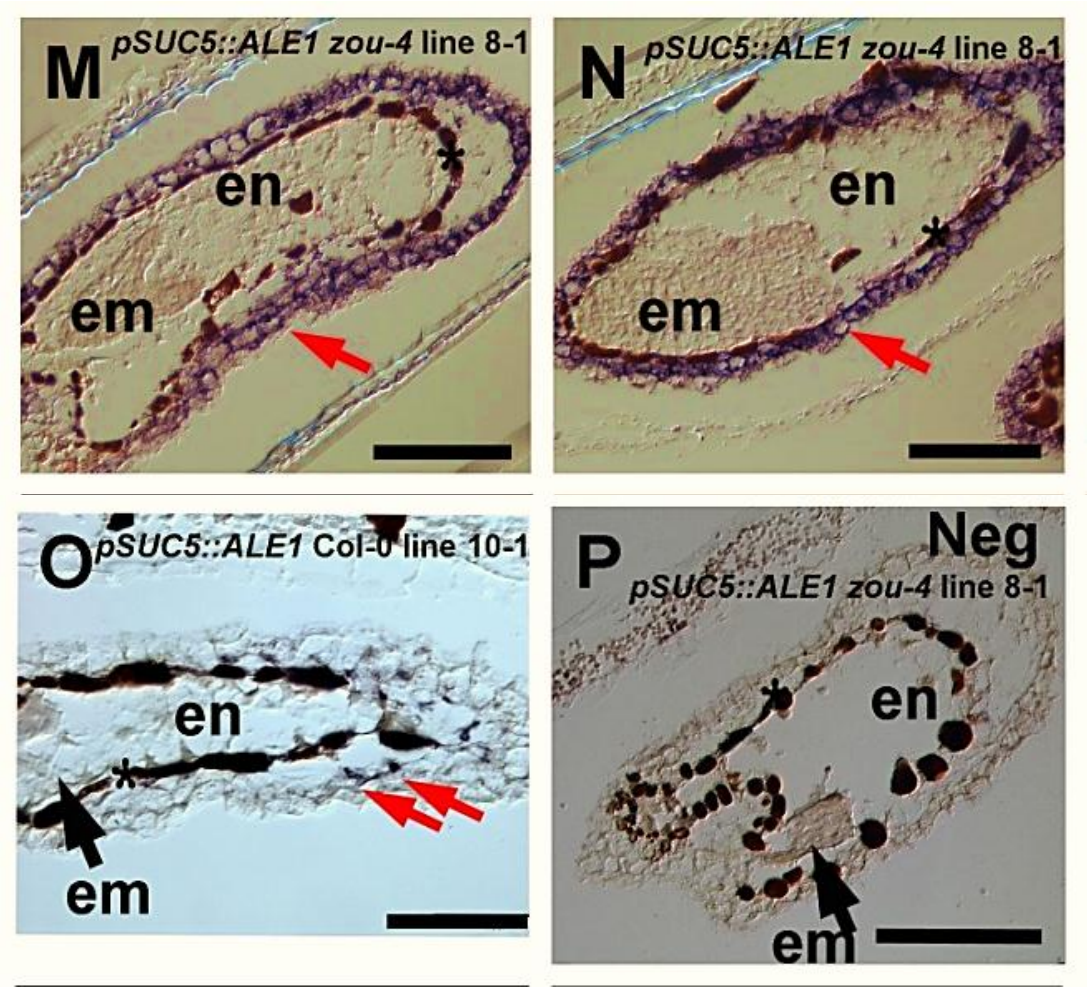

Figure 5.8 *RGP4* expression pattern during seed development by RNA *in situ* hybridizations.

A to P, images of RNA *in situ* hybridizations using digoxigenin-labelled *RGP4* antisense probes (A to C, E to G, I to K and M to O) and sense probes (D, H, L and P) viewed by DIC white light microscope. Signal shows as purple staining; the dark brown stained endothelium does not represent signal (marked by asterisks). Black arrows indicate embryos. Genotypes examined were Col-0 wild-type (A to D), *zou-4* mutants (E to H), *ale1-1* mutants (I to L), *pSUC5::ALE1 zou-4* line 8-1 (M, N and P), and *pSUC5::ALE1* Col-0 line 10-1 (O). A, seed with globular stage embryo. B, E, I, L, M, O and P, seeds with heart stage embryos. C, D, F to H, J, K and N, seeds with torpedo stage embryos.

Figure 5.8 Continued.

A and B, in wild-type plants, from the globular to the heart stage of embryo development the expression of *RGP4* is specifically localized in the inner integument (ii2) shown by purple stained cells (red arrows). C, in wild-type plants, at late torpedo stage of embryo development the inner integument undergoes programmed cell death and collapses the purple stained cells were seen in the outer integument with stronger intensity compared to A and B, suggesting an increase in *RGP4* expression in the outer integument. D, negative control by using sense probes of *RGP4*; no purple stained cells were observed. E to G, in *zou-4* mutants from the heart stage to torpedo stage the localization of *RGP4* expression is not change compared to the wild-type indicated by red arrows. However, at the heart stage the purple staining is much stronger in *zou-4* mutants (F, red arrow) than in the wild-type. I to K, in *ale1* mutants from the heart stage to torpedo stage the localization of *RGP4* expression is not changed compared to the wild-type indicated by red arrows. M and N, from the heart stage the localization of *RGP4* expression is not changed in *pSUC5::ALE1 zou-4* lines and *pSUC5::ALE1* Col-0 lines (O) compared to the wild-type (B and C), but shows increased expression in *pSUC5::ALE1 zou-4* lines at the heart stage (M) as indicated by red arrows. em, embryo; en, endosperm; Neg, negative control; scale bars represent 100 μm.

5.2.5 *RGP3* expression pattern during seed development

The *Arabidopsi*s eFP browser suggests similar temporal patterns of expression for *RGP3* and *RGP4*, although their expression patterns are spatially distinct, with *RGP3* apparently restricted to endosperm tissues (Winter et al., 2007). *RPG3* expression is down-regulated in *zou* mutant siliques compared to the wild-type according to the SOLEXA whole transcriptome sequencing and RT-PCR analysis (Figure 5.2). In order to confirm the localization of *RGP3* expression in the seed, RNA *in situ* hybridization using *RGP3* antisense probes was performed on wax embedded seed sections. In Col-0 wild-type seeds, at the globular stage of embryo development, no *RGP3* expression was detected in the seeds (Figure 5.9 A). From the heart stage to the late torpedo stage of embryo development, *RGP3* expression was detected exclusively in the endosperm surrounding the embryo, also known as the embryo surrounding region (ESR, Figure 5.9 B and 5.9 C, red arrows). *RGP3* sense probes were used as the negative control and no expression was detected in the seeds (Figure 5.9 D). In *zou* mutants, from the globular to the torpedo stage of embryo development, *RGP3* expression was strongly down-regulated and there was almost no signal detected anywhere in the seeds.

Since *ZOU* up-regulates both *RGP3* and *ALE1* and, moreover, since *ALE1* has ESR specific expression pattern, it is formally possible that *ALE1* might up-regulate *RGP3*. To test this hypothesis, *RGP3* expression was examined by RNA *in situ* hybridization in *ale1-1* mutants. In *ale1* mutants, at the globular stage of embryo development, almost no *RGP3* expression was detected in the seeds (Figure 5.9 I), which was the same as in the wild-type (Figure 5.9 A) and *zou* mutants (Figure 5.9 B). However, in *ale1* mutants from the heart stage to the late torpedo stage *RGP3*

expression was strongly detected in the ESR (Figure 5.9 J and 5.9 K, red arrows), suggesting that *ALE1* might not up-regulate *RGP3* expression.

To confirm this observation, *RGP3* expression was tested in *pSUC5::ALE1 zou-4* line 8-1 and *pSUC5::ALE1* Col-0 line10-1 seeds. In *pSUC5::ALE1 zou-4* line 8-1 from the heart stage to the mature stage of embryo development, no *RGP3* expression was detected by *in situ* hybridizations (Figure 5.9 M and 5.9 N). Whilst in *pSUC5::ALE1* Col-0 line10-1 seeds, at the torpedo stage of embryo development, *RGP3* displayed the same expression pattern in the ESR (Figure 5.9 O, red arrows) as was observed in the Col-0 wild-type seeds (Figure 5.9 C, red arrow). These results suggest that *ZOU* up-regulates *RGP3* expression independently of *ALE1*, even though both *ALE1* and *RGP3* expression are localized in the ESR (Tanaka et al., 2001). To summarize, *RGP3* has an ESR specific expression pattern during seed development and *RGP3* expression appears after the globular stage of embryo development. *RGP3* expression is up-regulated by *ZOU* independently of the expression of *ALE1*.

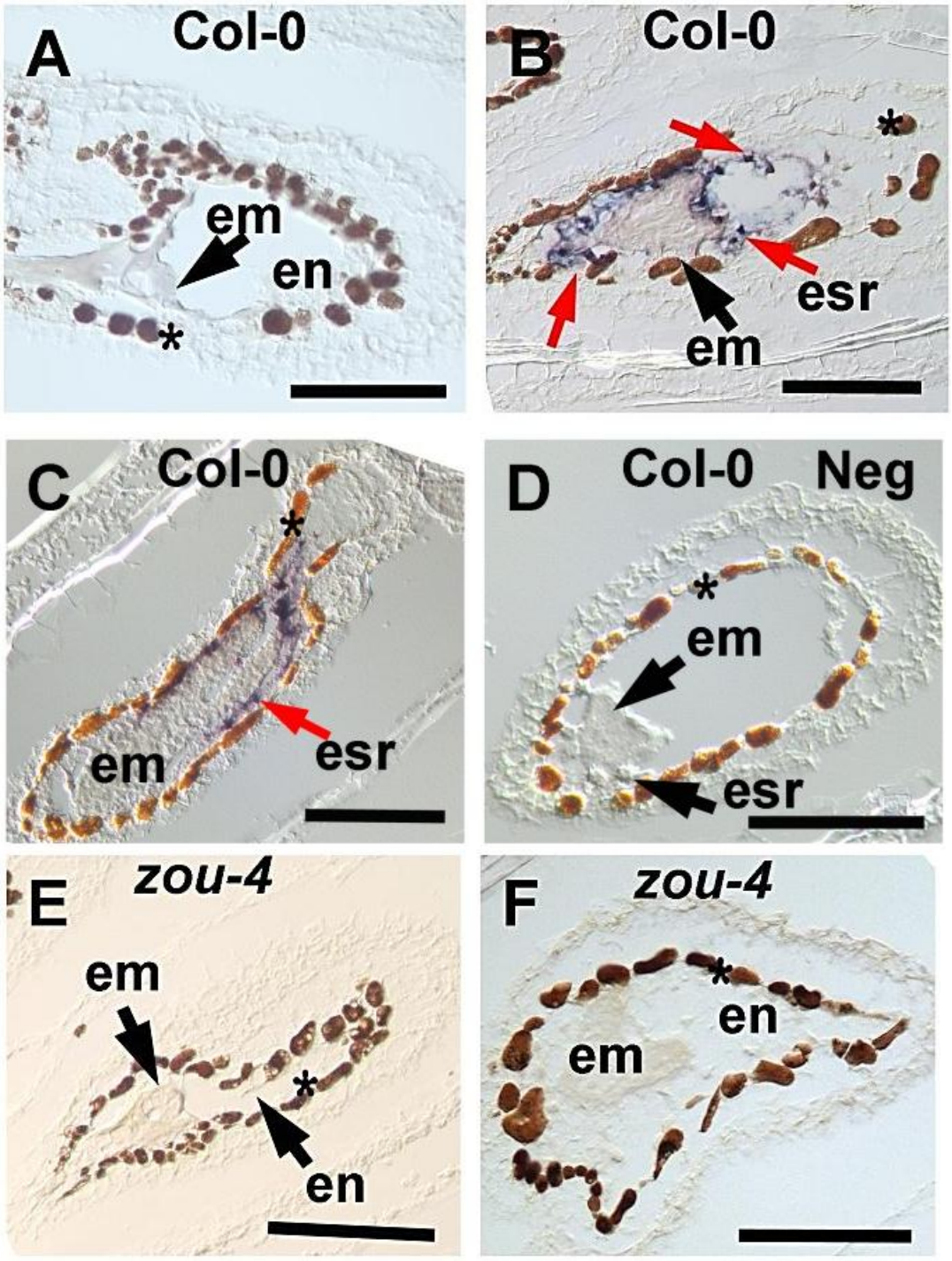
A
Col-0
em
en
*
B
Col-0
*
esr
em
C
Col-0
*
em
esr
D
Col-0
Neg
*
em
esr
E
zou-4
em
*
en
F
zou-4
*
en
em

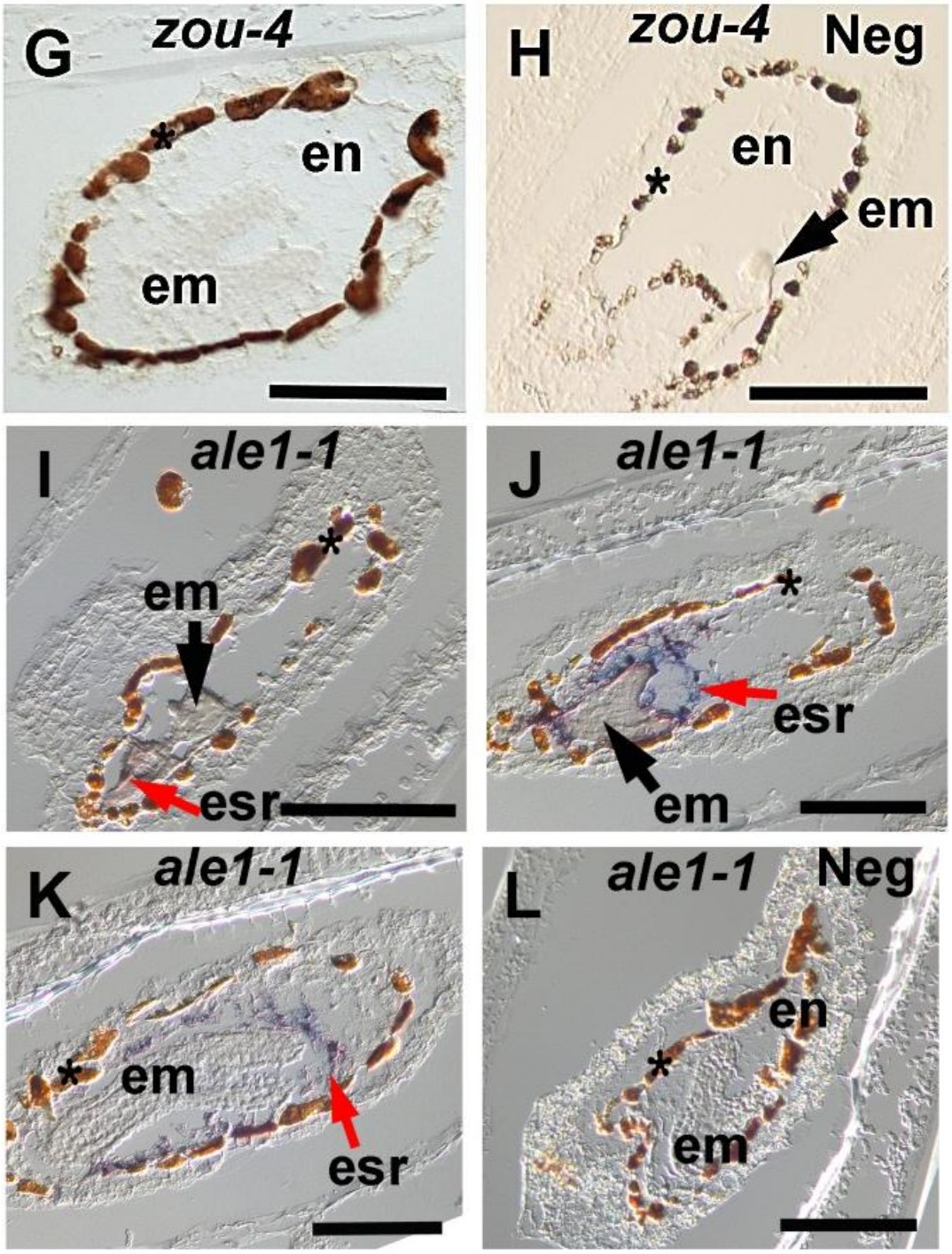
G
zou-4
*
en
em
H
zou-4
Neg
en
*
em
I
ale1-1
em
*
esr
J
ale1-1
*
esr
em
K
ale1-1
*
em
esr
L
ale1-1
Neg
en
*
em

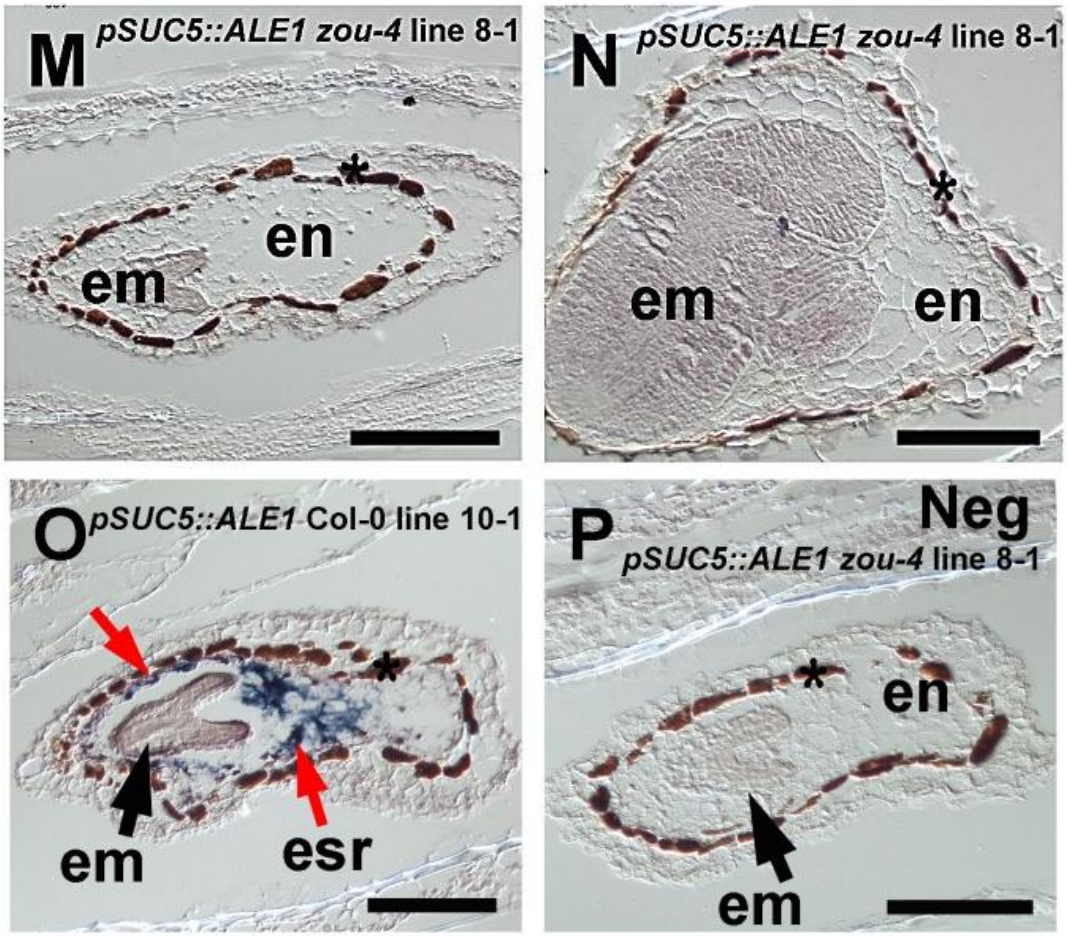
M
pSUC5::ALE1 zou-4 line 8-1
en
em
N
pSUC5::ALE1 zou-4 line 8-1
em
en
O
pSUC5::ALE1 Col-0 line 10-1
em
esr
P
Neg
pSUC5::ALE1 zou-4 line 8-1
en
em

Figure 5.9 *RGP3* expression pattern by RNA *in situ* hybridizations

A to P, images of RNA *in situ* hybridizations of digoxigenin-labelled *RGP3* antisense probes (A to C, E to G, I to K and M to O) and sense probes (D, H, L and P) viewed by DIC white light microscopy. Signal shows as purple staining; the dark brown stained endothelium does not represent signal (marked by asterisks). Genotypes examined were Col-0 wild-type (A to D), *zou-4* mutants (E to H), *ale1-1* mutants (I to L), *pSUC5::ALE1 zou-4* line 8-1 (M, N and P), and *pSUC5::ALE1* Col-0 line 10-1 (O). A, E, H and I, seeds with globular stage embryos. B, D, F, J and M, seeds with heart stage embryos. C, G, K, L, O and P, seeds with torpedo stage embryos. N, seed with mature stage embryo. A, in wild-type seeds, at the globular stage little purple staining was detected, suggesting almost no *RGP3* expression in the seeds. B and C, from the heart stage strong purple staining was defected exclusively in the embryo surrounding region (ESR) as indicated by red arrows. D, negative control with *RGP3* sense probes and no staining was detected in the seeds. E to J, in *zou* mutants from the globular stage to the late torpedo stage, no purple staining was detected in the seeds, suggesting that in *zou* mutants *RGP3* expression was strongly down-regulated. I, in *ale1-1* mutants at the globular stage no *RGP3* expression was detected in the seeds. J and K, in *ale1-1* mutants from the heart stage, *RGP3* expression was exclusively detected in the esr as indicated by the red arrows. M and N, from the heart stage to the mature stage of embryo development *RGP3* expression was not detected in *pSUC5::ALE1 zou-4* lines. O, *RGP3* expression was exclusively detected in the esr in *pSUC5::ALE1* Col-0 lines indicated by red arrows. em, embryo; en, endosperm; Neg, negative control; scale bars represent 100 μm.

5.2.6 Genetic interactions of *ZOU, ALE1, RGP3* and *RGP4*

SOLEXA whole transcriptome sequencing of wild-type and *zou* mutant siliques has shown that in *zou* mutants the expression of *ALE1* and *RGP3* is down-regulated and the expression of *RGP4* is up-regulated. I have validated this by RT-PCR and RNA *in situ* hybridizations (Figure 5.2, 5.8 and 5.9). However, in *ale1* mutants the expression of *RGP3* and *RGP4* did not show a difference compared to their expression in the wild-type (Figure 5.8 and 5.9), which was also confirmed by qRT-PCR (Gwyneth Ingram personal communication). My analyses also support the hypothesis that *ZOU* might regulate *RGP3* and *RGP4* independently from *ALE1*.

As *ALE1*expression is localized in the ESR and has a role in controlling embryonic epidermal cuticle development (Tanaka et al., 2001), and *RGP3* expression is also localized in the ESR but its function during embryo development is not clear, it is possible that *ALE1*or *ZOU* might interact genetically with *RGP3*. In order to test this hypothesis, double mutants of *rgp3-1 zou-4* (Figure 5.10 C) and *rgp3-1 ale1-1* (Figure 5.10 A) were generated by crossings between two homozygous mutants. Seed phenotypes of the double mutants were examined. *rgp3-1 zou-4* double mutants show the same shrivelled seed phenotype (Figure 5.10 C) as *zou-4* single mutants (Figure 5.10 D) and *rgp3-1 ale1-1* double mutants show the same seed phenotype (Figure 5.10 A) as *ale1-1* single mutants (Figure 5.10 B). Thus the possibility that loss of *RGP3* might modify the *zou-4* and the *ale1-1* phenotype was not supported.

RGP4 is exclusively expressed in the testa with an unknown function during seed development and *RGP4* expression is up-regulated in *zou* mutants shown by SOLEXA sequencing, RT-PCR (Figure 5.2) and RNA *in situ* hybridizations (Figure

5.8). To test the hypothesis that loss of *RGP4* might modify the phenotype of *zou-4*, *rgp4-1 zou-4* double mutants were generated by crossing the two single mutants. Figure 5.12 F shows that *rgp4-1 zou-4* mutants have a similar shrivelled seed phenotype to *zou-4* mutants (Figure 5.10 D) suggesting that loss of *RGP4* does not modify the *zou* phenotype.

Finally, although *RGP3* and *RGP4* are expressed in separate tissues, the predicted presence of both proteins in the secretory pathway prohibited us from excluding the possibility that they interact functionally or genetically. To test the possible genetic interaction between *RGP3* and *RGP4*, double mutants were generated by crossing the homozygous *rgp3-1* and *rpg4-1* single mutants. However, homozygous *rgp3-1 rgp4-1* double mutants did not show any difference in seed development (Figure 5.10 E) compared to the wild-type seeds (Figure 5.10 I), suggesting that *RGP3* and *RGP4* do not modify each other's functions during seed development.

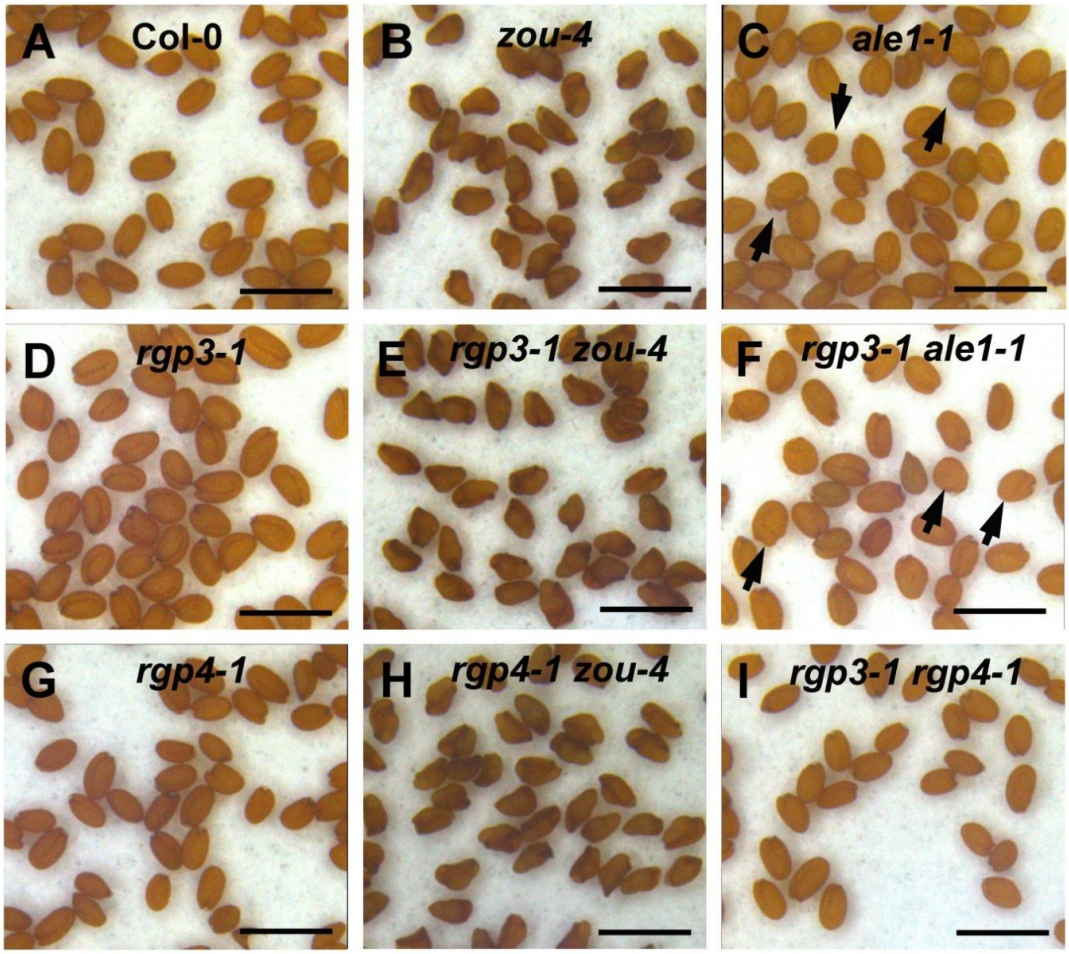

Figure 5.10 Seed phenotypes of double mutants among combinations of *rgp3-1, rgp4-1, ale1-1* and *zou-4* mutants.

A, *rgp3-1 ale1-1* double mutants show an *ale1-1* mutant seed phenotype. A and B, arrows indicate the abnormal seed shape phenotype. C, *rgp3-1 zou-4* double mutants show a *zou-4* seed phenotype. E, *rgp3-1 rgp4-1* double mutants show a wild-type seed phenotype. F, *rgp4-1 zou-4* double mutants show a *zou-4* seed phenotype. G and H, *rgp3-1* and *rgp4-1* single mutants show a wild-type seed phenotype. Arrow bars represent 2 mm.

5.3 Discussion

By analysing the SOLEXA whole transcriptome profiles of wild-type and *zou* mutant siliques, nine genes were selected as potential *ZOU* targets for expression and functional analysis. Among these genes, *LOL2*, *DP1*, *DOX1*and *RGP4* were up-regulated in *zou* mutants, and *RGP3*, *GDSL-Lipase 3* and *4*, *AtENODL10*, and *CSY1* were down-regulated in *zou* mutants. RT-PCR analysis on the expression of the nine genes in wild-type and *zou* mutant siliques confirmed the SOLEXA profiling results for all nine genes. The seed and seedling phenotypes of the T-DNA insertion mutants of the nine genes were examined, however, no visible defects of these mutants were identified.

RNA *in situ* hybridizations showed that *RGP4* expression was initiated in the inner integument from the globular embryo stage to the heart embryo stage, and after the heart embryo stage *RGP4* expression was detected in the outer integument with an increased expression level. In *zou* mutants, before the late heart embryo stage, *RGP4* showed stronger expression in the inner integument compared to the wild-type at the same stage, however, after the late heart embryo stage the difference was less prominent. Also shown by RNA *in situ* hybridization, *RGP4* expression was independent from *ALE1* expression.

RGP3 has an ESR specific expression pattern which initiates after the globular embryo stage. In *zou* mutants, *RGP3* expression is strongly down-regulated, and its regulation is independent from the expression of *ALE1*. My genetic analysis did not uncover any genetic interactions between *ZOU/ALE1* and either *RGP3* or *RGP4.* Moreover no genetic interactions were observed between *RGP3* and *RGP4.* However

it should be born in mind that the mutant alleles of *RGP3* and *RGP4* used in the analysis were not fully confirmed as null, despite the fact that they contained T-DNA insertions in protein coding sequences. RT-PCR analyses on *RPG3* and *RGP4* expression in *rgp3-1* and *rgp4-1* mutants have shown that *rgp3-1* has transcripts before and after the T-DNA insertion and *rgp4-1* has transcript before the T-DNA insertion. To solve the problem more alleles with T-DNA insertion near the transcription start sites should be screened. Moreover we cannot, for the moment, exclude the possibility that genetic and functional redundancy exist between *RGP3* or *RGP4* and other members of the *RGP* family, particularly *RGP1* and *2*. Both these genes are expressed ubiquitously, and they may act redundantly. Although neither gene shows obvious misregulation in our SOLEXA datasets, misregulation in the endosperm and testa could be masked by strong expression in other silique tissues. Unfortunately, the male sterility observed in *rgp1 rgp2* double mutant pollen (Drakakaki et al., 2006) could render the task of uncovering genetic redundancy during seed development very difficult. However, generation of further double mutant combinations within this gene family would be a valuable future perspective. Generating RNAi constructs under endosperm specific promoters to target the homologous genes could also help to solve the problem.

Although *RGP3* and *RGP4* are both predicted to be involved in cell wall modification, it should be noted that both genes are strong expressed in populations of cells which are destined to undergo imminent cell death. This is particularly noticeable for *RGP4*, which is expressed early in the inner integument prior to its collapse, and later in the outer integument, again prior to cell death in this tissue. Thus, although not proven in this study, there may well be either a functional or a

causal link between *RGP* expression and cell death. One possibility is that *RGP* gene expression is triggered by cell-wall-derived oligosaccharides released during cell autolysis. It has been suggested that changes in cell wall structure can activate defence pathways (Dumas et al., 2008). Perturbation of cellulose status which is the major component of the cell wall architecture causes calcium influx, activates the membrane cellulose integrity sensors (i.e. through cellulose synthase genes, CESAs and receptor-like kinase THESEUS1, THE1), and the calcium influx may also activate kinase cascades and downstream hormone (JA, SA, ABA and ET) signalling, leading to expression of defence genes (Dumas et al., 2008). Therefore, it is possible that cell wall related genes are involved in defence signalling and cell death pathways. Besides the different localization of transcripts, *RGP3* and *RGP4* may have divergent functions. Firstly, rice *RGP* homologies were shown to have a UDP-mutase activity which transfers uridine diphosphate (UDP)-arabinopyranose (UDP-Ara*p*) to UDP-arabinofuranose (UDP-Ara*f*) which is the key constituent of plant cell walls (Konishi et al., 2007). In *Arabidopsis*, only RGP1, RGP2 and RGP3 showed UDP-*Ara* mutase activity which can interconvert UDP-Ara*p* and UDP-Ara*f* in bacteria, whilst RGP4 and RGP5 did not show UDP-*Ara* mutase activity (Rautengarten et al., 2011). Secondly, phylogenetic analysis of *Arabidopsis* RGP family proteins has shown that RGP3 is closer to RGP1 and RGP2, than RGP4 in homology, and RGP5 displays the least homology to the others. Last but not the least, *ZOU* up-regulates *RGP3* and down-regulates *RGP4*. Taken together, differently regulated by seed specific gene *ZOU*, endosperm specific *RGP3* and testa specific *RGP4* may have different roles in controlling seed development, which are independent from *ALE1*.

The key aims of this chapter were to identify novel *ZOU* targets that may be involved in cell death pathways or epidermal cuticle pathways. The criteria for selecting promising candidate genes were based on the predicted protein type that they encode and the availability of expression data. Therefore, genes that were selected for expression and functional analysis were specifically expressed in the seeds, and could potentially be involved in endosperm and embryo cell-cell signalling. However, I was also interested in genes that are not seed specific but are cognate cell death regulators. For example, *LOL2* and *DOX1* are both known cell death regulators, and they are universally expressed (De León et al., 2002; Dietrich et al., 1997). The rest of the genes analysed in this chapter were all predicted or shown to be seed specific. The endosperm specific genes, *RGP3*, two *GDSL-Lipases*, the plastocyanin-like protein *AtENODL10* and *CSY1* were of great interest, because they could be direct targets of *ZOU*. *RGP3* is predicted to be involved in cell wall biosynthesis (Rautengarten et al., 2011), the two *GDSL-Lipases* in cuticle biosynthesis (Akoh et al., 2004), the *AtENODL10* in cell wall signalling (Borner et al., 2002) and *CSY1* in endosperm catalysis (Pracharoenwattana et al., 2005). These endosperm specific genes are all down-regulated in *zou* mutants, which is globally consistent with the *zou* persistent endosperm phenotype and embryonic cuticle defects. Comparison of the temporal and spatial expression profiles of these five endosperm specific genes down-regulated in *zou* mutants (Andrew Waters personal communication), suggests that these genes are all co-ordinately regulated with the possible exception of *CYS1* whose expression initiates later than the other four genes. Based on the fact that the expression of *RGP3*, *GDSL-Lipase3* and *4*, and *AtENODL10* initiate prior to the onset of endosperm cell death, those genes could be

direct *ZOU* targets, rather than genes whose expression is triggered by cell autolysis. Therefore future experiments could be conducted to test this hypothesis by creating reporter constructs containing 1 to 2 kb upstream sequences of the putative target genes fused to β-glucuronidase (GUS) and GFP, and ZOU activator constructs in transient assays in tobacco leaves. The promoter-reporter constructs could also contain truncated sequences with/without putative G-box motifs (bHLH binding sites) or ZOU activator constructs containing truncated ZOU protein (for instance, without the bHLH binding domain).

Homozygous T-DNA insertion lines of the candidate *ZOU* target genes were isolated and their seed and the cuticle phenotypes were analysed. Unfortunately no defects in these T-DNA insertion lines have been identified. It is possible that the alleles used were not null, and further molecular characterisation is necessary to clarify this point. Alternatively genetic redundancy could again be the cause of our perceived lack of phenotypes. Further genetic analysis and the isolation of novel mutant alleles will be the first step in pushing forward this analysis. This work is currently being pursued by another PhD student in the laboratory.

To conclude, *ZOU* down-regulates the expression of *LOL2*, *DP1*, *DOX1* and *RGP4*, up-regulates the expression of *RGP3*, *GDSL-Lipases 3* and *4*, *AtENODL10* and *CYS1*, and *ZOU* regulation on *RGP3* and *RGP4* expression is independent from the expression of *ALE1*. *RGP3* has an ESR specific expression pattern and *RGP4* has a testa specific expression pattern which initiates from the inner integument. There might be functional redundancy among *Arabidopsis* RGP family proteins in regulating seed development.

6 Discussion

6.1 *ZOU* has a role in promoting autolysis of gametophytic nutritive tissues in both, gymnosperms and angiosperms, and a new role in controlling cuticle formation only in angiosperms

Double fertilization is one of the major innovations in angiosperms: In the common ancestor of angiosperms, in addition to fertilization of the egg cell by one sperm nucleus, a second sperm nucleus is thought to have been recruited in order to tether the development of the newly sexualised precursor of nutritive female gametophyte-derived tissue to that of the embryo (Baroux et al., 2002). In gymnosperms, which are thought to be the group closest to ancestral angiosperms, the female gametophyte proliferates to form a nutritive tissue prior to fertilization, and after fertilization the embryo invades into the gametophytic nutritive tissue which autolyses as the embryo advances.

Unlike the situation in gymnosperms, the angiosperm embryo and the endosperm develop at the same time. Besides the autolysis of endosperm, it is critical for the embryo to maintain its boundaries, especially since the endosperm does not have a cuticle to stop it from fusing to the surrounding tissue. How embryos manage to maintain their invasive growth into the nutritive tissue and their boundaries with the surrounding tissue in angiosperms is mysterious. Studies on *zou* mutants provide us with an important tool to address these questions.

The phenotype of *zou* mutants show two clear distinguishable defects during seed development: Firstly, *zou* mutant seeds have a persistent endosperm, and consequently a small embryo at the mature stage, and when *zou* seeds desiccate

during maturation the seeds shrivel. In wild-type seeds the endosperm is consumed during the expansion of the embryo leaving only a single cell layer of endosperm, suggesting that *ZOU* likely regulates endosperm cell death which is necessary for embryo expansion. Secondly, *zou* mutant embryos have defects in their cuticle, so that the ESR cells adhere to the embryo throughout seed development, and after the germination *zou* mutants develop gaps between pavement cells, which is likely due to loss of cuticle integrity, suggesting *ZOU* plays a role in epidermal cuticle development.

ZOU expression initiates soon after the fertilization in the central cell and later it is exclusively expressed in the ESR, suggesting that *ZOU* function is fertilization dependent. Strikingly, *ZOU* is not only widely conserved in angiosperms but also *ZOU* homologues are found in gymnosperm and more ancient vascular plants such as mosses which do not have seeds. This suggests that *ZOU* might have a more ancestral role, which is controlling the autolysis of gametophytic nutritive tissue, while the embryo advances. It would be interesting to look at the expression pattern and function of *ZOU* homologues in gymnosperms which could help to explore the evolution of seeds.

Even if the role of *ZOU* in controlling the autolysis of gametophytic nutritive tissue is maintained in angiosperms, there could still be a secondary 'boundary formation' problem which does not exist in gymnosperms, and which is only encountered in angiosperms by developing embryos while they are in the seeds due to the concomitant development of the endosperm. If this is the case, one idea might be that the angiosperms have had to evolve specific pathways which allow the embryonic cuticle to form properly, thus ensuring that the embryo separates correctly

from the endosperm. Former lab members identified that the gene *ABNORMAL LEAF SHAPE1* (*ALE1*) is up-regulated by *ZOU* and has the same ESR expression pattern as *ZOU* does (Yang et al., 2008). *ale1* mutants also display defects in embryonic cuticle development (Tanaka et al., 2001) but I, in collaboration with colleagues, have shown that *ale1* mutants do not show an endosperm cell death phenotype. Firstly, *ale1* seeds are bigger than *zou* mutants and no apparent seed shrivelling is observed in *ale1* mutants. Secondly, although *ale1* mutants display slightly retarded embryo growth, the hypocotyl and cotyledons of *ale1* mutants are able to elongate and invade into the endosperm, and there is an empty space between the developing embryo and the endosperm. Thirdly, TUNEL assays have shown that active nuclear DNA fragmentation occurs in the ESR cells in *ale1* seeds during embryo elongation, in contrast to *zou* seeds in which is not visible Lastly, shown by micro sections at the mature stage of embryogenesis, unlike *zou* mutants, there is no bulk of endosperm cells remaining in *ale1* mutant seeds, but only one layer of aleurone-like cells observed, as in wild-type (Andrew Waters unpublished data). These results suggest that *ALE1* only has a role in cuticle development but not in endosperm cell death. Interestingly, the *ZOU* target *ALE1* is less widely conserved than *ZOU*, and *ALE1* homologues are only found in some of the angiosperms, such as rice and potatoes, but are not present, for example in maize, nor in gymnosperms and mosses (Andrew Waters personal communication). This allowed us to make the hypothesis that *ALE1* could be involved in establishing of the 'boundary' between gametophytic tissue and zygotic tissue, and its recruitment downstream of *ZOU* could be an exclusively angiosperm innovation. If this was true then we would

certainly expect the role of *ALE1* to be separate from the role of *ZOU* in endosperm cell death.

To test this hypothesis, *ALE1* expression in the ESR in *zou* mutants was rescued using the *ZOU*-independent *AtSUC5* promoter to investigate whether one or both of *zou* phenotypes were complemented, and other candidate *ZOU* target genes were validated and characterized to determine their functions in endosperm cell death and/or embryonic epidermal cuticle development. The *AtSUC5*::*ALE1 zou* transgenic lines produce the same small and shrivelled seeds as those of *zou* mutants. However, the epidermal cuticle defects of *AtSUC5*::*ALE1 zou* transgenic lines were partially rescued, giving significantly less Toluidine Blue staining of cotyledons and much more resistance to desiccation than those of *zou* mutants. These results suggest that *ALE1* can partially rescue *zou* cuticle defects but not the defects in endosperm cell death. In other words, my studies on *ALE1* have allowed us to partially separate the role of *ZOU* in endosperm cell death and embryonic cuticle development, which further supports the idea that during the evolution angiosperm embryos have adopted a secondary 'boundary forming' mechanism, which allows the embryonic cuticle to form properly, and thus ensures that the embryo separates correctly from the endosperm during seed development.

6.2 Metabolic pathways that are regulated by *ZOU* during endosperm cell death and epidermal cuticle formation

In order to elucidate the pathways regulated by *ZOU* during endosperm cell death and epidermal cuticle formation, and to screen for candidate *ZOU* target genes, a SOLEXA whole transcriptome sequencing experiment was performed and *zou* loss

of function mutant siliques and wild-type gene expression profiles were compared. The mis-expressed genes were found to be involved in response to biotic/abiotic stresses, cell death regulators, wax biosynthesis, cell wall biosynthesis and remodelling, Ca^{2+} signalling, and plant hormone JA, ET, and ABA signalling (as was summarised in Figure 1.5). These data link *ZOU* function to programmed cell death regulation, plant response to developmental stimuli and cuticle biogenesis.

Firstly, phenotypic analysis has shown that *zou* mutants have persistent endosperm and down-regulated cell death in endosperm cells compared to the wild-type plants. Consistent with *zou* mutant phenotype, two negative cell death regulators, *DOX1* and *LOL2* (De León et al., 2002; Petra Epple et al., 2001) were up-regulated in *zou* mutants. Besides, *DOX1* expression is seed specific and biochemically the α-dioxygenase coded by *DOX1* has the potential to catalyse the biosynthesis of JA precursors (De León et al., 2002). Therefore, the lack of cell death in *zou* endosperm and the mis-expression of many stress response genes could be caused by disturbed JA signalling which is an interesting hypothesis to be tested. *LOL2* is universally expressed in response to *Pseudomonas syringae* (Petra Epple et al., 2001), however, no evidence has shown that *lol2* mutants display phenotypes in endosperm cell death with or without *Pseudomonas syringae* treatment. Through what mechanism *LOL2* is regulated by *ZOU* is unknown.

Pathogen triggered defence signalling and developmental cell death (eg. senescence, root formation, and xylem formation) share some common signalling machinery (Love et al., 2008; Tsuda and Katagiri, 2010). In pattern-triggered defence signalling, membrane associated LRR-receptor kinases bind to elicitors, activating MAPK cascades which impinge on AtWRKY transcription factors to regulate the

defence response genes. Meanwhile, Ca^{2+} signalling is initiated after the perception of microbes which activates Ca^{2+} channels and Ca^{2+} dependent protein kinases, and in turn controls the expression of genes involved in defence peptide and metabolites synthesis, plant hormone signalling, and cell wall remodelling (Ronald and Beutler, 2010). In effector-triggered immunity, effector recognition activates MAPK cascades, production of reactive oxygen species (ROS), cell wall remodelling and synthesis of defence hormones (JA, SA and ET) (Ronald and Beutler, 2010). One phenomena of plant defence signalling is rapidly forming localized cell death at the infection sites, which is called the hypersensitive response (HR). Developmental cell death is also modulated by ROS, MAPK cascades, and SA, JA and ET dependent pathways (Love et al., 2008).

In our SOLEXA sequencing data set, genes involved in both pattern-triggered and effector-triggered defence signalling are mis-expressed in *zou* mutants. However, I have shown that *zou* mutants do not show change of immune response to pathogen attack, and that *zou* mutants do not show any difference in leaf and whole plant senescence compared to wild-type plants either, suggesting that *zou* cell death defects only exist in endosperm and *ZOU* only has a role in promoting endosperm cell death. This I have confirmed using TUNNEL assays. The reason why genes involved in plant immune signalling pathways are mis-regulated by *ZOU* is likely to be that the developmental cell death regulated by *ZOU* in seeds, and pathogen triggered plant immunity or cell death share the same machinery.

Last but not the least, cuticle biosynthesis genes are down-regulated in *zou* mutants, which is consistent with *zou* mutant's lack of cuticle integrity and suggests *ZOU* has a role in cuticle biogenesis. Some other cuticle biogenesis mutants,

including *fiddlehead* (*fdh*), *lateral root development 2* (*lacs2*), *lacerate* (*lcr*) and *bodyguard* (*bdg*) not only display defects in biosynthesis of the correct cuticlar polyesters, but also show secondary phenotypes including disease response, senescence and abnormal organ morphology (Kurdyukov et al., 2006; Wellesen et al., 2001; Yephremov et al., 1999). Bioinformatics analysis on the published microarray databases by other research groups has suggested that in cuticular mutants, genes involved in cell wall, cuticle biosynthesis and defence responses are up-regulated (Voisin et al., 2009). The explanation is that cuticle is closely interlinked with the cell wall, and the dysfunction of cuticle leads to specific compensatory response from the cell wall and altered homeostasis of the cell wall. The remodelling of cuticle and cell walls could then activate defences usually associated with the perception of abiotic stresses and pathogens (Voisin et al., 2009). In *zou* mutants the mis-expression of cell wall genes and defence response genes could be the consequence of defective cuticle.

Interestingly, we identified a *ZOU* target, *ALE1* which is only expressed in the ESR, up-regulated by *ZOU*, and most importantly *ale1* mutants only display an embryonic cuticle defect, but not any other defects outside the seeds or any endosperm cell death phenotypes. Therefore, it is likely *ALE1* only has a role in cuticle development, which could help to dissect the role of *ZOU* in endosperm cell death and embryonic cuticle formation.

6.3 Conclusion and future perspectives

ZOU has a putative ancestral role in promoting gametophytic nutritive tissue autolysis via programmed cell death pathways, and a new role in controlling embryonic epidermal cuticle formation separating endosperm tissue from embryo tissue during the seed development. In order to further support the hypothesis that *ZOU* has two independent roles, future experiments could focus on other *ZOU* targets in cell death pathways and cuticle pathway. *zou* mutants have a pleiotropic phenotype, and a large group of genes are mis-expressed in *zou* mutants. By reintroducing other *ZOU* target genes back into *zou* mutants and monitoring rescue or enhancement of *zou* phenotypes, we could explain which targets act in which pathway. In addition, suppressor/enhancer screens involving the mutagenesis of *zou* mutants, or crossing *ZOU* target gene mutants to *zou* mutants could help us to elucidate the mechanisms underlying *ZOU* function. By looking for common and discrete targets of *ZOU* and *ALE1* by SOLEXA sequencing of *ale1* mutants we should be able to separate out the cuticle biogenesis pathway. Finally, ZOU protein is predicted to be a bHLH transcription factor; therefore *ZOU* whole genome ChIPs followed by promoter binding assays on candidate genes will be useful to confirm ZOU direct targets. This technique has been tried unsuccessfully by another group (Kondou et al., 2008), but technical modifications may improve our likelihood of success.

7 References Cited

Abe, M., H. Katsumata, Y. Komeda, and T. Takahashi, 2003, Regulation of shoot epidermal cell differentiation by a pair of homeodomain proteins in Arabidopsis: Development, v. 130, no. 4, p. 635-643.

Aida, M., T. Ishida, and M. Tasaka, 1999, Shoot apical meristem and cotyledon formation during Arabidopsis embryogenesis: interaction among the CUP-SHAPED COTYLEDON and SHOOT MERISTEMLESS genes: Development, v. 126, no. 8, p. 1563-1570.

Aida, M., T. Vernoux, M. Furutani, J. Traas, and M. Tasaka, 2002, Roles of PIN-FORMED1 and MONOPTEROS in pattern formation of the apical region of the Arabidopsis embryo: Development, v. 129, no. 17, p. 3965-3974.

Akoh, C. C., G. C. Lee, Y. C. Liaw, T. H. Huang, and J. F. Shaw, 2004, GDSL family of serine esterases/lipases: Progress in Lipid Research, v. 43, no. 6, p. 534-552.

Andème Ondzighi, C., D. A. Christopher, E. J. Cho, S. C. Chang, and L. A. Staehelin, 2008, Arabidopsis Protein Disulfide Isomerase-5 Inhibits Cysteine Proteases during Trafficking to Vacuoles before Programmed Cell Death of the Endothelium in Developing Seeds: The Plant Cell Online, v. 20, no. 8, p. 2205-2220.

Balandín, M., J. Royo, E. Gomez, L. Muniz, A. Molina, and G. Hueros, 2005, A protective role for the embryo surrounding region of the maize endosperm, as evidenced by the characterisation of *ZmESR-6*, a defensin gene specifically expressed in this region: Plant Molecular Biology, v. 58, no. 2, p. 269-282.

Bannenberg, G., M. Martínez, M. J. Rodríguez, M. A. López, I. Ponce de León, M. Hamberg, and C. Castresana, 2009, Functional Analysis of a-DOX2, an Active a-Dioxygenase Critical for Normal Development in Tomato Plants: Plant Physiology, v. 151, no. 3, p. 1421-1432.

Baroux, C., C. Spillane, and U. Grossniklaus, 2002, Evolutionary origins of the endosperm in flowering plants: Genome Biology, v. 3, no. 9, p. reviews1026.

Barrero, J. M., P. Piqueras, M. González-Guzmán, R. Serrano, P. L. Rodríguez, M. R. Ponce, and J. L. Micol, 2005, A mutational analysis of the ABA1 gene of Arabidopsis thaliana highlights the involvement of ABA in vegetative development: Journal of Experimental Botany, v. 56, no. 418, p. 2071-2083.

Baud, S., V. Guyon, J. Kronenberger, S. Wuillème, M. Miquel, M. Caboche, L. Lepiniec, and C. Rochat, 2003, Multifunctional acetyl-CoA carboxylase 1 is essential for very long chain fatty acid elongation and embryo development in Arabidopsis: The Plant Journal, v. 33, no. 1, p. 75-86.

Baud, S., J. P. Boutin, M. Miquel, L. Lepiniec, and C. Rochat, 2002, An integrated overview of seed development in Arabidopsis thaliana ecotype WS: Plant Physiology and Biochemistry, v. 40, no. 2, p. 151-160.

Baud, S., S. Wuillème, R. Lemoine, J. Kronenberger, M. Caboche, L. Lepiniec, and C. Rochat, 2005, The AtSUC5 sucrose transporter specifically expressed in the endosperm is involved in early seed development in Arabidopsis: The Plant Journal, v. 43, no. 6, p. 824-836.

Bauer, M. J., and R. L. Fischer, 2011, Genome demethylation and imprinting in the endosperm: Current Opinion in Plant Biology, v. 14, no. 2, p. 162-167.

Bayer, M., T. Nawy, C. Giglione, M. Galli, T. Meinnel, and W. Lukowitz, 2009, Paternal Control of Embryonic Patterning in Arabidopsis thaliana: Science, v. 323, no. 5920, p. 1485-1488.

Becraft, P. W., 2001, Cell fate specification in the cereal endosperm: Seminars in Cell & Developmental Biology, v. 12, no. 5, p. 387-394.

Becraft, P. W., S. H. Kang, and S. G. Suh, 2001, The Maize CRINKLY4 Receptor Kinase Controls a Cell-Autonomous Differentiation Response: Plant Physiology, v. 127, no. 2, p. 486-496.

Becraft, P. W., K. Li, N. Dey, and Y. Asuncion-Crabb, 2002, The maize dek1 gene functions in embryonic pattern formation and cell fate specification: Development, v. 129, no. 22, p. 5217-5225.

Beeckman, T., R. De Rycke, R. Viane, and D. Inzé, 2000, Histological Study of Seed Coat Development in *Arabidopsis thaliana*: Journal of Plant Research, v. 113, no. 2, p. 139-148.

Belin, C., and L. Lopez-Molina, 2010, Endosperm rupture as a model for lateral root emergence in Arabidopsis?: Plant Signaling & Behavior, v. 5, no. 5, p. 564-566.

Bentsink, L., and M. Koornneef, 2008, Seed Dormancy and Germination: The Arabidopsis Book, p. e0119.

Berger, F., P. E. Grini, and A. Schnittger, 2006, Endosperm: an integrator of seed growth and development: Current Opinion in Plant Biology, v. 9, no. 6, p. 664-670.

Berger, F., 2003, Endosperm: the crossroad of seed development: Current Opinion in Plant Biology, v. 6, no. 1, p. 42-50.

Berleth, T., and G. Jurgens, 1993, The role of the monopteros gene in organising the basal body region of the Arabidopsis embryo: Development, v. 118, no. 2, p. 575-587.

Bessire, M., C. Chassot, A. C. Jacquat, M. Humphry, S. Borel, J. M.-C. Petetot, J. P. Metraux, and C. Nawrath, 2007, A permeable cuticle in Arabidopsis leads to a strong resistance to Botrytis cinerea: EMBO J, v. 26, no. 8, p. 2158-2168.

Bethke, P. C., I. G. L. Libourel, N. Aoyama, Y. Y. Chung, D. W. Still, and R. L. Jones, 2007, The Arabidopsis Aleurone Layer Responds to Nitric Oxide, Gibberellin, and Abscisic Acid and Is Sufficient and Necessary for Seed Dormancy: Plant Physiology, v. 143, no. 3, p. 1173-1188.

Bird, S. M., and J. E. Gray, 2003, Signals from the cuticle affect epidermal cell differentiation: New Phytologist, v. 157, no. 1, p. 9-23.

Blanvillain, R., B. Young, Y. m. Cai, V. Hecht, F. Varoquaux, V. Delorme, J. M. Lancelin, M. Delseny, and P. Gallois, 2011, The Arabidopsis peptide kiss of death is an inducer of programmed cell death: EMBO J, v. 30, no. 6, p. 1173-1183.

Boisnard-Lorig, C., A. Colon-Carmona, M. Bauch, S. Hodge, P. Doerner, E. Bancharel, C. Dumas, J. Haseloff, and F. Berger, 2001, Dynamic Analyses of the Expression of the HISTONE::YFP Fusion Protein in Arabidopsis Show That Syncytial Endosperm Is Divided in Mitotic Domains: The Plant Cell Online, v. 13, no. 3, p. 495-509.

Bonello, J.-F., S. Sevilla-Lecoq, A. Berne, M.-C. Risueño, C. Dumas, and P. M. Rogowsky, 2002, Esr proteins are secreted by the cells of the embryo surrounding region: Journal of Experimental Botany, v. 53, no. 374, p. 1559-1568.

Bonneau, L., Y. Ge, G. E. Drury, and P. Gallois, 2008, What happened to plant caspases?: Journal of Experimental Botany, v. 59, no. 3, p. 491-499.

Borner, G. H. H., D. J. Sherrier, T. J. Stevens, I. T. Arkin, and P. Dupree, 2002, Prediction of Glycosylphosphatidylinositol-Anchored Proteins in Arabidopsis. A Genomic Analysis: Plant Physiology, v. 129, no. 2, p. 486-499.

Bourdenx, B. et al., 2011, Overexpression of Arabidopsis ECERIFERUM1 Promotes Wax Very-Long-Chain Alkane Biosynthesis and Influences Plant Response to Biotic and Abiotic Stresses: Plant Physiology, v. 156, no. 1, p. 29-45.

Bozhkov, P. V., L. H. Filonova, M. F. Suarez, A. Helmersson, A. P. Smertenko, B. Zhivotovsky, and S. von Arnold, 2003, VEIDase is a principal caspase-like activity involved in plant programmed cell death and essential for embryonic pattern formation: Cell Death Differ, v. 11, no. 2, p. 175-182.

Brand, U., J. C. Fletcher, M. Hobe, E. M. Meyerowitz, and R. Simon, 2000, Dependence of Stem Cell Fate in Arabidopsis on a Feedback Loop Regulated by CLV3 Activity: Science, v. 289, no. 5479, p. 617-619.

Breeze, E. et al., 2011, High-Resolution Temporal Profiling of Transcripts during Arabidopsis Leaf Senescence Reveals a Distinct Chronology of Processes and Regulation: The Plant Cell Online, v. 23, no. 3, p. 873-894.

Breuninger,H, E Rikirsch, M Hermann, M Ueda, T Laux. Differential Expression of WOX Genes Mediates Apical-Basal Axis Formation in the Arabidopsis Embryo. Developmental Cell 14[6], 867-876. 2008.

Broun, P., P. Poindexter, E. Osborne, C. Z. Jiang, and J. L. Riechmann, 2004, WIN1, a transcriptional activator of epidermal wax accumulation in Arabidopsis: Proceedings of the National Academy of Sciences of the United States of America, v. 101, no. 13, p. 4706-4711.

Burlat, V., M. Kwon, L. B. Davin, and N. G. Lewis, 2001, Dirigent proteins and dirigent sites in lignifying tissues: Phytochemistry, v. 57, no. 6, p. 883-897.

Burton, R. A., M. J. Gidley, and G. B. Fincher, 2010, Heterogeneity in the chemistry, structure and function of plant cell walls: Nat Chem Biol, v. 6, no. 10, p. 724-732.

Buschhaus, C., and R. Jetter, 2011, Composition differences between epicuticular and intracuticular wax substructures: How do plants seal their epidermal surfaces?: Journal of Experimental Botany, v. 62, no. 3, p. 841-853.

Cai, G., C. Faleri, C. Del Casino, G. Hueros, R. Thompson, and M. Cresti, 2002, Subcellular localisation of BETL-1, -2 and -4 in Zea mays L. endosperm: Sexual Plant Reproduction, v. 15, no. 2, p. 85-98.

Capron, A., S. Chatfield, N. Provart, and T. Berleth, 2009, Embryogenesis: Pattern Formation from a Single Cell: The Arabidopsis Book, p. 1-28.

Chaudhury, A. M., L. Ming, C. Miller, S. Craig, E. S. Dennis, and W. J. Peacock, 1997, Fertilization-independent seed development in Arabidopsis thaliana: Proceedings of the National Academy of Sciences, v. 94, no. 8, p. 4223-4228.

Chen, X., S. M. Goodwin, X. Liu, X. Chen, R. A. Bressan, and M. A. Jenks, 2005, Mutation of the RESURRECTION1 Locus of Arabidopsis Reveals an Association of Cuticular Wax with Embryo Development: Plant Physiology, v. 139, no. 2, p. 909-919.

Chen, X., M. Truksa, C. L. Snyder, A. El-Mezawy, S. Shah, and R. J. Weselake, 2011, Three Homologous Genes Encoding sn-Glycerol-3-Phosphate Acyltransferase 4 Exhibit Different Expression Patterns and Functional Divergence in Brassica napus: Plant Physiology, v. 155, no. 2, p. 851-865.

Clough, S. J., and A. F. Bent, 1998, Floral dip: a simplified method forAgrobacterium-mediated transformation ofArabidopsis thaliana: The Plant Journal, v. 16, no. 6, p. 735-743.

Coello, P., S. J. Hey, and N. G. Halford, 2011, The sucrose non-fermenting-1-related (SnRK) family of protein kinases: potential for manipulation to improve stress tolerance and increase yield: Journal of Experimental Botany, v. 62, no. 3, p. 883-893.

Coll, N. S., D. Vercammen, A. Smidler, C. Clover, F. Van Breusegem, J. L. Dangl, and P. Epple, 2010, Arabidopsis Type I Metacaspases Control Cell Death: Science, v. 330, no. 6009, p. 1393-1397.

Concetta Giuliani, G. C. G. G. M. C. a. S. D., 2002, Programmed Cell Death during Embryogenesis in Maize: Annals of Botany, v. 90, no. 2, p. 287-292.

Costa, L. M., J. F. Gutièrrez-Marcos, and H. G. Dickinson, 2004, More than a yolk: the short life and complex times of the plant endosperm: Trends in Plant Science, v. 9, no. 10, p. 507-514.

Davin, L. B., and N. G. Lewis, 2005, Lignin primary structures and dirigent sites: Current Opinion in Biotechnology, v. 16, no. 4, p. 407-415.

Davis, R. W., J. D. Smith, and B. G. Cobb, 1990, A light and electron microscope investigation of the transfer cell region of maize caryopses: Canadian Journal of Botany, v. 68, no. 3, p. 471-479.

De León, I. P., A. Sanz, M. Hamberg, and C. Castresana, 2002, Involvement of the Arabidopsis a-DOX1 fatty acid dioxygenase in protection against oxidative stress and cell death: The Plant Journal, v. 29, no. 1, p. 61-72.

De Smet, I., S. Lau, U. Mayer, and G. Jürgens, 2010, Embryogenesis-the humble beginnings of plant life: The Plant Journal, v. 61, no. 6, p. 959-970.

DeBono, A., T. H. Yeats, J. K. C. Rose, D. Bird, R. Jetter, L. Kunst, and L. Samuels, 2009, Arabidopsis LTPG Is a Glycosylphosphatidylinositol-Anchored Lipid Transfer Protein Required for Export of Lipids to the Plant Surface: The Plant Cell Online, v. 21, no. 4, p. 1230-1238.

Delgado, I. J., Z. Wang, A. de Rocher, K. Keegstra, and N. V. Raikhel, 1998, Cloning and Characterization of AtRGP1: Plant Physiology, v. 116, no. 4, p. 1339-1350.

Dharmasiri, N., and M. Estelle, 2004, Auxin signaling and regulated protein degradation: Trends in Plant Science, v. 9, no. 6, p. 302-308.

Dietrich,RA, M H Richberg, R Schmidt, C Dean, J L Dangl. A Novel Zinc Finger Protein Is Encoded by the Arabidopsis LSD1 Gene and Functions as a Negative Regulator of Plant Cell Death. Cell 88[5], 685-694. 1997.

Doan, T. T. P., A. S. Carlsson, M. Hamberg, L. Bülow, S. Stymne, and P. Olsson, 2009, Functional expression of five Arabidopsis fatty acyl-CoA reductase genes in Escherichia coli: Journal of Plant Physiology, v. 166, no. 8, p. 787-796.

Drakakaki, G., O. Zabotina, I. Delgado, S. Robert, K. Keegstra, and N. Raikhel, 2006, Arabidopsis Reversibly Glycosylated Polypeptides 1 and 2 Are Essential for Pollen Development: Plant Physiology, v. 142, no. 4, p. 1480-1492.

Duan, H., and M. A. Schuler, 2005, Differential Expression and Evolution of the Arabidopsis CYP86A Subfamily: Plant Physiology, v. 137, no. 3, p. 1067-1081.

Dumas, B., A. Bottin, E. Gaulin, and M. Esquerré-Tugayé, 2008, Cellulose-binding domains: cellulose associated-defensive sensing partners?: Trends in Plant Science, v. 13, no. 4, p. 160-164.

Dumas, C., and P. Rogowsky, 2008, Fertilization and early seed formation: Comptes Rendus Biologies, v. 331, no. 10, p. 715-725.

Ellis, M., J. Egelund, C. J. Schultz, and A. Bacic, 2010, Arabinogalactan-Proteins: Key Regulators at the Cell Surface?: Plant Physiology, v. 153, no. 2, p. 403-419.

Elmore, J. M., Z. J. D. Lin, and G. Coaker, Plant NB-LRR signaling: upstreams and downstreams: Current Opinion in Plant Biology, v. In Press, Corrected Proof.

Epple, P., A. A. Mack, V. R. F. Morris, and J. L. Dangl, 2003, Antagonistic control of oxidative stress-induced cell death in Arabidopsis by two related, plant-specific zinc finger proteins: Proceedings of the National Academy of Sciences, v. 100, no. 11, p. 6831-6836.

Fiebig, A., J. A. Mayfield, N. L. Miley, S. Chau, R. L. Fischer, and D. Preuss, 2000, Alterations in CER6, a Gene Identical to CUT1, Differentially Affect Long-Chain Lipid Content on the Surface of Pollen and Stems: The Plant Cell Online, v. 12, no. 10, p. 2001-2008.

Finkelstein, R., W. Reeves, T. Ariizumi, and C. Steber, 2008, Molecular Aspects of Seed Dormancy: Annual Review of Plant Biology, v. 59, no. 1, p. 387-415.

Floyd, S. K., and J. L. Bowman, 2004, Gene regulation: Ancient microRNA target sequences in plants: Nature, v. 428, no. 6982, p. 485-486.

Franck, V., 2006, Arabidopsis endogenous small RNAs: highways and byways: Trends in Plant Science, v. 11, no. 9, p. 460-468.

Friedman, W. E., 1995, Organismal duplication, inclusive fitness theory, and altruism: understanding the evolution of endosperm and the angiosperm reproductive syndrome: Proceedings of the National Academy of Sciences, v. 92, no. 9, p. 3913-3917.

Friedman, W. E., 1990, Double Fertilization in Ephedra, a Nonflowering Seed Plant: Its Bearing on the Origin of Angiosperms: Science, v. 247, no. 4945, p. 951-954.

Friml, J., A. Vieten, M. Sauer, D. Weijers, H. Schwarz, T. Hamann, R. Offringa, and G. Jurgens, 2003, Efflux-dependent auxin gradients establish the apical-basal axis of Arabidopsis: Nature, v. 426, no. 6963, p. 147-153.

Friml, J. et al., 2004, A PINOID-Dependent Binary Switch in Apical-Basal PIN Polar Targeting Directs Auxin Efflux: Science, v. 306, no. 5697, p. 862-865.

Fu, S., R. Meeley, and M. J. Scanlon, 2002, empty pericarp2 Encodes a Negative Regulator of the Heat Shock Response and Is Required for Maize Embryogenesis: The Plant Cell Online, v. 14, no. 12, p. 3119-3132.

Fujimoto, S. Y., M. Ohta, A. Usui, H. Shinshi, and M. Ohme-Takagi, 2000, Arabidopsis Ethylene-Responsive Element Binding Factors Act as Transcriptional Activators or Repressors of GCC Box-Mediated Gene Expression: The Plant Cell Online, v. 12, no. 3, p. 393-404.

Galinha, C., H. Hofhuis, M. Luijten, V. Willemsen, I. Blilou, R. Heidstra, and B. Scheres, 2007, PLETHORA proteins as dose-dependent master regulators of Arabidopsis root development: Nature, v. 449, no. 7165, p. 1053-1057.

Gallois, J. L., F. R. Nora, Y. Mizukami, and R. Sablowski, 2004, WUSCHEL induces shoot stem cell activity and developmental plasticity in the root meristem: Genes & Development, v. 18, no. 4, p. 375-380.

Geldner,N, N Anders, H Wolters, J Keicher, W Kornberger, P Muller, A Delbarre, T Ueda, A Nakano, G Jürgens. The Arabidopsis GNOM ARF-GEF Mediates Endosomal Recycling, Auxin Transport, and Auxin-Dependent Plant Growth. Cell 112[2], 219-230. 2003.

Gifford, M. L., S. Dean, and G. C. Ingram, 2003, The Arabidopsis ACR4 gene plays a role in cell layer organisation during ovule integument and sepal margin development: Development, v. 130, no. 18, p. 4249-4258.

Glover, B. J., 2000, Differentiation in plant epidermal cells: Journal of Experimental Botany, v. 51, no. 344, p. 497-505.

Godfray, H. C. et al., 2010, Food Security: The Challenge of Feeding 9 Billion People: Science, v. 327, no. 5967, p. 812-818.

Gómez, E. et al., 2009, The Maize Transcription Factor Myb-Related Protein-1 Is a Key Regulator of the Differentiation of Transfer Cells: The Plant Cell Online, v. 21, no. 7, p. 2022-2035.

Graham, I. A., 2008, Seed Storage Oil Mobilization: Annual Review of Plant Biology, v. 59, no. 1, p. 115-142.

Greenwood, J. S., M. Helm, and C. Gietl, 2005, Ricinosomes and endosperm transfer cell structure in programmed cell death of the nucellus during Ricinus seed development: Proceedings of the National Academy of Sciences of the United States of America, v. 102, no. 6, p. 2238-2243.

Greer, S., M. Wen, D. Bird, X. Wu, L. Samuels, L. Kunst, and R. Jetter, 2007, The Cytochrome P450 Enzyme CYP96A15 Is the Midchain Alkane Hydroxylase Responsible for Formation of Secondary Alcohols and Ketones in Stem Cuticular Wax of Arabidopsis: Plant Physiology, v. 145, no. 3, p. 653-667.

Gregersen, P. L., P. B. Holm, and K. Krupinska, 2008, Leaf senescence and nutrient remobilisation in barley and wheat: Plant Biology, v. 10, p. 37-49.

Grigg,SP, C Galinha, N Kornet, C Canales, B Scheres, M Tsiantis. Repression of Apical Homeobox Genes Is Required for Embryonic Root Development in Arabidopsis. Current biology : CB 19[17], 1485-1490. 2009.

Grossniklaus, U., J. P. Vielle-Calzada, M. A. Hoeppner, and W. B. Gagliano, 1998, Maternal Control of Embryogenesis by MEDEA, a Polycomb Group Gene in Arabidopsis: Science, v. 280, no. 5362, p. 446-450.

Guitton, A. E., D. R. Page, P. Chambrier, C. Lionnet, J. E. Faure, U. Grossniklaus, and F. Berger, 2004, Identification of new members of Fertilisation Independent Seed Polycomb Group pathway involved in the control of seed development in Arabidopsis thaliana: Development, v. 131, no. 12, p. 2971-2981.

Guo, Y., and S. Gan, 2006, AtNAP, a NAC family transcription factor, has an important role in leaf senescence: The Plant Journal, v. 46, no. 4, p. 601-612.

Hamann, T., E. Benkova, I. Bäurle, M. Kientz, and G. Jürgens, 2002, The Arabidopsis BODENLOS gene encodes an auxin response protein inhibiting MONOPTEROS-mediated embryo patterning: Genes & Development, v. 16, no. 13, p. 1610-1615.

Hamberg, M., A. Sanz, M. J. Rodriguez, A. P. Calvo, and C. Castresana, 2003, Activation of the Fatty Acid a-Dioxygenase Pathway during Bacterial Infection of Tobacco Leaves: Journal of Biological Chemistry, v. 278, no. 51, p. 51796-51805.

Hann, D. R., S. Gimenez-Ibanez, and J. P. Rathjen, 2010, Bacterial virulence effectors and their activities: Current Opinion in Plant Biology, v. 13, no. 4, p. 388-393.

Harvey, J., J. Lincoln, and D. Gilchrist, 2008, Programmed cell death suppression in transformed plant tissue by tomato cDNAs identified from an *Agrobacterium rhizogenes*-based functional screen: Molecular Genetics and Genomics, v. 279, no. 5, p. 509-521.

Hatsugai, N., M. Kuroyanagi, K. Yamada, T. Meshi, S. Tsuda, M. Kondo, M. Nishimura, and I. Hara-Nishimura, 2004, A Plant Vacuolar Protease, VPE, Mediates Virus-Induced Hypersensitive Cell Death: Science, v. 305, no. 5685, p. 855-858.

Haughn, G., and A. Chaudhury, 2005, Genetic analysis of seed coat development in Arabidopsis: Trends in Plant Science, v. 10, no. 10, p. 472-477.

Hay, A., and M. Tsiantis, 2010, KNOX genes: versatile regulators of plant development and diversity: Development, v. 137, no. 19, p. 3153-3165.

He, R., G. E. Drury, V. I. Rotari, A. Gordon, M. Willer, T. Farzaneh, E. J. Woltering, and P. Gallois, 2008, Metacaspase-8 Modulates Programmed Cell Death Induced by Ultraviolet Light and H_2O_2 in Arabidopsis: Journal of Biological Chemistry, v. 283, no. 2, p. 774-783.

Hibara, K. i., M. Karim, S. Takada, K. i. Taoka, M. Furutani, M. Aida, and M. Tasaka, 2006, Arabidopsis CUP-SHAPED COTYLEDON3 Regulates Postembryonic Shoot Meristem and Organ Boundary Formation: The Plant Cell Online, v. 18, no. 11, p. 2946-2957.

Hülskamp, M., S. Miséra, and G. Jürgens, 1994, Genetic dissection of trichome cell development in Arabidopsis: Cell, v. 76, no. 3, p. 555-566.

Inoue, H., H. Nojima, and H. Okayama, 1990, High efficiency transformation of Escherichia coli with plasmids: Gene, v. 96, no. 1, p. 23-28.

Jeff, A., E. I. Moan, J. I. Medford, and M. K. Barton, 1996, A member of the KNOTTED class of homeodomain proteins encoded by the STM gene of Arabidopsis: Nature, v. 379, no. 6560, p. 66-69.

Jessen, D., A. Olbrich, J. Knöfer, A. Krüger, M. Hoppert, A. Polle, and M. Fulda, 2011, Combined activity of LACS1 and LACS4 is required for proper pollen coat formation in Arabidopsis: The Plant Journal, v. 68, no. 4, p. 715-726.

Johnson, K. L., K. A. Degnan, J. Ross Walker, and G. C. Ingram, 2005, AtDEK1 is essential for specification of embryonic epidermal cell fate: The Plant Journal, v. 44, no. 1, p. 114-127.

Johnson, K. L., C. Faulkner, C. E. Jeffree, and G. C. Ingram, 2008, The Phytocalpain Defective Kernel 1 Is a Novel Arabidopsis Growth Regulator Whose Activity Is Regulated by Proteolytic Processing: The Plant Cell Online, v. 20, no. 10, p. 2619-2630.

Kamigaki, A., M. Kondo, S. Mano, M. Hayashi, and M. Nishimura, 2009, Suppression of Peroxisome Biogenesis Factor 10 Reduces Cuticular Wax Accumulation by Disrupting the ER Network in Arabidopsis thaliana: Plant and Cell Physiology, v. 50, no. 12, p. 2034-2046.

Kang, B. H., Y. Xiong, D. S. Williams, D. Pozueta-Romero, and P. S. Chourey, 2009, Miniature1-Encoded Cell Wall Invertase Is Essential for Assembly and Function of Wall-in-Growth in the Maize Endosperm Transfer Cell: Plant Physiology, v. 151, no. 3, p. 1366-1376.

Kannangara, R. et al., 2007, The Transcription Factor WIN1/SHN1 Regulates Cutin Biosynthesis in Arabidopsis thaliana: The Plant Cell Online, v. 19, no. 4, p. 1278-1294.

Katsir, L., H. S. Chung, A. J. Koo, and G. A. Howe, 2008, Jasmonate signaling: a conserved mechanism of hormone sensing: Current Opinion in Plant Biology, v. 11, no. 4, p. 428-435.

Kawakatsu, T., and F. Takaiwa, 2010, Cereal seed storage protein synthesis: fundamental processes for recombinant protein production in cereal grains: Plant Biotechnology Journal, v. 8, no. 9, p. 939-953.

Kawashima, T., and R. B. Goldberg, 2010, The suspensor: not just suspending the embryo: Trends in Plant Science, v. 15, no. 1, p. 23-30.

Kazan, K., and J. M. Manners, 2008, Jasmonate Signaling: Toward an Integrated View: Plant Physiology, v. 146, no. 4, p. 1459-1468.

Kepinski, S., and O. Leyser, 2005, The Arabidopsis F-box protein TIR1 is an auxin receptor: Nature, v. 435, no. 7041, p. 446-451.

Kinoshita, T., R. Yadegari, J. J. Harada, R. B. Goldberg, and R. L. Fischer, 1999, Imprinting of the MEDEA Polycomb Gene in the Arabidopsis Endosperm: The Plant Cell Online, v. 11, no. 10, p. 1945-1952.

Kohler, C., L. Hennig, R. Bouveret, J. Gheyselinck, U. Grossniklaus, and W. Gruissem, 2003, Arabidopsis MSI1 is a component of the MEA/FIE Polycomb group complex and required for seed development: EMBO J, v. 22, no. 18, p. 4804-4814.

Kondou, Y. et al., 2008, RETARDED GROWTH OF EMBRYO1, a New Basic Helix-Loop-Helix Protein, Expresses in Endosperm to Control Embryo Growth: Plant Physiology, v. 147, no. 4, p. 1924-1935.

Konishi, T., T. Takeda, Y. Miyazaki, M. Ohnishi-Kameyama, T. Hayashi, M. A. O'Neill, and T. Ishii, 2007, A plant mutase that interconverts UDP-arabinofuranose and UDP-arabinopyranose: Glycobiology, v. 17, no. 3, p. 345-354.

Konishi, T. et al., 2011, Down-regulation of UDP-arabinopyranose mutase reduces the proportion of arabinofuranose present in rice cell walls: Phytochemistry, v. 72, no. 16, p. 1962-1968.

Kroemer, G. et al., 2008, Classification of cell death: recommendations of the Nomenclature Committee on Cell Death 2009: Cell Death Differ, v. 16, no. 1, p. 3-11.

Kurdyukov, S. et al., 2006, The Epidermis-Specific Extracellular BODYGUARD Controls Cuticle Development and Morphogenesis in Arabidopsis: The Plant Cell Online, v. 18, no. 2, p. 321-339.

Kwon, C. S., K. i. Hibara, J. Pfluger, S. Bezhani, H. Metha, M. Aida, M. Tasaka, and D. Wagner, 2006, A role for chromatin remodeling in regulation of CUC gene expression in the Arabidopsis cotyledon boundary: Development, v. 133, no. 16, p. 3223-3230.

Kwon, S. J., H. C. Jin, S. Lee, M. H. Nam, J. H. Chung, S. I. Kwon, C. M. Ryu, and O. K. Park, 2009, GDSL lipase-like 1 regulates systemic resistance associated with ethylene signaling in Arabidopsis: The Plant Journal, v. 58, no. 2, p. 235-245.

L'Haridon, F. et al., 2011, A Permeable Cuticle Is Associated with the Release of Reactive Oxygen Species and Induction of Innate Immunity: PLoS Pathog, v. 7, no. 7, p. e1002148.

Langeveld, S. M. J., M. Vennik, M. Kottenhagen, R. van Wijk, A. Buijk, J. W. Kijne, and S. de Pater, 2002, Glucosylation Activity and Complex Formation of Two Classes of Reversibly Glycosylated Polypeptides: Plant Physiology, v. 129, no. 1, p. 278-289.

Lee, D. S., B. K. Kim, S. J. Kwon, H. C. Jin, and O. K. Park, 2009, Arabidopsis GDSL lipase 2 plays a role in pathogen defense via negative regulation of auxin signaling: Biochemical and Biophysical Research Communications, v. 379, no. 4, p. 1038-1042.

Lee, K. P., U. Piskurewicz, V. Turecková, M. Strnad, and L. Lopez-Molina, 2010, A seed coat bedding assay shows that RGL2-dependent release of abscisic acid by the endosperm controls embryo growth in Arabidopsis dormant seeds: Proceedings of the National Academy of Sciences, v. 107, no. 44, p. 19108-19113.

Lee, S., H. Cheng, K. E. King, W. Wang, Y. He, A. Hussain, J. Lo, N. P. Harberd, and J. Peng, 2002, Gibberellin regulates Arabidopsis seed germination via RGL2, a GAI/RGA-like gene whose expression is up-regulated following imbibition: Genes & Development, v. 16, no. 5, p. 646-658.

Lefebvre, V., H. North, A. Frey, B. Sotta, M. Seo, M. Okamoto, E. Nambara, and A. Marion-Poll, 2006, Functional analysis of Arabidopsis NCED6 and NCED9 genes indicates that ABA synthesized in the endosperm is involved in the induction of seed dormancy: The Plant Journal, v. 45, no. 3, p. 309-319.

Lenhard, M., G. Jürgens, and T. Laux, 2002, The WUSCHEL and SHOOTMERISTEMLESS genes fulfil complementary roles in Arabidopsis shoot meristem regulation: Development, v. 129, no. 13, p. 3195-3206.

Lenhard, M., and T. Laux, 2003, Stem cell homeostasis in the Arabidopsis shoot meristem is regulated by intercellular movement of CLAVATA3 and its sequestration by CLAVATA1: Development, v. 130, no. 14, p. 3163-3173.

Li, Y., F. Beisson, A. J. K. Koo, I. Molina, M. Pollard, and J. Ohlrogge, 2007, Identification of acyltransferases required for cutin biosynthesis and production of cutin with suberin-like monomers: Proceedings of the National Academy of Sciences, v. 104, no. 46, p. 18339-18344.

Lid, S. E. et al., 2002, The defective kernel 1 (dek1) gene required for aleurone cell development in the endosperm of maize grains encodes a membrane protein of the calpain gene superfamily: Proceedings of the National Academy of Sciences, v. 99, no. 8, p. 5460-5465.

Lim, P. O., H. J. Kim, and H. Gil Nam, 2007, Leaf Senescence: Annual Review of Plant Biology, v. 58, no. 1, p. 115-136.

Lin, Z., S. Zhong, and D. Grierson, 2009, Recent advances in ethylene research: Journal of Experimental Botany, v. 60, no. 12, p. 3311-3336.

Lombardi, L., N. Ceccarelli, P. Picciarelli, and R. Lorenzi, 2003, DNA degradation during programmed cell death in Phaseolus coccineus suspensor: Plant Physiology and Biochemistry, v. 45, no. 3-4, p. 221-227.

Lorenzo, O., J. M. Chico, J. J. Sánchez-Serrano, and R. Solano, 2004, JASMONATE-INSENSITIVE1 Encodes a MYC Transcription Factor Essential to Discriminate between Different Jasmonate-Regulated Defense Responses in Arabidopsis: The Plant Cell Online, v. 16, no. 7, p. 1938-1950.

Love, A. J., J. J. Milner, and A. Sadanandom, 2008, Timing is everything: regulatory overlap in plant cell death: Trends in Plant Science, v. 13, no. 11, p. 589-595.

Lu, P., R. Porat, J. A. Nadeau, and S. D. O'Neill, 1996, Identification of a Meristem L1 Layer-Specific Gene in Arabidopsis That Is Expressed during Embryonic Pattern Formation and Defines a New Class of Homeobox Genes: The Plant Cell Online, v. 8, no. 12, p. 2155-2168.

Lukowitz, W., A. Roeder, D. Parmenter, and C. Somerville, 2004, A MAPKK Kinase Gene Regulates Extra-Embryonic Cell Fate in Arabidopsis: Cell, v. 116, no. 1, p. 109-119.

Ma, H., H. Zhao, Z. Liu, and J. Zhao, 2011, The Phytocyanin Gene Family in Rice (*Oryza sativa* L.): Genome-Wide Identification, Classification and Transcriptional Analysis: PLoS ONE, v. 6, no. 10, p. e25184.

Magnard, J. L., E. Le Deunff, J. Domenech, P. M. Rogowsky, P. S. Testillano, M. Rougier, M. C. Risueño, P. Vergne, and C. Dumas, 2000, Genes normally expressed in the endosperm are expressed at early stages of microspore embryogenesis in maize: Plant Molecular Biology, v. 44, no. 4, p. 559-574.

Mallory, A. C., B. J. Reinhart, M. W. Jones-Rhoades, G. Tang, P. D. Zamore, M. K. Barton, and D. P. Bartel, 2004, MicroRNA control of PHABULOSA in leaf development: importance of pairing to the microRNA 5' region: EMBO J, v. 23, no. 16, p. 3356-3364.

Martin, C., and B. J. Glover, 2007, Functional aspects of cell patterning in aerial epidermis: Current Opinion in Plant Biology, v. 10, no. 1, p. 70-82.

Martínez, M., I. Rubio-Somoza, P. Carbonero, and I. Díaz, 2003, A cathepsin B-like cysteine protease gene from Hordeum vulgare (gene CatB) induced by GA in aleurone cells is under circadian control in leaves: Journal of Experimental Botany, v. 54, no. 384, p. 951-959.

MASHIGUCHI, K., T. AsamiA, and Y. zuki, 2009, Genome-Wide Identification, Structure and Expression Studies, and Mutant Collection of 22 Early Nodulin-Like Protein Genes in Arabidopsis: Bioscience, Biotechnology, and Biochemistry, v. 73, no. 11, p. 2452-2459.

Matsuda, F., M. Y. Hirai, E. Sasaki, K. Akiyama, K. Yonekura-Sakakibara, N. J. Provart, T. Sakurai, Y. Shimada, and K. Saito, 2010, AtMetExpress Development: A

Phytochemical Atlas of Arabidopsis Development: Plant Physiology, v. 152, no. 2, p. 566-578.

Mayer,KFX, H Schoof, A Haecker, M Lenhard, G Jürgens, T Laux. Role of WUSCHEL in Regulating Stem Cell Fate in the Arabidopsis Shoot Meristem. Cell 95[6], 805-815. 1998.

McCormick, S., 1993, Male Gametophyte Development: The Plant Cell Online, v. 5, no. 10, p. 1265-1275.

Merrill, R. C., and R. W. Spencer, 1948, Spectral Changes of Some Dyes in Soluble Silicate Solutions: Journal of the American Chemical Society, v. 70, no. 11, p. 3683-3689.

Miao, Y., and U. Zentgraf, 2007, The Antagonist Function of Arabidopsis WRKY53 and ESR/ESP in Leaf Senescence Is Modulated by the Jasmonic and Salicylic Acid Equilibrium: The Plant Cell Online, v. 19, no. 3, p. 819-830.

Michniewicz,M, M K Zago, L Abas, D Weijers, A Schweighofer, I Meskiene, M G Heisler, C Ohno, J Zhang, F Huang, R Schwab, D Weigel, E M Meyerowitz, C Luschnig, R Offringa, J Friml. Antagonistic Regulation of PIN Phosphorylation by PP2A and PINOID Directs Auxin Flux. Cell 130[6], 1044-1056. 2007.

Millar, A. A., S. Clemens, S. Zachgo, E. M. Giblin, D. C. Taylor, and L. Kunst, 1999, CUT1, an Arabidopsis Gene Required for Cuticular Wax Biosynthesis and Pollen Fertility, Encodes a Very-Long-Chain Fatty Acid Condensing Enzyme: The Plant Cell Online, v. 11, no. 5, p. 825-838.

Molina, I., G. Bonaventure, J. Ohlrogge, and M. Pollard, 2006, The lipid polyester composition of Arabidopsis thaliana and Brassica napus seeds: Phytochemistry, v. 67, no. 23, p. 2597-2610.

Nadeau, J. A., and F. D. Sack, 2002, Control of Stomatal Distribution on the Arabidopsis Leaf Surface: Science, v. 296, no. 5573, p. 1697-1700.

Nakaune, S., K. Yamada, M. Kondo, T. Kato, S. Tabata, M. Nishimura, and I. Hara-Nishimura, 2005, A Vacuolar Processing Enzyme, deltaVPE, Is Involved in Seed Coat Formation at the Early Stage of Seed Development: The Plant Cell Online, v. 17, no. 3, p. 876-887.

Nawrath, C., 2006, Unraveling the complex network of cuticular structure and function: Current Opinion in Plant Biology, v. 9, no. 3, p. 281-287.

Nawy, T., W. Lukowitz, and M. Bayer, 2008, Talk global, act local--patterning the Arabidopsis embryo: Current Opinion in Plant Biology, v. 11, no. 1, p. 28-33.

Nemeth, C. et al., 2010, Down-Regulation of the CSLF6 Gene Results in Decreased (1,3;1,4)--d-Glucan in Endosperm of Wheat: Plant Physiology, v. 152, no. 3, p. 1209-1218.

Nishimura, M. T., and J. L. Dangl, 2010, Arabidopsis and the plant immune system: The Plant Journal, v. 61, no. 6, p. 1053-1066.

Ogawa, M., H. Shinohara, Y. Sakagami, and Y. Matsubayashi, 2008, Arabidopsis CLV3 Peptide Directly Binds CLV1 Ectodomain: Science, v. 319, no. 5861, p. 294.

Ohad, N., L. Margossian, Y. C. Hsu, C. Williams, P. Repetti, and R. L. Fischer, 1996, A mutation that allows endosperm development without fertilization: Proceedings of the National Academy of Sciences, v. 93, no. 11, p. 5319-5324.

Okushima, Y. et al., 2005, Functional Genomic Analysis of the AUXIN RESPONSE FACTOR Gene Family Members in Arabidopsis thaliana: Unique and Overlapping Functions of ARF7 and ARF19: The Plant Cell Online, v. 17, no. 2, p. 444-463.

Olsen, O. A., 2004, Nuclear Endosperm Development in Cereals and Arabidopsis thaliana: The Plant Cell Online, v. 16, no. suppl 1, p. S214-S227.

Opsahl-Ferstad, H. G., E. L. Deunff, C. Dumas, and P. M. Rogowsky, 1997, ZmEsr, a novel endosperm-specific gene expressed in a restricted region around the maize embryo: The Plant Journal, v. 12, no. 1, p. 235-246.

Panteris, E., and B. Galatis, 2005, The morphogenesis of lobed plant cells in the mesophyll and epidermis: organization and distinct roles of cortical microtubules and actin filaments: New Phytologist, v. 167, no. 3, p. 721-732.

Pennell, R. I., and C. Lamb, 1997, Programmed Cell Death in Plants: The Plant Cell Online, v. 9, no. 7, p. 1157-1168.

Petersen, K., J. L. Qiu, J. Lütje, B. K. Fiil, S. Hansen, J. Mundy, and M. Petersen, 2010, Arabidopsis MKS1 Is Involved in Basal Immunity and Requires an Intact N-terminal Domain for Proper Function: PLoS ONE, v. 5, no. 12, p. e14364.

Petra Epple, Veronica Franco, Amanda Mack, Jeffery L.Dangl. Regulation of cell death by LSD1 and it's homologues LOL1 and LOL2. 12th International conference on Arabidopsis research. Madison, WI, USA: University of Wisconsin Press. 2001.

Pfaffl, M. W., G. W. Horgan, and L. Dempfle, 2002, Relative expression software tool (REST) for group-wise comparison and statistical analysis of relative expression results in real-time PCR: Nucleic Acids Research, v. 30, no. 9, p. e36.

Pighin, J. A., H. Zheng, L. J. Balakshin, I. P. Goodman, T. L. Western, R. Jetter, L. Kunst, and A. L. Samuels, 2004, Plant Cuticular Lipid Export Requires an ABC Transporter: Science, v. 306, no. 5696, p. 702-704.

Pollard, M., F. Beisson, Y. Li, and J. B. Ohlrogge, 2008, Building lipid barriers: biosynthesis of cutin and suberin: Trends in Plant Science, v. 13, no. 5, p. 236-246.

Pracharoenwattana, I., J. E. Cornah, and S. M. Smith, 2005, Arabidopsis Peroxisomal Citrate Synthase Is Required for Fatty Acid Respiration and Seed Germination: The Plant Cell Online, v. 17, no. 7, p. 2037-2048.

Pruitt, R. E., J. P. Vielle-Calzada, S. E. Ploense, U. Grossniklaus, and S. J. Lolle, 2000, FIDDLEHEAD, a gene required to suppress epidermal cell interactions in Arabidopsis, encodes a putative lipid biosynthetic enzyme: Proceedings of the National Academy of Sciences, v. 97, no. 3, p. 1311-1316.

Rademacher,EH, A S Lokerse, A Schlereth, C I Llavata-Peris, M Bayer, M Kientz, A FreireáRios, J Borst, W Lukowitz, G Jürgens, D Weijers. Different Auxin Response Machineries Control Distinct Cell Fates in the Early Plant Embryo. Developmental Cell 22[1], 211-222. 2012.

Rademacher, E. H., B. Möller, A. S. Lokerse, C. I. Llavata-Peris, W. van den Berg, and D. Weijers, 2011, A cellular expression map of the Arabidopsis AUXIN RESPONSE FACTOR gene family: The Plant Journal, v. 68, no. 4, p. 597-606.

Raissig, M. T., C. Baroux, and U. Grossniklaus, 2011, Regulation and Flexibility of Genomic Imprinting during Seed Development: The Plant Cell Online, v. 23, no. 1, p. 16-26.

Rautengarten, C., B. Ebert, T. Herter, C. J. Petzold, T. Ishii, A. Mukhopadhyay, B. Usadel, and H. V. Scheller, 2011, The Interconversion of UDP-Arabinopyranose and UDP-Arabinofuranose Is Indispensable for Plant Development in Arabidopsis: The Plant Cell Online, v. 23, no. 4, p. 1373-1390.

Reape, T. J., E. M. Molony, and P. F. McCabe, 2008, Programmed cell death in plants: distinguishing between different modes: Journal of Experimental Botany, v. 59, no. 3, p. 435-444.

Reyes, F. C., T. Chung, D. Holding, R. Jung, R. Vierstra, and M. S. Otegui, 2011, Delivery of Prolamins to the Protein Storage Vacuole in Maize Aleurone Cells: The Plant Cell Online, v. 23, no. 2, p. 769-784.

Reyes, F. C., B. Sun, H. Guo, D. Gruis, and M. S. Otegui, 2010, Agrobacterium tumefaciens-Mediated Transformation of Maize Endosperm as a Tool to Study Endosperm Cell Biology: Plant Physiology, v. 153, no. 2, p. 624-631.

Riederer, M., and L. Schreiber, 2001, Protecting against water loss: analysis of the barrier properties of plant cuticles: Journal of Experimental Botany, v. 52, no. 363, p. 2023-2032.

Rodrigues, J., M. Luo, F. Berger, and A. Koltunow, 2010, Polycomb group gene function in sexual and asexual seed development in angiosperms: Sexual Plant Reproduction, v. 23, no. 2, p. 123-133.

Rojo, E., V. K. Sharma, V. Kovaleva, N. V. Raikhel, and J. C. Fletcher, 2002, CLV3 Is Localized to the Extracellular Space, Where It Activates the Arabidopsis CLAVATA Stem Cell Signaling Pathway: The Plant Cell Online, v. 14, no. 5, p. 969-977.

Ronald, P. C., and B. Beutler, 2010, Plant and Animal Sensors of Conserved Microbial Signatures: Science, v. 330, no. 6007, p. 1061-1064.

Rowe, M. H., and D. C. Bergmann, 2010, Complex signals for simple cells: the expanding ranks of signals and receptors guiding stomatal development: Current Opinion in Plant Biology, v. 13, no. 5, p. 548-555.

Sabelli, P. A., and B. A. Larkins, 2009, The Development of Endosperm in Grasses: Plant Physiology, v. 149, no. 1, p. 14-26.

Sagi, G., A. Katz, D. Guenoune-Gelbart, and B. L. Epel, 2005, Class 1 Reversibly Glycosylated Polypeptides Are Plasmodesmal-Associated Proteins Delivered to Plasmodesmata via the Golgi Apparatus: The Plant Cell Online, v. 17, no. 6, p. 1788-1800.

Sambrook, J., and D. Russell, 2001, Molecular Cloning: A Laboratory Manual Cold Spring Harbor Laboratory Press.

Samuels, L., L. Kunst, and R. Jetter, 2008, Sealing Plant Surfaces: Cuticular Wax Formation by Epidermal Cells: Annual Review of Plant Biology, v. 59, no. 1, p. 683-707.

Scanlon, M. J., and A. M. Myers, 1998, Phenotypic analysis and molecular cloning of discolored-1 (dsc1), a maize gene required for early kernel development: Plant Molecular Biology, v. 37, no. 3, p. 483-493.

Scheller, H. V., and P. Ulvskov, 2010, Hemicelluloses: Annual Review of Plant Biology, v. 61, no. 1, p. 263-289.

Schnurr, J., J. Shockey, and J. Browse, 2004, The Acyl-CoA Synthetase Encoded by LACS2 Is Essential for Normal Cuticle Development in Arabidopsis: The Plant Cell Online, v. 16, no. 3, p. 629-642.

Schoof,H, M Lenhard, A Haecker, K F X Mayer, G Jürgens, T Laux. The Stem Cell Population of Arabidopsis Shoot Meristems Is Maintained by a Regulatory Loop between the CLAVATA and WUSCHEL Genes. Cell 100[6], 635-644. 2000.

Schreiber, 2005, Polar Paths of Diffusion across Plant Cuticles: New Evidence for an Old Hypothesis: Annals of Botany, v. 95, no. 7, p. 1069-1073.

Schweighofer, A. et al., 2007, The PP2C-Type Phosphatase AP2C1, Which Negatively Regulates MPK4 and MPK6, Modulates Innate Immunity, Jasmonic Acid, and Ethylene Levels in Arabidopsis: The Plant Cell Online, v. 19, no. 7, p. 2213-2224.

Seifert, G. J., and C. Blaukopf, 2010, Irritable Walls: The Plant Extracellular Matrix and Signaling: Plant Physiology, v. 153, no. 2, p. 467-478.

Serna, A. et al., 2001, Maize endosperm secretes a novel antifungal protein into adjacent maternal tissue: The Plant Journal, v. 25, no. 6, p. 687-698.

Shen, B., C. Li, Z. Min, R. B. Meeley, M. C. Tarczynski, and O. A. Olsen, 2003, sal1 determines the number of aleurone cell layers in maize endosperm and encodes a class E vacuolar sorting protein: Proceedings of the National Academy of Sciences, v. 100, no. 11, p. 6552-6557.

Shpak, E. D., J. M. McAbee, L. J. Pillitteri, and K. U. Torii, 2005, Stomatal Patterning and Differentiation by Synergistic Interactions of Receptor Kinases: Science, v. 309, no. 5732, p. 290-293.

Simon, P., 2003, Q-Gene: processing quantitative real-time RT-PCR data: Bioinformatics, v. 19, no. 11, p. 1439-1440.

Smith, Z. R., and J. A. Long, 2010, Control of Arabidopsis apical-basal embryo polarity by antagonistic transcription factors: Nature, v. 464, no. 7287, p. 423-426.

Solano, R., A. Stepanova, Q. Chao, and J. R. Ecker, 1998, Nuclear events in ethylene signaling: a transcriptional cascade mediated by ETHYLENE-INSENSITIVE3 and ETHYLENE-RESPONSE-FACTOR1: Genes & Development, v. 12, no. 23, p. 3703-3714.

Sørensen, M. B., U. Mayer, W. Lukowitz, H. Robert, P. Chambrier, G. Jürgens, C. Somerville, L. Lepiniec, and F. Berger, 2002, Cellularisation in the endosperm of Arabidopsis thaliana is coupled to mitosis and shares multiple components with cytokinesis: Development, v. 129, no. 24, p. 5567-5576.

Spinelli, S. V., A. P. Martin, I. L. Viola, D. H. Gonzalez, and J. F. Palatnik, 2011, A Mechanistic Link between STM and CUC1 during Arabidopsis Development: Plant Physiology, v. 156, no. 4, p. 1894-1904.

Springer,NM. Small RNAs: How Seeds Remember To Obey Their Mother. Current biology : CB 19[15], R649-R651. 2009.

Sreenivasulu, N., V. Radchuk, M. Strickert, O. Miersch, W. Weschke, and U. Wobus, 2006, Gene expression patterns reveal tissue-specific signaling networks controlling programmed cell death and ABA- regulated maturation in developing barley seeds: The Plant Journal, v. 47, no. 2, p. 310-327.

Staswick, P. E., 2008, JAZing up jasmonate signaling: Trends in Plant Science, v. 13, no. 2, p. 66-71.

Staswick, P. E., and I. Tiryaki, 2004, The Oxylipin Signal Jasmonic Acid Is Activated by an Enzyme That Conjugates It to Isoleucine in Arabidopsis: The Plant Cell Online, v. 16, no. 8, p. 2117-2127.

Suarez, M. F., L. H. Filonova, A. Smertenko, E. I. Savenkov, D. H. Clapham, S. von Arnold, B. Zhivotovsky, and P. V. Bozhkov, 2004, Metacaspase-dependent programmed cell death is essential for plant embryogenesis: Current Biology, v. 14, no. 9, p. R339-R340.

Suh, M. C., A. L. Samuels, R. Jetter, L. Kunst, M. Pollard, J. Ohlrogge, and F. Beisson, 2005, Cuticular Lipid Composition, Surface Structure, and Gene Expression in Arabidopsis Stem Epidermis: Plant Physiology, v. 139, no. 4, p. 1649-1665.

Takada, S., K. Hibara, T. Ishida, and M. Tasaka, 2001, The CUP-SHAPED COTYLEDON1 gene of Arabidopsis regulates shoot apical meristem formation: Development, v. 128, no. 7, p. 1127-1135.

Takahashi, K., T. Shimada, M. Kondo, A. Tamai, M. Mori, M. Nishimura, and I. Hara-Nishimura, 2010, Ectopic Expression of an Esterase, Which is a Candidate for the Unidentified Plant Cutinase, Causes Cuticular Defects in Arabidopsis thaliana: Plant and Cell Physiology, v. 51, no. 1, p. 123-131.

Tanaka, H., H. Onouchi, M. Kondo, I. Hara-Nishimura, M. Nishimura, C. Machida, and Y. Machida, 2001, A subtilisin-like serine protease is required for epidermal surface formation in Arabidopsis embryos and juvenile plants: Development, v. 128, no. 23, p. 4681-4689.

Tanaka, H., M. Watanabe, M. Sasabe, T. Hiroe, T. Tanaka, H. Tsukaya, M. Ikezaki, C. Machida, and Y. Machida, 2007, Novel receptor-like kinase ALE2 controls shoot development by specifying epidermis in Arabidopsis: Development, v. 134, no. 9, p. 1643-1652.

Tanaka, H., M. Watanabe, D. Watanabe, T. Tanaka, C. Machida, and Y. Machida, 2002, ACR4, a Putative Receptor Kinase Gene of Arabidopsis thaliana, that is Expressed in the Outer Cell Layers of Embryos and Plants, is Involved in Proper Embryogenesis: Plant and Cell Physiology, v. 43, no. 4, p. 419-428.

Tanaka, T., H. Tanaka, C. Machida, M. Watanabe, and Y. Machida, 2004, A new method for rapid visualization of defects in leaf cuticle reveals five intrinsic patterns of surface defects in Arabidopsis: The Plant Journal, v. 37, no. 1, p. 139-146.

Tang, D., M. T. Simonich, and R. W. Innes, 2007, Mutations in LACS2, a Long-Chain Acyl-Coenzyme A Synthetase, Enhance Susceptibility to Avirulent Pseudomonas syringae But Confer Resistance to Botrytis cinerea in Arabidopsis: Plant Physiology, v. 144, no. 2, p. 1093-1103.

Terry, D. E., R. K. Chopra, J. Ovenden, and T. P. Anastassiades, 2000, Differential Use of Alcian Blue and Toluidine Blue Dyes for the Quantification and Isolation of Anionic Glycoconjugates from Cell Cultures: Application to Proteoglycans and a High-Molecular-Weight Glycoprotein Synthesized by Articular Chondrocytes: Analytical Biochemistry, v. 285, no. 2, p. 211-219.

Tester, M., and P. Langridge, 2010, Breeding Technologies to Increase Crop Production in a Changing World: Science, v. 327, no. 5967, p. 818-822.

Thomma, B. P., I. A. Penninckx, B. P. Cammue, and W. F. Broekaert, 2001, The complexity of disease signaling in Arabidopsis: Current Opinion in Immunology, v. 13, no. 1, p. 63-68.

Tian, Q. et al., 2007, Subcellular Localization and Functional Domain Studies of DEFECTIVE KERNEL1 in Maize and Arabidopsis Suggest a Model for Aleurone Cell Fate Specification Involving CRINKLY4 and SUPERNUMERARY ALEURONE LAYER1: The Plant Cell Online, v. 19, no. 10, p. 3127-3145.

Toledo-Ortiz, G., E. Huq, and P. H. Quail, 2003, The Arabidopsis Basic/Helix-Loop-Helix Transcription Factor Family: The Plant Cell Online, v. 15, no. 8, p. 1749-1770.

Tsiatsiani, L., F. Van Breusegem, P. Gallois, A. Zavialov, E. Lam, and P. V. Bozhkov, 2011, Metacaspases: Cell Death Differ, v. 18, no. 8, p. 1279-1288.

Tsuda, K., and F. Katagiri, 2010, Comparing signaling mechanisms engaged in pattern-triggered and effector-triggered immunity: Current Opinion in Plant Biology, v. 13, no. 4, p. 459-465.

Tsuwamoto, R., H. Fukuoka, and Y. Takahata, 2008, GASSHO1 and GASSHO2 encoding a putative leucine-rich repeat transmembrane-type receptor kinase are essential for the normal development of the epidermal surface in Arabidopsis embryos: The Plant Journal, v. 54, no. 1, p. 30-42.

Tucker, M. R., A. Hinze, E. J. Tucker, S. Takada, G. Jürgens, and T. Laux, 2008, Vascular signalling mediated by ZWILLE potentiates WUSCHEL function during shoot meristem stem cell development in the Arabidopsis embryo: Development, v. 135, no. 17, p. 2839-2843.

van der Hoorn, R. A. L., 2008, Plant Proteases: From Phenotypes to Molecular Mechanisms: Annual Review of Plant Biology, v. 59, no. 1, p. 191-223.

van Doorn, W. G. et al., 2011a, Morphological classification of plant cell deaths: Cell Death Differ, v. 18, no. 8, p. 1241-1246.

van Doorn, W. G., 2004, Is Petal Senescence Due to Sugar Starvation?: Plant Physiology, v. 134, no. 1, p. 35-42.

van Doorn, W. G., 2011b, Classes of programmed cell death in plants, compared to those in animals: Journal of Experimental Botany.

Vellosillo, T., M. Martínez, M. A. López, J. Vicente, T. Cascón, L. Dolan, M. Hamberg, and C. Castresana, 2007, Oxylipins Produced by the 9-Lipoxygenase Pathway in Arabidopsis Regulate Lateral Root Development and Defense Responses through a Specific Signaling Cascade: The Plant Cell Online, v. 19, no. 3, p. 831-846.

Vizcay-Barrena, G., and Z. A. Wilson, 2006, Altered tapetal PCD and pollen wall development in the Arabidopsis ms1 mutant: Journal of Experimental Botany, v. 57, no. 11, p. 2709-2717.

Voisin, D., C. Nawrath, S. Kurdyukov, R. B. Franke, J. J. Reina-Pinto, N. Efremova, I. Will, L. Schreiber, and A. Yephremov, 2009, Dissection of the Complex Phenotype in Cuticular Mutants of Arabidopsis Reveals a Role of SERRATE as a Mediator: PLoS Genet, v. 5, no. 10, p. e1000703.

Volokita, M., T. Rosilio-Brami, N. Rivkin, and M. Zik, 2011, Combining Comparative Sequence and Genomic Data to Ascertain Phylogenetic Relationships and Explore the Evolution of the Large GDSL-Lipase Family in Land Plants: Molecular Biology and Evolution, v. 28, no. 1, p. 551-565.

Vroemen, C. W., A. P. Mordhorst, C. Albrecht, M. A. C. J. Kwaaitaal, and S. C. de Vries, 2003, The CUP-SHAPED COTYLEDON3 Gene Is Required for Boundary and Shoot Meristem Formation in Arabidopsis: The Plant Cell Online, v. 15, no. 7, p. 1563-1577.

Wan, L., Q. Xia, X. Qiu, and G. Selvaraj, 2002, Early stages of seed development in Brassica napus: a seed coat-specific cysteine proteinase associated with programmed cell death of the inner integument: The Plant Journal, v. 30, no. 1, p. 1-10.

Wang, H., N. Ngwenyama, Y. Liu, J. C. Walker, and S. Zhang, 2007, Stomatal Development and Patterning Are Regulated by Environmentally Responsive Mitogen-Activated Protein Kinases in Arabidopsis: The Plant Cell Online, v. 19, no. 1, p. 63-73.

Watanabe, M., H. Tanaka, D. Watanabe, C. Machida, and Y. Machida, 2004, The ACR4 receptor-like kinase is required for surface formation of epidermis-related tissues in Arabidopsis thaliana: The Plant Journal, v. 39, no. 3, p. 298-308.

Watanabe, N., and E. Lam, 2011, Arabidopsis metacaspase 2d is a positive mediator of cell death induced during biotic and abiotic stresses: The Plant Journal, v. 66, no. 6, p. 969-982.

Weijers, D., A. Schlereth, J. S. Ehrismann, G. Schwank, M. Kientz, and G. Jurgens, 2006, Auxin Triggers Transient Local Signaling for Cell Specification in Arabidopsis Embryogenesis: Developmental Cell, v. 10, no. 2, p. 265-270.

Wellesen, K., F. Durst, F. Pinot, I. Benveniste, K. Nettesheim, E. Wisman, S. Steiner-Lange, H. Saedler, and A. Yephremov, 2001, Functional analysis of the LACERATA gene of Arabidopsis provides evidence for different roles of fatty acid w-hydroxylation in development: Proceedings of the National Academy of Sciences, v. 98, no. 17, p. 9694-9699.

Winter, D., B. Vinegar, H. Nahal, R. Ammar, G. V. Wilson, and N. J. Provart, 2007, An "Electronic Fluorescent Pictograph" Browser for Exploring and Analyzing Large-Scale Biological Data Sets: PLoS ONE, v. 2, no. 8, p. e718.

Wisniewska, J. et al., 2006, Polar PIN Localization Directs Auxin Flow in Plants: Science, v. 312, no. 5775, p. 883.

Wollmann, H., and F. Berger, 2012, Epigenetic reprogramming during plant reproduction and seed development: Current Opinion in Plant Biology, v. 15, no. 1, p. 63-69.

Wolters-Arts, M., W. M. Lush, and C. Mariani, 1998, Lipids are required for directional pollen-tube growth: Nature, v. 392, no. 6678, p. 818-821.

Wu, M., J. Huang, S. Xu, T. Ling, Y. Xie, and W. Shen, 2011, Haem oxygenase delays programmed cell death in wheat aleurone layers by modulation of hydrogen peroxide metabolism: Journal of Experimental Botany, v. 62, no. 1, p. 235-248.

Xiao, F., S. Mark Goodwin, Y. Xiao, Z. Sun, D. Baker, X. Tang, M. A. Jenks, and J. M. Zhou, 2004, Arabidopsis CYP86A2 represses Pseudomonas syringae type III genes and is required for cuticle development: EMBO J, v. 23, no. 14, p. 2903-2913.

Yadegari, R., and G. N. Drews, 2004, Female Gametophyte Development: The Plant Cell Online, v. 16, no. suppl 1, p. S133-S141.

Yang, S., N. Johnston, E. Talideh, S. Mitchell, C. Jeffree, J. Goodrich, and G. Ingram, 2008, The endosperm-specific ZHOUPI gene of Arabidopsis thaliana regulates endosperm breakdown and embryonic epidermal development: Development, v. 135, no. 21, p. 3501-3509.

Yang, Z., L. Tian, M. Latoszek-Green, D. Brown, and K. Wu, 2005, Arabidopsis ERF4 is a transcriptional repressor capable of modulating ethylene and abscisic acid responses: Plant Molecular Biology, v. 58, no. 4, p. 585-596.

Yephremov, A., E. Wisman, P. Huijser, C. Huijser, K. Wellesen, and H. Saedler, 1999, Characterization of the FIDDLEHEAD Gene of Arabidopsis Reveals a Link between Adhesion Response and Cell Differentiation in the Epidermis: The Plant Cell Online, v. 11, no. 11, p. 2187-2202.

York, W. S., and M. A. O'Neill, 2008, Biochemical control of xylan biosynthesis -- which end is up?: Current Opinion in Plant Biology, v. 11, no. 3, p. 258-265.

Young, T. E., and D. R. Gallie, 2000a, Programmed cell death during endosperm development: Plant Molecular Biology, v. 44, no. 3, p. 283-301.

Young, T. E., and D. R. Gallie, 2000b, Regulation of programmed cell death in maize endosperm by abscisic acid: Plant Molecular Biology, v. 42, no. 2, p. 397-414.

Zavaliev, R., G. Sagi, A. Gera, and B. L. Epel, 2010, The constitutive expression of Arabidopsis plasmodesmal-associated class 1 reversibly glycosylated polypeptide impairs plant development and virus spread: Journal of Experimental Botany, v. 61, no. 1, p. 131-142.

Zheng, H., O. Rowland, and L. Kunst, 2005, Disruptions of the Arabidopsis Enoyl-CoA Reductase Gene Reveal an Essential Role for Very-Long-Chain Fatty Acid Synthesis in Cell Expansion during Plant Morphogenesis: The Plant Cell Online, v. 17, no. 5, p. 1467-1481.

Zheng, Z. et al., 2010, The Protein Kinase SnRK2.6 Mediates the Regulation of Sucrose Metabolism and Plant Growth in Arabidopsis: Plant Physiology, v. 153, no. 1, p. 99-113.

Zimmermann, P., M. Hirsch-Hoffmann, L. Hennig, and W. Gruissem, 2004, GENEVESTIGATOR. Arabidopsis Microarray Database and Analysis Toolbox: Plant Physiology, v. 136, no. 1, p. 2621-2632.

Zuo, J., Q. W. Niu, G. Frugis, and N. H. Chua, 2002, The WUSCHEL gene promotes vegetative-to-embryonic transition in Arabidopsis: The Plant Journal, v. 30, no. 3, p. 349-359.